

**INTERMITTENT FASTING PROMOTES AXONAL  
REGENERATION THROUGH THE GUT MICROBIOME DERIVED  
METABOLITE: INDOLE-3-PROPIONIC ACID**

- by -

Elisabeth Serger

Imperial College London  
Department of Brain Sciences

Thesis submitted to Imperial College London for the degree of  
Doctor of Philosophy  
April, 2020

## Abstract

Spontaneous functional mammalian axonal regeneration following injury fails. High density and fast axon regeneration across distances are needed for efficient repair in humans. These are likely influenced by complex neuronal intrinsic and extrinsic metabolic and signalling mechanisms. Environmental factors such as exercise and diet have been shown to affect metabolism and signalling promoting health and repair processes in several diseases. Intermittent fasting (IF) has been shown to increase synaptic plasticity and neurogenesis that partially share molecular mechanisms with axonal regeneration. Recent publications showed that IF was followed by enhanced functional recovery following spinal cord injury. We hypothesized that IF would promote axonal regeneration after injury by a combinatorial effect of systemic and cell intrinsic mechanisms influencing neuronal metabolism and regenerative signalling pathways. Hence, we studied axonal regeneration after sciatic nerve injury in fasting (IF) versus non-fasting animals to discover that IF significantly promotes axonal regeneration. We next found IF-dependent upregulation of gut bacteria-derived indole metabolites and identified indole-3-propionic acid (IPA) as a key factor in IF dependent axonal regeneration. IPA treatment in *ad libitum*-fed mice increased axonal regeneration after injury. Further, RNA sequencing transcriptomic analysis from dorsal root ganglia neurons suggests that neutrophils and interferon gamma play an important role in IPA-dependent axonal regeneration. These studies offer both a novel mechanism and they have the potential to provide a novel translational approach for nerve repair and functional recovery after injury.

## **Statement of originality**

This is to certify that the content of this thesis is my own work and has not been submitted for any degree or other purposes.

## **Copyright declaration**

The copyright of this thesis rests with the author. Unless otherwise indicated, its contents are licensed under a Creative Commons Attribution-Noncommercial 4.0 International Licence (CC BY-NC).

Under this licence, you may copy and redistribute the material in any medium or format. You may also create and distribute modified versions of the work. This is on the condition that: you credit the author and do not use it, or any derivative works, for a commercial purpose.

When reusing or sharing this work, ensure you make the licence terms clear to others by naming the licence and linking to the licence text. Where a work has been adapted, you should indicate that the work has been changed and describe those changes.

Please seek permission from the copyright holder for uses of this work that are not included in this licence or permitted under UK Copyright Law.

## Acknowledgements

This page is dedicated to thank all the people who contributed in one way or the other to the successful completion of the presented work.

First of all I would like to thank the members of my lab and our collaborators. The experiments in this project required knowledge and techniques from a variety of fields (literally across the globe) and I could not have done it without them. I want to thank Dr. Antonis Myridakis for conducting the GC-MS metabolomics, Professor Dylan Dodd for providing us with the WT and *FldC Clostridium sporogenes* bacterial cultures, Dr. Matt Danzi for the raw data analysis of the RNA sequencing, Dr. Alexander Brandis for running the LC-MSMS for IPA quantification and Adesola Bello for the analysis of the 16S sequencing raw data. A special thanks will be given to Dr. Greg Crawford, who has taught me all I know about immunology lab techniques.

I am truly grateful for all I have learned in the last 4 years from the members of the Di Giovanni group. We are a true team, helping each other inside and outside the lab. Thanks to Simone, for providing the space to be creative and develop as a scientist and always sticking to his “open-door-policy”, being there when needed. A special thanks goes to Ilaria, whom I still believe is one of the most skilled molecular biologists out there and who always took the time to understand and help when help was needed. Thanks to my “Minions”, Jess and Fran, who have brought so much fun and love to my lab-life since they started 2 years ago. Especially to Jess for her positivity and an always open ear in those long hours in the animal house. I would also like to thank Francy, who was the biggest help when it came to large experiments and long hours of dissections, usually filled with inspiring conversations. Last, but not least, I want to thank all the others, Eilidh, Paolo, Tom, Luming and Guiping and Lucia for being the most supportive lab I have ever seen. Whatever it is, to simply talk science, exchange new exciting ideas or tackle some technical issues, EVERYONE is involved.

Finally, I would like to thank James, my “rock in the ocean”, keeping me sane, loving and supporting me no matter what happens. Additionally, I want thank all my friends and my wonderful family, who have believed in me and supported me over the years, significantly shaping the path which has led me to this point.



## Table of contents

Abstract.....	2
Statement of originality .....	3
Copyright declaration.....	3
Acknowledgements .....	4
List of Figures and Tables.....	7
Abbreviations .....	9
<b>Chapter 1: INTRODUCTION .....</b>	<b>13</b>
<b>1.1 Nervous system injury and regeneration .....</b>	<b>13</b>
1.1.1 Peripheral nervous system injury.....	13
1.1.1.1 The Dorsal root ganglion system .....	15
1.1.1.2 Wallerian degeneration and the role of extrinsic and intrinsic factors in sciatic nerve regeneration.....	17
1.1.2 Central nervous system injury.....	22
1.1.2.1 CNS regenerative failure – The role of extrinsic and intrinsic factors.....	22
1.1.3 Environmental changes and their potential impact on metabolic modulation of axonal regeneration.....	25
<b>1.2 Intermittent Fasting .....</b>	<b>28</b>
1.2.1 General Introduction.....	28
1.2.2 Intermittent fasting in health and disease.....	29
<b>1.3 The Gut microbiome .....</b>	<b>32</b>
1.3.1 General introduction .....	32
1.3.2 The Gut microbiome and the nervous system .....	34
1.3.3 The Gut microbiome – response to dietary interventions .....	35
<b>1.4 Immune response to nervous system injury .....</b>	<b>37</b>
1.4.1 General introduction .....	37
1.4.2 Peripheral nervous system injury – Immune response in the sciatic nerve.....	37
1.4.3 Central nervous system injury – Immune response in the spinal cord .....	42
<b>1.5 The mammalian system to study axonal regeneration .....</b>	<b>46</b>
<b>1.6 Hypothesis and Aims of the Thesis .....</b>	<b>48</b>
<b>Chapter 2: METHODS.....</b>	<b>49</b>
2.1 In vivo methods.....	49
2.2 Ex vivo and in vitro methods.....	53
<b>Chapter 3: RESULTS.....</b>	<b>61</b>
<b>3.1 Intermittent Fasting promotes axonal regeneration and target reinnervation following sciatic nerve crush.....</b>	<b>61</b>
<b>3.2 Schwann cells , macrophages and neurotrophic factors are unchanged in the sciatic nerve and DRG in IF vs AL .....</b>	<b>64</b>

3.3	Metabolomics analysis identifies IF-dependent induction of indole metabolites .....	66
3.4	IF-dependent axon regeneration requires the gram+ gut microbiome and strongly induces serum indole-3 propionic acid levels .....	68
3.5	16S sequencing reveals increased number of Clostridiales following intermittent fasting .....	74
3.6	IPA is required for and promotes axonal regeneration via a DRG neuron extrinsic mechanism .....	77
3.7	RNA sequencing reveals upregulation of immune regulatory pathways following IPA treatment .....	81
3.8	IPA increases the number of neutrophils and NK cells in the spleen, mesenteric lymph nodes and DRG following sciatic nerve crush.....	85
3.9	Neutrophil chemotaxis and IFN $\gamma$ signalling mediate the effect of IPA.....	88
3.10	IPA delivery after sciatic nerve crush injury improves sensory recovery .....	91
3.11	Dorsal column axotomy followed by IPA affects behavioural recovery and synaptic plasticity.....	93
<b>Chapter 4: Discussion .....</b>		<b>99</b>
4.1	Overview.....	99
4.2	Intermittent Fasting promotes axonal regeneration through Indole-3-propionic acid....	100
4.3	Indole-3-propionic Acid mimics IF facilitated axonal regeneration through immunoregulatory mechanisms .....	103
4.4	Indole-3-propionic acid promotes functional recovery following Sciatic nerve and spinal cord injury.....	107
4.5	Limitations and future perspectives .....	109
4.6	Conclusion .....	111
<b>Bibliography .....</b>		<b>112</b>

## List of Figures and Tables

*Figure 1. Anatomy of the Central- and Peripheral nervous system*

*Figure 2. The dorsal root ganglion system and the conditioning lesion*

*Figure 3. Peripheral nerve injury induced signalling*

*Figure 4. Adaptive physiological response of major organs to intermittent fasting*

*Figure 5. Multifactorial communication of the gut microbiome with the body, specifically the brain.*

*Figure 6. Overview of the gut-microbiota-brain axis in neurology and psychiatry*

*Figure 7. Immune response and related events after peripheral nerve injury*

*Figure 8. Schematic representation of the spinal cord injury site*

*Figure 9. Intermittent Fasting promotes axonal regeneration and target reinnervation following sciatic nerve crush*

*Figure 10. Weight and food intake screen during 10 days of intermittent fasting*

*Figure 11. Assessment of Macrophages and Schwann cells in the nerve and DRGs in IF vs AL following injury and biochemical analysis of neurotrophic factors following intermittent fasting.*

*Figure 12. Untargeted metabolomics analysis identifies Indole-3-propionic acid, a microbiome derived metabolite as candidate, as upregulated after IF.*

*Figure 13. The proregenerative effect of intermittent fasting is partially mediated by the gut microbiome*

*Figure 14. Metabolomics analysis identifies Indole-3-propionic following 10 days of intermittent fasting*

*Figure 15. GC-MS targeted metabolomics analysis identifies no changes for SCFAs*

*Figure 16. 16S-sequencing reveals increased number of Clostridiales following intermittent fasting*

*Figure 17. Indole-3-propionic acid indirectly promotes axonal regeneration of DRG neurons*

*Figure 18. RNA sequencing reveals upregulation of immune regulatory pathways following IPA treatment*

*Figure 19. Immunohistochemical analysis of DRG and nerve crush side following IPA treatment.*

*Figure 20. IPA increases the number of neutrophils and NK cells in spleen and mesenteric lymph nodes following sciatic nerve crush.*

*Figure 21. Neutrophil chemotaxis and IFN $\gamma$  signalling seem to mediate the effect of IPA*

*Figure 22. Sciatic nerve crush followed by IPA treatment showed improved thermal heat sensation at 2 weeks post injury.*

*Figure 23. Dorsal column axotomy followed by IPA treatment showed a decrease in adhesive tape touch time within 1 week following injury.*

*Figure 24. Dorsal column axotomy followed by IPA treatment leads to reduced GFAP intensity in the lesion core and increased number of synaptic connections to motor neurons below the injury site*

*Table 1. Indole-3-propionic Acid is significantly increased in the serum in IF vs AL.*

## Abbreviations

Acetyl-Coa = acetyl coenzyme A  
AD = Alzheimers disease  
ADF = alternate day fasting  
ADP = Adenosine diphosphate  
AKT = phosphoinositide 3-kinases (PI3K)/serine/threonine protein kinase B  
AL = Ad libitum  
AMP = Adenosine monophosphate  
ANOVA = analysis of variance  
ASV = amplicon sequence variant  
ATF3 = Activating Transcription Factor 3  
ATP = Adenosine triphosphate  
BBB = Basso-Beattie-Bresnahan  
BBB = blood brain barrier  
BDNF = Brain derived neurotrophic factor  
bFGF = basic fibroblast growth factor  
BMS = Basso mouse scale for locomotion  
BP = Biological Process  
BSA = bovine serum albumin  
*C.s.* = *Clostridium sporogenes*  
Ca<sup>2+</sup> = Calcium  
CaMK = Ca<sup>2+</sup>-calmodulin-dependent protein kinases  
cAMP = 3',5'-cyclic adenosine monophosphate  
Casp4 =Caspase 4  
CBP = CREB-Binding Protein  
Ccl19 = Chemokine (C-C motif) ligand 19  
CCR2 = C-C chemokine receptor type 2  
CD = cluster of differentiation  
CEBP = CCAAT-enhancer-binding proteins  
CFU = colony forming unit  
ChAT = choline acetyl transferase  
CMT1A = Charcot-Marie-Tooth type 1A  
CNS = central nervous system  
CR = caloric restriction  
CREB = cAMP - response element binding protein  
CSPGs = Chondroitin sulfate proteoglycan  
CST = Corticospinal tract  
CTB = *Cholera toxin B*  
CTLA4 = cytotoxic T-lymphocyte-associated Protein 4  
CVF = Cobra venom factor  
CXCL1 = chemokine (C-X-C motif) ligand 1  
CXCR2 = C-X-C Motif Chemokine Receptor 2  
DAVID = Database for Annotation, Visualization, and Integrated Discovery  
DLK1 = Delta Like Non-Canonical Notch Ligand 1  
DMEM = Dulbecco's Modified Eagle Medium  
DNA = Deoxyribonucleic acid  
DRG = dorsal root ganglion  
EAE = Experimental autoimmune encephalomyelitis  
ECM = extracellular matrix

EDTA = Ethylenediaminetetraacetic acid  
EE = enriched environment  
EGFR = Epidermal growth factor receptor  
ELISA = Enzyme-linked Immunosorbent Assay  
ErbB2 = Erythroblastic oncogene B 2  
ErbB3 = Erythroblastic oncogene B 3  
ERK = Extracellular-*signal*-regulated kinase  
FACS = fluorescence activated cell sorting  
FBS = Foetal bovine serum  
FGF2 = Fibroblast Growth Factor 2  
fldC = phenyllactate dehydratase complex  
FT = Faecal transplantation  
GABA = gamma-Aminobutyric acid  
GAP43 = Growth Associated Protein 43  
GC-MS = Gas chromatography – Mass Spectrometry  
GDNF = glial cell line-derived neurotrophic factor  
GFAP = glial fibrillary acidic protein  
GO = Gene Ontology  
GPRs = G Protein-coupled receptors  
Gr-1 = gamma response 1  
GRP-78 = Glucose-Regulated Protein, 78kD  
Gsdmd = Gasdermin D  
HBSS = Hanks balanced salt solution  
HDAC 3 = Histone deacetylase 3  
HDAC 5 = Histone deacetylase 5  
HDL = high density lipoprotein  
HO-1 = *Heme oxygenase-1*  
HPA = hypothalamic-pituitary-adrenal axis  
*HSP70* = Heat shock protein 70  
IF = intermittent fasting  
IFN $\beta$  = Interferon beta  
IFN $\gamma$  = Interferon gamma  
IFN $\gamma$ R = Interferon gamma receptor  
IGF-1 = Insulin like growth factor 1  
IHC = immunohistochemistry  
IL1 = Interleukin 1  
IL10 = Interleukin  
IL-10R1 = Interleukin 10 receptor 1  
IL13 = Interleukin 13  
IL17b = Interleukin 17B  
IL18 = Interleukin 18  
IL1 $\alpha$  = Interleukin 1 alpha  
IL1 $\beta$  = Interleukin 1 beta  
IL6 = Interleukin 6  
ILA = Indole-lactic acid  
IP = intraperitoneal  
IPA = indole-3-propionic acid  
JAK = Janus kinase  
JIP3 = JNK-interacting protein 3  
JNK = JUN N-terminal kinase  
JUN = Jun Proto-Oncogene  
KA = kainic acid

KAT2B = Lysine Acetyltransferase 2B  
LC-MSMS  
LDL = low density lipoprotein  
LIF = Leukemia inhibitory factor  
LN = lymph node  
logFC = log<sub>2</sub> Fold Change  
Ly6G = Lymphocyte antigen 6 complex locus G6D  
MAG = Myelin associated glycoprotein  
MAPK = Mitogen-activated protein kinase  
MBP = Myelin basic protein  
MCP-1 = Monocyte chemoattractant protein-1  
MHCI = major histocompatibility complex I  
MIP1 $\alpha$  = Macrophage Inflammatory Protein 1alpha  
MIP1 $\beta$  = Macrophage Inflammatory Protein 1beta  
MLN – mesenteric lymph node  
mRNA = messenger RNA  
NAD = nicotinamide adenine dinucleotide  
NADPH = Reduced nicotinamide adenine dinucleotide phosphate  
NF200 = neurofilament 200  
NGF = nerve growth factor  
NGFb = Nerve Growth Factor (Beta Polypeptide)  
NgR1 = Nogo receptor 1  
NK cell = Natural killer cell  
NKT cell = Natural killer T-cell  
NLRP3 = NOD-, LRR- and pyrin domain-containing protein 3  
NogoA = Neurite outgrowth inhibitor A  
NR =nuclear receptor  
Nr1i2 = Pregnane X Receptor gene  
NRG-1 = Neuregulin  
NT-3 = Neurtrophin-3  
NT-4 = Neurtrophin-4  
NTR = neurotrophin receptor  
OMgp = oligodendrocyte myelin glycoprotein  
OPLS-DA = orthogonal partial least-squares-discriminant analysis  
P0 = Myelin protein zero  
PBS = Phosphate buffered saline  
PDL = Poly-D-lysine  
PGC1 $\alpha$  = Peroxisome Proliferator-Activated Receptor Gamma Coactivator 1-Alpha  
PI3K = Phosphoinositide 3-kinases  
PKA = Protein kinase A  
PKC = Protein kinase C  
PLC = Phospholipase C  
PLS-DA = partial least-squares-discriminant analysis  
PMP22 = peripheral myelin protein 22  
PMP22 = Peripheral protein 22  
PNI = peripheral nerve injury  
PNS = peripheral nervous system  
PRKD1 = Protein Kinase D1  
PTEN = Phosphatase and tensin homologue  
PTP = Receptor protein tyrosine phosphatase  $\delta$   
PXR = Pregnane X Receptor  
RAGs = regeneration-associated genes

RNA = Ribonucleic acid  
ROS = reactive oxygen species  
SCFAs = short chain fatty acids  
SCG-10 = Superior cervical ganglion-10  
SCI = spinal cord injury  
SEM = standard error of the mean  
SIRT3 = sirtuin 3  
SNC = Sciatic nerve crush  
SNPH = Syntaphilin  
SOX10 = SRY-Box Transcription Factor 10  
SOX11 = SRY-Box Transcription Factor 11  
STAT = signal transducers and activators of transcription  
STAT3 = signal transducers and activators of transcription 3  
Teff = effector T-cell  
TET3 = tet methylcytosine dioxygenase 3  
TF = transcription factor  
Th1 cell = Type 1 helper T-cells  
TLR = Toll like receptor  
TLR4 = Toll like receptor  
TNFR = tumor necrosis factor receptor  
TNF $\alpha$  = tumor necrosis factor alpha  
Treg = regulatory T-cell  
Tregs = regulatory T-cells  
TrKA = receptor tyrosine kinase A  
TrKB = receptor tyrosine kinase B  
TrKC = receptor tyrosine kinase C  
TX100 = Triton X 100  
vGAT = synaptic vesicle GABAergic transporter  
VGCC = voltage gated calcium channel  
vGLUT = synaptic vesicle Glutamatergic transporter  
XBP1 = X-Box Binding Protein 1  
 $\beta$ IIITub =  $\beta$  III Tubulin



# Chapter 1: INTRODUCTION

## 1.1 Nervous system injury and regeneration

### 1.1.1 Peripheral nervous system injury

The peripheral nervous system (PNS) transmits signals between the central nervous system (CNS) and the rest of the body<sup>1</sup>. It consists of glial cells, stromal cells and neuronal cells, of which the latter can be subdivided into motor, sensory and autonomic neurons. Efferent neurons (motor and autonomic) receive signals from the CNS, whereas afferent neurons relay signals from cells, including Pacini cells, Golgi cells and muscle spindles to the brain and interneurons of the spinal cord<sup>1</sup>. Peripheral nerves are composed of nerve fibers which are assembled in individual fascicle bundles. Each fascicle is surrounded a perineurium membrane, and all fascicles are collectively encompassed by the epineurium, thus enclosing individual nerves<sup>1</sup> (Figure 1). Contrary to motoneurons, which are classified as A $\alpha$  neurons, sensory neurons can be subdivided into tactile and proprioceptive neurons (A $\beta$ ), muscle tone neurons (A $\gamma$ ), pain, cold, temperature and touch neurons (A $\delta$ ) and pain, warm temperature and touch neurons (dC). Others such as, B and sC neurons, have various anatomical functions<sup>2</sup>.

Injuries to the peripheral nervous system occur between 13 - 23 per 100,000 persons per year in developed countries<sup>3-5</sup>, resulting in approximately \$150 billion spent on annual healthcare in the United States alone<sup>5</sup>. Nerve injuries emerge from traction or stretch, contusion, missiles (gunshot wounds), crush (compression, ischemia) or thermal and electric injuries, resulting in partial or total loss of sensory, motor and autonomic function. Accordingly, injury severity can range from mild segmental demyelination (first degree injury, neuropraxia) to total loss of continuity of the entire nerve trunk (5<sup>th</sup> degree injury, neurotmesis)<sup>2</sup>. Often nerve injuries occur as secondary injuries following surgeries<sup>6</sup> or muscle injections, and despite of some retained regenerative capacity of adult peripheral neurons, the functional outcome of such injury is often poor<sup>7</sup>. This is because the injured neurons regenerative response and the response of cells surrounding the axon, cannot maintain an effective growth-promoting response for long periods. Investigation into cellular processes and signalling pathways that promote peripheral nerve regeneration will be crucial for improving clinical outcomes following peripheral nerve injury (PNI).

In early developmental stages mammalian neurons extend growth cones into axons and form synapses with other neurons. However, during transition into adulthood this growth capacity is partially or completely lost, in both the PNS and CNS, respectively<sup>8,9</sup>. The ability to reinitiate axon growth following injury is usually termed axon “regeneration” and has mainly been studied utilising developmental pathways and genes<sup>10,11</sup>, regenerative organisms<sup>12,13</sup> and post-injury

experimental models<sup>14</sup>. Adult mammalian nerves regenerate poorly and rarely reinnervate their target tissue, whereas invertebrates, such as aplysia, crayfish, leeches and cockroaches, manage to refuse the proximal and distal stump, months after nerve injury<sup>15-19</sup>. The ability to regenerate axons to full functional recovery makes them valuable model organisms to investigate the structural and molecular adaptations leading to successful axonal regeneration. The giant axons found in aplysia and cockroaches have been crucial in the dissection of events that initiate growth cone formation following transection in vitro. Additionally, studies in aplysia have uncovered many of the proteins retrogradely transported following injury, illuminating a better understanding of the communication between the injury site and the transcriptional changes in the cell soma<sup>20-23</sup>. These findings were built on further by studies in the mammalian sciatic nerve<sup>24-26</sup>. Invertebrates such as *Drosophila melanogaster* and *C.elegans* have also been found to undergo processes similar to mammalian neurons upon axotomy, resulting in a proximal stump that succeeds to form a new growth cone and a distal axon that degenerates<sup>27,28</sup>. The genomes between *C.elegans* and mammals are highly conserved<sup>29</sup>. Therefore, the transparent body, short life cycle and single neuron resolution of *C.elegans* allows for large scale genetic screens to dissect pathways required for axonal regeneration after injury. This approach has led to the discovery of more than 100 genes that influence the regrowth of axons, including the Delta Like Non-Canonical Notch Ligand 1 - Mitogen-activated protein kinase (DLK1-MAPK) pathway<sup>30-32</sup>, Phosphatase and tensin homologue (PTEN) homologue daf-18<sup>33</sup> and Notch homologue lin12<sup>34</sup>. Invertebrates have been used to investigate the sequence of events following peripheral nerve injury and further guided our understanding of regenerative signalling. Intracellular signals are required to activate cell repair and initiate regenerative reprogramming. A number of signalling pathways, detected first in *c.elegans*, have been associated with axonal regeneration, of which the most well studied are the DLK-JIP3-JNK complex and Importin-vimentin-ERK complex signalling.

Finally, neurons will have to rebuild a functional circuit by reconnecting with the original target to form synaptic contacts. In early development this is established by the release of nerve growth factors (NGFs) by the target itself<sup>35</sup>, whereas in the mammalian PNS, Schwann cells and macrophages release NGFs<sup>36-38</sup> and Schwann cells form tubes to physically guide axons<sup>39</sup>. However, reaching a functional endpoint equivalent to that observed during development or in some invertebrate species is still to be achieved in mammalian peripheral nerves. Studies using mammalian animal models have further unravelled the intrinsic and extrinsic mechanisms contributing to axonal regeneration.

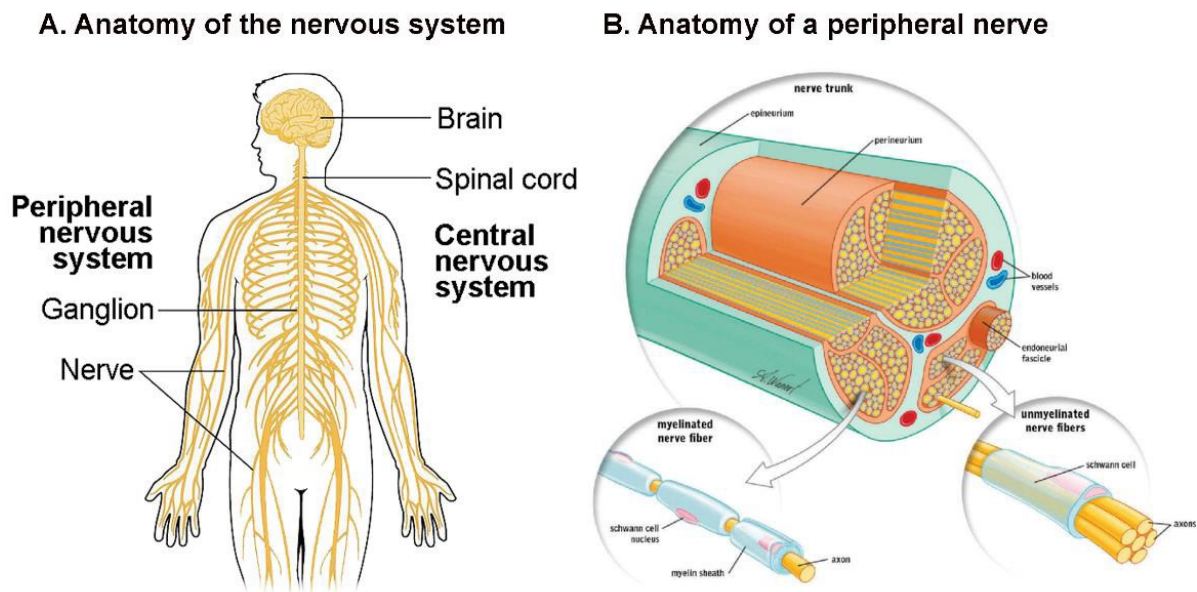


**Figure 1.** *Anatomy of the Central- and Peripheral nervous system*

This figure shows (A) the anatomy of central and peripheral nervous system and (B) a detailed anatomy of a peripheral nerve (From Kandel et al., 2003)<sup>1</sup>.

### 1.1.1.1 The Dorsal root ganglion system

One of the most established mammalian models to study the anatomical and molecular changes following axonal injury in rodents are the sciatic dorsal root ganglia. These ganglia, located lateral to the spinal cord<sup>1</sup>, contain the cell bodies of somatosensory pseudounipolar neurons which extend one regenerative competent branch into the sciatic nerve and one regeneration incompetent central branch in the spinal cord, the dorsal column and antero-lateral ascending pathways<sup>1</sup> (Fig. 2). This is an elegant system to study the dichotomy of the regenerative response between the two nervous systems by enabling the investigation of pro-regenerative mechanisms in the CNS and the PNS within the same cell soma. Indeed, it was found that a prior injury to the sciatic nerve enhances regeneration of the central branch in the dorsal column (conditioning lesion)<sup>40</sup> (Fig. 2). It demonstrated for the first time that, following injury, the signals that retrogradely propagate from the injury side to the soma in PNI, are not activated upon CNS injury. Additionally, it proved that PNI activates an intrinsic growth programme that enables axonal regeneration in both the peripheral and the central branch. This robust proregenerative signalling cascade relies on both axonal signalling and transcriptional mechanisms.

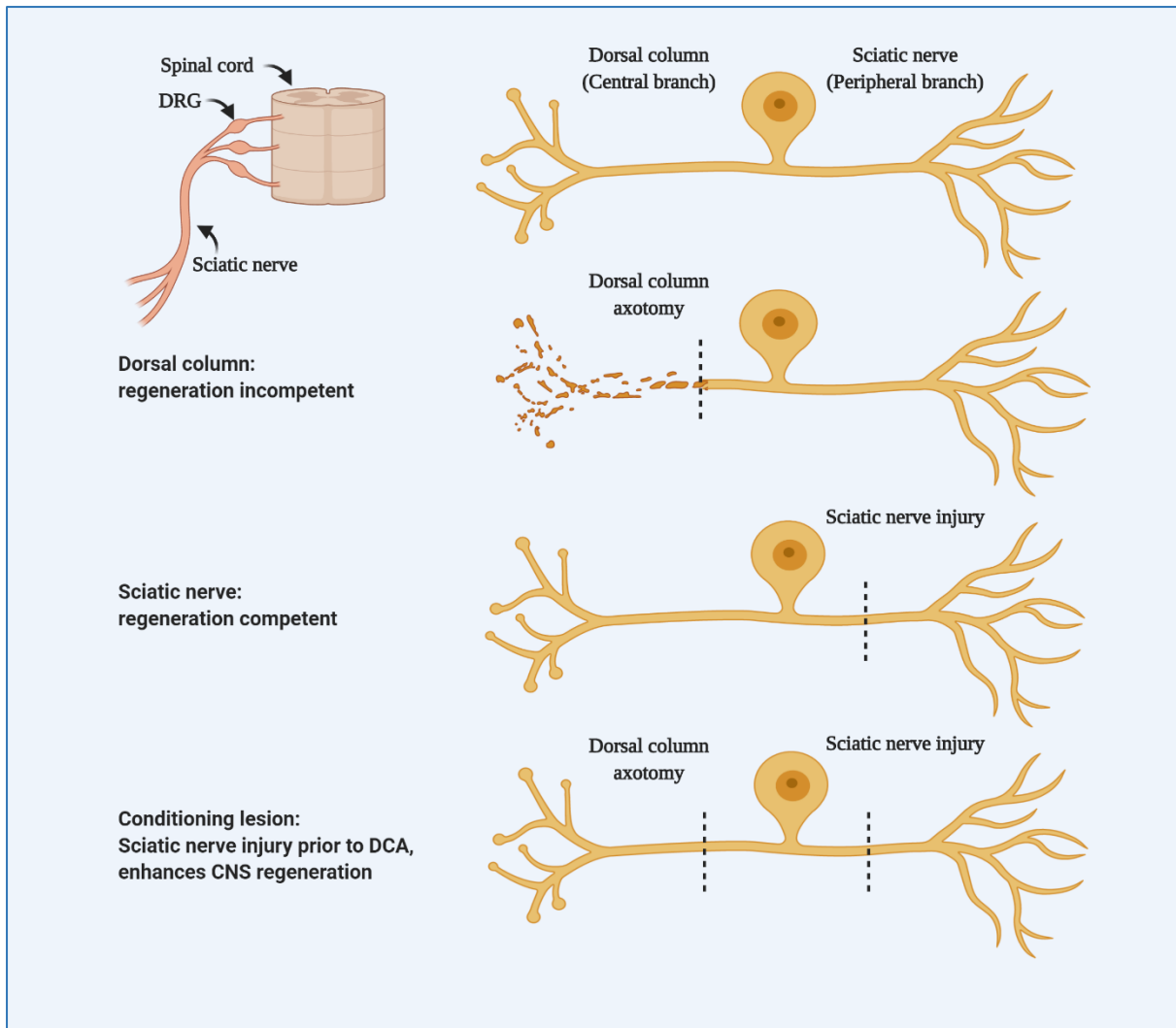


***Figure 2. The dorsal root ganglion system and the conditioning lesion***

*The dorsal root ganglion somatosensory neurons extend one regeneration incompetent central branch in the spinal cord, the dorsal column, and one regenerative competent branch into the sciatic nerve. Injury to the sciatic nerve prior to dorsal column axotomy enhances regeneration of the central branch (conditioning lesion).*

### **1.1.1.2 Wallerian degeneration and the role of extrinsic and intrinsic factors in sciatic nerve regeneration**

The term ‘Wallerian degeneration’ was first described by Augustus Waller in 1851. The first minutes after nerve injury are called the ‘Lag phase’ in which the distal nerve still propagates action potentials. This is followed by the fragmentation phase which is characterised by the breakdown of axons. While the proximal axon segment of invertebrate and mammalian nerves can form a growth cone and begin extending, the lesion site and distal nerve stump undergo Wallerian degeneration<sup>41,42</sup>. Following nerve transection in mice and rats, axons swell, form beads and disintegrate<sup>43</sup>, initiated by cytoskeleton degradation following calcium entry in the first wave of intracellular signalling<sup>44-46</sup>. Consequently, the blood-nerve barrier is strongly compromised<sup>47</sup> as membrane permeability peaks 4-7 days post injury, coinciding at the height of the acute inflammatory response<sup>48,49</sup>. Following axonal injury in vivo, the inflammatory environment contributes substantially to the neuronal response which will be discussed in greater detail in chapter 1.4.

Schwann cells are the first to respond following injury<sup>50,51</sup>. Within 48 hours Schwann cells cease myelin synthesis and upregulate regeneration associated genes (e.g Growth Associated Protein 43 [GAP43]), neurotrophic factors and neuregulin<sup>52</sup>, activating signalling between and within damaged neurons. Simultaneously, Schwann cells proliferate and migrate into the injury side, releasing cytokines and chemokines (e.g. tumour necrosis factor alpha (TNF $\alpha$ ), LIF, IL6, Interleukin 1 alpha [IL1 $\alpha$ ]). Trophic factors and cytokines/chemokines secreted by Schwann cells<sup>53,54</sup> and cell-cell communication between neurons and immune cells<sup>42,55,56</sup> provide pro-regenerative signalling to promote axonal growth. The extracellular matrix of the intact nerve consists of a Schwann cell generated basal lamina, required for ensheathment and myelination of axons. The main component of the basal lamina is Laminin, which has been shown to play an important role in neurite outgrowth in vitro and is highly upregulated by Schwann cells upon PNS injury<sup>57-59</sup>. Monoclonal antibodies against  $\alpha$ 2-Laminin reduced neurite outgrowth in vitro<sup>60</sup> and conditional knock-out of Laminin  $\gamma$ 1 severely impaired regeneration following sciatic nerve crush in vivo<sup>61</sup>. Conversely, overexpression of Laminin in DRG neurons promoted outgrowth even on inhibitory myelin substrate<sup>62</sup>. Although the direct mechanism through which Laminin promotes outgrowth, axon regeneration and guidance is not yet completely uncovered, Laminin binding to its receptor, Integrin, has been shown to activate the proregenerative PI3K-AKT signalling cascade<sup>63,64</sup>.

Conversely, DRG growth is largely inhibited by the presence of myelin-associated Glycoprotein (MAG) and Oligodendrocyte myelin glycoprotein (OMG). Both are expressed in the PNS, but

myelin debris is rapidly removed by infiltrating macrophages and Schwann cells following nerve injury<sup>65</sup>. Additionally, Schwann cells dedifferentiate and downregulate the expression of myelin proteins. The process of myelin removal in the PNS, which does not occur in the CNS, is an important factor contributing to the successful regeneration of the PNS. Interestingly, when the sciatic nerve is lesioned prior to DRG in-vitro culture, the neurons successfully initiate neurite growth on MAG or myelin<sup>66,67</sup>, indicating that intrinsic signalling can overcome the inhibitory effect of myelin-associated molecules.

Four days post injury, the formation of bands of Büngner by non-myelinating, proliferating Schwann cells provide supportive substrate and growth factors for injured axons<sup>68,69</sup>. Activated Schwann cells produce multiple neurotrophins<sup>70</sup> which are known to support neuronal survival during development<sup>71</sup>. Some neurotrophins, such as Brain derived neurotrophic factor (BDNF) and Neuronal growth factor (NGF), are upregulated in injured nerves and adjacent Schwann cells and have been found to support neuronal regeneration<sup>72-74</sup>. However, even though NGF, NT3 and BDNF induce axon growth in vitro<sup>75-77</sup>, exogenous Brain derived neurotrophic factors (BDNF) after acute or chronic SNI did not increase the number of successfully regenerated motor neurons, but rather led to neurotrophin induced axonal sprouting<sup>78,79</sup>. Schwann cells finally remyelinate newly regenerated axons<sup>52</sup> and neurotrophic factors have been found to critically modulate peripheral nerve myelination, with BDNF positively and NT3 negatively affecting axonal myelination by Schwann cells<sup>80</sup>. Glial cell line-derived neurotrophic factor (GDNF), is a trophic factor increased in the distal segment of the injured nerve and surrounding Schwann cells<sup>36-38</sup> and is believed to primarily act through stimulation of Schwann cell proliferation and migration resulting in enhanced myelination<sup>81,82</sup>. Similarly, Neuregulin-1 (NRG1), responsible for Schwann cell proliferation and survival during development, is increased following axotomy, as well as their receptors ErbB2 (erythroblastic oncogene B 2) and ErbB3 (erythroblastic oncogene B 3)<sup>83</sup>. However, determining if NRG-1/ErbB signalling induces Schwann cell myelination requires further clarification. While the extracellular environment has proven to be crucial for successful axonal regeneration, intracellular signalling to the cell soma, activated by the injury, initiates the intrinsic growth program. Immediately following injury, at the local proximal nerve stump site, calcium influx leads to the resealing of the cell membrane and activates proteases that accelerate reassembly of neurofilaments and microtubules<sup>44,45,84</sup>. A rapid calcium wave propagates from the lesion site towards the cell body as the first signal arriving at the cell soma following injury. Subsequently, the main phase of retrograde signalling involves retrograde transport of signalling molecules by motor proteins<sup>85,86</sup> and is primarily mediated by protein kinases triggering the activation of multiple signalling events<sup>87</sup>

During an early phase following injury, the calcium- dependent enzyme adenylyl cyclase activates a number of proteins at the injury site, including DLK<sup>88</sup> (Fig. 3a). DLK mediates the retrograde transport of injury signaling proteins, such as JUN N-terminal kinase (JNK) and JNK-interacting protein 3 (JIP3)<sup>89</sup>. Simultaneously, retrograde transport of the Importin-B/Vimentin/ERK complex allows for the translocation of the Histone-acetyl transferase PCAF to the nucleus<sup>25,90</sup>. The lesion-initiated calcium wave induces nuclear export of Histone deacetylase 5 (HDAC5), resulting in enhanced histone acetylation and gene expression<sup>91,92</sup> (Fig 3b). In response to peripheral injury, DRG neurons dramatically alter their gene expression pattern switching to a regenerative phenotype<sup>93</sup>, which is likely controlled by a number of chromatin regulators and transcription factors. Non-surprisingly, the subcellular localisation of histone modifiers and chromatin remodelers leads to formation of a more accessible and transcription permissive chromatin structure<sup>94,95</sup>, required for proregenerative transcriptional changes. For example, the CTCF chromatin remodeler has been found to be crucial for axonal regeneration in the PNS<sup>94</sup>. Additionally, STAT3 activation, induced following PNS, but not CNS injury, initiates its translocation to the nucleus where it acts as a transcription factor, leading to the expression of a number of proteins involved in regeneration, such as GAP43<sup>96</sup> (Fig. 3a,b). Other transcription factors are also upregulated in DRG cell bodies following peripheral nerve injury and have been linked to regeneration, with the most prominent and well-studied being 3',5'-cyclic adenosine monophosphate (cAMP) response element binding protein (CREB), Activating Transcription Factor 3 (ATF3), STAT3, SRY-Box Transcription Factor 11 (SOX11) and the early response proteins c-Jun and JunD<sup>97-101</sup>. Manipulation of these factors can improve neuronal regenerative potential in the CNS<sup>102-106</sup>. However, knock-out and overexpression studies revealed that discrete aspects of regeneration are likely controlled by separate transcription factors. For example STAT3 seems to be important in regulating the initiation but not continuation of axonal regeneration in both central and peripheral axons<sup>107</sup>. Together, injury induced retrograde transport and signalling activates a number of chromatin remodelers and transcription factors which further initiate the expression of proteins required for regeneration. In coherence with these events DRG neurons when downregulating synaptic proteins, such as voltage-gated calcium channels (VGCCs), switch from synaptic transmission to a state of repair and growth<sup>108</sup>. This has been suggested to recapitulate some of the developmental processes that occur during neurogenesis, switching the neuron from an active to and electrically silent, growth-competent state<sup>109</sup>.

However, a few molecules have been identified as endogenous inhibitors of axonal regeneration, with the most investigated one being phosphatase and tensin homologue (PTEN). A great number of studies has focused on this suppressor of the PI3K-AKT signalling pathway, which has been shown to increase regeneration when inhibited<sup>110</sup>. Even though PI3K-AKT signalling is

upregulated upon peripheral injury, PTEN is similarly expressed, partially inhibiting downstream signalling<sup>110</sup>.

In addition to the robust injury response in the peripheral nerve, the activation and retrograde transport of the before mentioned signalling molecules, its intrinsic growth capacity is largely influenced by the external environment. The signalling pathways and molecules mentioned here are grossly related in axonal regeneration and are tightly coordinated to ensure successful repair and growth. However, PNS axons regenerate within the basal lamina tubes and are likely guided to the correct targets via these tubes. Often, in severe nerve injuries axons fail to reach their targets and unguided sprouting may lead to the development of neuroma or chronic pain<sup>111</sup>.

Together, this chapter summarizes the multifactorial input required to achieve functionally successful axonal regeneration. Undoubtedly, a full understanding of the events following sciatic nerve injury will be necessary to tackle the incomplete regenerative capacity of the PNS. By studying extrinsic and intrinsic factors that promote or inhibit PNS axon regeneration, we may discover treatments to improve repair after spinal cord injury or brain injury.



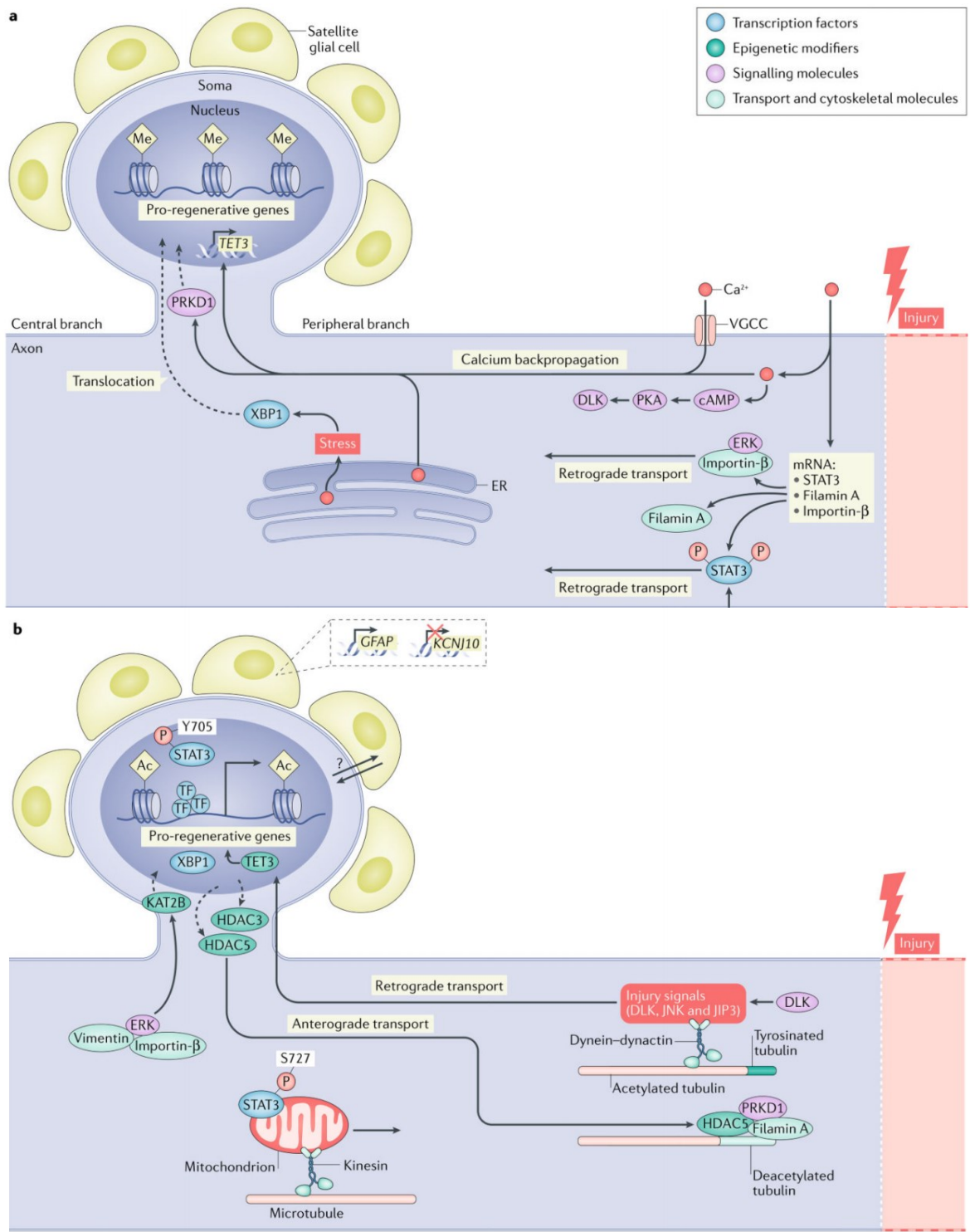


**Figure 3. Peripheral nerve injury induced signalling**

Schematics illustrating some of the early phase calcium- and cytokine dependent pathways (a) and late phase transport-dependent signalling (b) initiating epigenetic reprogramming and expression of regeneration-associated genes (RAGs). (From Mahar and Cavalli et al., 2018)<sup>93</sup>

### **1.1.2 Central nervous system injury**

The most common CNS injuries include traumatic brain injury (TBI) and Spinal cord injury (SCI). The spinal cord is the primary connection between the brain and peripheral nervous system, located between the medulla oblongata and the lumbar region of the vertebral column<sup>1</sup>. Therefore, a traumatic spinal cord injury often leads to permanent sensory, motor, autonomic and cognitive deficits<sup>112</sup>. In developed countries spinal cord injuries are predominantly contusions, with about 45 % of complete and 55 % incomplete SCI, and are primarily caused by traffic (40-50%), work (10-25%) and sports accidents (10-25%)<sup>113</sup>. More than 2.5 million people suffer a spinal cord injury yearly with 150 000 new cases per annum (<https://www.spinal-research.org/injury>). Disparate to the peripheral nervous system, the CNS is profoundly regeneration- incompetent and non-permissive for axonal growth. This has been found to be due to both intrinsic incapability and an inhibitory extrinsic environment.

#### **1.1.2.1 CNS regenerative failure – The role of extrinsic and intrinsic factors**

The unique and complex pathophysiology that occurs in and around the injury site contributes significantly to the regenerative failure following spinal cord injury. In the primary phase following injury leukocytes infiltrate the lesion site together with changes in calcium and potassium concentrations due to the disruption of the blood-brain barrier<sup>114</sup>. Over the following weeks and months, the injury site enters a second phase defined by progressive neurodegeneration and the development of a glial scar. The second phase is defined by inflammation, glial and neuronal apoptosis, axonal demyelination, glial apoptosis and reactive astrogliosis. Alongside this, there is an upregulation of inhibitory ECM proteins and activation of a robust immune response consisting of activation of microglia, macrophages and astrocytes. In this chapter I will briefly discuss the impact of the extracellular environment and the neuronal intrinsic capacity in the regenerative failure of the CNS. The CNS extracellular matrix consists of an interactive network of glycoproteins and proteoglycans, which can either promote cell migration and axon growth during development<sup>115</sup> or impair synaptogenesis, axonal regeneration and sprouting after injury<sup>116,117</sup>. As the CNS matures during development, oligodendrocytes form myelin sheaths around the axons containing proteins that might function as protection of aberrant sprouting in the adult CNS. The myelin consists of a number of growth inhibitory molecules, such as neurite outgrowth inhibitor A (NogoA), myelin-associated glycoprotein (MAG) and oligodendrocyte/myelin glycoprotein (OMgp), the ephrins B3 and A3 and Semaphorins 4D, 5A and 3F. The three major inhibitors NogoA, MAG and OMgp all bind to the same neuronal receptor, Nogo receptor 1 (NgR1), which mediates the inhibitory effect<sup>118-121</sup> via a number of coreceptors: p75 neurotrophin receptor (p75 (NTR)) or TROY and LINGO-1. Monoclonal antibodies against NogoA induced robust increase

in axonal growth in the spinal cord following injury as well as drastically improve sensory and motor function in both rats and primates<sup>122</sup>. Many signalling pathways are involved in myelin inhibitory signalling, such as the small GTPase signal transducer Rho in Nogo-A-induced inhibition or protein kinase C (PKC) and Epidermal growth factor receptor (EGFR) signalling, and have been targeted to antagonise myelin induced inhibition of regeneration. For example, inhibition of PKC was shown to stimulate injured dorsal column axons<sup>123</sup> and increased regeneration in the injured CST<sup>124</sup>. Another factor that significantly counteracts axonal regeneration in the CNS is the formation of the glial scar. The lesion site manifests a zone of intensive inflammation, rapidly infiltrated with inflammatory immune cells<sup>125</sup> that further activate local astrocytes and microglia. Reactive astrocyte hypertrophy results in the upregulation of intermediate filament proteins, such as glial fibrillary acidic protein (GFAP), vimentin and nestin<sup>126-128</sup>. Additionally, they contribute to the production extracellular matrix (ECM) molecules, such as Proteoglycans. Astrocytes produce Chondroitin sulfate proteoglycans (CSPGs) to limit structural plasticity and stabilize neuronal circuitry in the healthy spinal cord<sup>129-131</sup>, contributing to the dense ECM structure of the CNS, the perineuronal net<sup>132,133</sup>. After CNS injury, CSPG expression changes strongly in the lesion site and contributes to the inhibition of axon regrowth<sup>116,134,135</sup>, by sterically hindering growth-promoting adhesion molecules (laminin/integrins)<sup>136</sup>, but also via direct binding to receptors, such as Receptor protein tyrosine phosphatase  $\sigma$  (PTP), LAR, and Nogo receptors 1 and 3<sup>137-141</sup>. Deletion of PTP or LAR increased growth of sensory, corticospinal and serotonergic axons after spinal cord injury<sup>137,140,141</sup>. Both receptors share similar, but also distinct downstream targets, and deficiency of both receptors resulted in additive enhancement of axonal growth invitro<sup>142</sup>. Scar-forming reactive astrocytes form a barrier between the lesion center, a region of inflammation and fibrosis, and the spared tissue of the spinal cord. Consequently, axons cannot regenerate beyond the scar which forms a physical and biochemical barrier and thus form dystrophic endbulbs<sup>143</sup>. However, astrocytes seem to have an aiding function as attenuation of scar formation or chronic deletion reduced spontaneous as well as stimulated axonal growth into and past the lesion site<sup>144</sup>. Additionally, the intrinsic regenerative ability of neurons gradually declines during development. CNS neurons undergo a decrease in the expression of pro-growth genes and a corresponding increase in the expression of growth inhibitory genes during maturation and aging<sup>8</sup>. This has been linked to a decrease in chromatin accessibility at promoters and enhancers of proregenerative genes<sup>94</sup>. Accordingly, increasing chromatin accessibility<sup>90,94</sup> and upregulation of regeneration associated transcription factors<sup>94,145-147</sup> have been linked to increased neuroregeneration. Compared to the PNS, adult CNS axons possess a strongly reduced growth capacity and, thus, require effective therapeutic strategies to enhance CNS axon regeneration following injury.

Signalling pathways identified in the PNS can be manipulated to improve regenerative capacity in the CNS. For example the suppressor of cytokine signalling 3 (SOCS3) represses the gp130 dependent JAK-STAT pathway<sup>148</sup>. Accordingly, deletion of SOCS3 promotes robust axonal regeneration in the CNS<sup>149</sup>. Another well-studied pathway promoting CNS and PNS regeneration is the mTOR/PTEN signalling cascade<sup>110,150-152</sup>. PTEN is a phosphatase that converts PIP3 to PIP2, consequently counteracting PI3K. Therefore, PTEN deletion results in the accumulation of PIP3 and downstream AKT activation<sup>151</sup>. Downstream signalling of AKT activation leads to the activation of mTOR via Ras homolog enriched in brain (Rheb). PTEN deletion in cortical neurons promote CST axonal sprouting and regeneration of injured axons past the lesion site<sup>153,154</sup> forming active synaptic contacts distal to the injury site<sup>153</sup>. Conversely, inhibition of mTOR using rapamycin, attenuated the effect of PTEN deletion, indicating that the PTEN inhibitory effect on axonal regeneration is mTOR dependent<sup>151</sup>. Furthermore, deletion of other upstream inhibitors of the mTOR pathway, such as hamartin (TSC1) and tuberin (TSC2), also increased regeneration in both, the CNS and PNS<sup>151,155</sup>. Altogether these results show that mTOR/PTEN signalling is important in axon regeneration in the central and peripheral nervous system. Understanding regenerative competent mechanisms within the PNS may eventually elucidate effective treatments for CNS injury, facilitating axonal regeneration in a hostile environment.

### **1.1.3 Environmental changes and their potential impact on metabolic modulation of axonal regeneration**

As described in the previous chapters successful axonal regeneration requires a multitude of extracellular and intracellular factors. Doubtlessly, the transition of a neuron to a proregenerative state is metabolically demanding and requires the ability to cope with stress and energy demands. Environmental changes, such as the transition to an enriched environment (EE), dietary changes (ketogenic diet, caloric restriction (CR), intermittent fasting (IF)) and exercise have been shown to improve neuronal health in models of brain and spinal injury and neurodegeneration by increasing stress resistance, cell growth and plasticity primarily via systemic and cellular metabolic switching<sup>156</sup>. Increasing amounts of data generated using EE, exercise or IF/CR in mice found strong overlaps between the non-invasive systemic, and primarily metabolic, changes and proregenerative factors. These include neurotrophic factor signalling<sup>11</sup>, epigenetic changes<sup>157-159</sup>, metabolic modulation<sup>156</sup> and increased mitochondrial biogenesis<sup>160,161</sup>. This chapter introduces the most prevalent metabolic adaptations induced by systemic changes and their potential benefits for successful axonal regeneration.

The most explicit proregenerative signalling pathway, which is clearly susceptible to systemic metabolism, is insulin and insulin-like growth factor 1 (IGF-1) signalling. Both growth hormones mediate their effect via the PI3K-AKT-mTOR signalling pathway and have been shown to promote axonal regeneration in the CNS<sup>162-164</sup>. Insulin treatment following acute optic nerve transection in retinal ganglion cells significantly increased dendritic length<sup>162</sup>, indicating that insulin receptor signalling could promote axonal regeneration. However, impaired insulin sensitivity is a common health risk factor in individuals suffering spinal cord injury<sup>165,166</sup>, precluding insulin as treatment option. IF, CR and exercise, increase insulin sensitivity<sup>167</sup> and therefore its signalling efficiency and glucose uptake. IF, as well as CR, could provide a non-invasive treatment to restore insulin sensitivity in individuals with spinal cord injury. The insulin pleiotropic hormone IGF-1 provides a more promising treatment option. It significantly improved functional recovery of cortico spinal tract (CST) neurons following spinal cord hemisection<sup>163</sup>, as well as after spinal cord crush injury with neural stem cell graft<sup>164</sup>. Interestingly, IF, but not CR, has been shown to increase IGF-1 levels in the serum<sup>168</sup>.

While IF, CR and exercise improve glucose uptake efficiency via increased insulin sensitivity, they impose strict metabolic cellular changes which are believed to strongly contribute to their impact on neuronal health in injury and disease<sup>156</sup>. Healthy neurons transport mitochondria into the distal dendrites and axons for energy efficiency and to support local translation<sup>169</sup>. Following sciatic nerve injury in the mouse, mitochondrial anterograde transport increases by more than 80% supporting the elevated metabolic demand of the regenerating axon<sup>170</sup>. Enhanced axonal

mitochondrial transport via knock-out of the mitochondria-anchoring protein syntaphilin (SNPH) resulted in accelerated regeneration, suggesting dependency on local energy production at the injury site for successful regeneration<sup>161</sup>. Indeed, a conditioning lesion to the peripheral branch increases mitochondrial transport into the peripheral and central branch of the spinal cord<sup>171</sup>.

Ketogenic diet, intermittent fasting and exercise improve mitochondrial function in multiple tissues<sup>172-175</sup>, including the nervous system<sup>173,176</sup>. Evidence from studies in rodents has shown that intermittent fasting and exercise reduce mitochondrial oxidative stress and stimulate autophagy and mitophagy in order to remove dysfunctional mitochondria, but induce mitogenesis simultaneously in neurons<sup>176</sup>. This process of renewing mitochondria may play a significant role in the prevention of diseases associated with dysfunctional mitochondria, such as Alzheimer's and Parkinson's disease<sup>177</sup> and may have similarly beneficial effects in axonal regeneration. However, the fact that fasting and exercise ubiquitously increase cellular autophagy and mitophagy, a mechanism genuinely believed to antagonise regeneration, as the activation of mTOR significantly promotes axonal growth<sup>151,155</sup>, seems controversial with regard to regeneration. The mTOR pathway regulates protein synthesis in response to fluctuations in nutrient availability. During intermittent fasting or exercise, in a fed or rest state mTOR is activated and induces anabolic processes such as ribosome biogenesis, protein synthesis, cellular growth and the secretion of mitogenic factors required for healing and growth<sup>178</sup>. Conversely, during fasting and exercise mTOR activity decreases, activating autophagy and catabolic pathways. Intermittent fasting and exercise might be beneficial for neuronal regeneration, because both provide an 'intermittent' metabolic switch between anabolism and catabolism, resulting in activation of cell growth and mitochondrial biogenesis and simultaneously inducing molecular recycling and repair pathways<sup>156</sup>. Interestingly, a recent study found evidence of autophagy facilitated central nervous system regeneration by microtubule stabilization during growth via degradation of SCG-10, a microtubule disassembly protein in neurons<sup>179</sup>. Interestingly, EE<sup>180</sup> in addition to IF<sup>181</sup> was shown to alleviate pain in a model of peripheral nerve neuropathic pain. Madorsky et al., demonstrated IF increased the autophagy-lysosomal pathway in peripheral neurons of a mouse model of Charcot-Marie-Tooth disease, enhancing chaperone production and protein degradation. This led to decreased accumulation of the peripheral myelin protein 22 (PMP22) protein aggregate, typical for Charcot-Marie-Tooth type 1A (CMT1A) neuropathies<sup>181</sup>.

Furthermore, changes in cellular metabolism can influence epigenetics (histone/DNA methylation, histone acetylation) and therefore transcription<sup>182-184</sup>. Following PNS injury the neuron undergoes dramatic changes in gene expression and epigenetic marks, which are not observed after CNS injury<sup>94,185</sup>. Increased histone acetylation has been closely associated with the conditioning lesion and a pro-regenerative neuronal state, suggesting that a more 'open' chromatin supports

regenerative gene expression<sup>94</sup>. In line with this, enriched environment and exercise increase axonal regeneration in the CNS and PNS via Creb-binding protein (CBP)-mediated histone acetylation facilitating the expression of genes associated with the regenerative program<sup>157</sup>. Additionally, histone-acetylation is strongly interlinked with metabolism via glycolysis and the krebs-cycle, such as Acetyl-Coa, as well as the histone-deacetylase activity of ketones. It can be hypothesised that increased glucose uptake by DRG neurons following sciatic nerve injury might supply the elevated demand for acetylgroups via acetyl-coa synthesis. However, the direct impact of metabolic changes on epigenetic signatures and gene expression in axonal regeneration remains to be investigated. A study by Streijger et al., found that ketogenic diet treatment significantly improved functional recovery and reduced lesion volume following cervical spinal cord injury<sup>186</sup>, proving a first direct link between metabolism and axonal regeneration. While ketogenic diet has been found to increase histone acetylation<sup>187,188</sup>, Caloric restriction (CR) decreases it<sup>158,159</sup>. Not much is known about the extent of IF impacting histone acetylation, however in contrast to CR, IF increases ketogenesis resulting in elevated levels of ketone  $\beta$ -hydroxybutyrate in the serum<sup>168</sup>.  $\beta$ -hydroxybutyrate is a histone-deacetylase inhibitor and once entered the cell, can be metabolized to acetyl coenzyme A, which can either supply the Krebs cycle or provide the acetyl-group for protein acetylation<sup>189,190</sup>. While EE, exercise and ketogenic diet trigger proregenerative signalling in neurons to significantly increase axonal regeneration, mechanisms through with IF or CR might facilitate axonal growth remain to be investigated. The various similarities between intermittent fasting and proregenerative metabolic adaptations provide a promising foundation to study a potential proregenerative effect of IF.

## 1.2 Intermittent Fasting

### 1.2.1 General Introduction

Throughout evolution, from single cell organisms to the early stages of humanity and up to the beginning of industrialisation long periods of little or no food were considered normality. Highly conserved mechanisms allowed to compensate for the lack of energy supply in fasting periods. Mammals have developed physiological mechanisms, such as energy storage in adipose tissue and the liver, to overcome long periods of food deprivation. Interestingly, these mechanisms do not only enable survival, but signal to other tissues promoting metabolic and cognitive adaptation. Metabolic, endocrine and nervous system processes are designed to generate high physical and mental performance when in a fasted state<sup>156,191,192</sup>. Perhaps the first evidence that Intermittent fasting (IF) (also alternate day fasting: ADF) may induce systemic health benefits came from a study published in 1982, showing rats that had undergone life-long intermittent fasting lived almost twice as long as the control group<sup>193</sup>. When IF was induced at middle age, rats lived 30-40% longer than the control, which could be even further prolonged with exercise<sup>193</sup>. Since then, many studies have investigated the systemic and tissue specific effects of intermittent fasting and caloric restriction, as well as exercise (summarized in these reviews<sup>156,167,191,194-197</sup>). Caloric restriction describes a feeding regimen in which the daily food intake is reduced to 60-80%<sup>198</sup> or sometimes even 20-40%<sup>199</sup> of their normal Ad libitum food intake. IF is characterised by alternating periods of complete fasting<sup>168</sup> (or very low-calorie intake<sup>200,201</sup>) with ad libitum (AL) food. Most experimentally imposed IF patterns switch from 24 hours of fasting to 24 hours of AL food supply, with IF cycles lasting from days up to 6 months. An impressive amount of metabolic data has been accumulated comparing caloric restriction (CR) and IF. Both dietary regimens are highly comparable in changes of metabolic markers, such as systemic lipid, glucose and insulin levels, leading to multiple systemic and tissue specific changes ranging from decreased visceral fat and improved insulin sensitivity to increased learning and memory<sup>168,176,195,202</sup>. Both, CR and IF have been suggested to modulate the circadian clock through variable eating patterns, which may be partially responsible for increased longevity measurements across species in both<sup>193,203-211</sup>. However, while CR seems more successful in reducing body weight, intermittent fasting has been shown to have a stronger control on systemic glucose and insulin, a significant increase of ketone production and improved cell survival following injury compared to CR<sup>168</sup>. Other effects, such as body fat distribution and Adiponectin levels are similarly altered between both<sup>201</sup>. Conclusively, IF enables the body to undergo health- associated changes by modulating the metabolic rhythm (eating and sleeping patterns), without losing as much bodyweight<sup>168,194</sup>. These data in addition to the strong overlap between metabolic and epigenetic changes in cells undergoing IF and neurons with



high axonal regeneration capacity, described in the previous chapter, resulted in the prioritisation of IF over CR.

### **1.2.2 Intermittent fasting in health and disease**

Intermittent Fasting affects every organ and cell of the mammalian and non-mammalian body with systemic as well as molecular ramifications<sup>167</sup>. Increase of life span due to fasting or caloric restriction has been observed in single cell organisms like bacteria<sup>204</sup> and *S.cerevisiae*<sup>205</sup> as well as in *C.elegans*<sup>206,207</sup> and mammals<sup>193,208-210</sup>. The fact that fasting increases longevity in species going as far back in evolution as *E.coli*, indicates compensatory mechanisms starting at the single cell and increasing to the adaptive systemic changes observable in larger vertebrates. In mammals under fasting conditions, blood glucose reduction results in the depletion of liver glycogen and the mobilization of fatty acids through beta-oxidation and the subsequent production of ketones ( $\beta$ -hydroxybutyrate) in the liver<sup>168</sup>. Systemically, this leads to a general reduction of insulin levels<sup>201,212,213</sup> and systemic leptin<sup>214</sup>, an elevation of adiponectin as well as decreased systemic cholesterol, triglycerides and high-density lipoprotein (HDL)<sup>215,216</sup>. This metabolic switch from liver glucose to fatty acid and amino acid derived ketones leads to a greater efficiency of energy production, in which ketone metabolites function as signalling molecules, activating the expression of metabolic regulators, such as PGC1a (Peroxisome Proliferator-Activated Receptor Gamma Coactivator 1-Alpha) and NAD (nicotinamide adenine dinucleotide)<sup>217</sup>. However, other compensatory adaptations are activated upon IF. Conserved across taxa and found in most, if not all organs, IF increases the expression of proteins involved in antioxidant defence and protein quality control, increased mitochondrial biogenesis and autophagy<sup>218</sup>. Following ischemic brain injury, Arumugam et al. found an upregulation of neuroprotective proteins, such as basic fibroblast growth factor (bFGF) and BDNF, stress response proteins (Heat shock protein 70 [HSP70]) and antioxidant enzymes (Heme oxygenase-1 [HO-1]) in mice that had undergone 3-4 months of IF compared to AL<sup>219</sup>. In line with this, it was discovered that prophylactic IF attenuates the systemic and tissue specific inflammatory reaction to injury<sup>168,219-223</sup>. Intermittent fasting prior to intraperitoneal injections of Lipopolysaccharide, significantly decreased inflammatory cytokines systemically and in the brain and reduced cognitive impairment<sup>222</sup>. Concordantly, IF prior to an injection of the excitotoxin kainic acid (KA) to the hippocampus<sup>168</sup> or induction of ischemic stroke in rodents<sup>219,220,224</sup> showed increased neuronal survival and reduced inflammatory markers in the brain. In summary, IF is potentially creating a protective microenvironment resulting in a cell “prepared” against stress, acting as a preconditioning mechanism to enhance stress resistance and cell survival throughout many tissues of the body (Fig. 4). This indicates processes activated by intermittent fasting may have a protective function in metabolic and immune system-controlled

diseases. Metabolic diseases, such as diabetes or obesity, are affected by high blood sugars and insulin resistance<sup>225</sup>. Intermittent fasting has been found to prevent obesity induced by high fat diet in mice and ameliorates diabetes<sup>212</sup>. This seems to be due to its effects on increasing insulin receptor sensitivity (Fig. 4), leading to improved glucose uptake, specifically in high energy consuming cells, such as muscle, liver and neurons<sup>167,226</sup>. In humans, alternate days of 70% caloric restriction (a modified version of IF) has been found to reduce weight, body fat and blood cholesterol<sup>227</sup> (Fig.4). The reduction of cholesterol, LDL/HDL (low density lipoprotein/high density lipoprotein) levels, blood glucose and triglycerides<sup>201,212,228-230</sup> in addition to reduced systemic inflammation and oxidative stress, may be the reason IF also reduces the risk of cardiovascular disease in non-obese humans<sup>231-233</sup>. The concept that IF induces longevity has created the hypothesis that IF counteracts ageing processes. Neurodegenerative diseases are age-related and believed to be induced by impaired mitochondrial function, oxidative damage, impaired lysosome function and hyperexcitability<sup>192</sup>. Conversely, IF is known to increase neuronal stress resistance through multiple mechanisms, including strengthening of mitochondrial function and antioxidant defences, stimulation of autophagy and the production of neurotrophic factors, such as BDNF and Fibroblast Growth Factor 2 (FGF2)<sup>219,234,235</sup>. Indeed, in several animal models of neurodegeneration it has been shown that IF is able to counteract the disease process of Alzheimers (AD), Parkinsons and Huntingdon disease<sup>167,236-240</sup>. Transgenic mouse models of AD accumulate A $\beta$  or Tau and develop symptoms of learning and memory deficits during ageing. Intermittent fasting of these animal models successfully prevented cognitive impairment<sup>238,240,241</sup> and ameliorated A $\beta$  plaques<sup>237,241</sup>. Interestingly, a recent paper by Liu et al. found IF was able to reduce the hyperexcitability of hippocampal neurons in a mouse model of AD by enhancing GABAergic neuron activity through Sirtuin 3 (SIRT3) upregulation, revealing a new mechanism through which IF regulates synaptic adaptations<sup>241</sup>. The mechanisms safeguarding neurons from deteriorating diseases and injury, may likewise enhance neuronal function and plasticity in the healthy brain. Unsurprisingly, IF is shown to improve learning and memory as well as synaptic plasticity in the hippocampus of mice<sup>213,242-244</sup>. Additionally, comparable to exercise, IF increases neural stem cell proliferation and survival of newly born neurons, resulting in increased neurogenesis in the hippocampus<sup>245</sup> (Fig. 4). BDNF, which is increased in the brains of animals which have undergone IF<sup>213,219</sup>, has been shown to partially mediate the effects of exercise and IF on synaptic plasticity, neurogenesis and neuronal resistance to injury and disease<sup>246,247</sup>.

A study by Jeong et al. investigated IF vs AL induced functional recovery after a thoracic rat contusion spinal cord injury. The authors found improvement in several functional tests (BBB, grid walk, cat walk etc.) in both groups, when IF started prior to injury and continued thereafter, and when IF was started post-injury<sup>248</sup>. Another publication by the same group found increased

functional recovery in the cylinder and ladder test, as well as reduced lesion size, when IF was initiated post injury<sup>249</sup>. This shows that intermittent caloric restriction improves motor function after spinal cord injury.

In summary, IF modifies multiple signalling pathways that modulate synaptic plasticity and promote stress resistance, including in post-nervous system injury. However, whether IF delivers conditioning signals to prime neurons for axonal regeneration remains to be investigated.

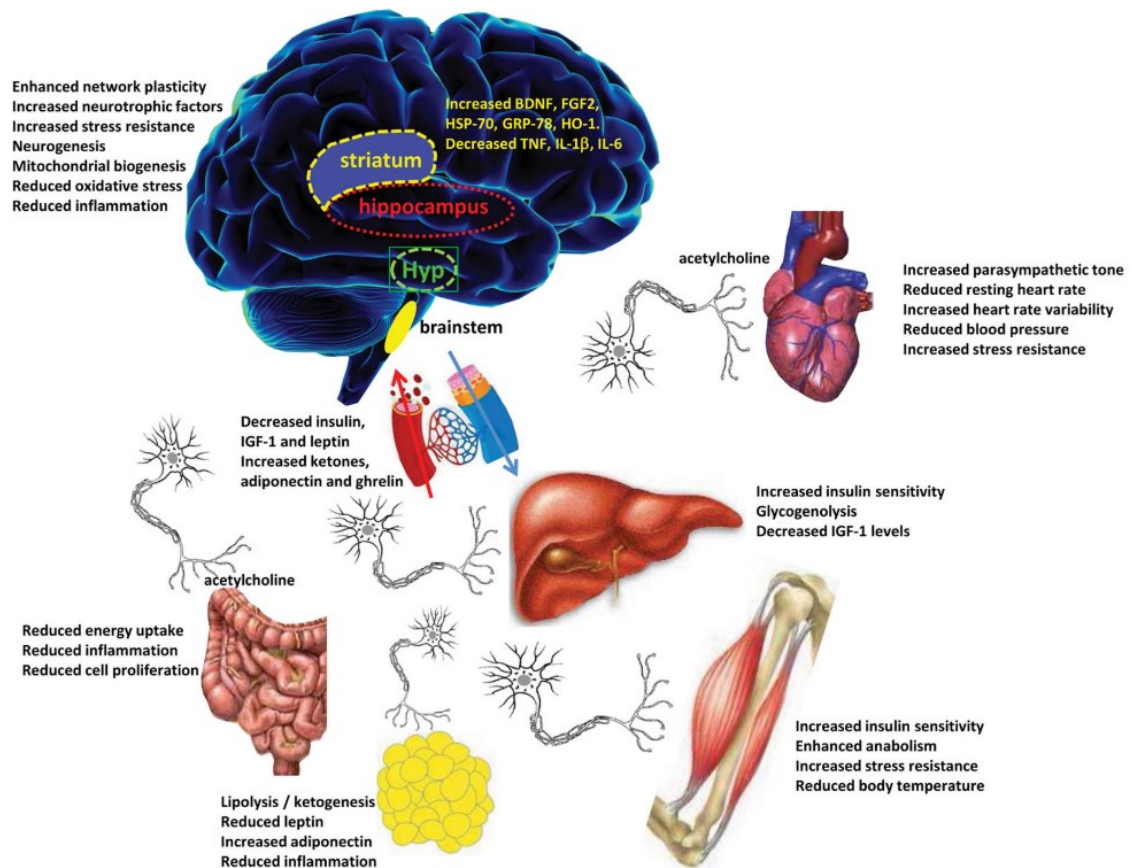


**Figure 4.** Adaptive physiological response of major organs to intermittent fasting

IF modifies brain neurochemistry and neuronal networks resulting in optimized brain function. Four brain regions have been identified to be important in adaptive responses in IF, which include hippocampus, striatum, hypothalamus and brain stem. Through these, IF is believed to reduce the resting heart rate and blood pressure. By depleting liver glycogen levels, fasting activates lipolysis and the synthesis of ketone bodies, which results in the reduction of body fat. IF enhances insulin sensitivity and reduces levels of systemic inflammation throughout the body and brain (From Longo et al., 2014)<sup>176</sup>.

## 1.3 The Gut microbiome

### 1.3.1 General introduction

The human gastrointestinal tract is colonised by a collection of bacteria, archaea and eukarya, which are collectively termed the “gut microbiome”. The number of bacteria cultivated in the mammalian gut ranges from  $10^{14}$  (10 times more than human cells<sup>250</sup>, to a value similar to the total human cell number, estimated at a 1:1 human: bacteria ratio<sup>251</sup>. Over thousands of years the co-evolution between the gut microbiota and its host has formed a mutually beneficial relationship<sup>250,252</sup>, affecting the hosts’ health through a range of physiological functions. These include the shaping of intestinal epithelium and supporting gut integrity<sup>253-256</sup>, facilitating energy harvest<sup>257</sup>, protection against pathogens<sup>258</sup> and regulation of host immunity<sup>255,259,260</sup> (Fig. 5). Intestinal nutrient sensing is mediated by the gut enteroendocrine cells which extend their apical processes to directly interact with the gut lumen (and microbiome) and primarily sensory fibres, from the vagus nerve and spinal DRG neurons<sup>261</sup> (Fig. 5). Enteroendocrine cells and sensory nerves mediate responses to changes in gut peptide secretion and nutrient content<sup>261</sup>. It has been found that specific bacterial species support the digestion and degradation of otherwise indigestible nutrients, such as the synthesis of short chain fatty acids (SCFAs) from polysaccharides<sup>262,263</sup> (Fig. 5). SCFAs and some other gut microbiome derived metabolites function as an energy source and signalling molecules, in many tissues and cell types of the body<sup>259,264-272</sup>. SCFAs signal through a number of G Protein-coupled receptors (GPRs) to regulate the immune response to injury, adapt metabolic reactions to high glucose/fat<sup>264,273</sup>, regulate neuronal activity<sup>271</sup> and influence neuronal, as well as global levels of histone acetylation<sup>265,274</sup>. Additionally, regulation of tryptophan uptake and further metabolization of tryptophan to various indole-metabolites, have been linked to hormone production (serotonin) and regulation of intestinal immunity<sup>259</sup> (Fig. 5). Interestingly, mice fed with a low-tryptophan diet are more susceptible to experimentally induced inflammation<sup>275</sup>. Conversely, tryptophan treatment improved gut motility and decreased intestinal inflammation in mice with dextran sodium sulfate-induced colitis<sup>276</sup>. Several tryptophan derived microbial metabolites have been associated with changes in immune reactivity, including Indole-3-acetic acid<sup>277</sup>, indole-3-propionic acid<sup>256</sup> and indole-3-aldehyde<sup>278</sup>. Venkatesh et al., showed that indole-3-propionic acid signalling to its receptor PXR in gut epithelial cells, restored gut integrity following TLR4 ligand induced intestinal inflammation<sup>256</sup>. Collectively, one can conclude the gut microbiome significantly influences the host physiology, immunity, epigenetic signatures and even the brain.

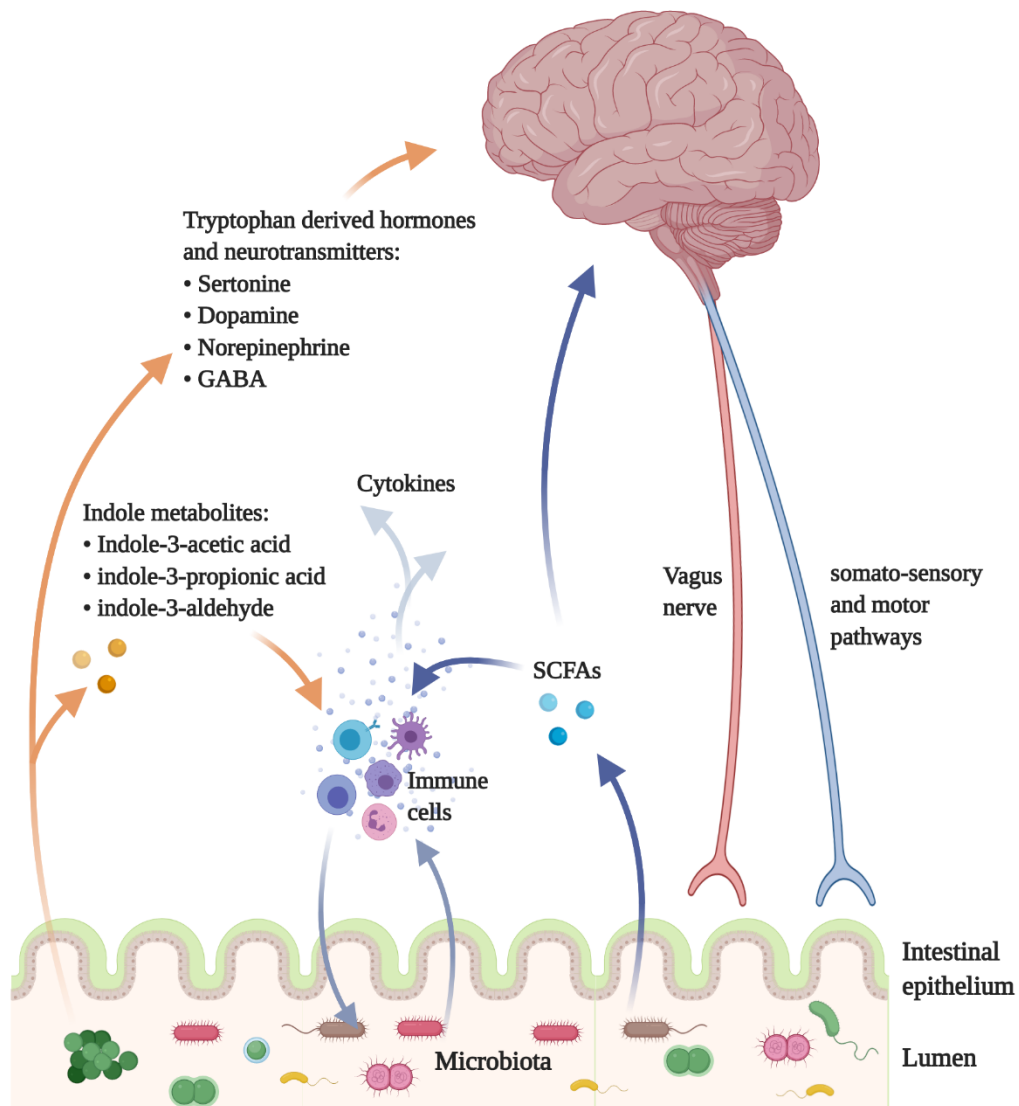


**Figure 5.** Multifactorial communication of the gut microbiome with the body, specifically the brain. Bidirectional routes of communication between the brain and the gut microbiota, including vagus nerve, spinal pathways, the immune system, tryptophan uptake and metabolism to indole metabolites and the production of short chain fatty acids (SCFA).

### **1.3.2 The Gut microbiome and the nervous system**

Many hormones and metabolites secreted by the microbiota and enterochromaffin cells intersect with biochemical pathways which influence the CNS. These can be summarized into three communication formats: neuronal (vagal afferents, DRG sensory fibres), endocrine messages (gut hormones) and immune regulation (cytokines)<sup>279,280</sup> (Figure 5). Together they create the Microbiote-Gut-Brain-axis, a bidirectional neuroendocrine system<sup>281</sup>. Interestingly, changes in gut microbiome composition have been indirectly associated with a number of neuronal diseases and psychiatric disorders (Figure 6). Experiments which transplanted microbiota from depressed patients into mice or rats, observed that the depression behavioural phenotype was also transferred to the animals<sup>282,283</sup>. Similar results were found from the transplantation of microbiota from patients with irritable bowel syndrome with anxiety to germ-free mice, inducing gastrointestinal symptoms and anxiety-related behaviour<sup>284</sup>. In contrary, transplantation of the bacterial strain *B. infantis* was able to reverse the aberrant stress response of germ-free mice, demonstrating that the microbial presence in the gut is critical to the development of an appropriate stress response and a normal development of the HPA axis<sup>285</sup>. Moreover, similarly designed experiments demonstrated a link between symptoms of neurodegenerative diseases and gut microbiome composition. Patients suffering neurodegenerative diseases not only appeared to own an altered microbiome compared to healthy controls<sup>286-288</sup>, but transfer of their microbiota to germ-depleted mice, conveyed disease symptoms<sup>289,290</sup>. The colonisation of  $\alpha$ Synuclein-overexpressing mice with microbiota from Parkinsons disease affected patients enhanced the physical impairments compared to control microbiota from healthy human donors<sup>289</sup>. Likewise, in models of Alzheimers disease, probiotic treatment was able to attenuate age related deficits and improved memory in rats<sup>291</sup>. Additionally, central nervous system injuries, such as brain ischemia and spinal cord injury have been shown to trigger formation of gut dysbiosis, leading to gut leakage and increased inflammation<sup>292-294</sup>. This is believed to be directly associated with an altered gut microbiome<sup>293</sup>. A study by Kigerl et al., concluded SCI induces gut dysbiosis associated with changes in microbiome composition, which is worsened by antibiotic treatment. Conversely, probiotic treatment following spinal cord injury improved locomotor recovery, inducing a protective immunological response to injury<sup>294</sup>. These results indicate communication between the gut microbiome and the nervous system, which evidently influence physiology and activity bidirectionally (Fig. 6).

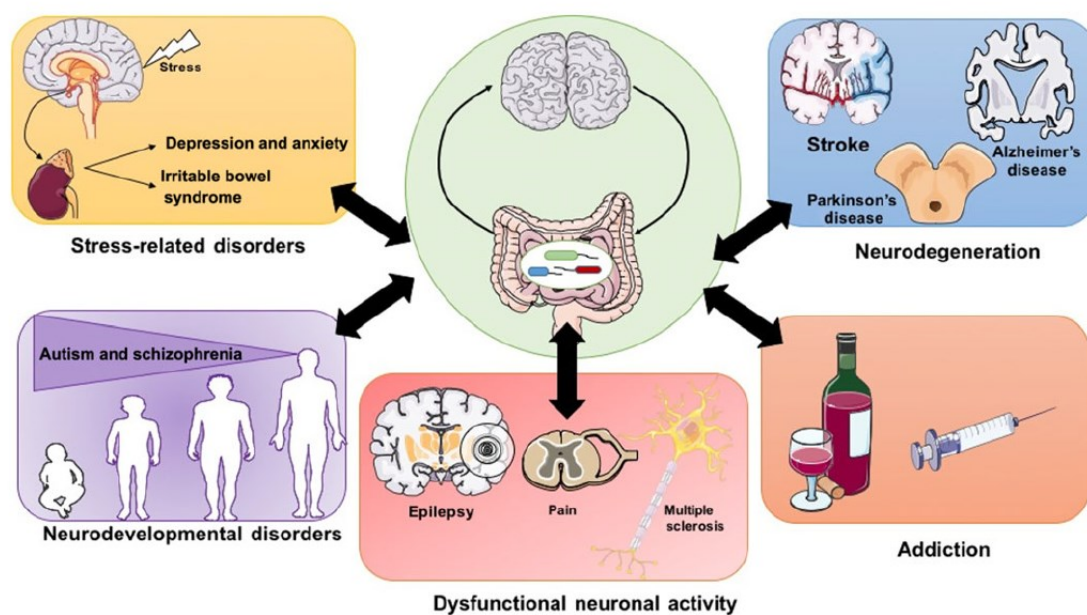


**Figure 6.** *Overview of the gut-microbiota-brain axis in neurology and psychiatry*

*Microbiome-gut-brain axis is involved in a number of neurological and psychiatric conditions. These include depression, addiction, stroke, epilepsy and Parkinsons disease (From Sherwin et al., 2017)<sup>295</sup>.*

### **1.3.3 The Gut microbiome – response to dietary interventions**

Those studying the gut microbiome primarily focus on the bacterial composition of certain phyla and bacterial classes, with occasional identification of single bacterial species. The majority of microbiota are composed of two main bacterial phyla, the Firmicutes (51%) and Bacteroidetes (~48%), with the remaining 1% distributed between Proteobacteria, Actinobacteria, Fusobacteria, Spirochaetes, Verrucomicrobiota and Lentisphaerae<sup>296</sup>. Bacterial abundance and composition in the human digestive system are strongly dependent on content, volume and frequency of nutrient intake<sup>297-300</sup>. Different dietary regimens are able to modify the composition and diversity of the gut microbiome in human and mice<sup>264,300-304</sup>. Interestingly, several publications concluded a high fat diet reduces bacterial diversity in the gut, favouring bacterial phyla/strains associated with obesity<sup>305,306</sup>. Conversely, caloric restriction and intermittent fasting have been shown to increase bacterial diversity<sup>213,264,302</sup>. Unsurprisingly, 30 days of IF in mice was sufficient to reverse induced obesity, by converting white adipose tissue to brown via changes in the gut microbiome<sup>264</sup>). Furthermore, recent work by Cignarella et al., showed that for the first time changes in the gut microbiome, induced by IF, were able to ameliorate the pathological symptoms in a mouse model of Multiple sclerosis, Experimental autoimmune encephalomyelitis (EAE)<sup>302</sup>. Similar results were

found in a diabetes mouse model showing significant recovery of cognitive impairment mediated by increase in gut microbiome derived metabolites following 30 days of IF<sup>213</sup>.

Research collated over the past 20 years can conclude IF and caloric restriction are associated with an increased Firmicutes to Bacteroidetes ratio<sup>213,264,307</sup> and an overall increase in bacterial diversity in the gut<sup>301,302</sup>. Currently, disease and injury related studies primarily show a very narrow and indistinct picture of the vast effect the gut microbiome has on the human body. In order to better understand the systemic impact of single bacterial species in health and disease, further investigation into the functional mechanism by which they influence development, disease onset, aggravation and improvement, is required.



## **1.4 Immune response to nervous system injury**

### **1.4.1 General introduction**

Injury to the nervous system initiates a cascade of events which activate immune and non-immune cells, found to facilitate or inhibit the success of wound healing and axonal regeneration. Interestingly, in the peripheral nervous system these events are predominantly neuroprotective and pro-regenerative, enabling time- limited successful regeneration in mild to moderate injuries. However, in the central nervous system the events following injury are not adapted to prevent further damage or facilitate axonal regeneration. For example, while inhibitory myelin and axonal debris is rapidly cleared in the PNS within weeks, the same process may take several months in the CNS. This chapter will introduce the differing immune responses following sciatic nerve (PNS) and spinal cord (CNS) injury.

### **1.4.2 Peripheral nervous system injury – Immune response in the sciatic nerve**

Transection or crush injury to the sciatic nerve results in axonal break down of the distal stump of the injured nerve, known as Wallerian degeneration<sup>41</sup>. Myelin collapses and Schwann cells dedifferentiate around the injury site, start proliferating and downregulate myelin protein synthesis. Endoneurial, resident, immune cells as well as recruited leukocytes and lymphocytes play a crucial role in the process of rapid and efficient myelin debris clearance and initiation and resolution of the inflammatory response. The mechanical injury damages the nerve exposing axonal and myelin epitopes, which further activate the classical and alternative pathways of the complement system. This is the initial response to prevent infection and eliminate microbes. The products C3 and C5 opsonize myelin and membrane debris which is crucially required for phagocytosis by immune cells, primarily macrophages (Fig. 7). Experiments using C3-deficient serum in co-cultures showed that macrophages were unable to invade degenerating nerves<sup>308</sup>. In vivo C3 depletion in rats, using intravenous administration of cobra venom factor (CVF), reduced macrophage recruitment to the injured nerve<sup>309</sup>. Similar results were found using mice which are deficient of complement component C5, resulting in inefficient myelin clearance by Schwann cells<sup>310</sup>.

The intact peripheral nerve consists of stable mast cells, ensheathing Schwann cells and resident macrophages. Resident mast cells<sup>311,312</sup> are the first responders of inflammation and release mediators such as histamine, serotonin, proteases, prostaglandins and a number of pro- and anti-inflammatory cytokines<sup>311</sup>. Mast cells closely interact with nerve endings throughout the body, communicating external inflammatory signals<sup>313</sup> and have been shown to play a crucial role in

wound healing<sup>314</sup>. No specifics are known about the role of mast cells in peripheral nerve injury, with the exception that they produce factors capable of neutrophil recruitment<sup>315-317</sup> which peak in and around the injury site about 24 hours following PNI<sup>318</sup> (Fig. 7). Neutrophils are recruited by chemoattractants such as NGFb, CXCL1, Monocyte chemoattractant protein-1 (MCP-1) and Leukotrine B4<sup>319,320</sup> and have been demonstrated to be the first inflammatory leukocytes to invade the injured tissue<sup>318</sup>. Neutrophils contribute to the inflammatory response via the release of superoxides and other reactive oxygen species<sup>321</sup> and have been linked to increased nociceptor activation and allodynia<sup>322,323</sup>. However, their primary function in phagocytosis seems to play a crucial role in successful myelin clearance following sciatic nerve injury<sup>324</sup>. Work by Lindborg et al. showed that neutrophils effectively cleared the myelin in mice with C-C chemokine receptor type 2 positive (CCR2+) macrophage deletion. Conversely, neutrophil depletion impaired myelin clearance in WT and CCR2<sup>-/-</sup> mice<sup>324</sup>. Additionally, besides their primary function in proteolysis and phagocytosis at the injury site, neutrophils appear to modulate the recruitment and activation of other leukocytes following tissue injury<sup>321</sup>. Neutrophils release mediators chemotactic for macrophages such as macrophage inflammatory protein-1 $\alpha$  and -1 $\beta$  (MIP-1 $\alpha$  and MIP-1 $\beta$ ), IL-1 $\beta$  and defensins<sup>325-327</sup>, which would explain the decreased number of macrophages following neutrophil depletion<sup>324</sup>. This suggests that besides their reputation as non-specific inflammatory leukocytes<sup>321</sup>, they may play a crucial role in successful tissue clearance and axonal regeneration following injury. Furthermore, within 5 hours following nerve transection in mice, Schwann cells become activated and release pro-inflammatory cytokines TNF $\alpha$  and IL1 $\alpha$  with a slightly delayed synthesis of IL1 $\beta$ <sup>328</sup>. These initiate the expression of Interleukin 6 (IL6) in fibroblasts and Schwann cells<sup>329</sup> which activate the synthesis of RAGs in neurons, facilitating neurite growth<sup>330,331</sup>. Interestingly, IL6 is crucial for the induction of conditioning injury signalling<sup>330</sup>, underlining the importance of neurotrophic cytokine signalling following nervous system injury. Additionally, this cytokine cascade induces the production of MCP-1, Macrophage Inflammatory Protein 1alpha (MIP1a) and Leukemia inhibitory factor (LIF) in Schwann cells, neutrophils and macrophages, which are responsible for the recruitment and transmigration of bone marrow monocytes, starting at 24 hours (likely dependent on neutrophil derived chemokines) and peaking around 2-3 days post injury<sup>332,333</sup> (Fig. 7). Cytokines, released by infiltrating immune cells and activated Schwann cells, such as LIF and IL6, are well established factors of regeneration<sup>330,334,335</sup>, activating the Janus kinase/signal transducers and activators of transcription (JAK-STAT) signalling pathway<sup>336,337</sup>, resulting in STAT3 phosphorylation. Knock-out of either of the two cytokines significantly impairs conditioning injury induced spinal axon regeneration<sup>330,334</sup>. Monocytes transdifferentiate into phagocytosing macrophages when recruited into injured tissue which in nerve injury assists the resident macrophages. Both, Schwann cells and macrophages, phagocytose the remaining cellular

and myelin debris created by the injury, which act as barriers to re-growing axons (debris contains proteins inhibitory to axonal growth: Myelin associated glycoprotein [MAG], oligodendrocyte myelin glycoprotein [OMgp]) and is a crucial step of Wallerian degeneration as it eventually enables axon regrowth. Innate inflammatory mediators are crucially involved in successful myelin debris clearance. Complement system C3 deposition, was found in the sciatic nerve as little as 6 hours following peripheral nerve lesion (PNI)<sup>338</sup> and C3 opsinisation of myelin debris increases myelin phagocytosis by macrophages by two folds<sup>339</sup>. Additionally, inflammatory cytokines released by macrophages and Schwann cells, specifically tumour necrosis factor- $\alpha$  (TNF $\alpha$ ), Interleukin-1 $\alpha$  (IL1 $\alpha$ ), and Interleukin-1 $\beta$  (IL-1 $\beta$ ), augmented myelin phagocytosis by macrophages<sup>328</sup>. Unsurprisingly, depletion of CD11b positive macrophages 12 hours before a sciatic nerve crush, resulted in reduced debris clearance, loss of neurotrophin synthesis, decreased axon regeneration and slower functional recovery<sup>340</sup>. Although, pro-inflammatory M1-like and anti-inflammatory M2-like macrophages seem to be present simultaneously in and around the injury site<sup>341</sup>, throughout the process of myelin phagocytosis the expression of anti-inflammatory cytokines increases, indicating a transition to a more inflammation resolving/pro-repair state. Specifically, increasing levels of macrophage secreted IL10, between day 7 and 14 post injury, gradually downregulates the production of inflammatory cytokines<sup>42</sup>. Additionally, Sequeira Mietto et al. showed that lack of Il-10 induces a more pro-inflammatory environment, marked by an increased influx and prolonged retention of macrophages after sciatic nerve crush, resulting in reduced axonal regeneration and impaired functional recovery<sup>342</sup>. Importantly, macrophage activation after nerve injury turned out to be crucial for the conditioning lesion dependent increase in regenerative capacity in the CNS<sup>343,344</sup> and PNS<sup>345</sup>. Kwon et al. demonstrated that macrophages engage in direct cell-cell contact via CCL2 release by DRG neurons in the dorsal root ganglion<sup>343</sup>. Another study by Hervera et al., found that macrophage released exosomes are retrogradely transported to the neuronal cell soma, promoting axonal regeneration of the sciatic nerve via NOX2 mediated PTEN-oxidization<sup>55</sup>. These studies show that, in addition to their contribution to the degeneration of the distal stump, macrophages stimulate regeneration of the proximal axons of DRG neurons via direct macrophage-neuron interaction. Other immune cells have been shown to infiltrate the dorsal root ganglion, including neutrophils which seem to accumulate in the meninges and perineural membranes following axotomy<sup>346</sup> and may be responsible for further immune cell recruitment.

The adaptive immune response at the injury site after peripheral nerve injury is primarily mediated by T lymphocyte infiltration starting at 3 days and peaking at 21 days in sciatic nerve chronic constriction lesion (CCL) injury, a model of neuropathic pain<sup>347</sup> (Fig. 7). T lymphocyte function largely depends on their distinctive cytokine profiles. Th1 (Type 1 helper) T cells produce

predominantly pro-inflammatory cytokines such as interferon-g (IFN $\gamma$ ), IL-2 and TNF $\alpha$  that activate macrophages, neutrophils and natural killer cells. Th2 (Type 2 helper) T cells secrete anti-inflammatory cytokines, IL-4, IL-5, IL-10 and IL-13, which suppress the production of pro-inflammatory cytokines and are required for balancing the initial immune response. Type 1 and type 2 helper T-cells (Th1 and Th2 cells) are the last immune cells to arrive and while their function in axonal regeneration remains largely unknown, it has been suggested that Th1 cytokines may be central to the pain sensitivity in neuropathic pain, whilst Th2-derived cytokines maybe protective<sup>347</sup>. Further work is required to elucidate the mechanisms in which innate and adaptive immune cells signal to neurons directly at the site of transection, as well as far from the primary injury at the site of the cell body (Fig. 7).

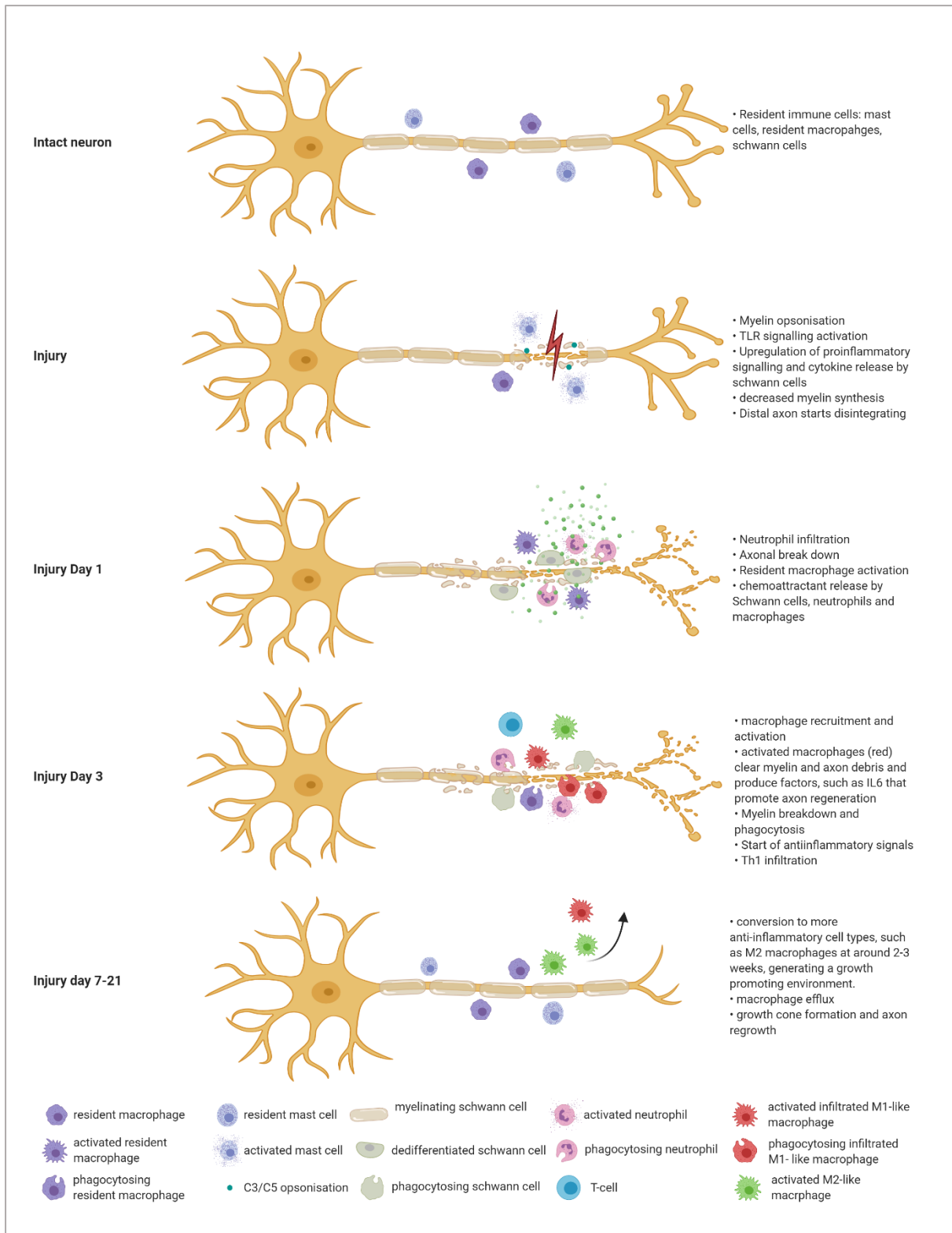


**Figure 7. Immune response and related events after peripheral nerve injury**

Shown is a peripheral neuron, consisting of axon, Schwann cells (grey) and resident macrophages and mast cells (purple). **Injury – Day 1.** Myelinating and non-myelinating Schwann cells cease myelin synthesis and produce cytokines/trophic factors. Distal axon disintegrates in the fragmentation phase. Schwann cells and the injured axon produce factors that activate resident

*macrophages. Neutrophils arrive and phagocytose myelin and axon debris Day 3-7. Schwann cells produce soluble factors that recruit monocytes/macrophages from the blood. The activated macrophages (red) clear myelin and axon debris and produce factors, such as IL6 that promote axon regeneration. Th1 cells infiltrate and contribute to the immune environment Day 7 - >21 Pro-inflammatory cytokines that dominate the lesion site promote the conversion to more anti-inflammatory state at around 2-3 weeks, generating a growth promoting environment. Injured axons form a growth cone and begin to regenerate along Bands of Büngner formed by Schwann cells. If the axon is able to transverse the injury site, it can reconnect with its peripheral targets.*

### **1.4.3 Central nervous system injury – Immune response in the spinal cord**

Immune cascades following a central injury are significantly divergent to those after a peripheral injury. Injury to the spinal cord instigates an acute inflammatory response from resident immune cells and microglia, followed by infiltration of peripheral immune cells, such as Neutrophils, mast cells, monocytes/macrophages and eventually T-cells<sup>125</sup> (Figure 8). Resident microglia are the first immune cells to respond, activated by the disruption of the neurovascular unit and the resulting release of damage-associated molecular patterns, they migrate toward the lesion site where they participate in glial scar formation<sup>348,349</sup>. The CNS, normally isolated from the peripheral immune system, experiences a blood- spinal cord barrier damage, enabling peripheral immune cells to infiltrate the lesion site. In rodents, starting at 2 hours and peaking at twenty-four-hours post injury, neutrophils are the first to arrive from the periphery, responding to CNS derived chemoattractants<sup>350,351</sup>. Neutrophils traditionally phagocytose debris, secrete proteases and release reactive oxygen species (ROS)<sup>352</sup>. Following spinal cord injury, neutrophils are responsible for early activation of astrocytes and recruitment of macrophages, via the release of Reduced nicotinamide adenine dinucleotide phosphate (NADPH) oxidase, Transforming growth factor alpha (TGF $\alpha$ ), ROS, Interleukin 1 (IL1) and IL6 production<sup>143</sup>. Despite their destructive reputation, neutrophils contribute to the early events of tissue healing and immune cell regulation following spinal cord injury. Mice treated with anti-Ly6G/Gr-1 (Lymphocyte antigen 6 complex locus G6D/gamma response 1) showed reduced early astrogliosis resulting in a lower neurological recovery and increased lesion size<sup>353</sup>. Surprisingly, a study by de Castro et al., found that neutrophils also prevent the accumulation of destructive ROS at the lesion site<sup>354</sup>. Monocytes and macrophages from the blood infiltrate the injury site around 3 days post- injury, reaching its first peak at 7 days post-injury<sup>350</sup>. Macrophages include a wide array of phenotypes, which are primarily determined by environmental cues, such as specific cytokines, that influence the macrophage polarization state of which the “classically activated” proinflammatory M1-type and the “alternatively activated” anti-inflammatory M2-type describe the two extremes of the spectrum<sup>355</sup>.

The capacity to switch from one phenotype to another is regulated by factors in the inflammatory microenvironment following injury<sup>355</sup>. While both types are present following SCI, proinflammatory M1-like macrophages, associated with secondary tissue damage, neuronal loss, axon retraction and demyelination, appear to dominate the lesion site<sup>356</sup>, with anti-inflammatory macrophages M2-like macrophages found reduced or completely eliminated after only one week post injury<sup>357</sup>. Interestingly, while macrophages and Schwann cells in the PNS are primarily responsible for myelin debris clearance after nerve injury, this is not the case for the CNS<sup>358</sup>. Here, oligodendrocytes and macrophages fail to remove the growth-inhibiting myelin debris left behind at the lesion site, but instead contribute to further demyelination of injured axons<sup>358</sup>. Additionally, macrophages release reactive oxygen species (ROS) and NO, as well as proinflammatory cytokines such as TNF $\alpha$ , IL1b, but also LIF and IL6, contributing to tissue damage and promoting astrocytic differentiation of progenitor cells. Reactive astrocytes and chondroitinase proteoglycans (CSPGs) form a stabilizing but impenetrable barrier; the astroglial scar. Additionally, astrocyte proliferation can directly repair the BBB<sup>359</sup> and prevent propagation of the inflammatory immune response<sup>360</sup>. The presence of Th2 T-cells, which express anti-inflammatory cytokines, such as Interleukin 4 (IL4), Interleukin 13 (IL13) and IL10 can activate the conversion of pro-inflammatory to anti-inflammatory macrophages<sup>355</sup>. IL10 expressing macrophages promote axon growth in vitro, even on inhibitory substrates<sup>356</sup> and seem to remodel the glial scar into a more permissive environment for axonal regeneration<sup>361</sup>. Furthermore, they have been shown to enhance remyelination via activation of oligodendrocytes<sup>362</sup>. The transient conversion of pro-inflammatory macrophages to a more anti-inflammatory profile, that can be observed in normal wound healing, does not take place in SCI, largely due to the accumulation of unphagocytosed myelin and accumulation of apoptotic neutrophils<sup>357</sup>. This largely contributes to the chronic inflammation characteristic of spinal injury pathology<sup>363</sup>. Therefore, one could conclude a generally detrimental effect of macrophages in spinal cord injury healing and regeneration. Work by Zhu et al., showed reduced scar tissue and increased axonal regeneration following macrophage depletion in SCI<sup>364</sup>. However, one study using macrophage/monocyte depletion demonstrated poorer neurological outcomes and wound healing following macrophage depletion<sup>365</sup>, indicating a more complex function for macrophages in SCI.

The role for the adaptive immune system in axonal regeneration following spinal cord injury is still not fully understood. Little is known about the function of CD4+ or CD8+ effector T-cells (Teff) or natural killer (NK) cells in spinal cord injury. Antigen presenting cells, such as microglia, macrophages and dendritic cells promote the recruitment and activation of helper T-cells, which can be anti-inflammatory (Th2 cells) or Pro-inflammatory (Th1 cells), and regulatory T-cells (Tregs). T-cell infiltration occurs at 3-7 dpi in rats and 7-14 days in mice, with twice as many CD4 Teffs present than CD8 Teffs<sup>356</sup>. Non-surprisingly, CD4-, CD8- Teffs and regulatory T-cells likely

participate in both, injury and recovery, processes<sup>366-369</sup>, underlining a required balance between inflammation and repair. A recent paper by Walsh et al., revealed the controversial role of Tregs in optic nerve injury. It was found that depletion of Tregs exacerbated neurodegeneration, resulting in an exaggerated response of effector T-cells. Interestingly, exogenous transfer of T-regs, inhibited effector T-cells and their beneficial effects on spinal cord injury. Additionally, both resulted in the reduction of alternatively activated M2-like macrophages<sup>370</sup>. Tregs suppress the proliferation of CD4 effector T-cells (Teff) via the expression of the signalling molecules Interleukin-10 (IL-10) and transforming growth factor (TGF)- $\beta$ <sup>371</sup>. Early experiments using low-dose irradiation<sup>372</sup> or thymectomy<sup>369</sup>, strongly reducing or depleting systemic Tregs, identified improved neurological outcomes following CNS injury in optic nerve or spinal cord, increasing neuronal survival and neuroprotection by decreasing immune suppression. These early results were supported by the hypothesis that CD4 effector T-cells are required for neuroprotection following injury. However, later it was found that exogenous Tregs injected following CNS injury have opposing effects based on the mouse genetic background, with neuroprotection increased in C57/B6 mice and decreased in Balb/c mice<sup>373</sup>. Interestingly, this dichotomy was resolved when Tregs were transferred into immunodeficient mice with beneficial effects in both genetic backgrounds<sup>373</sup>. It is increasingly understood that Tregs respond with a suppressive or inflammatory phenotype depending on the immune environment at the injury site and further studies investigating T-cell interactions in more or less immunocompromised phenotypes will be required for immune system based proregenerative and neuroprotective therapies.

In summary, immune cell activation and the response to spinal cord injury depicts a scenario of conflicting results. The immune response to injury in the mammalian body is a well-controlled system of cell activation, communication and inhibition, in which each cell type is crucial for the successful healing of the wound. Due to the unique anatomical and physiological circumstances of spinal cord injury, this system malfunctions at numerous levels, leading to chronic inflammation. However, uncontrolled depletion of most immune cell types has resulted in worsening of the healing process and inhibition of neuronal survival and neuroregeneration<sup>340,353,365,370,374</sup>. Further understanding of the time, location and nature of cell activation, will fully elucidate the fascinating orchestra of events following injury and how it can be manipulated for the benefit of neuronal survival and regeneration.



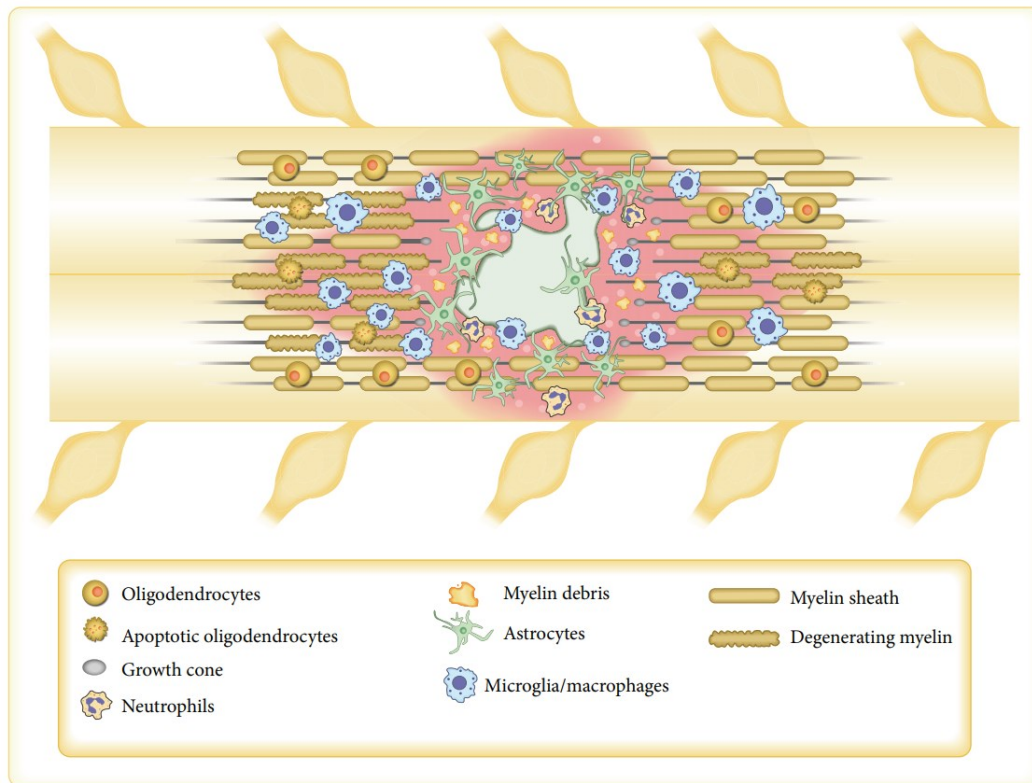


**Figure 8.** Schematic representation of the spinal cord injury site

Injury to the spinal cord immediately generates a blood-spinal cord barrier damage. Infiltration of neutrophils followed by monocytes/macrophages and activation of microglia leads to the activation and migration of astrocytes into the lesion site. CSPGs and astrocytes then form a stabilizing but impenetrable barrier, the astroglial scar. Eventually, at around 3-7 days post injury T-cells infiltrate the lesion site and a short period of anti-inflammatory cytokines and M2 macrophages takes place (From Mietto et al., 2015)<sup>375</sup>.

## **1.5 The mammalian system to study axonal regeneration**

In contrast to non-vertebrate organisms described in the first chapter, the adult mammalian peripheral and central nervous system partially or fully lack regenerative capacity, respectively. In order to test growth enhancing mechanisms in the mammalian system, several animal models have been selected for CNS and PNS regeneration studies. Rodents, dogs, rabbits, pigs and non-human primates are most commonly applied in CNS studies<sup>376</sup>, with rodents, rabbits, dogs and sheep used in PNS studies<sup>377</sup>. Larger animal models are rarely used in basic cellular and molecular studies, for obvious reasons of cost, size, availability, housing facilities, medical care and ethics. However, due to their size and similarity to human physiology pigs have become more important as preclinical model of spinal cord injury, representing intermediates between rodents and humans, in recent years<sup>378,379</sup>. Further, the use of non-human primates seems the obvious choice for pre-clinical studies, but this has been limited for ethical reasons. These studies, however, have provided important information on anatomical plasticity and behaviour in spinal cord and peripheral nerve repair<sup>380-382</sup>. For studies of basic molecular and cellular biology following both, PNS and CNS injury, rodent animal models provide sufficient physiological similarity to humans in addition to higher economical suitability with lower costs (housing facilities, medical care) and lower ethical concern. For central nervous system injury studies rats have higher similarities with humans in the cellular composition of the spinal injury scar, compared to mice<sup>383</sup>. Conversely, mice are mostly available as transgenic models<sup>384</sup> enabling greater mechanistic insights into the cellular and molecular processes of axon regeneration, allowing for temporo-spatial control of the knock-out strategy. Therefore mice are usually used to gain mechanistic insight into basic cellular and molecular biology of the spinal cord injury and rats are preferably used in preclinical studies<sup>385</sup>. PNS nerve injury research is usually conducted on the sciatic nerve, since it is the largest nerve in the body and therefore facilitates experimental microsurgery in such small animal models<sup>377</sup>. Rats are most commonly used in peripheral regeneration due to large dimensions of the nerve and functional testing of sensory- motor recovery is more standardized<sup>386,387</sup>. However, transgenic models<sup>384</sup> as well as rat specific antibodies are less available. As mentioned before, mice have a greater availability as transgenic models and are therefore more suitable when aiming to study cellular and molecular mechanisms of regeneration. Just like rat, they are economical to keep, easy to handle and can therefore be studied in large groups. However, in mouse even the largest nerve is rather small and in vivo work requires more advanced microsurgical skills. Additionally, the intrinsic regenerative capacity of peripheral nerves in rodents is higher than in humans resulting in a faster and complete recovery from nerve injury<sup>387</sup>. Continued studies in physiologically and anatomically more similar animal models to humans, such as sheep, pig and non-human primates

are required to assess if pro-regenerative mechanisms identified in mouse or rat are translatable to humans.

## **1.6 Hypothesis and Aims of the Thesis**

Here, we hypothesized that Intermittent Fasting will facilitate axonal regeneration upon sciatic nerve injury via changes in systemic and/or local modifications in metabolic or cellular signalling pathways.

This thesis aims to:

- (1) Investigate the regenerative effect of Intermittent Fasting after peripheral nerve injury
- (2) Investigate the systemic and or local changes affecting axonal regeneration after intermittent fasting and investigate the mechanism behind it
- (3) Discover novel systemic and/or local signalling pathways that can be targeted and used as therapy for peripheral nerve and eventually spinal cord injury.

## **Chapter 2: METHODS**

### **2.1 In vivo methods**

#### **Animal Husbandry**

All animal experiments were carried out according to UK Home Office regulations in line with the Animals (Scientific Procedures) Act of 1986 under personal and project licenses registered with the UK Home Office. The experiments were carried out using male C57BL6 mice (20-30 g, 6-8 weeks of age). For all surgeries, mice were anesthetized with isoflurane (5% induction, 2% maintenance) and a mixture of buprenorphine (0.1mg/kg) and carprophen (5mg/kg) was administered subcutaneous peri-operatively as analgesic. Body temperature was maintained by keeping the mice on a heating pad (37°C) during the whole procedure.

#### **Intermittent Fasting**

C57BL/6 mice were randomly assigned to intermittent fasting (IF), or *ad libitum* (control) treatment groups. The IF group did not have access to food (fasting) during the first 24 h and then every second day after that (e.g. fasting during 0–24 h, 48–72 h, 96–120 h) with ad libitum access to food on the alternating days (24–48 h, 72–96 h, 120–144 h). Pre-weighed food was be provided in the food hopper of their home cage at 9:30 am (unless a fasting day for the IF groups), and leftover food was weighed 24 h later. On the day following the last food day, sciatic DRGs were dissected, dissociated and cultured for 12 hours.

#### **Sciatic nerve crush (SNC) surgery**

The sciatic nerve crush surgery was executed under isoflurane anaesthesia (5% induction, 2% maintenance). Following the skin incision, the biceps femoris and the gluteus superficialis were opened by blunt dissection and the sciatic nerve was exposed using a surgical hook. The sciatic nerve crush was performed orthogonally for 20 seconds (45 seconds for functional recovery experiment) using a 5 mm surgery forceps (91150-20 Inox-Electronic). The crush was performed at approximately 20 mm distally from the L4-L6 DRGs.

#### **Intramuscular injection**

Ten days after sciatic nerve crush, 5 µl of 1% Cholera toxin B (CTB; List Biological Laboratories) was injected into the tibialis anterior and medial gastrocnemius muscles using a 10µl Hamilton syringe ((NDL small RN ga34/15mm/pst45o ) (Hamilton). Three days post injection, the L4-L6

DRGs were dissected, fixed in 4% PFA, followed by incubation in 30% sucrose for at least 24 hours.

### **Dorsal column axotomy**

Mice were kept under anaesthesia with 2% isoflurane/1% O<sub>2</sub> mixture. The skin over the thoracic area was shaved and brushed with iodine. The skin was incised, the superficial fat shifted apart, and the muscle tissue dissected to expose laminae T9–T11. A T10 laminectomy was performed, the dura mater was removed, taking care not to damage the spinal cord during this procedure. A dorsal column axotomy was performed using micro scissors. Muscle tissue and skin were sutured up separately. After surgery, mice were placed into a 38 °C warm box until woken up and assessed for abnormalities. Mice underwent daily check for general health, mobility within the cage, wounds, swelling, infections, or autophagy of the toes throughout the experiment.

### **Axonal tracing**

Six weeks post spinal cord injury the sensory axons in the dorsal columns were traced by injecting 3 µl of 1% CTB (List Biological Laboratories) diluted in saline into the sciatic nerve using a 10 µl Hamilton syringe and Hamilton needle (NDL small RN ga34/15mm/pst45o) (Hamilton). 4 days post-tracing, mice were terminally anaesthetised and transcardially perfused with 20 ml PBS (pH 7.4) (Sigma) followed by 20 ml 4% paraformaldehyde in PBS (Sigma).

### **Behavioural assessment**

Mice were trained daily for 1-week pre-surgery before baseline measurements and then assessed on day 3 post-surgery and weekly or daily thereafter. The tests were performed at the same time of day throughout the study in a suitable room for behavioural assessment. External stimuli such as noise were minimized. All behavioral testing and analysis were done by an observer blinded to the experimental groups.

#### Grid walk:

The grid walk consists of a 50 cm × 5 cm plastic grid placed between two vertical 40 cm high wood blocks. The mesh is formed by 1 cm × 1 cm spaces. Mice were allowed to run the grid walk 3 times per session. The number of total steps and missteps per run for each hind paw were analyzed by a blind investigator.

### Adhesive removal test:

An 8 mm diameter adhesive pad was placed on each hind-paw, or only the left one for the sciatic nerve crush experiment. The mouse was then placed into plexi-glass box and the time until it first contacted each of the adhesive pads was recorded, followed by the time until it removed the adhesive pads from each hind-paw. The maximum time allowed for each animal was 5 mins. Each animal was tested twice per time- point and values represent the average time from both hind paws from both runs.

### Basso Mouse Scale for Locomotion (BMS)

The test was performed by two testers located at opposite sides of an open field (115 cm diameter, 20 cm sidewall height). Each mouse was evaluated for 4 minutes. Carried out based on the original guidelines<sup>388</sup>.

### Von Frey Test

The Von Frey test was carried out daily until mice recovered to baseline levels. In this test, animals were placed individually in small transparent cages with a grid bottom. The animals were acclimatized to the behavioural room and their own compartment of enclosure for 30 min every day for 1 week before the test was started. Baseline reading was obtained 1 day before surgery. Every day the mice were acclimatized for 20-30 min to the enclosure until they were calm. A monofilament was applied perpendicularly to the plantar surface of the hind paw, delivering a constant pre-determined target force (0.008 - 8 grams, equivalent to 0.078 – 78.431 milli-Newtons) for 2–5 s. A response is considered positive if the animal exhibits brisk paw withdrawal, licking, or shaking of the paw, either during application of the stimulus or immediately after the filament is removed.

### Hargreaves

The Hargreaves test was carried out daily until mice recovered to baseline levels.

A complete set of Hargreaves test (Ugo Basile, catalog number: 37370 or Harvard Apparatus, catalog number: 72-6692) was used for this assessment. The animals were acclimatized to the behavioural room and their own compartment of enclosure for 30 min every day for 1 week before the test was started. Baseline reading was obtained 1 day before surgery. Every day the mice were acclimatized for 20-30 min to the enclosure until they were calm. The reaction time at the controller was set to 10 seconds at 50 units infrared intensity. The infrared emitter/detector was positioned underneath the center of the paw being tested (the left hind paw) and by pressing the start button the test was started. The time was stopped automatically when the animals elicited a withdrawal

response due to sensing of thermal heat and the record time was recorded manually. This was repeated for 3 times per animal with approximately 5 min between the tests.

### **Faecal transplantation**

Fresh faeces was collected every day from the cage of 5 healthy C57BL/6 mice, approximately 200 mg / mouse. The cage was changed thereafter to a fresh cage. 1g of faeces was then homogenized in 10 ml of PBS and centrifuged for 30 seconds at 3000 rpm at 4°C. Following on that the supernatant was transferred to a new tube and centrifuged for 5 min at 12000 rpm at 4°C. The pellet was resuspended in 2.5 ml PBS and 500 µl gavaged to each mouse.

### **Antibiotic administration**

Vancomycin antibiotics (Sigma, V2002) was administered through the drinking water (50mg/kg/day; 214.27 mg/l), which was renewed every second day.

### **Indole-3-propionic Acid treatment**

Indole-3-propionic acid (Sigma, 57400) was diluted at 0.5 mg/200 µl in sterile PBS. Mice were treated with 20 mg/kg/day via gavage or IP injection.

### **Clostridium sporogenes recolonization**

*WT and FldC Clostridium sporogenes bacterial cultures were obtained in collaboration with Professor Dylan Dodd, Stanford University, USA*

WT and *fldC* (mutant for (R)-phenyllactyl-CoA dehydratase beta subunit of the phenyllactate dehydratase complex [*fldC*]) *Clostridium sporogenes* cultures were obtained in collaboration with Dr. Dylan Dodd (Stanford University). Bacterial cultures were mixed with glycerol to reach the final concentrations of: WT 6.01E+06 CFU/ml and *C.s. fldC* mutant 5.46E+06 CFU/ml. Mice were pretreated with Vancomycin in drinking water for 3 days. *C.s. WT* or *C.s. fldC* were transplanted to the cecum via oral gavage for 10 consecutive days at 1E+06 CFU/day.

### **Monoclonal Antibody injection**

Preceding and following nerve injury monoclonal antibodies, mouse αLy6G (Bioxcell, Clone 1A8), mouse αIFNγ (Bioxcell, Clone XMG1.1), Rat IgG2a isotype control (Bioxcell, Clone 2A3), Rat αIgG1 (Bioxcell, Clone HRPN) were administered at 200ug/day for 10 consecutive days via IP injection.



## 2.2 Ex vivo and in vitro methods

### **Serum and cecum preparation**

Blood was extracted via heart punctation and collected into a covered test tube. The blood was allowed to clot for a minimum of 30 min at room temperature and centrifuged at 2000 g for 10 min at 4 °C. The supernatant was then collected into a fresh tube and stored at -20 °C until use.

Cecum content was removed from the cecum using sterile forceps into a tube and snap-frozen in liquid nitrogen immediately.

### **Gas chromatography – Mass Spectrometry (GC-MS) untargeted metabolomics**

*GC-MS was carried out in collaboration with Professor Marc-Emmanuel Dumas (ICL) and Dr. Antonis Myridakis, Department of Metabolism, Digestion and Reproduction, Imperial College, London. Sample preparation, GC-MS and data analysis was done by Antonis Myridakis and me.*

Serum samples (100 µL) were prepared as follows: I) samples were spiked with 10 µL internal standard solution (myristic acid-d27, 750mg/mL), II) 850 µL of ice cold methanol were added, followed by centrifugation for 20 min (4° C, 16000 g), III) 750 µL of supernatants were transferred to silanized dark 2mL autosampler vials and were evaporated to dryness in a rotational vacuum concentrator (45° C, 20 mbar, 2 h), IV) 50 µL of methoxyamine solution (2% in pyridine) were added and the samples were incubated overnight at room temperature and finally, V) 100 µL of N-methyl-trimethylsilyl-trifluoroacetamide (MSTFA) +1% trimethylchlorosilane (TMCS) solution were added, the samples were incubated at 60o C for 1 h and were transferred to dark autosampler vials with 250 µL silanized inserts. The samples were analysed in an Agilent 7890B-5977B Inert Plus GC-MS system. 2 µL of each sample were injected in a split inlet (1:10 ratio). The chromatographic column was an Agilent ZORBAX DB5- MS (30 m X 250 µm X 0.25 µm + 10m Duraguard). The temperature gradient was 37.5 min long and the mass analyser was operated in full scan mode between 50-600 m/z. The detailed instrumental conditions are described elsewhere ([Agilent G1676AA Fiehn GC/MS Metabolomics RTL Library, User Guide, Agilent Technologies, https://www.agilent.com/cs/library/usermanuals/Public/G1676-90001\\_Fiehn.pdf](https://www.agilent.com/cs/library/usermanuals/Public/G1676-90001_Fiehn.pdf)). Quality

Control (QC) samples were created by pooling equal amounts of every serum sample of the study and were analysed interspaced in the analytical run. Study samples were randomized before sample preparation. Peak deconvolution, alignment and annotation and were performed with the use of the Fiehn library via the software packages AMDIS (NIST), Mass Profiler Pro and Unknowns (Agilent technologies) in the pooled QC samples. Peak picking was performed with the GAVIN package (A software complement to AMDIS for processing GC-MS metabolomics data. doi:

10.1016/j.ab.2011.04.009). Non-reproducible (CV>30% in QC samples) and contaminated (blank > 20% of the mean QC levels) metabolic features were removed from the dataset.

This data set was then used to build orthogonal partial least-squares-discriminant analysis (OPLS-DA) (IF vs AL) or partial least-squares-discriminant analysis (PLS-DA) (IF, IF-V, AL, AL-V), focusing on the differences among the experimental groups. The OPLS algorithm derives from the partial least-squares (PLS) regression method<sup>389</sup>. The method explains the maximum separation between class samples Y (n dummy variables for n classes) by using the GCMS data X. Here the ropls R package (<http://bioconductor.org/packages/release/bioc/html/ropls.html>) was used, which implements the PCA, PLS-DA and OPLS-DA approaches<sup>390</sup>. It includes the R2 and Q2 quality metrics, permutation diagnostics, the computation of the VIP values, the score and orthogonal distances to detect outliers, as well as scores, loadings, predictions, diagnostics, outliers graphics<sup>390</sup>.

### **Liquid chromatography-tandem mass spectrometry (LC-MSMS)**

*LC-MSMS was carried out by Dr Alexander Brandis, Weizmann Institute, Tel Aviv, Israel*

#### Materials

Indole-3-propionic acid (Aldrich 1 g) as standard and indole-3-propionic-2,2-d<sub>2</sub> acid (0.05 g, C.D.N. Isotopes) as internal standard (IS) were used. Acetonitrile, methanol and formic acid were of ULC-MS grade and were supplied from Bio-Lab. Water with resistivity 18.2 MΩ was obtained using Direct 3-Q UV system (Millipore). Standard curve was built using concentration range of 3-indolepropionic acid 0.01-12 µg/mL, with final concentration of IS 100 ng/mL.

#### Extract preparation

Plasma (30 µL) and IS (10 µL, 1 µg/mL) was incubated 10 min, then 500 µL of methanol was added. The mixture was shaken at 10°C for 30 min (ThermoMixer C, Eppendorf), and centrifuged at 21,000 g for 10 min. Collected supernatant was evaporated in speedvac and then in lyophilizer. Before LC–MC analysis, the obtained residue was re-suspended in 100 µL of 20%-aq methanol, centrifuged twice at 21,000 g for 5 min to remove insoluble material. The soluble part was placed to insert of LC-MS vial. Some samples were diluted 1/20 with 20%-aq methanol.

#### LC-MS analysis

The LC–MS/MS instrument consisted of an Acquity I-class UPLC system (Waters) and Xevo TQ-S triple quadrupole mass spectrometer (Waters) equipped with an electrospray ion source and operated in positive ion mode. MassLynx and TargetLynx software (version 4.1, Waters) were applied for the acquisition and analysis of data. Chromatographic separation was done on a 100

mm × 2.1 mm internal diameter, 1.7-µm UPLC BEH C18 column equipped with 50 mm × 2.1 mm internal diameter, 1.7-µm UPLC BEH C18 pre-column (both Waters Acquity) with mobile phases A (0.01% formic acid) and B (0.01% formic acid in acetonitrile) at a flow rate of 0.6 ml min<sup>-1</sup> and column temperature 60°C. A gradient was used as follows: 0–5 min a linear increase from 20 to 25 % B, then increase to 95 % B during 0.1 min, 5.1–7 min held at 95 % B, then back to 20 % B in 0.1 min, and equilibration at 20 % B for 1.9 min, providing total run time of 9 min. Samples kept at 8 °C were automatically injected in a volume of 1 µl. MS parameters: capillary voltage - 1kV, cone 0 V, Source temperature -150°C, Desolvation temperature - 550°C, Desolvation gas - 110 L/Hr, Cone gas - 200 L/Hr, Nebulizer - 7.0 Bar, Collision gas 0.10 mL/min. MRM transitions (collision energy, eV): 190>55.0 (17), 190>130.1 (12), 190>172.1 (9) for 3-indolepropionic acid, and 192.1>56.0 (12), 192.1>130.1 (14), 190>174.1 (14) for IS.

### 16S sequencing

Cecum content was collected from mice and immediately frozen in liquid nitrogen. Samples were stored at -80 °C. Faecal DNA was extracted using Fast DNA spin kit (MP Biomedicals). Libraries were prepared using the 16S Metagenomic Sequencing Library Preparation protocol for the Illumina MiSeq System. In brief, PCR primers (16S Amplicon PCR Forward Primer = 5' TCGTCGGCAGCGTCAGATGTGTATAAGAGACAGCCTACGGGNGGCWGCAG; 16S Amplicon PCR Reverse Primer = 5' GTCTCGTGGGCTCGGAGATGTGTATAAGAGACAGGACTACHVGGGTATCTAATCC) directed at the V3/V4 region of bacterial rRNA genes were used to generate libraries and libraries were validated by the Agilent 2100 Bioanalyzer. Sequencing was performed with 250 bp paired-end reads on Illumina Miseq2500 (Imperial BRC Genomics Facility).

### 16S rRNA gene sequencing data analysis

*Carried out by Adesola Temitope Bello and Prof Elaine Holmes, Department of Metabolism, Digestion and Reproduction, Faculty of Medicine, Imperial College London*

Only single-end R1 sequences were analysed. Data processing was carried out in R statistical environment version 3.5.2 according to the DADA2 pipeline<sup>391</sup> as follows; primers were trimmed from de-multiplexed sequences, amplicon sequence variants (ASVs) were generated using DADA2 package version 1.10.1, and taxonomic assignment was performed using the SILVA rRNA database version 132 [<https://www.arb-silva.de/>]. ASVs with no phylum assigned were excluded from analyses to yield a final number of  $n = 906$  annotated ASVs.

Alpha and beta diversity analyses were carried out using phyloseq package version 1.26.1<sup>392</sup>. Alpha diversity (Shannon Index) was calculated using raw counts<sup>393</sup> (Compared to rarefied counts, results

were identical). Groups were compared using Mann Whitney U statistical tests. For beta diversity analyses, data was normalised by log-transformation with a pseudo count of +1. Differential abundance of groups were compared in the DESeq2 package version 1.22.2<sup>394</sup> using the Wald test with adjustments for multiple testing carried out by the Benjamini and Hochberg method (p set as 0.05).

### **RNA sequencing**

DRGs were collected from animals that had undergone 10 days of IPA or PBS treatment and/or followed by sciatic sciatic nerve crush. L4-L6 DRGs were extracted 72h after sciatic nerve crush or from naïve animals (surgeries were performed as described above), and collected into RNAlater. DRGs were crushed with RNase free micropestle and RNA was then immediately extracted using RNAeasy kit (Qiagen), according to manufacturer's guidelines. Residual DNA contamination was removed by treating the spin column with 40 units of RNase-free DNase I (Qiagen) for 15 min at 23 °C prior to RNA elution. RNA concentrations and purity were verified for each sample following elution with the Agilent 2100 Bioanalyzer (Agilent). RNA with RIN factor above 7.5 was used for library preparation. cDNA libraries for each sample were generated by the Imperial BRC Genomics Facility using the TruSeq Sample Preparation Kit A (Illumina, San Diego CA) and sequenced using Illumina HiSeq 4000 (PE 2x75 bp) sequencing.

*Bioinformatics analysis of the raw data files was carried out by Dr Matt Christopher Danzi, University of Miami. Further GO analysis of the processed data was done by me.*

Gene ontology (GO) was performed on the differentially expressed genes with DAVID (Database for Annotation, Visualization, and Integrated Discovery (<http://david.abcc.ncifcrf.gov/>)) using a threshold of  $P < 0.05$ . Upregulated genes that resulted enriched in the GO BP “immune system” functional clustering were added to a Venn diagram (<https://bioinfogp.cnb.csic.es/tools/venny/>) and immune regulated genes upregulated in the PBS-SNC control dataset were excluded from the analysis. Genes uniquely upregulated in IPA and IPA-SNC, as well as genes upregulated at least 1.5 fold higher in the IPA-SNC compared to the PBS-SNC dataset were uploaded into STRING to build a protein-protein interaction network. The network was visualized by Cytoscape, where each node represents a differentially regulated gene (RNA-seq) and edges represent protein-protein interactions.

### **Sciatic nerve regeneration**

24 hours or 72 hours following the surgery, sciatic nerves were dissected and post-fixed in 4% PFA, incubated at 4°C for 1h and transferred into 30 % sucrose for at least 3 days. Subsequently, the tissue was embedded and frozen in Tissue-Tek OCT and maintained at -80°C until cut into 11

µm sagittal sections. Tissue sections were immunostained for SCG10 (1:1000, Rabbit, Novus) a marker for regenerating axons. The crush side was identified by deformation of the nerve and disruption of axon coinciding with highest SCG-10 intensity. The SCG-10 intensity was measured in 500 µm intervals along the length of the nerve distal to sciatic nerve crush side. The intensity was normalised to the SCG-10 intensity before the crush side and plotted as fold-change. 4-6 sections per animal were analysed and imaged with a HWF1 - Zeiss Axio Observer with a Hamamatsu Flash 4.0 fast camera using 10x magnification.

### **Dorsal Root Ganglia (DRG) cell culture.**

Glass coverslips were coated with 0.1 mg/ml PDL, washed and coated with mouse Laminin 2µg/ml (Millipore) for 1-2 hours each previous to the start of the experiment. Sciatic DRGs from adult animals were dissected and collected in Hanks balanced salt solution (HBSS) on ice. The DRGs were transferred into a digest solution (5mg/ml Dispase II (Sigma), 2.5 mg/ml Collagenase Type II (Worthington) and incubated in a 37 °C water bath for 45 min, with occasional mixing. Following on that the DRGs were washed and manually dissociated with a 1ml pipette in media containing 10 % heat inactivated FBS (Invitrogen) and 1x B27 (Invitrogen) in F12:DMEM (Invitrogen). Pipetting was continued until DRGs were fully dissociated and no clumps could be observed. Next, the cell suspension was spun down at 1000 rpm for 4 min and resuspended in culture media containing 1x B27 and Penicillin/Streptomycin in F12 : DMEM. 3500 cells were plated on each coverslip (laminin and PDL coated) and maintained in a humidified culture chamber with 5% CO<sub>2</sub> at 37 °C, for 12 hours before fixed with 4% PFA and immunostained. Following cell plating, DRGs were treated with Indole-3-propionic acid (1 µM, 10 µM or 100 µM, Sigma 57400) or IFN $\gamma$  (5 ng/ml, 100 ng/ml, Peprotech 250530). For IFN $\gamma$  treated ex-vivo DRG outgrowth, animals were injected intraperitoneal with 10 µg IFN $\gamma$ /mouse 48 hours before DRG cell culture.

### **Immunohistochemistry**

Immunohistochemistry on tissue sections was performed according to standard procedures. Tissue sections were rehydrated with PBS and blocked and permeabilized for 1 hour with 8% BSA containing 0.3% PBS-TX100. Secondly, the sections were incubated with anti-SCG10 (1:1000, Rabbit, Novus), SOX10 (1:1000, Rabbit, Abcam), CD68 (1:1000, Rabbit, Abcam), Ly6G (1:500, mouse, BioxCell, clone 1A8), ChAT (1:200, goat, Chemocon), vGLUT (1:1000, rabbit, Synaptic Systems), vGAT (1:1000, rabbit, Synaptic Systems), GFAP (1:500, Rabbit, Merck Millipore) antibodies (diluted in 2% BSA in 0.1% PBS-TX100) at room temperature over night. The sections were washed three times with PBS, followed by incubation with Alexa Fluor conjugated goat

secondary antibodies (diluted in 2% BSA in 0.1% PBS-TX100). All tissue sections were counterstained with DAPI (Molecular Probes) and cover slipped with moviol.

### **Immunocytochemistry (ICC)**

Plated cells were fixed by incubation with cold 4 % PFA for 15 min. Following on that they were blocked and permeabilized for 1 hour with 0.3 % TX100 in PBS containing 2 % BSA. The primary antibody staining was performed using anti- $\beta$ III Tubulin (1:1000, mouse, Promega) in 0.1 % TX100 in PBS containing 2 % BSA, which O/N incubation at RT. The goat secondary antibody (Alexa) was diluted in 0.1 % TX100 in PBS containing 2 % BSA and cells were incubated for 1 hour. All cells were counterstained with DAPI.

### **FACS staining**

Cells were isolated from spleens or lymph nodes by mashing using a 70  $\mu$ m cell strainer and a pestle and transferred into Media (RPMI media 1640 [Thermo Fisher scientific] + 2% Foetal calf serum + 1x Penicillin/Streptomycin + 1x HEPES [Thermo Fisher scientific]). Spleen cells were centrifuged at 1200 rpm for 6 min and resuspended in 10 ml of Red blood cell lysis buffer Hybrid Max (Sigma) for 5 min. Following on that 9 ml of media was added and centrifuged at 1200 rpm for 6 min. Spleen cells or lymph node (LN) cells were resuspended in Media and plated at  $1 \times 10^6$ - $2 \times 10^6$  cells per well in a 96-well plate. The plate was centrifuged at 2000 rpm for 1 min and 50  $\mu$ l of blocking stain (1:50 dilution Rat Serum [Sigma], 1:50 dilution TruStain FcX™ [anti-mouse CD16/32] [Biolegend] in FACS buffer [PBS supplemented with with 5% FCS, 2mM EDTA and 0.09% NaAzide]) was added. Cells were blocked for 30 min at 4 °C and subsequently washed three times with 140  $\mu$ l of FACS buffer. Antibodies were added and cells were incubated for 30 mins in the dark. Following on that cells were washed another 3 times and imaged on a BD LSR Fortessa X-20 (BD Biosciences, 4 laser).

<u>Marker (clone)</u>	<u>Colour</u>	<u>Dilution</u>	<u>Company</u>
CD45 (30-F11)	V450	1:100	BD Biosciences
CD11b (M 1/70)	BV421	1:200	Biolegend
CD11c (3.9)	PECy7	1:200	Biolegend
Ly6G (1A8)	BV711	1:200	Biolegend
Ly6C (HK1.4)	FITC	1:200	Biolegend
NK1.1 (PK136)	PE	1:100	Biolegend
TCRb (H57-597)	BV786	1:200	Biolegend

CD4 (GK 1.5)	APCCy7, BV605	1:200	Biolegend
CD8 (5.3-6.7)	PECy7	1:400	Biolegend
B220 (RA36B2)	BV605	1:200	Biolegend
CD19 (6D5)	APCCy7	1:100	Biolegend
CD23 (B3B4)	BV421	1:100	Biolegend
CD21 (7G6)	FITC	1:100	BD Biosciences
LIVE/DEAD™	Aqua (405 nm)	1:100	Thermo Fisher Scientific

### **Microscopy**

Photomicrographs were taken with a Nikon Eclipse TE2000 microscope with an optiMOS scMOS camera using 10x or 20x magnification - Zeiss Axio Observer with a Hamamatsu Flash 4.0 fast camera using 10x or 20x magnification. Confocal images were taken with a Leica TCS SP5 II confocal microscope at 40X magnification and processed with the LAS-AM Leica software (Leica).

### **Image analysis**

Image analysis was conducted using ImageJ (Fiji) software. All analysis was performed by the same experimenter who was blinded to the experimental groups.

### **Image Analysis for IHC and ICC**

DRG images were taken using a Nikon Eclipse TE2000 microscope with an optiMOS scMOS camera at either 10x or 20x magnification. Images were analysed by calculating the percentage of cells with positive staining. Approximately between 100 and 200 cells were counted and analysed per animal per condition. This was done in triplicate or quadruplicate and blind to the experimental group.

### **Neurite Length Analysis**

DRG neurons were imaged using a Nikon Eclipse TE2000 microscope with an optiMOS scMOS camera at 10x or 20x magnification. Between 15 and 20 images were taken per coverslip and analysed using Neurite J plugin for Image J software (Image J). All analyses were performed in blind. Approximately 45-60 cells were analysed per animal and condition.

### **Statistical analysis**

Results are graphed as mean  $\pm$  SEM. Statistical analysis was carried out using GraphPad Prism 7. Normally distributed data was evaluated using a two-tailed unpaired Student's t-test or a one-way

ANOVA when experiments contained more than two groups. Dunnetts multiple comparisons test or multiple comparison testing corrected by FDR method of Benjamini and Hochberg were applied when appropriate. The Two-way ANOVA, Tukey's or Sidak's test, was applied when two independent variables on one dependent variable were assessed. A threshold level of significance was set at  $P < 0.05$ . Significance levels were defined as follows: \*  $P < 0.05$ ; \*\*  $P < 0.01$ ; \*\*\*  $P < 0.001$ ; \*\*\*\*  $p < 0.0001$ . All data analysis was performed blind to the experimental group.



## Chapter 3: RESULTS

### **3.1 Intermittent Fasting promotes axonal regeneration and target reinnervation following sciatic nerve crush**

I initially tested the hypothesis that IF will facilitate axonal regeneration upon sciatic nerve injury. Sciatic nerve regeneration was tested 24 hours after sciatic nerve crush following 10 or 30 days of IF preceding sciatic injury. Regeneration past the crush side was visualized and measured by Superior cervical ganglia-10 (SCG-10) immunostaining, which selectively labels regenerating axons. Interestingly, we observed that 30 or 10 days of IF vs AL significantly enhanced regeneration past the crush side to a similar extent, up to 1mm, 24 post-injury (Fig. 9A-C). Therefore, all subsequent experiments were performed following 10 days of IF. Importantly, when we extended the post-injury time to 72 hours (AL after the injury), we observed an enhanced number of regenerating axons up to 2.5 mm past the injury site in the IF group (Fig. 9A-C). In confirmation of these findings, we found an increase in neurite outgrowth in cultured dorsal root ganglia (DRG) neurons from mice that underwent 10 days of IF vs AL (AL:  $1624 \pm 127.2 \mu\text{m}$ ; IF:  $2221 \pm 193.1 \mu\text{m}$ ; 12 hours in culture) (Fig. 9D-F). In order to investigate whether IF would also promote target reinnervation after injury, we measured sciatic reinnervation into its target gastrocnemius and tibialis anterior muscles 2 weeks following a nerve crush. CTB tracer was injected into the gastrocnemius and tibialis anterior muscles 11 days after SNC and DRG were extracted 3 days later. Re-innervated nerve fibres incorporate CTB tracer and innervation efficiency can be studied by the quantification of CTB positive DRG neurons. Interestingly, we found a 25% increase NF200 positive neurons co-labelled with CTB in the IF group compared with control, specifically, 8% double-positive neurons in the AL group and 10% double-positive neurons in the IF group. This indicates a greater muscle reinnervation following IF (Fig. 9H-I). We next assessed whether 10 days of IF led to any change in food intake or weight. We found that the average food intake of IF mice on a feeding day (5.78 g) exceeded the daily amount of the AL group (4.16 g) resulting in slightly reduced average “daily” food intake in the IF group (2.88 g) (Fig. 10A). However, while the body weight fluctuated depending on whether mice were weighed on a fasting or feeding day, the average body weight remained unchanged compared to the AL control group (day 11: AL=  $26.58 \pm 0.63 \text{ g}$ ; IF=  $26.4 \pm 0.41 \text{ g}$ ) (Fig. 10B).

We can conclude that IF prior to nerve injury facilitates sciatic nerve regeneration and reinnervation of sciatic nerve fibres into the leg muscles without affecting the body weight of the animals.

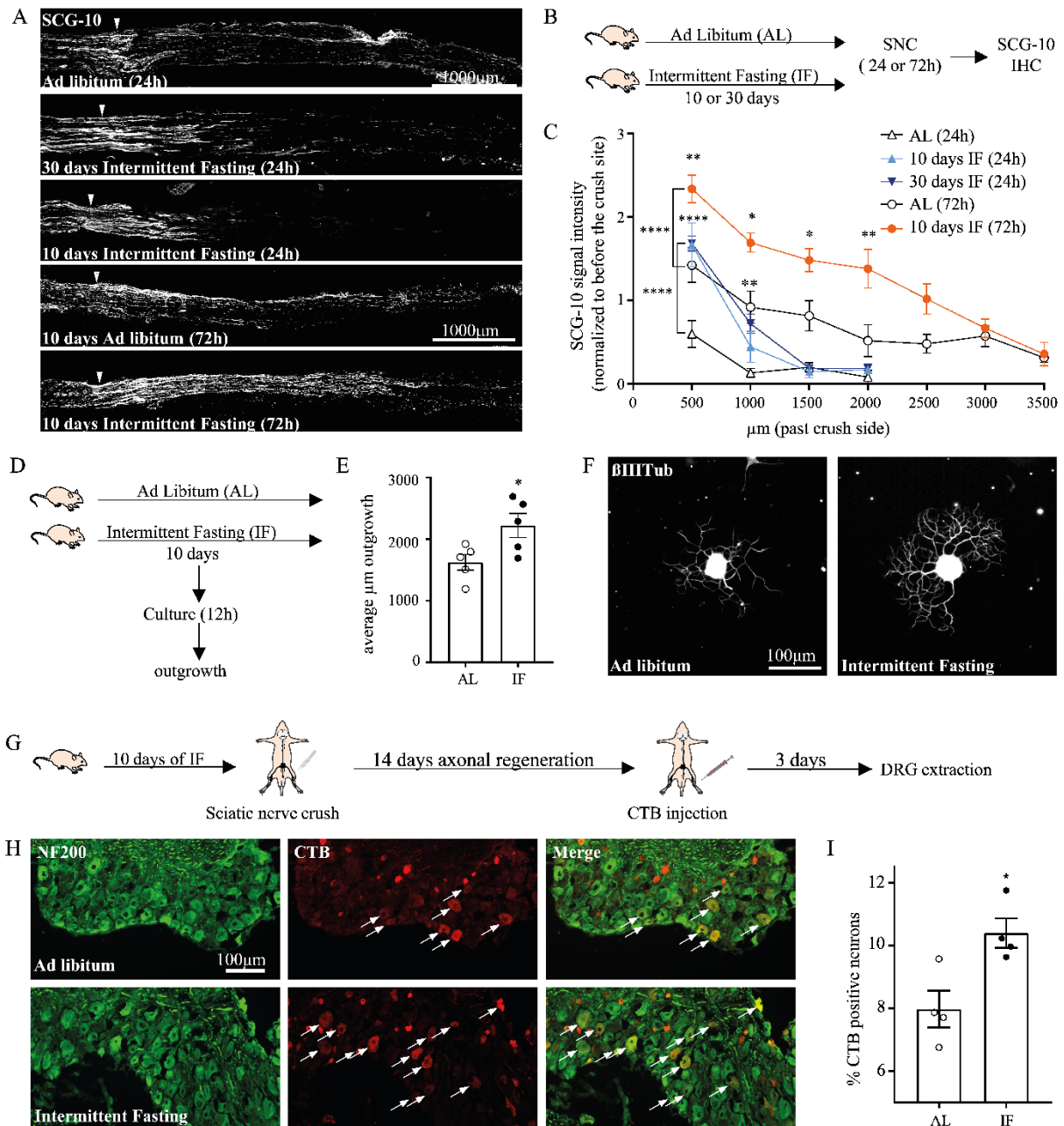


**Figure 9.** Intermittent Fasting promotes axonal regeneration and target reinnervation following sciatic nerve crush

**A-C.** Nerve regeneration following 10 or 30 days of IF or AL and 24h and 72h upon sciatic nerve crush. **A.** micrograph showing representative longitudinal images of sciatic nerves stained with SCG-10 of mice following 10 or 30 days of IF or AL and 24h and 72h upon sciatic nerve crush (scheme in **B**. scale bar: 1000 μm. Arrowhead indicates the crush side). **C.** Quantification of SCG-10 intensity at the indicated distances and normalized to the intensity before the crush site. Normalised SCG-10 intensity was plotted as a function of the distance from the crush site. (N=5-6 nerves per group from 3 mice per group with a bilateral sciatic nerve crush; \*\*\*\*p < 0.0001, \*\*p < 0.01, \*p < 0.05 by Two-way-ANOVA with Tukey's test, mean ± SEM). **D-F.** Neurite outgrowth

measurements from mice following 10 days of IF vs AL revealed significantly more outgrowth of DRG neurons in culture, following 10 days of IF (scheme in **D**). **E**. Quantification of  $\beta$ III-Tubulin ( $\beta$ IIITub, green) immunostained neurite outgrowth by measuring the length of neurites ( $N=5$  animals per group, with 4 technical replicates each;  $*p<0.05$  by students t-test, mean $\pm$ SEM). **F**. Representative images of DRG neurons immunostained with  $\beta$ III-Tubulin, cultured for 12 hours. **G-I**. Axonal muscle reinnervation was assessed by CTB tracing following 10 days of IF vs AL. **G**. Schematics illustrates the experimental timeline: 10 days of IF/AL was followed by a sciatic nerve crush and CTB injection into gastrocnemius and tibialis anterior muscles 14 days later. DRGs were extracted 3 days post CTB injection. **H**. Images showing CTB (red) co-staining of DRGs with NF200 (green). Arrows indicate CTB+NF200+ (yellow) double positive DRG neurons. scale bar: 100 $\mu$ m. **I**. Average percentage CTB+NF200+ DRG neurons displaying a 1.3 fold increase in double-positives in IF vs AL DRGs ( $N=4$ ,  $*p<0.05$  by students t-test, mean $\pm$ SEM).

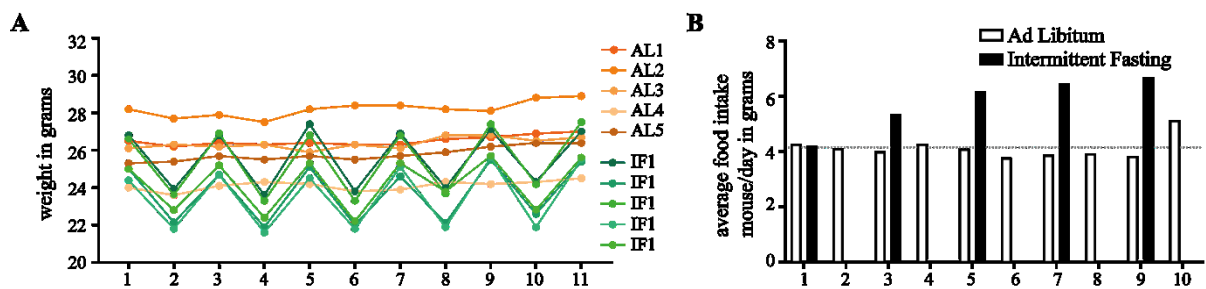


**Figure 10.** Weight and food intake screen during 10 days of intermittent fasting

**A.** Body weight measurements of AL and IF mice ( $N=5$ ). **B.** Average food intake per Mouse / day between AL and IF ( $N=5$ ).

### **3.2 Schwann cells , macrophages and neurotrophic factors are unchanged in the sciatic nerve and DRG in IF vs AL**

Next we investigated Schwann cell migration and macrophage recruitment, since they both contribute to support axonal regeneration<sup>55,395</sup>, to the crush side 72 hours post-injury. The immunostaining intensity of the Schwann cell marker SOX-10 was measured up to 1000 $\mu$ m proximal and distal to the crush side (Fig. 11A, D). We found no significant difference in SOX-10 intensity between IF and AL. Anti-CD68 immunostaining was used as macrophage marker. While an increased staining intensity was found in and at 500 $\mu$ m distal and proximal to the crush side (Fig. 11A and C), similarly to SOX10, CD68 intensity did not differ between IF and AL (Fig. 11B and D). In summary, no changes were observed between IF and AL in the number of Schwann cells and macrophages accumulating in the injured tissue 72 hours following the crush. Neurotrophic factors have been shown to protect neurons following an injury and promote axonal regeneration<sup>11,396-399</sup>. Interestingly, increased levels of neurotrophic factors, such as BDNF, have been found in the hippocampus following IF<sup>243</sup>. Consequently, we measured by ELISA the concentration of the neurotrophic factors NGF, BDNF, NT3 and NT4/5 in the DRG following 10 days of IF vs AL, to find no difference between the groups (Fig. 11E). In summary, these data suggest that Schwann cells, macrophages and neurotrophic factors likely do not play a major role in the IF-dependent axonal regenerative phenotype.

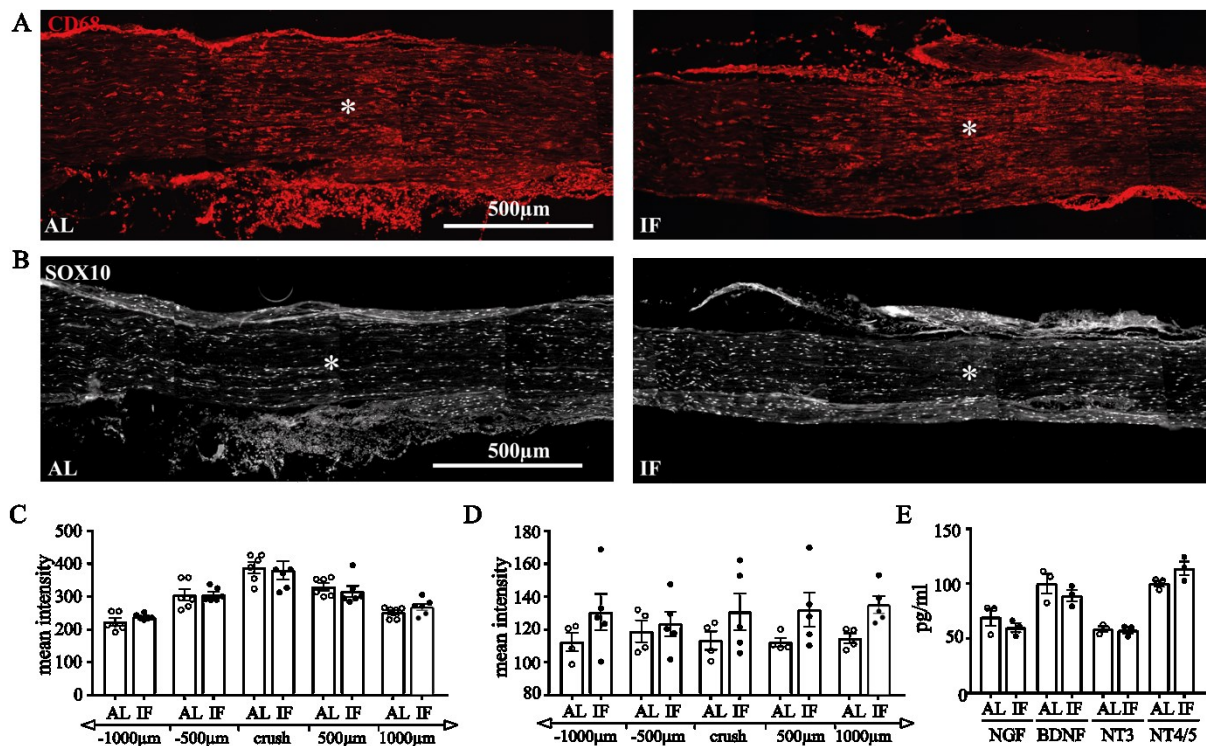


**Figure 11.** *Assessment of Macrophages and Schwann cells in the nerve and DRGs in IF vs AL following injury and biochemical analysis of neurotrophic factors following intermittent fasting.*

*A-B.* Representative images of Nerves dissected from 10 days AL and IF animals at 3 days post injury. Sections were immunostained for *A.* CD68 (macrophage marker, red) or *B.* SOX10 (Schwann cell marker, white). Scalebar 500 µm. Asterisk indicates the crush site. *C.* Quantification of CD68 (red) was conducted by intensity measurements 1000µm proximal and distal to the crush side. No difference was observed between IF and AL. (N=6 nerves per group from 3 mice, significance was assessed using Two-way ANOVA, Tukey's test, mean±SEM). *D.* Quantification of SOX10 (white) was conducted by intensity measurements 1000µm proximal and distal to the crush side. No difference was observed between IF and AL (N=5 nerves per groups from 3 mice significance was assessed using Two-way ANOVA, Tukey's test, mean±SEM). *E.* ELISA measurements of NGF, BDNF, NT3 and NT4/5 from DRG tissue following 10 days IF or AL (N=3 mice per group, Significance was assessed by students t-test, mean±SEM). Samples were collected at the refed state.

### **3.3 Metabolomics analysis identifies IF-dependent induction of indole metabolites**

Due to the impact of IF on metabolism<sup>168,194</sup> and the gut microbiome<sup>264,301,400</sup>, we next hypothesised that changes in metabolism might underpin the IF-dependent regenerative effects we observed following a nerve crush injury. Therefore, we conducted untargeted gas chromatography-mass spectrometry allowing for an unbiased identification of metabolites in the serum. 79 metabolites were found to be differentially concentrated in the serum 10 days following IF vs AL diet (N=10 mice per group; samples taken at refed day). Pairwise orthogonal projection to latent structure-discriminant analysis (OPLS-DA) was performed on the normalized GC-MS data (Fig. 12 A-C). This supervised modelling approach, commonly used for metabolomics datasets, allows to identify differences between two groups or systems. The OPLS discriminant analysis indicates which variables are the driving forces that separate two groups and therefore have the largest discriminatory power. These differences can then be visualised in score plots. The predictive score plot (Fig. 12A) and permutation-based significance diagnostic (Fig. 12B) reveal significant ( $p < 0.0001$ ) stability of the OPLS-DA model. This suggests a significant goodness of fit between the OPLS-DA model and the data point distribution between the groups. Running the observation diagnostics allowed us to identify outlier groups that were subsequently removed from the differential analysis (Fig. 12C). The significantly differentially represented metabolites upon IF can be clustered into 4 groups: microbiome derived, glycolysis intermediates (glycogen breakdown), amino acids (solely convertible to pyruvate and Acetyl-CoA through transamination) and the chemical compounds of AMP/ADP/ATP (Fig. 12D). Interestingly, the 4 most increased metabolites upon IF were microbiome derived: 3-indolelactic acid 2, 2,3-butanediol 2, xylose 2 and indole-propionic acid (IPA) (shown in red, Fig. 12E-H).

Taken together these data show that 10 days of IF alters the serum metabolome, primarily by increasing indole and microbiome derived metabolites (Fig. 12I).

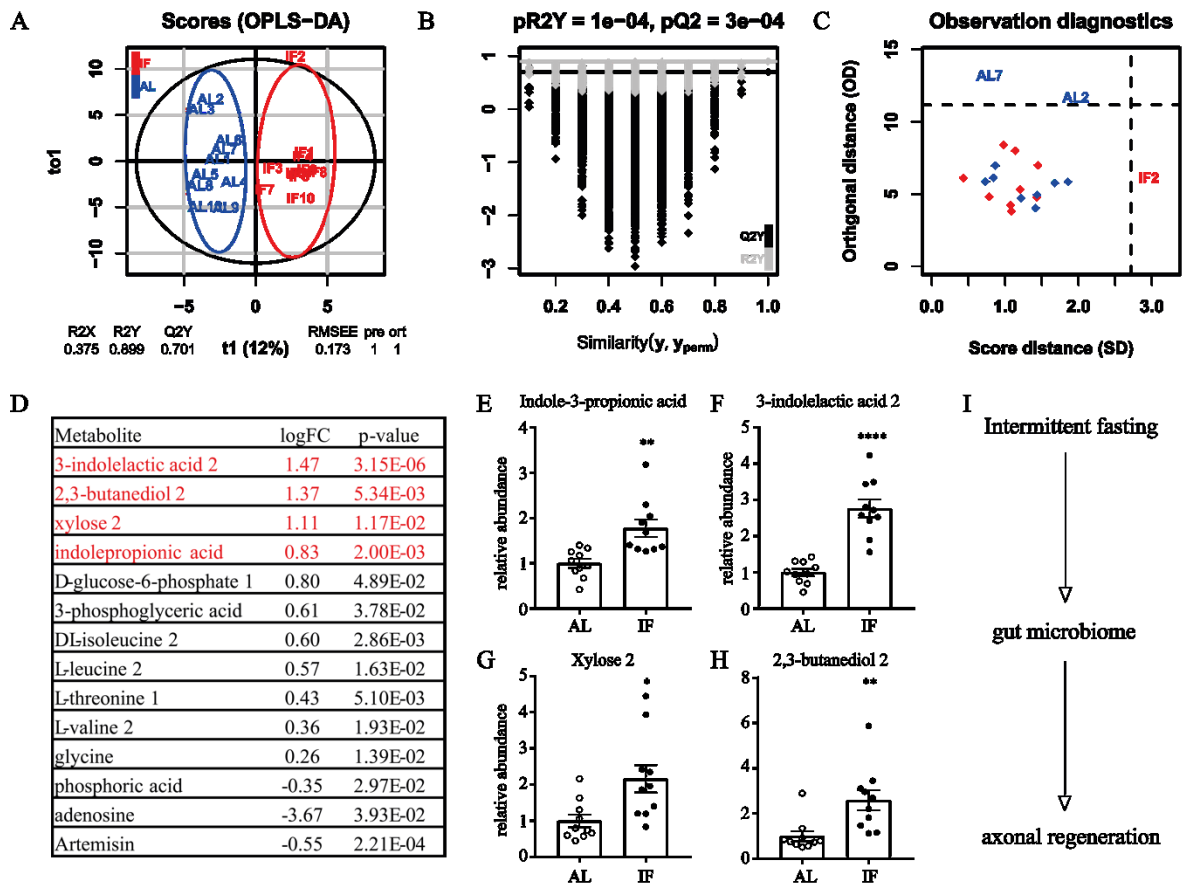


**Figure 12.** Untargeted metabolomics analysis identifies Indole-3-propionic acid, a microbiome derived metabolite as candidate, as upregulated after IF.

GC-MS metabolomics analysis was conducted from serum after 10 days of IF/AL and identified 79 metabolites of which 14 were differentially enriched between the two groups. **A.** X-score plot of the OPLS-DA analysis. The number of components and the cumulative R2X, R2Y and Q2Y are indicated below the plot. Analysis performed on normalised GC-MS data, reveals clear separation of the IF group from AL. **B.** Permutation based significance diagnostic reveals significant ( $p < 0.0001$ ) stability of the OPLS-DA model, specifically that the model remains a good fit ( $R2Y > 0.01$ ) and explains comparable to non-permuted model ( $Q2Y > 0$ ). **C.** Observation diagnostics identifies outliers of the model. **D.** Table listing significantly upregulated ( $n=11$ ) and downregulated ( $n=3$ ) metabolites in IF vs AL serum ( $p < 0.05$ ). Shown are the logarithmic fold changes (logFC) and the p-value (students t-test) between IF and AL groups ( $N=AL: 8$ ,  $IF: 9$  mice per group, excluded outliers). **E-H.** Bar graphs plotting the relative abundance of gut microbiome derived metabolites from the GC-MS analysis: Indole-3-propionic acid (**E**), 3-indolelactic acid 2 (**F**), Xylose 2 (**G**) and 2,3-butanediol 2 (**H**) ( $N=AL:8$ ,  $IF:9$ ;  $*p < 0.05$ ,  $**p < 0.01$ ,  $****p < 0.0001$ , significance was assessed by students t-test, mean $\pm$ SEM), **I.** Schematics summarizing the hypothesis that the modulation of the gut microbiome by IF might lead to the increase in axonal regeneration following injury.



### **3.4 IF-dependent axon regeneration requires the gram+ gut microbiome and strongly induces serum indole-3 propionic acid levels**

Next, since our metabolomics findings indicated that IF changes the gut microbial composition with a significantly higher concentration of serum indole-metabolites, we tested whether the microbiome influences sciatic nerve regeneration upon IF. Therefore, we designed a gain-of-function experiment by implanting the microbiota collected from IF animals into AL mice by faecal transplantation (FT) and observed whether this would enhance axonal regeneration (Fig. 13A-D). Faeces were freshly collected every day from animals undergoing IF or AL. The faeces were dissociated, and the faecal matter removed in order to obtain a clean bacterial solution. The bacteria were then transplanted by gavage to animals which had AL access to food at all times (Fig 13A). Transplanted mice were pre-treated with the antibiotic vancomycin for 3 days prior the start of faecal transplantation, which has previously been shown to deplete the microbiome<sup>401</sup>. Following 10 days of FT, mice underwent a sciatic nerve crush. 72 hours later sciatic nerve anti-SCG-10 immunolabelling was performed and SCG-10 intensity measurements showed a significant increase in regenerating fibres past the crush side (Fig. 13C-D). Measurement of the regeneration index, which measures the distance between the crush side and the point in which SCG-10 intensity is 50% of that at the crush site also showed a significant increase (AL-FT:  $1697 \pm 73.74$ , IF-FT:  $2400 \pm 99.75$ ) (Fig. 13D).

Since indole metabolites (e.g. Indole-3-lactate, Indole-3-aldehyde, Indole-sulfate, Indole-propionate) are primarily synthesized by the gram-positive bacteria *Bifidobacterium* (indole-3-lactic acid)<sup>402</sup>, *Lactobacillus* and *Clostridium sporogenes* (indole-propionic acid)<sup>403</sup>, we next tested whether gram+ bacteria were required for IF-dependent axonal regeneration. To this end, we treated mice with vancomycin or vehicle during 10 days IF vs AL diet before performing a sciatic nerve crush injury. Vancomycin is a common antibiotic against gram-positive bacteria and has been shown to deplete the gut microbial diversity in humans<sup>401</sup>. Four experimental groups (N=6-7 nerves, 4 animals/group) underwent either IF or AL, with or without antibiotic treatment for 10 days. Next, we induced a sciatic nerve crush and assessed regeneration by SCG-10 immunostaining 72 hours later (Fig. 13E-F). Indeed, we found that vancomycin treatment abolished the effect of IF on axonal regeneration. Only about half as many fibres extended past the crush side in the IF + vancomycin group compared to IF alone. There was no difference in the regenerative potential between AL and AL + vancomycin (Fig. 13G). Additional analysis of the regeneration index showed an almost two fold increase in regeneration following IF (AL:  $1001 \pm 126 \mu\text{m}$ , IF:  $1959 \pm 200.5 \mu\text{m}$ ), which was limited to AL levels by vancomycin treatment (IF+V:  $1236 \pm 114.4 \mu\text{m}$ ) (Fig. 13H). Together these results reveal that IF-dependent regenerative phenotype are largely dependent upon the gut microbiome, suggesting a prominent role for gram+ bacteria.



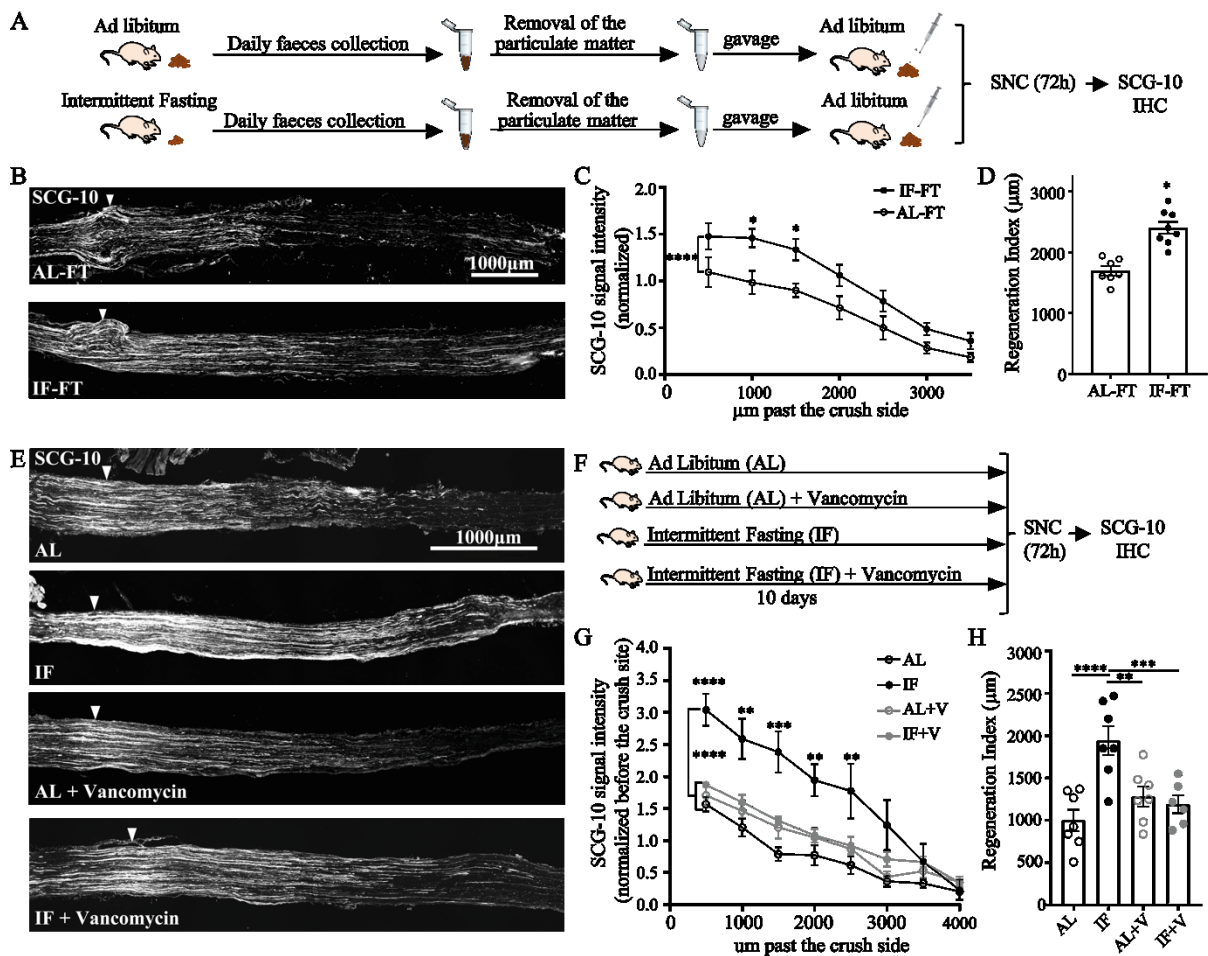


**Figure 13.** *The proregenerative effect of intermittent fasting is partially mediated by the gut microbiome*

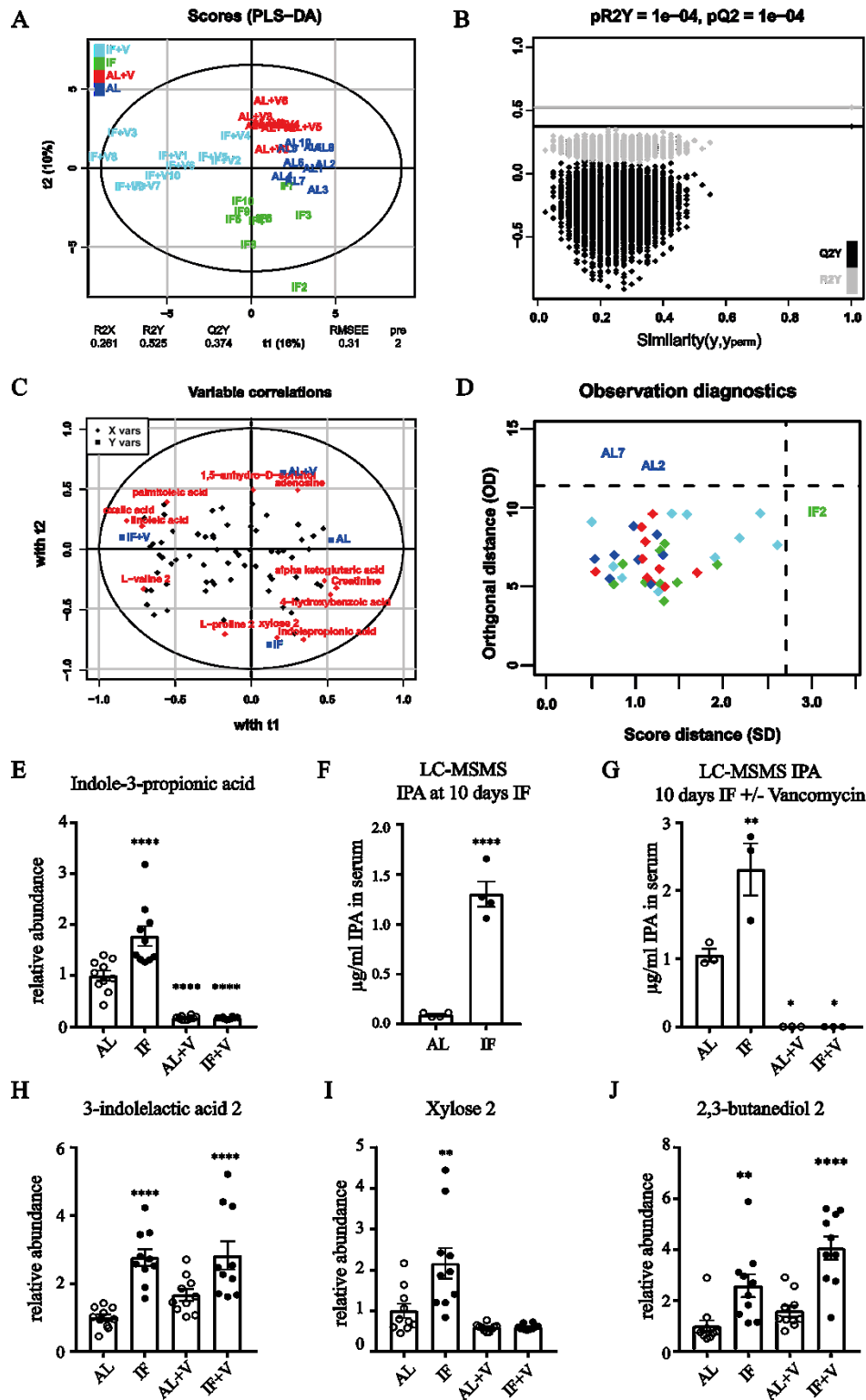
**A-D.** *Quantification of regenerative potential following 10 days of faecal transplantation from IF or AL mice (N=7-8).* **A.** *schematics showing experimental setup. Faeces was collected for 10 days from IF or AL mice and bacterial extract gavaged to AL mice, which were treated with Vancomycin 3 days prior to the start of the experiment. The sciatic nerve crush was followed by 72h regeneration time.* **B.** *micrograph of representative longitudinal section images of sciatic nerves for faecal transplanted groups from AL and IF, 3 days post sciatic nerve crush immunostained with SCG-10. Scale bar: 1000 μm. The arrowhead indicates the crush site.* **C.** *Quantification of SCG-10 intensity at the indicated distances and normalized to the intensity before the crush site. Normalised SCG-10 intensity was plotted as a function of the distance from the crush site. (N=7-8 nerves per group from 4 mice per group with a bilateral sciatic nerve crush; \*\*\*\* $p < 0.0001$ , \* $p < 0.05$ , by Two-way ANOVA with Tukeys test, mean  $\pm$  SEM) revealed increased regeneration in IF-FT mice compared to AL-FT.* **D.** *SCG-10 intensity was measured from the crush site towards the distal end and normalised to the crush site as percentage of intensity. SCG-10 intensity percentage of 50% was plotted as a function of the distance from the crush site. (N=7-8 nerves per*

group from 4 mice with bilateral sciatic nerve crush;  $*p < 0.05$ . by students t-test, mean $\pm$ SEM). **E-H.** Quantification of the regenerative potential following 10 days IF or AL +/- vancomycin. **E.** micrograph of representative longitudinal section images of sciatic nerves for all groups immunostained with SCG-10 following 10 days of IF/AL with or without Vancomycin treatment and 3 days post sciatic nerve crush (Scheme in **F**). Scale bar: 1000  $\mu$ m. The arrowhead indicates the crush site **G.** Quantification of SCG-10 intensity at the indicated distances and normalized to the intensity before the crush site. Normalised SCG-10 intensity was plotted as a function of the distance from the crush site. (N=6-7 nerves per group from 4 mice per group with a bilateral sciatic nerve crush; \*\*\*\* $p < 0.0001$ , \*\* $p < 0.01$ , by Two-way ANOVA with Tukeys test, mean $\pm$ SEM) revealed increased regeneration following IF, which was lost with vancomycin treatment. **H.** In vivo regeneration index was calculated from images in (**A**). SCG-10 intensity was measured from the crush site towards the distal end and normalised to the crush site as percentage of intensity. SCG-10 intensity percentage of 50 % was plotted as a function of the distance from the crush site. (N=6-7 nerves per group from 4 mice with bilateral sciatic nerve crush; \*\* $p < 0.01$ , \*\*\* $p < 0.001$ , \*\*\* $p < 0.0001$  Significance was assessed using One-way ANOVA, Multiple comparison testing: corrected by FDR method of Benjamini and Hochberg, if not indicated otherwise p-value compares to PBS group, mean $\pm$ SEM).

In order to investigate potential specific metabolites underpinning the microbiome-dependent regenerative phenotype, untargeted serum gas chromatography-mass spectrometry was performed in four experimental groups including mice that underwent 10 days of IF vs AL with and without vancomycin. 79 metabolites were identified and partial least squares Discriminant Analysis (PLS-DA) was performed on the normalized GC-MS data (Fig. 14A-D). Comparable to the OPLS-DA modelling approach, PLS-DA allows for supervised clustering of the samples aiming to identify the key variables that drive such discrimination. In addition to OPLS-DA, PLS-DA allows for the analysis of multiple samples. The analysis of our data showed that the predictive score plot (Fig. 14A) and permutation-based significance diagnostic (Fig. 14B) reveal significant ( $p < 0.0001$ ) stability of the PLS-DA model. This suggests a significant goodness of fit between the PLS-DA model and the data point distribution among the groups. Metabolites were visualized by most differentially represented in each group, revealing indole-3-propionic acid (IPA) as most differentially regulated in the IF group (Fig. 14C). Table 1 shows the log fold change for all differentially abundant metabolites, the p-values between the two dietary regimens (IF and AL), antibiotics treatment (vancomycin vs non-vancomycin) and the interaction p-value. Interestingly, IPA showed the most significant increase between IF and AL and was the only metabolite significantly affected by vancomycin treatment with the lowest interaction p-value, suggesting that

its amount critically depended on IF and vancomycin. Indeed, serum IPA was found among the highest increased metabolites in the serum of IF vs AL, with total depletion in the vancomycin treated mice (Fig. 14E). Importantly, the IPA concentration in the serum was assessed using Liquid Chromatography Mass Spectrometry (LC-MS/MS) that allows accurate and sensitive measurements of metabolites. Initially we measured serum IPA in IF vs AL fed mice and found a very significant increase in serum IPA following IF (Fig. 14F). Next, we confirmed that vancomycin led to complete depletion of serum IPA (Fig. 14G).

While indole-3-lactic acid and 2,3- butanediol 2 were found to be highly represented in IF mice, they were not affected by vancomycin treatment (Fig. 14H, J). Xylose 2 appeared to be increased by IF but depleted with vancomycin treatment (Fig. 14I). Xylose 2 appears to be poorly utilized by vertebrates for energy production, however, some evidence suggests a way of oxidation for xylose sugar molecules in mammalian cells<sup>404</sup>. Further, we sought to investigate if microbiome derived short chain fatty acids (SCFA) may be changed upon IF as well. Short chain fatty acids have been shown to be potent signalling molecules, involved in immune regulation, energy homeostasis and epigenetic reprogramming<sup>265,405,406</sup>. Serum and cecum samples were collected following 10 days IF and AL and acetate, propionate and butyrate concentrations were assessed via targeted GC-MS metabolomics. No difference in SCFA concentrations were found between IF and AL in neither serum (Fig. 15A-C) nor cecum (Fig. 15D-F). Acetic acid (Fig. 15D) and butyric acid (Fig. 15E) were decreased or depleted, respectively, in the cecum upon vancomycin treatment. Together, these data allow to conclude that IF mainly affects metabolites synthesized by the gut microbiome, with the strongest effect on IPA.

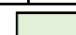


**Figure 14.** Metabolomics analysis identifies Indole-3-propionic following 10 days of intermittent fasting

GC-MS metabolomics analysis was conducted from serum after 10 days of IF/AL and identified 79 metabolites of which 14 were differentially enriched between the two groups. A. X-score plot of the PLS-DA analysis performed on normalized GC-MS data reveals clear separation of the groups:

IF, IF+Vancomycin, AL, AL+Vancomycin. The number of components and the cumulative R2X, R2Y and Q2Y are indicated below the plot. **B.** Permutation based significance diagnostic reveals significant ( $p < 0.0001$ ) stability of the PLS-DA model, specifically that the model remains a good fit ( $R2Y > 0.01$ ) and explains comparable to non-permuted model ( $Q2Y > 0$ ). **C.** Variable Correlations analysis models the overlap between loadings and score plot revealing metabolites that are primarily represented in specific groups. **D.** Observation diagnostics analysis revealed outliers of the dataset that do not conform to the general correlation structure. **E-J.** Gut microbiome derived metabolites reveal to be highest upregulated in the serum following IF. **E.** Indole-3-propionic acid is shown to be completely depleted by vancomycin treatment. (N= AL: 8, IF: 9 mice per group;  $***p < 0.01$ , significance assessed by One-way ANOVA, Dunnett's multiple comparisons test, p-value indicates comparison to AL. mean±SEM). **F.** LC-MSMS measurements of IPA in serum from mice following 10 days of intermittent fasting vs. Ad libitum (N=5, significance assessed using students t-test, mean±SEM) **G.** LC-MSMS measurements of IPA in serum from mice following 10 days of IF vs AL with and without Vancomycin treatment (N=3, significance assessed using One-way ANOVA, Dunnett's multiple comparisons test, p-value indicates comparison to AL. mean±SEM) **H-J.** 3-indolelactic acid 2, Xylose 2 and 2,3-butanediol 2 upregulated in the IF groups. Xylose 2 acid shown to be depleted to AL levels by vancomycin treatment. (N= AL: 8, IF: 9 mice per group;  $*p < 0.05$ ,  $**p < 0.01$ ,  $***p < 0.001$ ,  $****p < 0.0001$  significance assessed by One-way ANOVA, Dunnett's multiple comparisons test, p-value indicates comparison to AL control group. mean±SEM).

Metabolite	log FC	p-value			Rsq
		IF vs AL	Ab vs non-Ab	interaction	
indole-3-propionic acid	0.83	1.11E-05	4.26E-06	9.07E-04	7.94E-01
3-indolelactic acid 2	1.47	2.73E-05	7.67E-02	2.50E-01	4.50E-01
xylose 2	1.11	3.47E-04	1.72E-01	8.79E-03	4.74E-01
2,3-butanediol 2	1.37	3.03E-04	2.40E-01	2.25E-01	5.06E-01
L-threonine 1	0.43	3.89E-03	7.72E-01	3.54E-01	4.02E-01
adenosine	-3.67	7.00E-03	6.61E-01	8.21E-01	2.84E-01
glycine	0.26	7.28E-03	8.04E-01	2.44E-01	1.85E-01
DL-isoleucine	0.6	1.39E-02	8.63E-02	3.13E-01	3.56E-01
phosphoric acid	-0.35	1.80E-02	9.14E-02	2.32E-02	9.13E-02
L-proline 2	0.50	2.00E-02	6.02E-01	7.89E-01	1.73E-01

 P<0.001

**Table 1.** Indole-3-propionic Acid is significantly increased in the serum in IF vs AL.

Listed are metabolites differentially abundant in the serum of IF vs AL treated mice. Shown are the log fold change (logFC), IFvsAL p-value, Vancomycin vs non-Vancomycin p-value (Ab vs non-Ab) and the interaction p-value between intermittent fasting condition and vancomycin treatment (interaction). R-square (Rsq, the coefficient of determination) showed the highest predictability (79.4%) for indole-3-propionic acid.

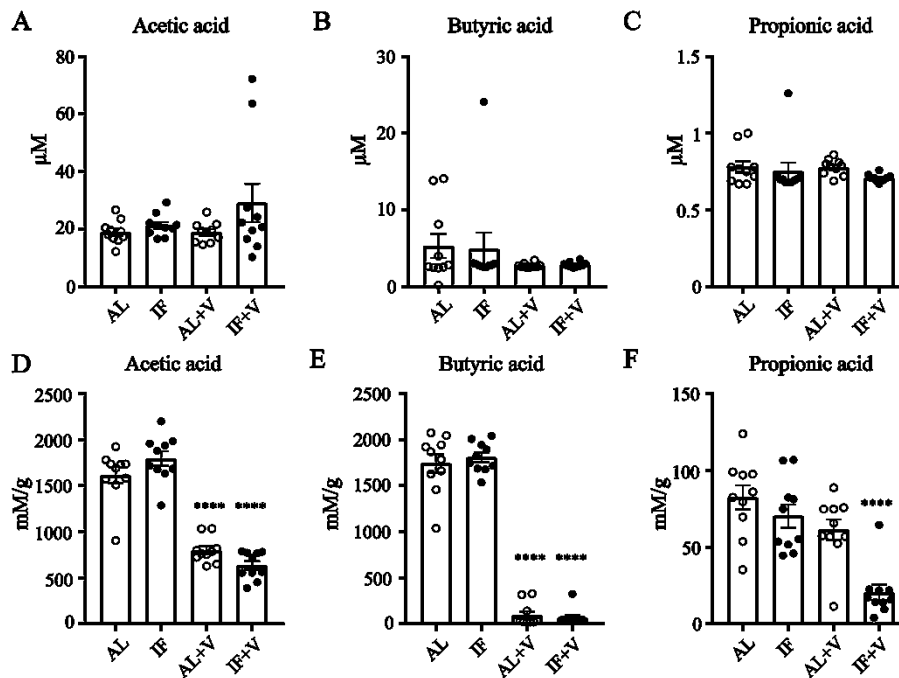


**Figure 15.** GC-MS targeted metabolomics analysis identifies no changes for SCFAs

**A-D.** Short chain fatty acid concentrations were analysed using targeted GC-MSMS metabolomics in the serum of AL, IF, AL+V and IF+V treatment conditions. No difference was observed for acetic acid (A), butyric acid (B) and propionic acid (C). **D-F.** Short chain fatty acid concentrations in the cecum of AL, IF, AL+V and IF+V treatment conditions. No difference was observed for acetic acid (E), butyric acid (F), propionic acid (G). Acetic acid (E) and butyric acid (F) were reduced and depleted by Vancomycin, respectively (N=10 mice per group; One-way ANOVA, Dunnett's multiple comparisons test, p-value indicates comparison to AL control group. mean±SEM).

### 3.5 16S sequencing reveals increased number of Clostridiales following intermittent fasting

So far, we established that IF improves axonal regeneration in mice that it requires gram+ microbiota and that it leads to a significant increase in serum IPA. Recent studies found that IF increases the microbial diversity<sup>301,302</sup> as well as the Firmicutes/Bacteroidetes ratio<sup>264,307</sup> in the cecum. Therefore, we next aimed to analyse how IF changes the microbial composition and diversity in the gut that could align with the increased production of IPA. We conducted 26S sequencing from microbial DNA extracted from the cecum of IF vs AL fed mice (8 per group) with and without vancomycin treatment. The relative abundance of the bacterial phyla showed an increase for Firmicutes in IF vs AL. Non-surprisingly, vancomycin treatment decreased the number of Firmicutes and Bacteroidetes resulting in a larger population of most gram negative Proteobacteria and gram negative Verrucomicrobia (Fig. 16A). As expected, bacterial order composition analysis revealed a nearly total depletion of Clostridiales in vancomycin treated

groups. (AL: 35.22%, IF: 38.51%, AL+V: 12.43%, IF+V: 1.77%) (Fig. 16B). A close look at the two graphs (Fig. 15A and B) reveals that the main increase of Firmicutes upon IF belongs to the order of Clostridiales. Figure 8C shows the quantification of Clostridiales by overall log (abundance), with strong reduction of Clostridiales by vancomycin treatment (Fig. 16C). Assessment of the Alpha diversity of the bacterial populations was used to explore the intra-sample variation to assess overall bacterial diversity (Alpha diversity was calculated using raw counts). The Shannon-Weaver index (Fig. 16D) is commonly used to assess bacterial diversity based on operational taxonomic units. Indeed, vancomycin treatment reduced the bacterial diversity as expected (Fig. 16D). However bacterial diversity was not found to be significantly increased in IF vs AL (Fig. 16D). Lastly, we plotted the top 25 amplicon sequence variants (ASVs) that are statistically different ( $FDR < 0.05$ ) between IF and AL, which belonged to either the order of Bacteroidales or Clostridiales (Fig. 16E). Interestingly, the top 5 most increased bacterial orders (ASV 390, ASV 246, ASV 6, ASV 99 and ASV 86) belonged to the order of Clostridiales, which have previously been associated with the maintenance of gut health and normal weight<sup>407</sup>. Importantly, Clostridiales are largely responsible for IPA production<sup>254</sup>. Together, we can conclude that while as expected vancomycin depletes gram+ bacteria, 10 days of IF affects the gut microbial composition mainly increasing the Firmicutes/Bacteroidetes ratio and the bacterial order of Clostridiales.

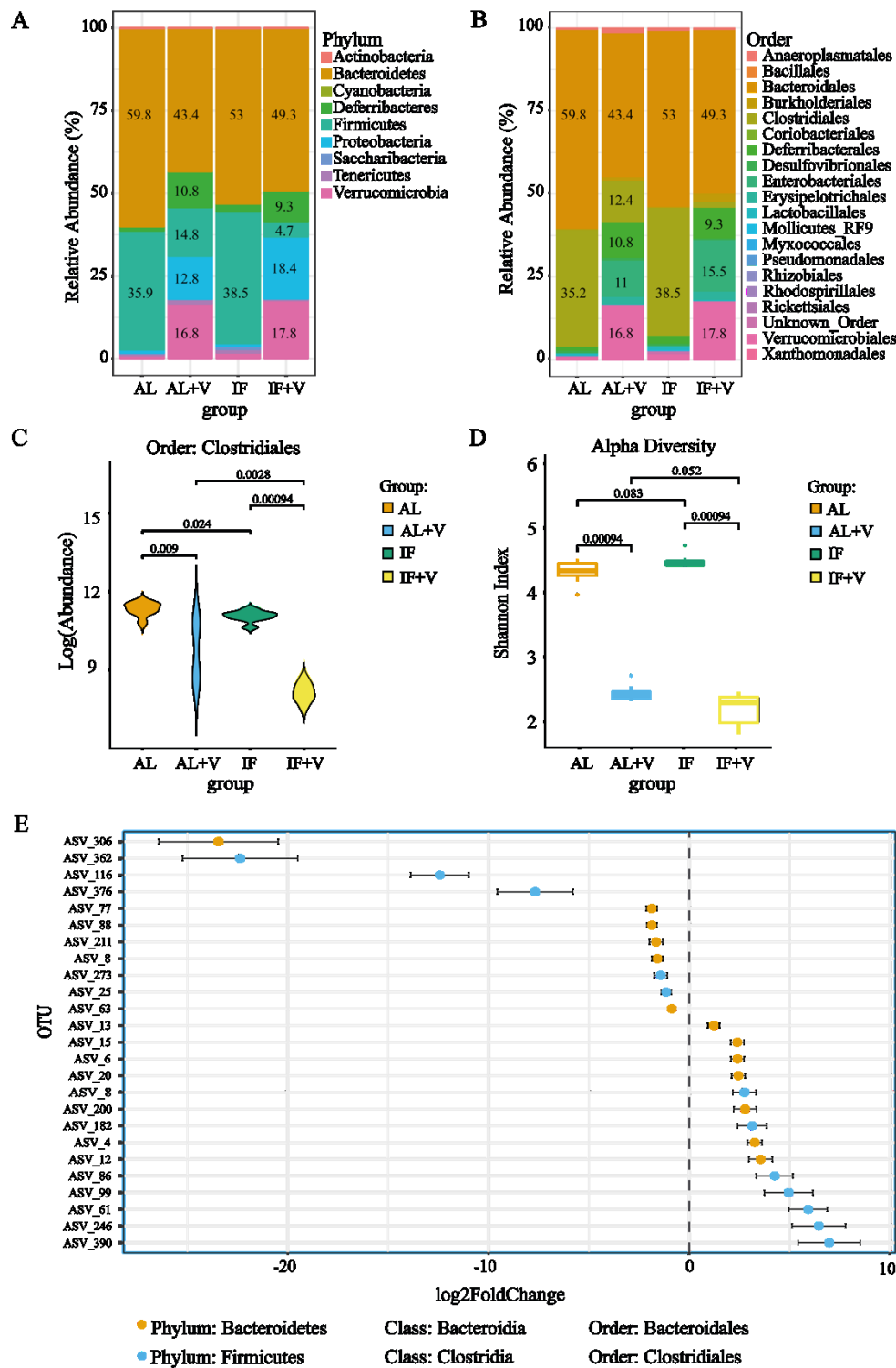


**Figure 16.** 16S-sequencing reveals increased number of Clostridiales following intermittent fasting. 16S sequencing was carried out from cecum of AL, AL+Vancomycin, IF, IF+Vancomycin treated animals (N=8). **A+B.** Relative abundance (%) of bacterial phyla (**A**) and bacterial order (**B**) between AL, AL+Vancomycin, IF and IF+Vancomycin. **C.** Log(abundance) of bacterial Order of Clostridiales. Mann Whitney U test was used for significance assessment, showing significant reduction of gut bacteria upon vancomycin treatment. **D.** Shannon index reveals significant



differences in Alpha diversity between Vancomycin vs non-vancomycin treated groups (Significance between samples was assessed using Mann Whitney U test). **E.** Plot showing that the top 25 bacterial Amplicon sequence variants (ASVs) that are statistically different ( $p < 0.05$ , FDR corrected, plotted as  $\log_2\text{FoldChange}$ ) between IF and AL belong to either of Bacteroidetes or Firmicutes phyla, Bacteroida or Clostridia classes and Bacteroidales or Clostridiales order of bacteria. The highest increase bacterial order was 5 ASVs of Clostridiales.

### **3.6 IPA is required for and promotes axonal regeneration via a DRG neuron extrinsic mechanism**

So far, we have found that IPA is the top candidate bacteria metabolite with the potential to underpin the IF-dependent regenerative phenotype that was reversed by vancomycin, which depleted gram+ bacteria and IPA.

IPA is solely synthesised by the gut microbiome, primarily by bacteria belonging to the Phylum of the Firmicutes and the bacterial species *Clostridium sporogenes*. Therefore, we first designed an experiment to test whether *Clostridium sporogenes* producing IPA were needed for axonal regeneration after sciatic nerve crush. Specifically, we took advantage of a *Clostridium sporogenes fldC* (*C.s. fldC*) bacterial strain recently generated by our collaborators Dr. Dodd (Stanford) that is mutant for the (R)-phenyllactyl-CoA dehydratase beta subunit, which results in the loss of IPA production. We recolonised the gut via a two-step protocol, starting with bacterial depletion using vancomycin for 3 days followed by 10 days of bacterial gavage until the execution of a sciatic nerve crush (Fig. 17A). As expected, LC-MSMS analysis showed total depletion of IPA from the serum of mice recolonised with the *C.s. fldC* compared to the *C.s. WT* strain (*C.s. WT*:  $0.232 \pm 0.126 \mu\text{g/ml}$ , *C.s. fldC*:  $0.002 \pm 0.002 \mu\text{g/ml}$ ) (Fig. 17B). Regeneration was assessed by SCG-10 immunostaining of the injured sciatic nerve. We found that recolonization of the gut with *C.s. fldC* significantly reduced the number of SCG-10 positive fibres up to 3000  $\mu\text{m}$  past the crush side, by about 50% (Fig. 17C-D). The quantification of the regeneration index further supported these findings (Fig. 17E). Subsequently, we aimed to test if IPA in vivo treatment prior to injury would promote axonal regeneration of the sciatic nerve. Treatment was conducted via gavage at 20 mg/kg/day for 10 consecutive days (Fig. 17F). Serum measurements using LC-MSMS showed a 13.6-fold increase in IPA half an hour after gavage (PBS:  $1.92 \pm 0.247 \mu\text{g/ml}$ , IPA:  $26.05 \pm 2.526 \mu\text{g/ml}$ ) (Fig. 17G). Following 10 days of IPA administration, a sciatic nerve crush was carried out and axonal regeneration was assessed 72 hours later by SCG-10 immunostaining (Fig. 17H). SCG-10 intensity measurements revealed a significant increase in the number of fibres up to 4000  $\mu\text{m}$  past the crush side, which was further confirmed by the quantification of the regeneration index (PBS:  $1841 \pm 101.8 \mu\text{m}$ , IPA:  $2463 \pm 161.3 \mu\text{m}$ ) (Fig. 17I-J).

To this point gain and loss of function experiments have been conducted by oral gavage. Previous publications have found that IPA binds to its receptor PXR in the gut epithelium affecting the gut permeability significantly possibly by modulating tight junctions<sup>254,256</sup>. In order to assess if IPA production within the gut and gut epithelium is required to enhance axonal regeneration, we repeated IPA treatments, this time via intraperitoneal (IP) injection. Injection of IPA (20 mg/kg/day, 10 days) mirrored the effects on regeneration that we found via gavage (Fig. 17K-N). In fact, IPA treatment led to significantly increased SCG-10 intensity up to 4500  $\mu\text{m}$  past the crush side with a regeneration index of  $1538 \pm 170.5 \mu\text{m}$  for PBS and  $2325 \pm 159.3 \mu\text{m}$  for IPA treated mice (Fig. 17M-N). Finally, we asked if the effect on axonal regeneration requires direct IPA signalling to DRG neurons. To test this hypothesis, we treated DRG neurons in culture with increasing concentrations of IPA for 12 hours and quantified neurite outgrowth (1  $\mu\text{M}$ , 10  $\mu\text{M}$ , 100  $\mu\text{M}$ ) (fig. 17O-Q). All three concentrations of IPA showed a very similar outgrowth to the non-treated control condition (PBS control:  $1594 \pm 262.4 \mu\text{m}$ , 1 $\mu\text{M}$  IPA:  $1651 \pm 459.2 \mu\text{m}$ , 10 $\mu\text{M}$  IPA:  $2003 \pm 303.8 \mu\text{m}$ , 100 $\mu\text{M}$  IPA:  $1849 \pm 139.9 \mu\text{m}$ ) (Fig. 16P).

In summary, we can conclude that *Clostridium sporogenes*-dependent IPA production is required for axonal regeneration and that oral as well as systemic IPA delivery prior to sciatic injury enhance axonal regeneration by a tissue resident DRG extrinsic mechanism.

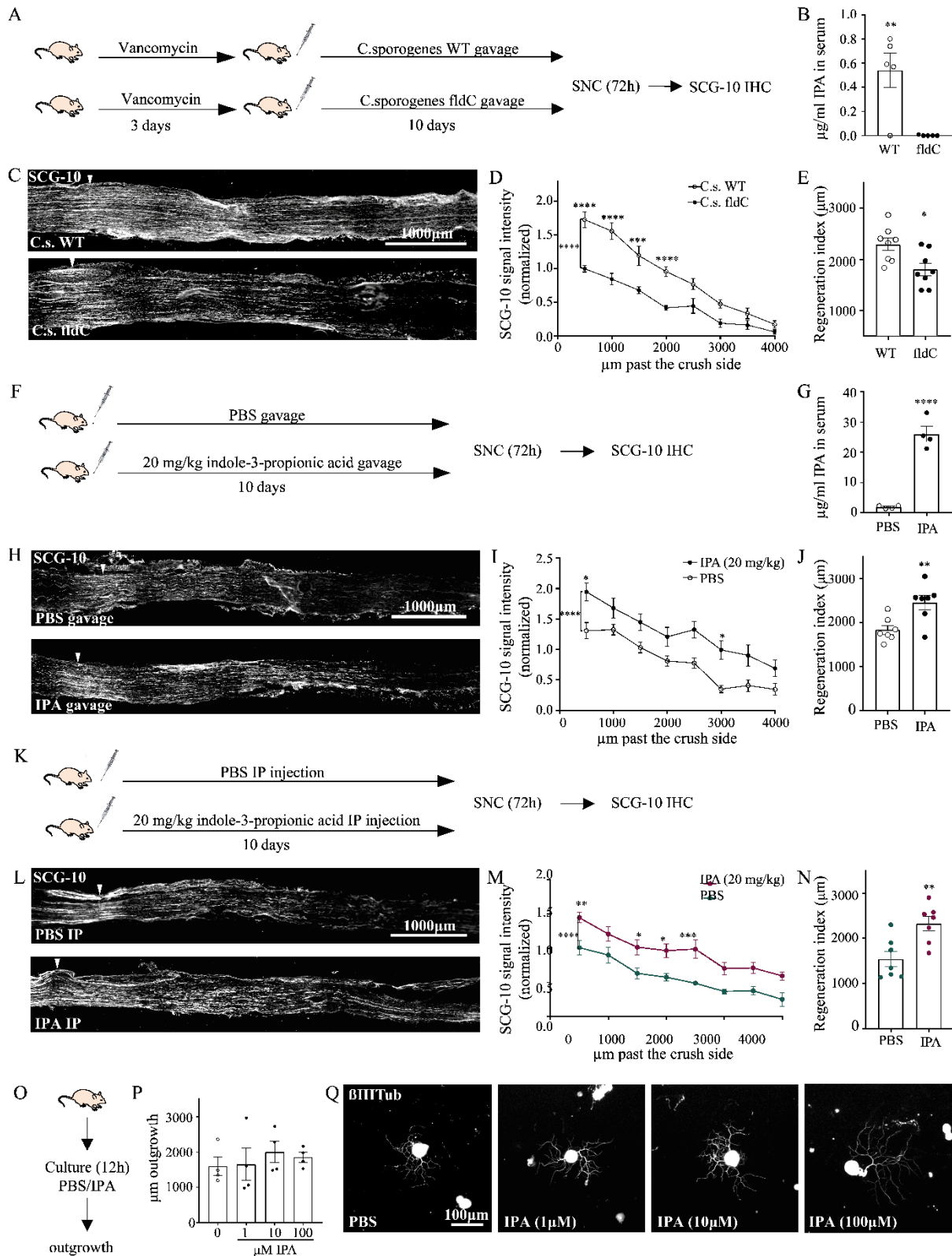


**Figure 17. Indole-3-propionic acid indirectly promotes axonal regeneration of DRG neurons**  
**A-E.** Recolonization of the gut microbiome with *C. sporogenes fldC* and wildtype (WT). **A.** Schematics outlines the experimental setup. **B.** LC-MSMS measurements of IPA in serum from mice following 10 days of *Clostridium sporogenes* wildtype vs mutant (*fldC*) transplantation via gavage

( $N=5$ , significance assessed using students  $t$ -test,  $\text{mean}\pm\text{SEM}$ ) **C.** micrograph of representative longitudinal section images of sciatic nerves immunostained with SCG-10 following 10 days of recolonising with *C.s. fldC* or *WT* and 3 days post sciatic nerve crush (Scheme in **A**). Scale bar:  $1000\ \mu\text{m}$ . The arrowhead indicates the crush site **D.** Quantification of SCG-10 intensity at the indicated distances and normalized to the intensity before the crush site. Normalised SCG-10 intensity was plotted as a function of the distance from the crush site. ( $N=8$  nerves from 4 mice per group with a bilateral sciatic nerve crush; \*\*\*\* $p<0.0001$ , \*\*\* $p<0.001$ , by Two-way-ANOVA with Sidaks test,  $\text{mean}\pm\text{SEM}$ ) revealed decreased regeneration when colonised with *C.s. fldC*. **E.** SCG-10 intensity was measured from the crush site towards the distal end and normalised to the crush site as percentage of intensity. SCG-10 intensity percentage of 50% was plotted as a function of the distance from the crush site and revealed loss of regeneration following the sciatic nerve crush in *C.s fldC* vs *C.s. WT* gavage groups. ( $N=8$  nerves per group from 4 mice with bilateral sciatic nerve crush; \* $p<0.05$ . by students  $t$ -test,  $\text{mean}\pm\text{SEM}$ ). **F-J.** Administration of IPA by gavage promotes axonal regeneration of the sciatic nerve. **F.** Schematics outlines the experimental setup. **G.** LC-MSMS quantification of IPA in serum from mice following 10 days of IPA gavage ( $N=4$ , significance was assessed using students  $t$ -test,  $\text{mean}\pm\text{SEM}$ ). **H.** micrograph of representative images of sciatic nerves immunostained with SCG-10 following 10 days of IPA gavage (20 mg/kg/day) and 3 days post sciatic nerve crush. Scale bar:  $1000\ \mu\text{m}$ . The arrowhead indicates the crush site **I.** Quantification of SCG-10 intensity at the indicated distances and normalized to the intensity before the crush site. Normalised SCG-10 intensity was plotted as a function of the distance from the crush site. ( $N=8$  nerves from 4 mice per group with a bilateral sciatic nerve crush; \*\*\*\* $p<0.0001$ , \* $p<0.05$ , by Two-way-ANOVA with Sidaks test,  $\text{mean}\pm\text{SEM}$ ) revealed increased regeneration in mice gavaged daily with IPA **J.** In vivo regeneration index was calculated and revealed increased regeneration following the sciatic nerve crush in IPA vs PBS gavage groups. ( $N=7$  nerves per group from 4 mice with bilateral sciatic nerve crush; \* $p<0.05$ . by students  $t$ -test,  $\text{mean}\pm\text{SEM}$ ). **K-N.** Systemic administration of IPA by intraperitoneal (IP) injection promotes axonal regeneration of the sciatic nerve. **K.** Schematics outlines the experimental setup. **L.** micrograph of representative longitudinal section images of sciatic nerves immunostained with SCG-10 following 10 days of IPA IP injection (20 mg/kg/day) and 3 days post sciatic nerve crush. Scale bar:  $1000\ \mu\text{m}$ . The arrowhead indicates the crush site **M.** Quantification of SCG-10 intensity at the indicated distances and normalized to the intensity before the crush site. Normalised SCG-10 intensity was plotted as a function of the distance from the crush site. ( $N=7$  nerves from 4 mice per group with a bilateral sciatic nerve crush; \* $p<0.05$ . \*\* $p<0.01$ , \*\*\* $p<0.001$ , \*\*\*\* $p<0.0001$  by Two-way-ANOVA with Sidaks test,  $\text{mean}\pm\text{SEM}$ ) revealed increased regeneration in mice injected daily with IPA **N.** In vivo regeneration index was

calculated and revealed increased regeneration following the sciatic nerve crush in IPA vs PBS IP groups. ( $N=7$  nerves per group from 4 mice with bilateral sciatic nerve crush;  $**p<0.01$ . by students  $t$ -test,  $mean\pm SEM$ ). **O-Q** *in vitro* IPA treatment of DRG cell cultures does not affect neurite outgrowth. DRG neurons were treated with  $1\mu M$ ,  $10\mu M$  and  $100\mu M$  IPA (schematics in **O**). **P**. Quantification of  $\beta III$ -Tubulin ( $\beta III$ Tub, green) immunostained neurite outgrowth by measuring the length of neurites ( $N=4$  replicates per group; significance assessed by One-way ANOVA, Dunnett's multiple comparisons test,  $mean\pm SEM$ ). **Q**. Representative images of DRG neurons immunostained with  $\beta III$ -Tubulin, cultured for 12 hours.

### **3.7 RNA sequencing reveals upregulation of immune regulatory pathways following IPA treatment**

In order to investigate IPA-dependent molecular changes in gene expression and signalling pathways that would prime DRG neurons for axonal regeneration, we conducted RNA sequencing from DRG preceding (naïve) or 3 days after a sciatic nerve crush injury following 10 days of IPA or PBS oral gavage.

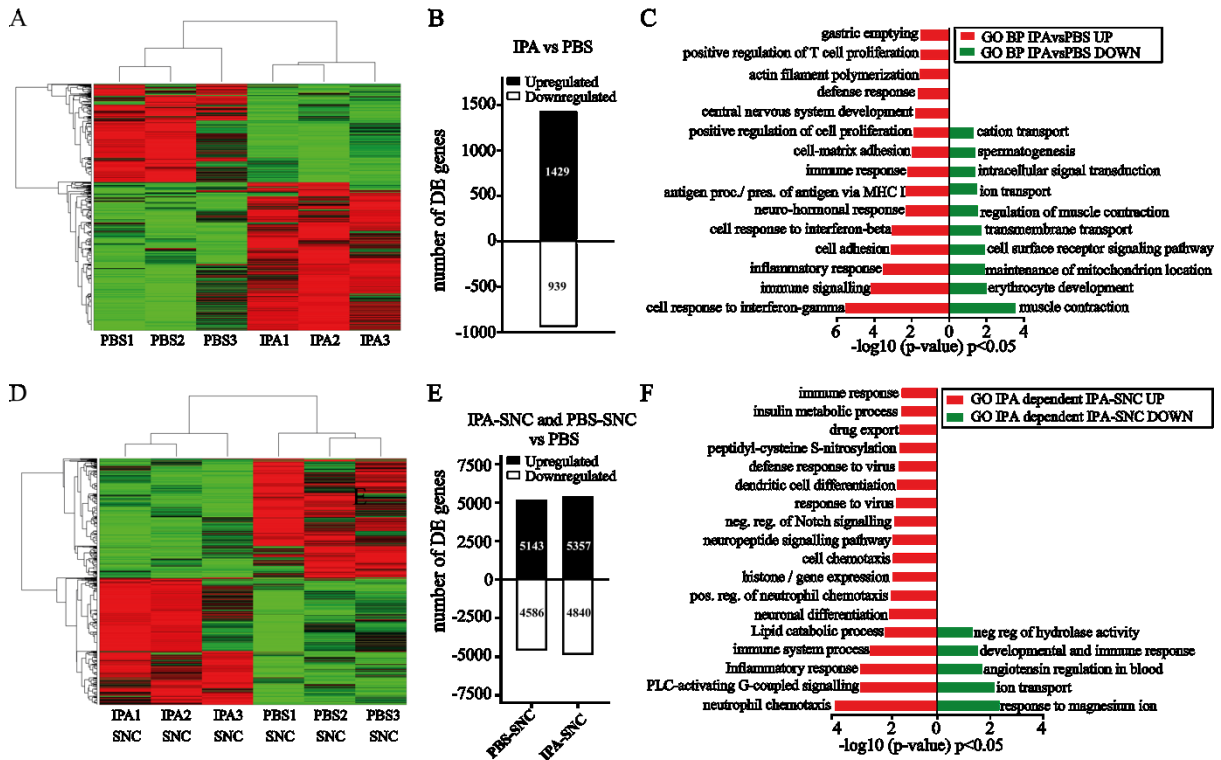
RNA sequencing analysis from naïve DRG showed that IPA treatment strongly alters the gene expression programme inside the DRG tissue. Clear separation of the two groups is shown by heat map clustering (Fig. 18A). We found 1429 differentially upregulated and 939 downregulated genes between IPA vs PBS treated animals (Fig. 18B). Interestingly, GO biological process (GO BP) analysis of the upregulated genes between IPA and PBS were dominated by immune-regulatory categories, with the most significant ones being “cell response to interferon-gamma”, “immune system process”, “inflammatory response”, “cell response to interferon-beta” and “antigen processing and presenting of antigen via MHC-I”. Most significantly down regulated GO categories were related to rather intracellular processes such as “muscle contraction”, “maintenance of mitochondria location” or “cell surface receptor signalling” (Fig. 18C). Heat map clustering from IPA vs PBS treated DRG following 3 days of SNC revealed that IPA continues to significantly alter gene expression following injury (Fig 18F). RNA sequencing analysis revealed more upregulated and downregulated genes in IPA vs PBS treated animals (IPA-SNC: UP: 5357, DOWN: 4840; PBS-SNC: UP: 5143, DOWN: 4586) (Fig. 18D). GO biological process (GO BP) analysis was carried out with exclusion of genes that overlap between IPA-SNC and PBS-SNC. Consequently, solely injury dependent changes in gene expression were removed, enabling to focus on IPA-dependent alterations in gene expression following SNC. Analysis of the down regulated genes showed a decrease in ion transport and response as most significant, however it also contained the category “immune response”. Upregulated categories were dominated by immune regulatory processes, with the most significant one being “neutrophil chemotaxis”, followed by

“Inflammatory response” and “immune system process”. However, signalling pathways such as “PLC-activating G-coupled signalling”, “neuropeptide signalling pathway”, as well as “positive regulation of gene expression” were also upregulated upon IPA-SNC treatment (Fig 18G).

It is striking that the majority of the IPA dependently upregulated GO BP clusters can be categorised as ‘immune signalling’, which is largely maintained and aggregated at 3 days after SNC. We found that IPA increased immunostimulatory (TNFR, IL17b) but also anti-inflammatory signalling molecules (IL10, CLTA4) in the DRG tissue indicating a complex IPA dependent immune regulatory microenvironment. Importantly, expression of the gene encoding Pregnane X Receptor (Nr1i2), the nuclear receptor that IPA binds to, was increased by 3-fold in DRG from IPA vs PBS and IPA-SNC vs PBS-SNC treated animals.

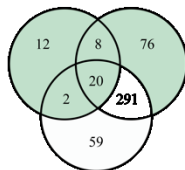
In order to visualise the functional clusters that drive the GO BP results, we extracted the genes classified in immune related GO BP categories and excluded genes that were solely injury induced (Fig 18H, Venn diagram). Next, we generated a protein-protein interaction network using the STRING database and labelled the genes by their primary cell type or signalling function. This network of IPA dependent immune signalling genes emphasized what was previously found in the GO BP analysis, with the main clusters summarized in following categories: “IFN $\gamma$ / $\beta$  signalling”, “MHCI subunits and assembly”, “T-cell/NK-cell activation/signalling” and “Innate immune signalling”, “CEBP TFs” and “TNF signalling” (Fig. 18H). The cluster “innate immune signalling” primarily contains genes of the antibacterial complement component complex, genes involved in neutrophil chemotaxis and genes indicating inflammasome activation and IL1b secretion. Interestingly, genes categorised in “PLC-activating G-coupled signalling” in the GO BP analysis (Fig. 17G) are functionally involved in immune cell signalling, of which Gpr84, Ltb4r1/2 and Cxcr2 specifically have been shown to take part in neutrophil chemotaxis and signal transduction<sup>408-411</sup>. In line with this analysis, we found that neutrophil ligand Cd177, endothelial neutrophil chemoattractant chemokine (C-X-C motif) ligand 1 (Cxcl1) and its receptor C-X-C Motif Chemokine Receptor 2 (Cxcr2) were exclusively upregulated in the IPA-SNC dataset, and not following injury only (PBS-SNC vs PBS) (Figure 18I). Specifically, CXCL1 is one of the major attractants of neutrophils binding to its receptor CXCR2.

In summary, we can conclude that IPA increases immune signalling inside the DRG tissue, which is further increased following sciatic nerve injury. Specifically, the most significantly upregulated GO categories suggest IPA to be involved in neutrophil recruitment and the activation of IFN $\gamma$  signalling.



**G. DE genes from upregulated immune regulatory pathways (GO BP)**

IPA vs PBS      IPA-SNC vs PBS



PBS-SNC vs PBS

- IFN $\gamma$ / $\beta$
- MHC I subunits and assembly
- T-/NK-cell activation/signalling
- CBBP TFs
- Innate immune signalling
- TNF signalling
- Other

**H**

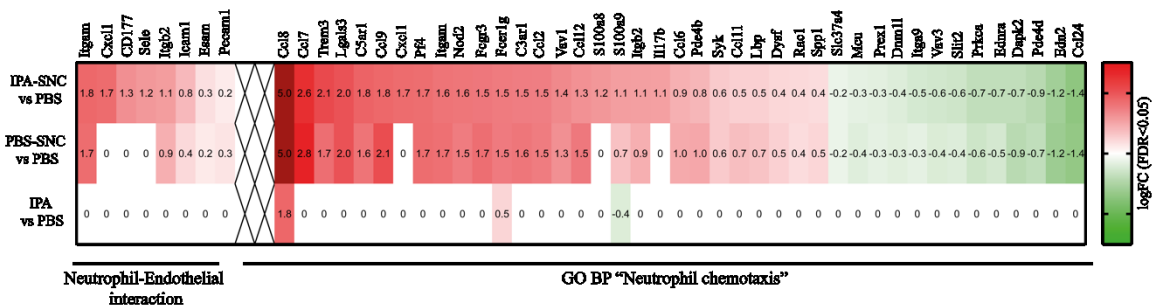


**Figure 18. RNA sequencing reveals upregulation of immune regulatory pathways following IPA treatment**

RNA sequencing from DRG bulk tissue following 10 days of IPA treatment (A-C) and following IPA treatment combined with a 72 hours of sciatic nerve injury (D-G). A-B. Shown are differentially regulated genes following IPA vs PBS treatment for 10 days as heat map (A) and graph (B). C. GO biological process analysis of up- and downregulated genes following IPA treatment. Shown are significantly up- and downregulated GO pathways categorized by DAVID Bioinformatics Database and Graphed as  $-\log_{10}$  of p-value ( $p < 0.05$ ). D-F. Shown are differentially regulated genes between PBS-SNC and IPA-SNC as heat map (D) and IPA-SNC vs PBS and PBS-SNC vs PBS as graph (E). G. GO biological process analysis of up- and downregulated genes following IPA treatment and 72 hours post injury. Shown are IPA dependent significantly up or downregulated GO pathways categorized by DAVID Bioinformatics Database and Graphed as  $-\log_{10}$  of p-value ( $p < 0.05$ ) H. Network showing IPA dependently upregulated genes from significant GO BP pathways classified as immune regulatory. The Venn diagram shows the number of genes from each dataset included in the network (green background). Injury dependently upregulated immune regulatory genes were excluded (PBS-SNC vs PBS overlap with IPA-SNC vs PBS, 281 genes). Nodes circled in red are genes categorised in the GO BP: "Neutrophil chemotaxis". Network was generated using <https://string-db.org/> and was annotated into gene functions categories. I. Heat map showing the logarithmic expression fold change ( $\log_{2}FC$  ( $FDR < 0.05$ )) of all genes categorized as involved in "Neutrophil-Endothelial interaction" or "GO BP Neutrophil chemotaxis" for the comparisons IPA-SNC vs PBS, PBS-SNC vs PBS and IPA vs PBS.



### **3.8 IPA increases the number of neutrophils and NK cells in the spleen, mesenteric lymph nodes and DRG following sciatic nerve crush.**

RNA sequencing analysis suggested a potential recruitment of neutrophils to the DRG tissue, implicating a role of IPA in neutrophil chemotaxis.

Immunostaining for neutrophils was carried out using the neutrophil marker Ly6G and the number of neutrophils per DRG section was quantified. Due to the localization of neutrophils surrounding the DRG tissue, the number was normalised to the area between the perimeter and 30  $\mu\text{m}$  off the perimeter of the DRG (Fig 19A). We found that IPA treatment alone increased the number of neutrophils around the DRG tissue by 3.8-fold (PBS:  $1.73 \pm 0.28$ , IPA:  $6.623 \pm 0.68$ ). At 3 days post injury the number of neutrophils in the PBS treated control increased by 2-fold (PBS+SNC:  $3.68 \pm 0.699$ ) compared to non-injured (PBS:  $1.73 \pm 0.28$ ). Not a significant difference was observed in the IPA+SNC group compared to IPA alone (IPA:  $6.623 \pm 0.68$ , IPA+SNC:  $7.99 \pm 1.69$ ). This indicates that IPA treatment increases the number of neutrophils largely independently from sciatic nerve crush (Fig. 19B). Next we immuno-stained sciatic nerve sections for Ly6G to assess neutrophil infiltration into the injury site at 3 days post injury. Ly6G immunofluorescence intensity was measured up to 1000 $\mu\text{m}$  proximal and distal to the crush side. No significant difference was found between the IPA and PBS treated groups (Fig 19C-D).

IPA has previously been reported to broadly affect immune regulation locally in the gut<sup>256</sup> as well as systemically<sup>254</sup>. In order to analyse the effect of IPA on the immune environment around the ileum and cecum as well as systemically, we performed an immune screen by using fluorescence activated cell sorting (FACS) from spleen and mesenteric lymph nodes from IPA and PBS treated animals naïve (PBS, IPA) as well as 3 days post SNC injury (PBS+SNC, IPA+SNC). The cells were immunolabeled for cell markers of the innate and adaptive immune system, specifically: monocytes, neutrophils, NK cells, NKT cells, CD4 T-cells, CD8 T-cells and B-cells. Analysis of the spleen revealed an increase of neutrophils and NK cells in the IPA+SNC group (Fig. 20C, D). No change in cell numbers was found for T-cells, B-cells, monocytes and NKT cells (Fig. 20B, E-H). Analysis of the mesenteric lymph nodes showed significantly more CD45-positive immune cells in IPA+SNC samples compared to PBS+SNC. Consistently with data from the spleen, we found an increase in neutrophils and NK cells in the IPA+SNC group, as well as an additional rise in the number of NKT-cells and B-cells upon IPA+SNC (Fig. 20K-M). No changes in cell numbers between the 4 groups were observed for monocytes and T-cells (Fig. 20J, N-O). These data suggest that IPA directly affects neutrophil and NK cell numbers systemically and in mesenteric lymph nodes following sciatic nerve injury. Intriguingly, these results strongly align with the RNA sequencing data suggesting an effect of IPA on neutrophil chemotaxis. In conclusion we could show that IPA treatment increases the number of neutrophils locally into the DRG tissue and,

coupled with injury, systemically. This suggests that the regenerative effect of IPA on the sciatic nerve may be mediated through neutrophil signalling to DRG neurons.

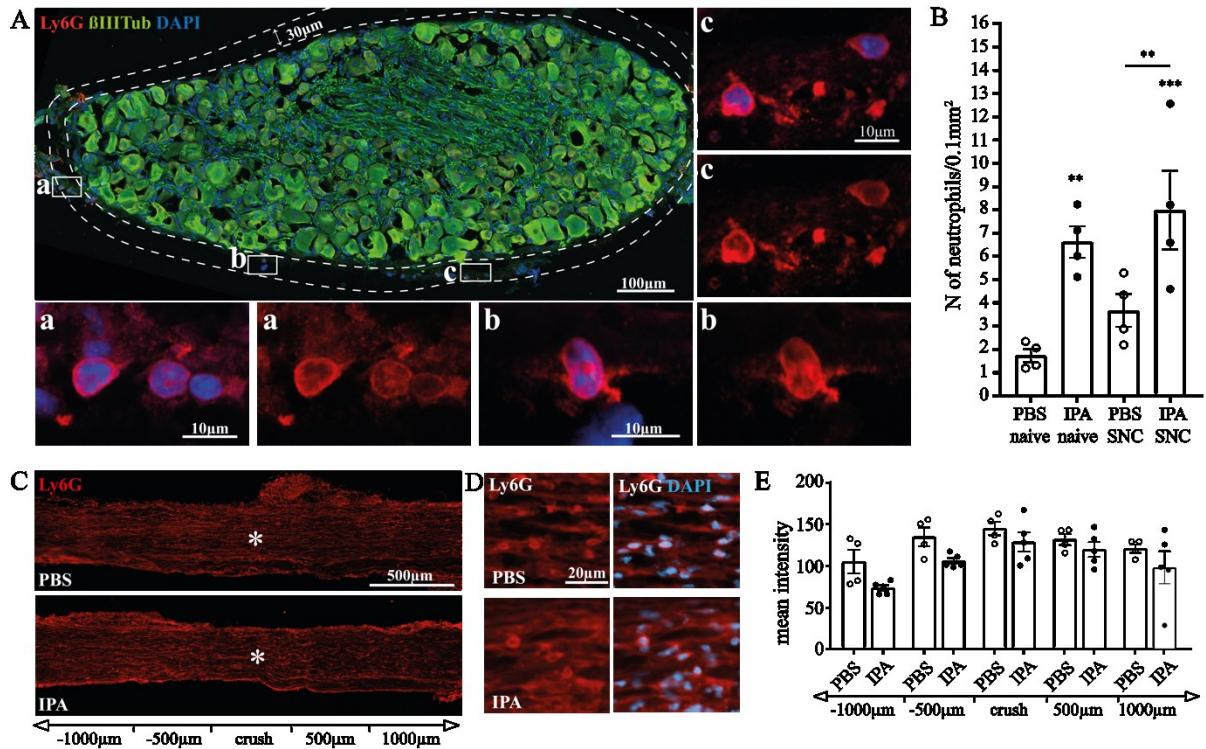
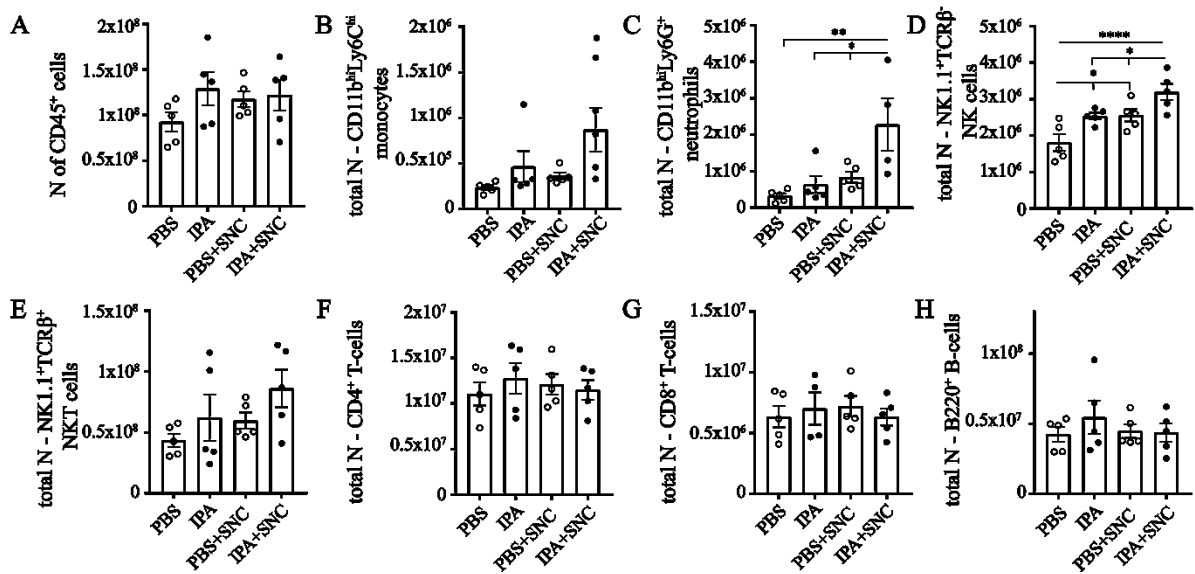


**Figure 19.** Immunohistochemical analysis of DRG and nerve crush side following IPA treatment.

**A+B.** Quantification of Neutrophils (Ly6G) at the DRG tissue following 10 days of PBS/IPA treatment, naive or 3 days after SNC. **A.** Representative image of a DRG stained for Ly6G (red),  $\beta$ IIITubulin ( $\beta$ IIITub, green) and DAPI (blue). Dotted line indicates the area neutrophils were identified and quantified in. Scale bar: 100  $\mu$ m. Boxes labelled as **a**, **b**, **c** show higher magnification images of Ly6G positive neutrophils. Scale bar: 10  $\mu$ m **B.** Quantitative analysis of neutrophils, shown as number of neutrophils per 0.1 mm<sup>2</sup> (N=4 mice per group; \* $p$ <0.05, \*\* $p$ <0.01, significance assessed by One-way ANOVA, multiple comparison testing: corrected by FDR method of Benjamini and Hochberg, if not indicated otherwise  $p$ -value compares to PBS group, mean $\pm$ SEM) **C-D.** Quantification of neutrophils (Ly6G) at the Nerve injury site at 3 days post injury. **C.** Longitudinal image of the sciatic nerve. Ly6G (red) IHC staining of the nerve crush side after IPA and PBS treatment. Asterix indicates the crush site. Scale bar: 500  $\mu$ m **D.** Higher magnification images of Ly6G-positive Neutrophils from panel C. Scale bar: 20 $\mu$ m **E.** Quantitative analysis by intensity measurements 1000 $\mu$ m proximal and distal to the crush side did not show any difference between IPA and PBS treated nerves (N=4-5 nerves from 3 mice per group, significance was assessed by two-way ANOVA using Tukeys test, mean $\pm$ SEM).

## Spleen



## Mesenteric lymph nodes

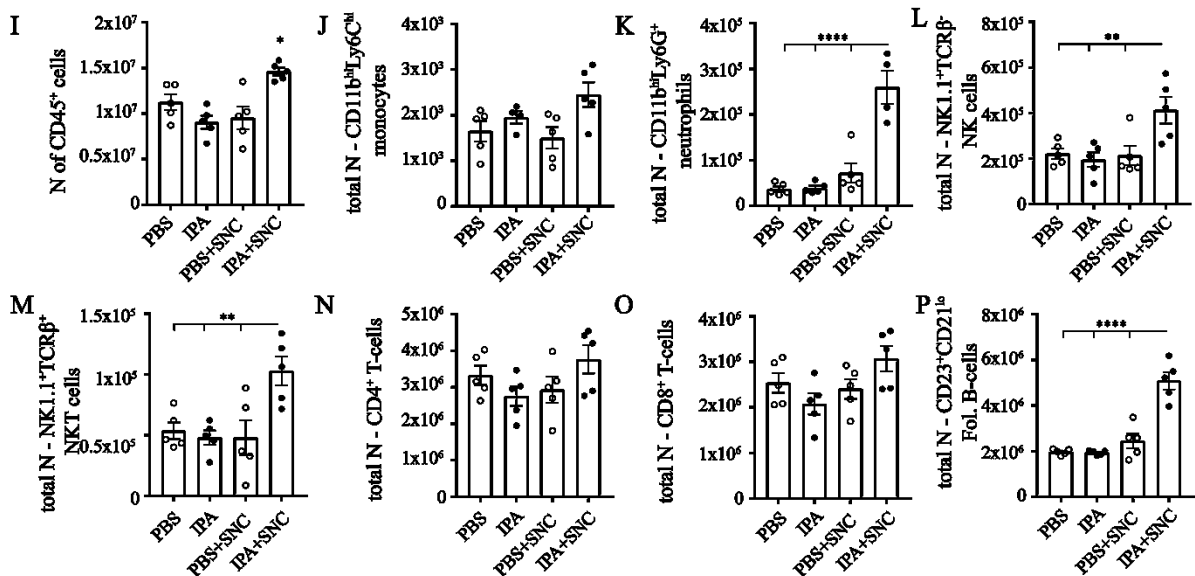


**Figure 20.** IPA increases the number of neutrophils and NK cells in spleen and mesenteric lymph nodes following sciatic nerve crush.

Immune cell screen of spleen (A-H) and mesenteric lymph (I-P) nodes using flow cytometry analysis following IPA treatment. Quantification of total number of CD45<sup>+</sup> cells (A+I), monocytes (B+J), neutrophils (C+K), NK-cells (D+L), NKT cells (E+M), CD4<sup>+</sup> T-cells (F+N), CD8<sup>+</sup> T-cells (G+O) and Follicular B-cells (H+P) in spleen and mesenteric lymph nodes, respectively (N=5, \*p<0.05, \*\*p<0.01, \*\*\*\*p<0.0001. Significance was assessed using One-way ANOVA, Multiple comparison testing: corrected by FDR method of Benjamini and Hochberg, if not indicated otherwise p-value compares to PBS group, mean±SEM).

### **3.9 Neutrophil chemotaxis and IFN $\gamma$ signalling mediate the effect of IPA**

These data imply that IPA might facilitate axonal regeneration in the sciatic nerve through the activation of neutrophil chemotaxis and neutrophil signalling in proximity of DRG neurons. Since RNA sequencing revealed that IPA treatment led to increased expression of IFN $\gamma$ , which is typically released upon neutrophil activation, we hypothesised that neutrophils and IFN $\gamma$  might be required for IPA-dependent axonal regeneration.

In order to test this hypothesis, mice were treated by gavage with either 20 mg/kg/day IPA or PBS for 10 consecutive days alongside intraperitoneal injections of monoclonal antibodies against neutrophils or IFN $\gamma$  (Fig. 21A-F). Following treatment, a sciatic nerve crush was induced, and nerves were immunostained for SCG-10 at 3 days post injury (Fig. 21B). In line with previous experiments, IPA treatment alone and IPA co-treated with IgG control antibody increased axonal regeneration following injury up to 3000  $\mu$ m past the crush side. Anti-Ly6G monoclonal antibody co-treatment with IPA decreased the regenerative potential to PBS control levels. No difference was observed between PBS and PBS co-treated with anti-Ly6G (Fig. 21C). These results were mirrored by the analysis of the regeneration index, showing 1.6-fold increase for IPA vs PBS (IPA:  $2066 \pm 204\mu$ m, PBS:  $1288 \pm 117.4\mu$ m) and a significant decrease down to control levels of IPA co-treated with anti-Ly6G ( $1455 \pm 164.7\mu$ m) (Fig. 21D). Anti-IFN $\gamma$  antibody treatment neutralises IFN $\gamma$  and prevents signalling through the IFN $\gamma$  receptor (IFN $\gamma$ R) (Fig 21A-B, E-F). Interestingly, anti-IFN $\gamma$  treatment closely phenocopies the inhibition of regenerative ability observed with the anti-Ly6G treatment. The number and distance of regenerating fibres in the IPA - anti-IFN $\gamma$  group showed overlap with the PBS control. As expected, no difference was observed between PBS and PBS co-treated with anti-IFN $\gamma$  antibody (Fig. 21E). Analysis of the regeneration index confirms these results, showing a significant decrease of regenerative potential to control levels when IPA was co-treated with anti-IFN $\gamma$  ( $1382 \pm 144.6\mu$ m) (Fig. 21F). Next, we decided to assess if IFN $\gamma$  treatment has the potential to facilitate axonal growth directly in cultured DRG neurons since this remains to be investigated. DRG neuronal cultures were treated for 12 hours with a low (5 ng/ml) or high dose (100 ng/ml) of IFN $\gamma$ . Neurite outgrowth measurement revealed that both the low and high IFN $\gamma$  dose significantly enhanced neurite outgrowth (PBS:  $652.5 \pm 65.49\mu$ m, IFN $\gamma$  (5ng/ml):  $1115 \pm 51.14\mu$ m; (100 ng/ml):  $1048 \pm 94.86\mu$ m), with no detrimental effect on neuronal viability (Fig. 21G). Finally, we investigated whether delivery of IFN $\gamma$  in vivo can mimic IPA-mediated neurite outgrowth in DRG neurons. IFN $\gamma$  was injected intraperitoneally 48 hours before dissection followed by DRG culture for 12 hours. Neurite outgrowth analysis revealed twice as much growth in DRG cultures from mice injected with IFN $\gamma$  ( $864.6 \pm 101.3 \mu$ m) compared to PBS ( $423.9 \pm 6.404 \mu$ m). Together, these data indicate that IPA-dependent axonal regeneration following sciatic nerve crush needs neutrophils and IFN $\gamma$  signalling.

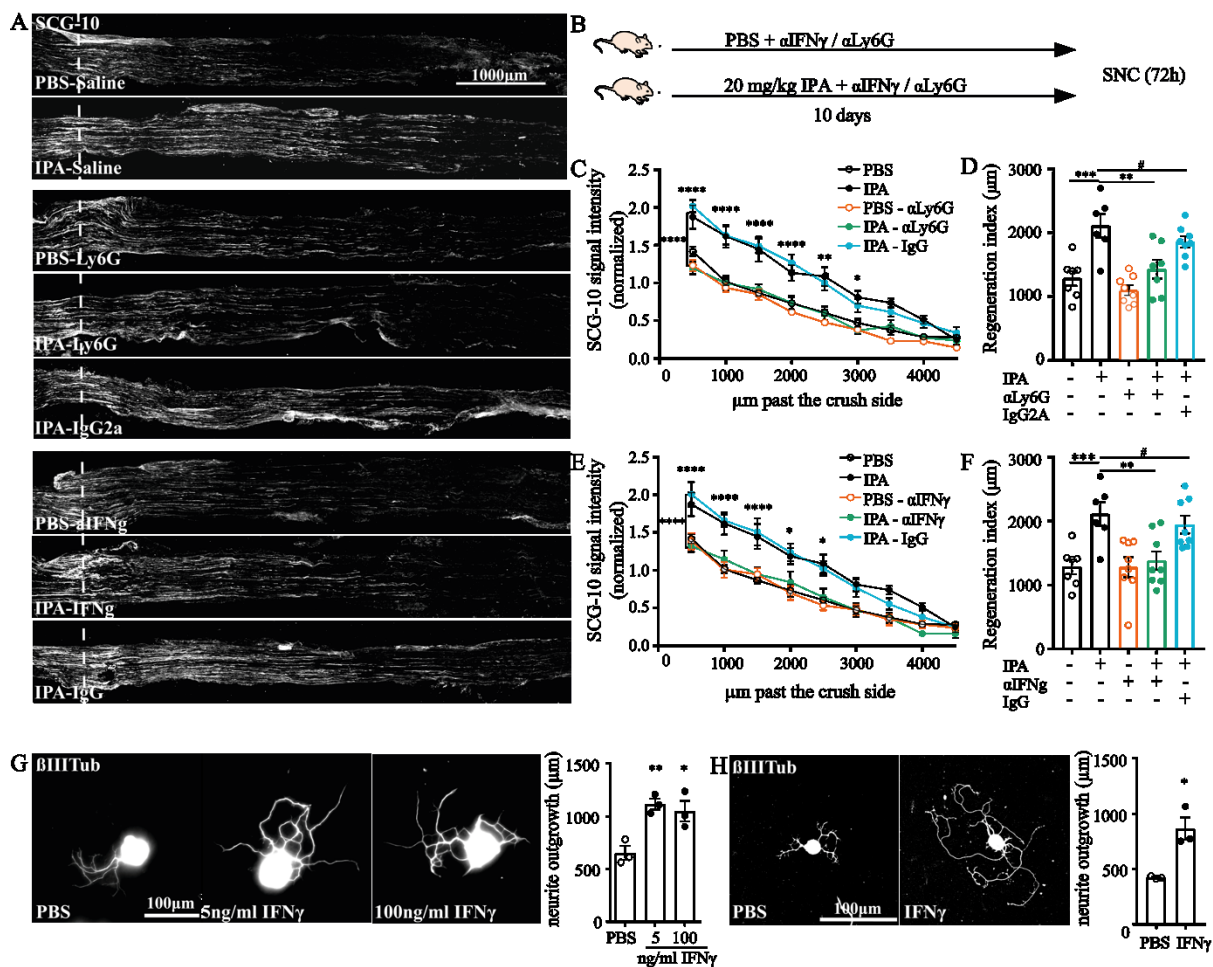


**Figure 21.** Neutrophil chemotaxis and IFN $\gamma$  signalling seem to mediate the effect of IPA

**A-E.** Mice were treated with either with IPA or PBS (by gavage) and IPA injected with either anti-Ly6G antibody (neutrophil depletion) or anti-IFN $\gamma$  (IFN $\gamma$  neutralisation). Axonal regeneration was assessed at 3 days post sciatic nerve crush. **A.** Micrograph of representative longitudinal section images of sciatic nerves for all groups immunostained with SCG-10 following 10 days of monoclonal antibody injection and 3 days post sciatic nerve crush (Scheme in **B**). Scale bar: 1000  $\mu$ m. The dotted line indicates the crush site. **B.** Schematics of the experimental setup. **C.** Quantification of SCG-10 intensity at the indicated distances and normalized to the intensity before the crush site. Normalised SCG-10 intensity was plotted as a function of the distance from the crush site revealed loss of IPA dependently increased regeneration with anti-Ly6G treatment. ( $N=7-8$  nerves per group from 4 mice per group with a bilateral sciatic nerve crush; \* $p<0.05$ , \*\* $p<0.001$ , \*\*\*\* $p<0.0001$ , significance assessed by Two-way-ANOVA with Tukeys test, significance shown above the graph comparing IPA- $\alpha$ Ly6G and IPA- $\alpha$ IgG, mean $\pm$ SEM) **D.** In vivo regeneration index was calculated from images in (A). SCG-10 intensity was measured from the crush site towards the distal end and normalised to the crush site as percentage of intensity. SCG-10 intensity

percentage of 50% was plotted as a function of the distance from the crush site. Increased regeneration in IPA treated groups was lost when combined with anti-Ly6G treatment (N=7-8 nerves per group from 4 mice with bilateral sciatic nerve crush; \*\* $p < 0.01$ , \*\*\* $p < 0.001$ , # $p = n.s.$  by One-way ANOVA, Multiple comparison testing: corrected by FDR method of Benjamini and Hochberg, mean $\pm$ SEM). **E.** Quantification of SCG-10 intensity at the indicated distances and normalized to the intensity before the crush site. Normalised SCG-10 intensity was plotted as a function of the distance from the crush site revealed loss of IPA dependently increased regeneration with anti-IFN $\gamma$  treatment. (N=7-8 nerves per group from 4 mice per group with a bilateral sciatic nerve crush; \* $p < 0.05$ , \*\*\*\* $p < 0.0001$ , significance assessed by Two-way-ANOVA with Tukeys test, significance shown above the graph comparing IPA- $\alpha$ IFN $\gamma$  and IPA- $\alpha$ IgG, mean $\pm$ SEM). **F.** In vivo regeneration index was calculated from images in (A). Increased regeneration in IPA treated groups was lost when combined with anti-IFN $\gamma$  treatment (N=7-8 nerves per group from 4 mice with bilateral sciatic nerve crush; \*\* $p < 0.01$ , # $p = n.s.$  by One-way ANOVA, Multiple comparison testing: corrected by FDR method of Benjamini and Hochberg, mean $\pm$ SEM). **G.** DRG neurons were treated with 5ng/ml, 50 ng/ml or 100ng/ml of IFN $\gamma$  in vitro and neurite outgrowth was assessed. Representative images of DRG neurons for each treatment, immunostained with  $\beta$ III-Tubulin ( $\beta$ IIITub). Cultured for 12 hours. Scale bar: 100 $\mu$ m. Quantification of  $\beta$ III-Tubulin ( $\beta$ IIITub, green) immunostained neurite outgrowth by measuring the length of neurites (N=3 technical replicates per group; \* $p < 0.05$ , significance assessed by One-way ANOVA with Dunnett's multiple comparisons test, mean $\pm$ SEM). **H.** Ex-vivo culture of DRG neurons 48 hours after IFN $\gamma$  I.P. injection (10  $\mu$ g/mouse). Neurite outgrowth was assessed 12 hours after plating. Representative images of DRG neurons for each treatment, immunostained with  $\beta$ III-Tubulin ( $\beta$ IIITub, white). Scale bar: 100 $\mu$ m. Quantification of  $\beta$ III-Tubulin ( $\beta$ IIITub, white) immunostained neurite outgrowth by measuring the length of neurites (N=3 technical replicates per group; \* $p < 0.05$ , significance assessed by students t-test, mean $\pm$ SEM).

### **3.10 IPA delivery after sciatic nerve crush injury improves sensory recovery**

The axonal regeneration rate is very slow following peripheral axonal injury limiting target reinnervation that is critical for functional recovery<sup>412</sup>. This is particularly significant for recovery in clinical injuries<sup>7,195,412</sup> where the growth capacity is not fully sustained for the duration required to enable muscle and skin reinnervation leading to functional recovery. Therefore, we aimed to investigate whether IPA administration at a clinically suitable time (24 hours) after injury was able to speed up the rate of sensory recovery following sciatic nerve injury. We performed a severe sciatic nerve crush injury approximately 20 mm distally from the L4-L6 DRG for 45 seconds, followed by 4 weeks of every other day IPA (20 mg/kg) or PBS oral gavage starting from 24 hours after nerve crush (Fig. 22A). During the four weeks of recovery time, we conducted several behavioural tests that measure sensory and motor function, as well as mechanical allodynia. These include the tape removal test (Fig. 22B1) that measures sensorimotor recovery, mechanical stimulation with the Von Frey filaments that measures mechanical allodynia (Fig. 21B2) and the Hargreaves test that assesses thermal nociception (Fig. 22B3). At the tape removal test, both “time to touch the tape” (Fig. 22C) and “time to remove the tape” (Fig. 22D) increased similarly at 3 days post-injury for both groups and gradually declined until day 29 compared to pre-injury (-1), showing no changes in the recovery rate between IPA and PBS. The Von Frey test uses filaments that stimulate the hind paw of the animals with variable forces (quantified in grams) whose intensity is recorded when the animal withdraws the paw. Data analysis showed no significant differences between the two groups (Fig. 22E). Finally, the mice were tested daily with the Hargreaves test to assess thermal nociception. An infrared emitter/detector is used to measure the time needed to elicit a paw withdrawal response following thermal heat exposure under the hind paw. Interestingly, both groups displayed an increased withdrawal response from 3.2 seconds pre-injury (-1) to about 8 seconds 3 days post-injury. However, IPA treated mice showed a faster speed of recovery shown by a reduced withdrawal response time compared to PBS between day 7 (PBS: 6.18±0.34, IPA: 5.25±0.4) and day 19 (PBS: 5.6±0.59, IPA: 3.78±0.24) (Fig. 22F), with a significant difference was found between days 16 and 17 (Fig. 21F). As expected both groups returned to baseline response levels 28 days post-injury (Fig. 22F).

These data show that IPA leads to an accelerated recovery in thermal nociception while it does not induce mechanical allodynia following sciatic nerve injury. No changes were found in sensorimotor recovery. Together, these experiments suggest that IPA might be a suitable treatment to induce sensory recovery without causing neuropathic pain in a sciatic crush model of peripheral nerve injury.



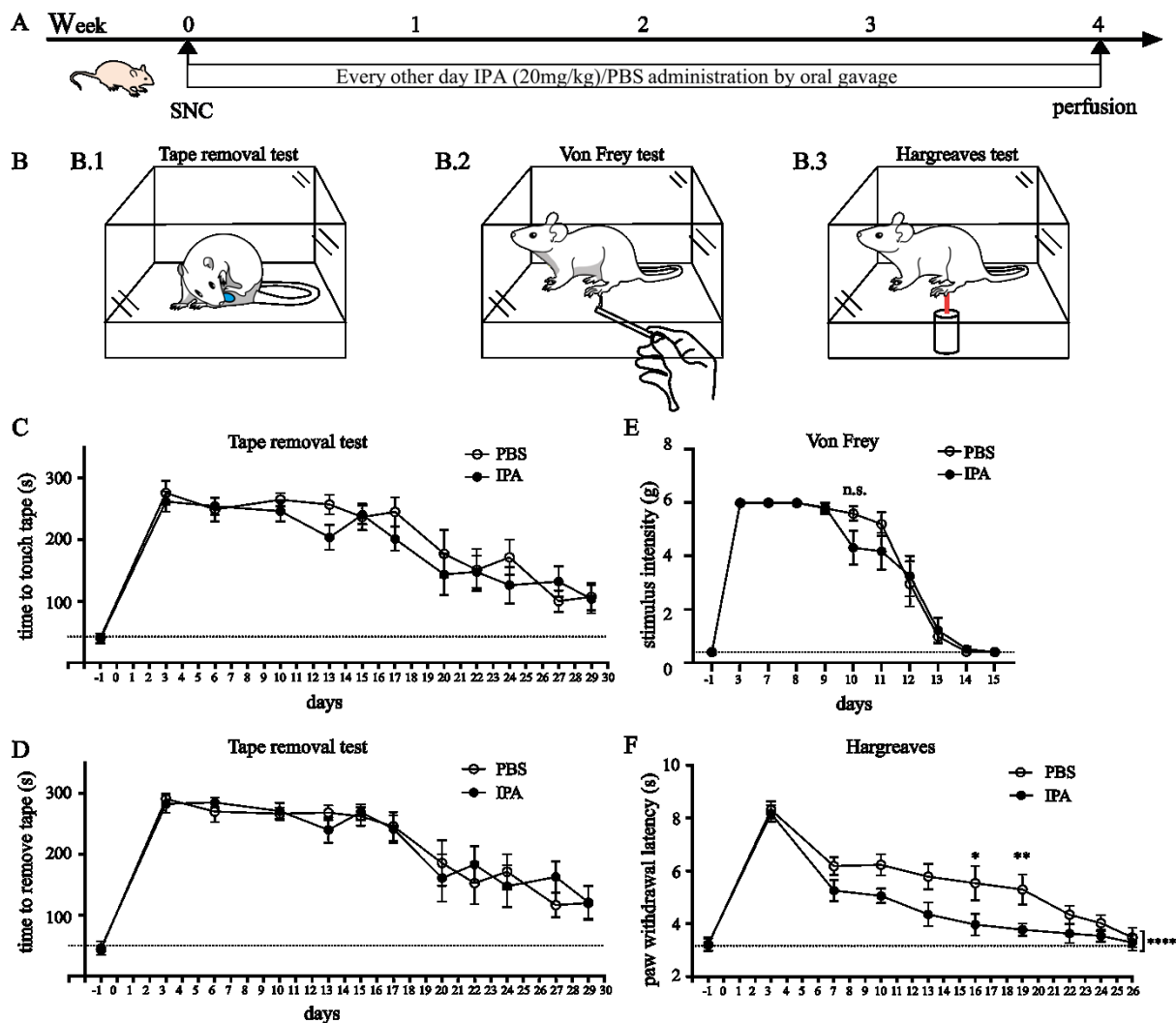


**Figure 22.** Sciatic nerve crush followed by IPA treatment showed improved thermal heat sensation at 2 weeks post injury.

**A.** Schematics showing the outline of the experimental setup. Sciatic nerve crush (SNC) was carried out on the left hind leg and IPA treatment (20 mg/kg) was administered via gavage every second day for 4 weeks (N=10 mice per group). **B.** Schematics showing the behavioural tests. Animals were assessed for tape removal test (**B1**) 3 times a week or for sensory behavioural tests (Von Frey (**B2**), Hargreaves (**B3**)) daily for 5 weeks following SNC. **C.** Quantification of the time required to first contact an adhesive pad placed on the left hind paw showed no significance between the two groups (N= 10 mice per group. Significance assessed by two-way ANOVA, Sidaks test, mean ± SEM) **D.** Quantification of the time required to remove an adhesive pad placed on the hind paws showed no significance between the two groups (N=10. mice per group. Significance assessed by two-way ANOVA, Sidaks test, mean ± SEM). **E.** Von Frey analysis for nociception (stimulus intensity shown in grams) showed no significant difference between the groups when plotted in a timeline. (N=10 per group, n.s. = not significant, Significance assessed by two-way ANOVA, Sidaks



test, mean  $\pm$  SEM) *F*. Visualisation of the paw withdrawal latency in seconds for the Hargreaves test for thermal pain sensation ( $N=10$ ,  $*p<0.05$   $**p<0.001$  significance assessed by two-way ANOVA, Sidaks test, mean  $\pm$  SEM).

### **3.11 Dorsal column axotomy followed by IPA affects behavioural recovery and synaptic plasticity**

Following a spinal cord injury, axons fail to regenerate across the lesion site, since in contrast to the sciatic nerve, spinal cord axons lie in a growth inhibiting environment and are halted from growing through the glial scar<sup>413</sup>. It has been found that an injury to the sciatic nerve preceding a spinal cord injury (conditioning lesion), activates a signalling cascade that induces pro-regenerative gene expression in DRG neurons that enable axonal regeneration in the spinal cord<sup>40</sup>. Therefore, treatments that successfully enhance axonal regeneration in the peripheral nervous system might have the capacity to translate the same effect to a central nervous system injury.

Here I we investigated if IPA affects the regenerative capacity of the spinal cord centrally projecting DRG axons following a spinal cord injury. A dorsal column axotomy was carried out and was followed by 7 weeks recovery. We delivered every other day IPA (20 mg/kg) or PBS by oral gavage that we initiated 24 hours after spinal injury ( $N$ : 10 mice per group) (Fig. 23A). Finally, 3 days before dissection we injected CTB into the sciatic nerve in order to visually trace axonal fibres regenerating into and across the lesion site. The tests were selected since they provide information on sensory and motor function as well as proprioceptive recovery. They include the grid walk (Fig. 23B1) and adhesive tape removal test (Fig. 23B2), as well as the Basso mouse scale for locomotion (BMS) (Fig. 23B3). Assessment of the number of hind paw foot slips on the grid walk showed a non-significant decrease in foot slips between IPA and PBS treated mice (Fig. 23C). We observed a significant recovery in IPA vs PBS animals in the adhesive tape removal test, with a decrease in the time it took to sense and then remove a piece of adhesive tape attached to the hind paws at day 7 after the injury. Thereafter, the time plateaued over the next 4 weeks with none to minimal changes (Fig. 23D-E). Finally, as expected, the BMS score and sub score did not show any difference in locomotion recovery between IPA and PBS (Fig. 23F-G).

Sensory inputs from muscle spindles to the spinal cord plays a crucial role in the regulation of motor circuit organisation and output. Proprioceptive afferents signal to the spinal cord via dorsal root ganglia and synapse on motor neurons or interneurons. This circuit provides positive feedback about muscle contractions, adjusting movements to environmental clues<sup>414</sup>. vGLUT positive proprioceptive afferents that signal to motoneurons are feedback inhibited by GABAergic interneurons, which act pre- and post-synaptically to inhibit the sensory transmitter release and motor neuron excitability, respectively. This balancing act enables locomotor function and is

commonly disrupted following spinal cord injury<sup>415,416</sup>. Part of the improved recovery we observed in the sensorimotor behavioural tests may be explained by a rescue of synaptic function. Hence, we hypothesised that IPA may improve synaptic plasticity below the lesion site. We immunolabeled section of the ventral horn caudal to the injury site for synaptic vesicle Glutamatergic transporter (vGLUT) and synaptic vesicle GABAergic transporter (vGAT) and determined the number of vGLUT and vGAT boutons co-labelled with the motor neuron marker ChAT. Interestingly, we found that the number of vGAT and vGlut contacts per motor neuron increased significantly in IPA treated spinal cords (vGAT: PBS=6.26 ± 0.27, IPA=12 ± 0.44; vGlut: PBS=3.45 ± 0.14, IPA=5.71 ± 0.21) (Fig. 24B-E).

Following spinal cord injury (SCI), innate immune cells infiltrate the injury site, including monocytes and macrophages. Consequently, they activate astroglial cells which proliferate resulting in the formation of the glial scar<sup>125</sup>. The glial scar is known to have dual properties, achieving stability for the spinal cord following injury, but also forming a barrier which axons fail to cross. Spinal cord sections from IPA and PBS treated mice were immunolabelled for glial fibrillary acidic protein (GFAP, astroglia cell marker) and CD68 (Monocytes/Macrophage marker) (Fig. 24F, G). Quantification of the lesion area showed no difference between IPA and PBS treated cords (Fig. 24H). Further, intensity measurements of GFAP in the lesion core revealed that IPA treated cords contained only 50% as many astroglia as the PBS treated control (IPA: 4580 ± 775.1 um, PBS: 2546 ± 543.4), suggesting decreased astrocyte activation and proliferation, resulting in reduced scar tissue, following SCI in combination with IPA treatment (Fig. 24I). CD68 intensity measurements inside the lesion core, as well as 2 mm rostral and caudal to the lesion core did not show any difference in monocyte/macrophage infiltration between treatment and control group (Fig. 24J-L). Additionally, immunostaining for neutrophil marker Ly6G at the lesion site did not show any positive staining of neutrophils in or around the lesion site at 5 weeks post injury. Earlier time points will be required to quantify neutrophils following spinal cord injury with IPA treatment (data not shown). CTB tracing for sensory fibre regeneration after DCA did not show robust tracing in all animals. For the spinal cord samples with positive tracing, we could not see a clear difference in the number of fibres regenerating into the lesion site between IPA and PBS treatment (data not shown).

Together, these data indicate that IPA leads to a decrease in GFAP positive scar tissue and to an increased synaptic plasticity below the lesion site that is in line with the improved recovery observed at the adhesive tape removal test.

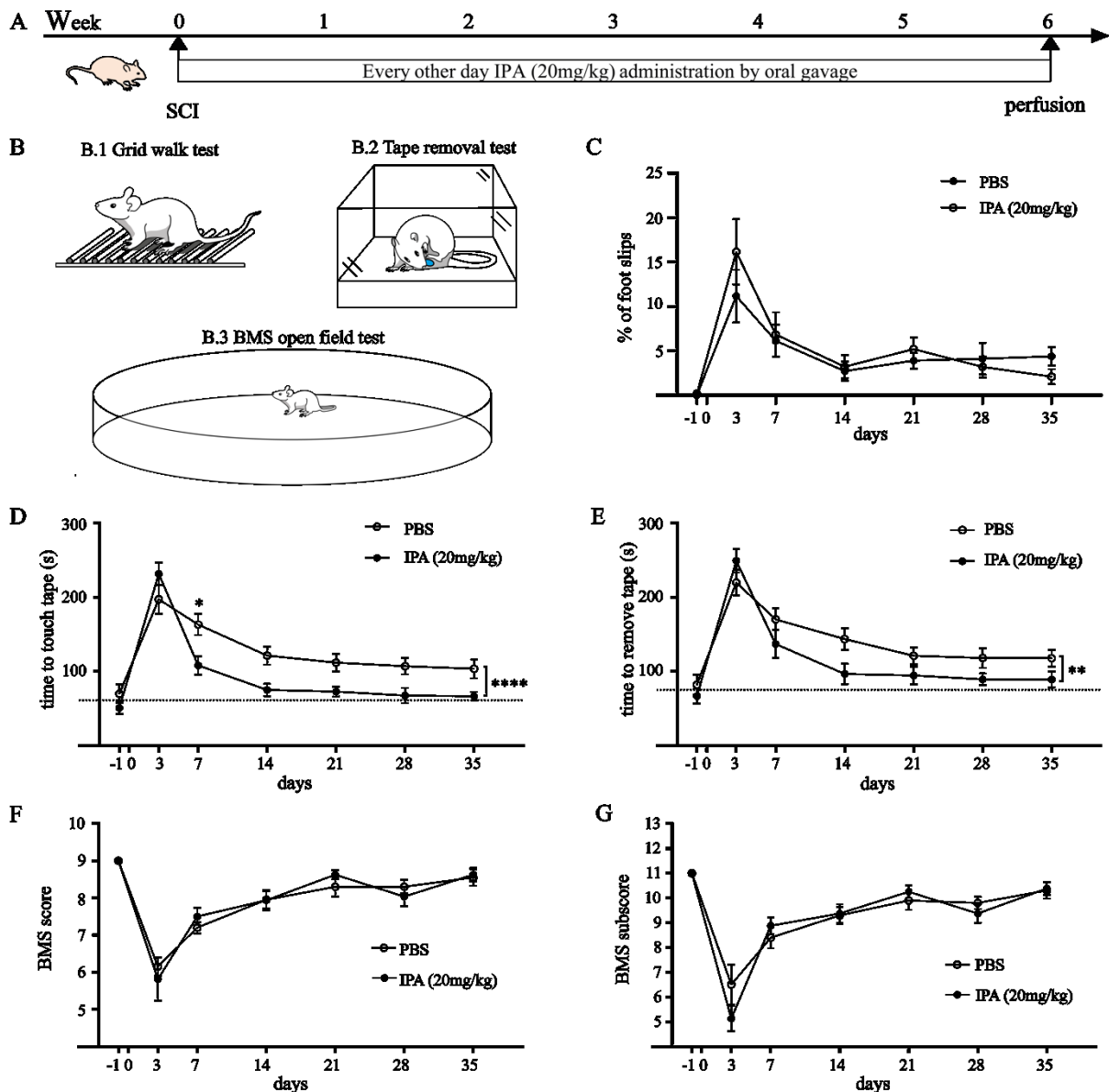


**Figure 23.** Dorsal column axotomy followed by IPA treatment showed a decrease in adhesive tape touch time within 1 week following injury.

**A.** Schematics showing the outline of the experimental setup. Dorsal column axotomy was carried out and IPA treatment (20 mg/kg) was administered via gavage every second day for 7 weeks ( $N=8-10$  mice per group). **B-G.** Animals were assessed for sensory and motor function behavioural tests weekly for 5 weeks following SCI. **B.** Schematic images of the behavioural tests: Grid walk (**B1**), Adhesive tape removal test (**B2**), Basso mouse scale for locomotion (BMS) (**B3**). **C.** Quantification of slips from Grid walk analysis showed no significant difference between the groups. ( $N=9$  per group, significance assessed by two-way ANOVA, Sidaks test, mean  $\pm$  SEM) **D.** Quantification of the time required to first contact an adhesive pad placed on the hind paws showed significant improvement in the IPA treated group for “time to touch tape” at 7 days post-injury and over all

significance between the two treatment groups (N= 8-10. mice per group. \* $p < 0.05$ , \*\* $p < 0.01$ , \*\*\* $p < 0.0001$ , significance assessed by two-way ANOVA, Sidaks test, mean  $\pm$  SEM) **E.** Quantification of the time required to remove an adhesive pad placed on the hind paws showed over all significance between the two treatment groups (N= 8-10. mice per group. \*\* $p < 0.01$  significance assessed by two-way ANOVA, Sidaks test, mean  $\pm$  SEM). **F-G.** Graphs show BMS score and subscore. No difference between IPA and PBS treated animal groups (N=9, significance assessed using two-way ANOVA, mean  $\pm$  SEM).

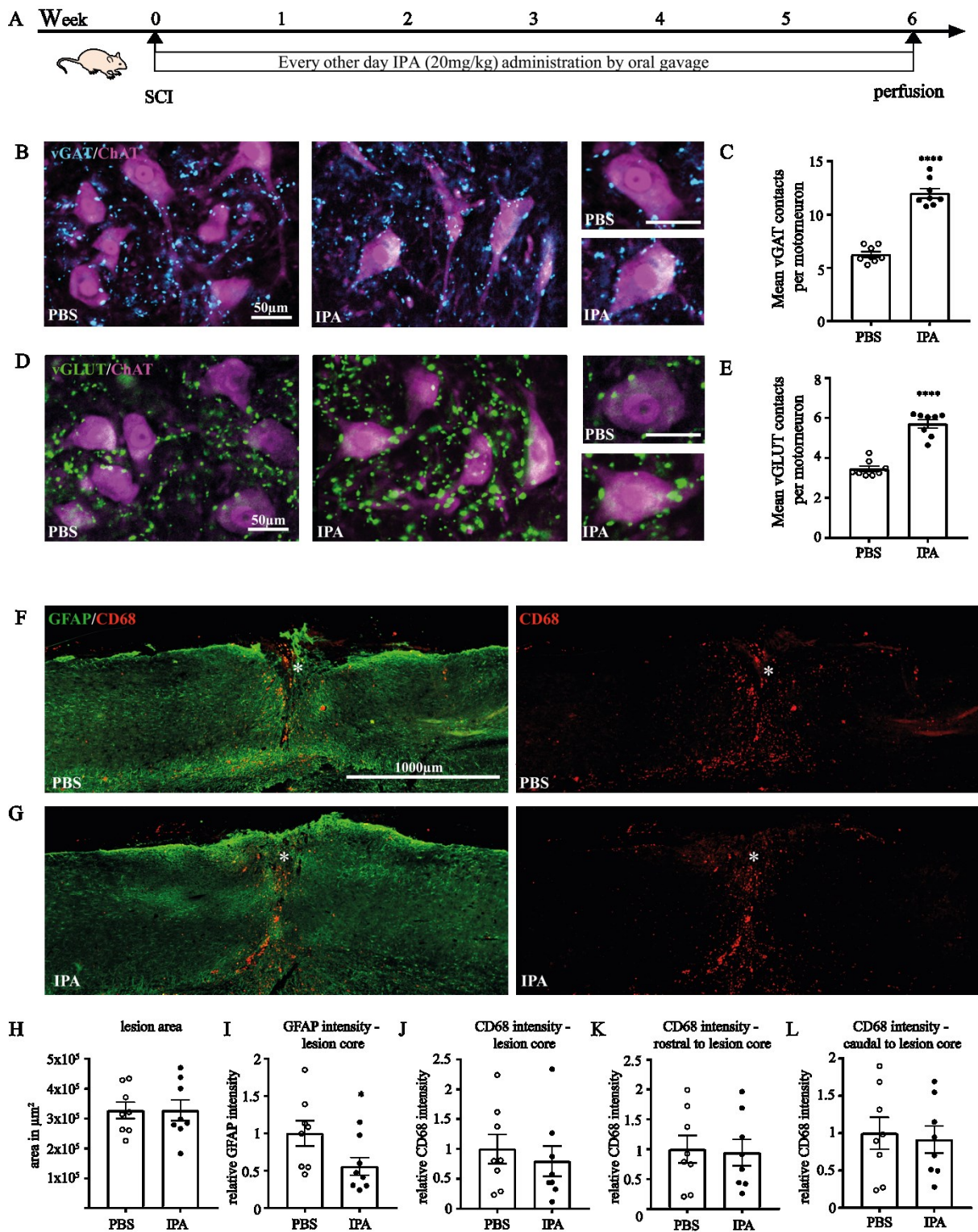


**Figure 24.** Dorsal column axotomy followed by IPA treatment leads to reduced GFAP intensity in the lesion core and increased number of synaptic connections to motoneurons below the injury site

**A.** Dorsal column axotomy was carried out and IPA treatment (20 mg/kg/day) was administered via gavage every second day for 7 weeks. **B-H.** IHC analysis of the spinal cord lesion site. **B-E.**

Quantification of number of vGAT (synaptic vesicle GABAergic transporter) and vGLUT (synaptic vesicle Glutamatergic transporter) contacts to motoneurons (ChAT). **B.** Representative images showing sections of the ventral horn caudal to the injury site immunolabeled for vGAT (blue) and ChAT (motoneuron marker, purple) of IPA and PBS treated animals. **C.** Quantification of boutons colabeled for vGAT and ChAT showed 2 fold more vGAT contacts per motor neuron compared to control (scale bar: 50  $\mu$ m, N= 8 mice per group, \*\*\*\* $p$ <0.0001, significance assessed using students  $t$ -test, mean $\pm$ SEM). **D.** Representative images showing sections of the ventral horn caudal to the injury site immunolabeled for vGLUT (green) and ChAT (motoneuron marker, purple) of IPA and PBS treated animals. **E.** Quantification of boutons colabeled for vGLUT and ChAT showed 1.65 fold more vGLUT contacts per motoneuron (scale bar: 50 $\mu$ m, N= 8 mice per group, \*\*\*\* $p$ <0.0001, significance assessed using students  $t$ -test, mean $\pm$ SEM). **F-G.** IHC staining for GFAP and CD68, for astroglial and macrophage/monocyte quantification at the injury site, respectively. **H.** Quantification of the lesion area in  $\mu$ m<sup>2</sup> showed no difference between the two treatments. **I.** intensity measurements of GFAP inside the lesion core reveals 44.4% less GFAP intensity in the lesion core in IPA treated animals. **J-L.** CD68 intensity measurements inside the lesion core (**J**), 2 mm rostral to the lesion core (**K**) and 2mm caudal to the lesion core (**L**) showed no difference between the two groups (scale bar: 1000  $\mu$ m, N=8, \* $p$ <0.05, significance was assessed using students  $t$ -test, mean $\pm$ SEM).

## **Chapter 4: Discussion**

### **4.1 Overview**

Injured mammalian adult peripheral nerves have a limited regenerative growth rate that is too slow and is not fully sustained for the duration required to enable muscle and skin reinnervation that are needed for functional recovery.

The vast heterogeneity of cell types involved in the events following injury and the complexity of responses at the injury site and neuronal cell bodies contribute together to the failure or success of axonal regeneration. Recently, a publication by our laboratory showed that exercise and environmental enrichment promote axonal regeneration in the PNS and CNS<sup>157</sup>. The manipulation of environmentally induced systemic stimuli, such as exercise and diet, impacts neuronal health<sup>417-419</sup> and promotes recovery from experimentally induced ischemic stroke or spinal cord injury<sup>157,219,224,420</sup>. Dietary interventions, such as IF, alleviate the immune-mediated neuronal damage and prevent neuronal death following brain ischemia<sup>219,224</sup>. Additionally, IF was found to increase neurotrophic factors and synaptic plasticity in the brain<sup>195,242</sup>. Together, published data suggested that IF might not only favour protection against “damage” in the nervous system but it might also be capable of promoting plasticity, regeneration and recovery following axonal injury. Testing this hypothesis was indeed the focus of my work.

In summary, 10 days of IF enhanced axonal regeneration after sciatic nerve crush in both the short- and long term. Further mechanistic investigation revealed that the IF-dependent composition of the gut microbiome was key to IF mediated regeneration, as shown by faecal transplantation and vancomycin microbiome depletion experiments. Detailed metabolomics studies and microbiome gene sequencing allowed to identify IPA as the preferential IF and microbiome-dependent metabolite associated with an increase in Clostridiales. Gain and loss of function experiments determined that IPA produced by *Clostridium Sporogenes* or directly delivered either orally or systemically was needed and sufficient to promote axonal regeneration after sciatic nerve injury. Additionally, RNA sequencing analysis of the DRG enabled to detect a role for neutrophils and IFN $\gamma$  signalling as novel IPA-dependent regenerative mechanism. Finally, behavioural tests in mice treated with IPA following SNC or dorsal column axotomy (DCA) showed faster and improved neurological recovery, proposing IPA as a novel treatment to promote repair and recovery after axonal injuries.

#### **4.2 Intermittent Fasting promotes axonal regeneration through Indole-3-propionic acid**

Intermittent Fasting has a multidimensional impact on the body, from changing metabolites and hormones systemically to promoting catabolic metabolism at the cellular level by increasing autophagy<sup>234</sup>. While the metabolic adaptations to food deprivation are well characterised, the mechanism through which IF modulates immune responses<sup>168,219-223</sup> and augments neurotrophic factors<sup>219</sup> and synaptic plasticity<sup>242,243</sup>, remains to be fully understood. Importantly, these adaptations have been found to prevent excessive inflammation and promote tissue healing upon brain ischemia<sup>219,220,224</sup> and prevent neuronal death upon excitotoxin exposure<sup>168</sup>. A study by Jeong et al., showed increased functional recovery from a thoracic contusion in the spinal cord upon IF. IF 3 weeks before injury improved functional recovery in the catwalk and Basso-Beattie-Bresnahan (BBB) open field assessment. The catwalk parameters of forelimb-hind limb swing duration and the BBB even showed recovery when IF was initiated after the injury<sup>248</sup>. Unfortunately, the mechanism of action was not investigated in this study.

It is essential to unravel the signalling pathways through which IF promotes regeneration and tissue healing in order to develop treatment strategies that can be applied to patients after nervous system injury.

To understand the impact of IF on axonal regeneration, two IF regimes were investigated. In this study I tested 30 days and 10 days of IF followed by a sciatic nerve crush and assessment of axonal regeneration past the crush site at the 24-hour time point (Figure 8). Both increased axonal regeneration to the same extent and therefore, subsequent IF regimens continued with 10 days of IF. Additionally, regeneration post sciatic nerve crush was tested at the 72-hour time point and at 14 days post injury via assessment of muscle reinnervation. Both experiments showed a successful increase in axonal regeneration and reinnervation, demonstrating that IF sustains regeneration for longer time points post-injury. Previous publications found increased BDNF levels in the hippocampus<sup>219</sup> upon IF and neurotrophic factors have been found to promote axonal outgrowth and regeneration<sup>11,396-399</sup>. However, IF did not affect the levels of BDNF, NGF, NT3 and NT4/5 in the DRG tissue (Figure 10). BDNF has been strongly correlated with enhanced cognition upon IF, likely by increase of synaptogenesis and neurogenesis in the hippocampus<sup>421</sup>. It has been suggested that IF or food deprivation induces BDNF expression in neuronal circuits involved in cognition by increasing their activity and shifting their energy state from glucose to ketones<sup>421</sup>. The expression and release of BDNF are stimulated by excitatory synaptic activity, resulting in the activation of Ca<sup>2+</sup>-calmodulin-dependent protein kinases (CaMK), eventually leading to the transcription of the *bdnf* gene<sup>422</sup>. Unfortunately, primarily brain (hippocampus, cortex, striatum)<sup>243,423</sup> or blood have been tested in these studies following 3-6 months of IF and nothing is known about IF induced BDNF production in peripheral neuronal tissues. Here we can hypothesise that 10 days of IF was



either not sufficient to induce neurotrophic factor synthesis in DRG neurons, or mechanism through which food deprivation acts on other nervous system tissues differ from the brain.

Further investigation into the two main cell types influencing regeneration at the injury site such as macrophages and Schwann cells showed that both cell numbers were not affected by IF (Figure 10). Schwann cells play a crucial role in the immediate events following nerve injury, providing neurotrophic factors<sup>36-38</sup>, supporting neuronal growth via signalling<sup>52,70,330,331</sup> and recruiting macrophages for the crucial phagocytosis of myelin from the injury site<sup>342,424</sup>. Other than cell numbers, IF could alter Schwann cell or immune cell signalling in and around the nerve injury site promoting recovery and regeneration. A recent study in our lab showed macrophage dependent signalling to injured axon promoted regeneration<sup>55</sup>. It is possible that IF further supports nerve regeneration via activation of macrophage signalling to the injured neurons, which could be investigated via monoclonal antibody depletion experiments. In a different study, remyelination of sciatic nerve axons by Schwann cells has been shown to be restored in a neuropathic mouse model (similar genetically to a Charcot–Marie–Tooth disease type 1A, myelin deficiency) upon 5 weeks of IF with increased myelin protein levels in the mutant, but not the WT<sup>181</sup>. No difference in the number of macrophages and Schwann cells was observed in the WT animals, but were reduced in the mutant. It would be interesting to identify if IF affects axon remyelination following nerve injury, which could be tested via additional IHC staining or western blot for myelin proteins such as Myelin basic protein (MBP), Myelin protein zero (P0) or PMP22. However, IF has been shown to alter signalling pathways involved in metabolism, autophagy and immunity and further experiments would be required to investigate its impact at the injury site following nerve injury.

It has been shown that IF for 30 days modifies the microbial composition, consequently affecting nutrient uptake<sup>264</sup>. We established that 10 days of IF promoted axonal regeneration following injury and hypothesised that this may be mediated through changes of the gut microbiome. Therefore we presumed that 10 days of IF might be sufficient to alter the production of microbiome derived metabolites, which in turn directly or indirectly impact axonal regeneration.

The finding that IF increased serum levels of indole-metabolites was in line with previous publications showing increased tryptophan uptake and tryptophan derived metabolites in the blood upon IF<sup>213,425,426</sup>. Indole-metabolites have been linked to hormone production (serotonin) and regulation of intestinal<sup>256</sup>, systemic<sup>259,277,427</sup> and CNS immunity<sup>427,428</sup>. Both, Indole-lactic acid (ILA) and indole-3-propionic acid (IPA) have been upregulated by IF (Figure 11), however depletion of the gram positive gut microbiome that reduced IF mediated axonal regeneration, only significantly reduced IPA from the blood serum, but not ILA (Figure 13). In line with our findings, IPA in addition to other gut derived metabolites, has recently been shown upregulated in the plasma of mice following 30 days of IF and was strongly linked to improved cognitive functions in an

animal model of diabetes<sup>213</sup>. This, in agreement with our findings, is supporting the hypothesis that the effect of IF might be at least partially mediated by the indole metabolite IPA.

Additionally, in contrast to others<sup>213,264</sup>, we did not find SCFAs increased by IF in our dataset, which may be due to the short term IF cycles (10 days vs 30 days) we employed and it indicates that SCFAs are not necessarily required for the regenerative effects of IF.

Next we performed a phylogenetic analysis, using 16S sequencing, aiming to identify the bacterial communities in the cecum of mice that had undergone 10 days of IF (Figure 15). The 16S rRNA gene sequence contains both highly conserved regions and hypervariable regions to identify phylogenetic characteristics of microorganisms. Based on previous literature, I expected an increase in bacterial diversity<sup>213,302</sup> and a shift towards a higher Firmicutes / Bacteroidetes ratio following IF<sup>264</sup>. 16S sequencing analysis of the gut microbiome from mice that had undergone 10 days of IF or AL was not able to show the expected rise in bacterial diversity, which might be due to the relatively short amount of IF cycles compared to previous publications<sup>302</sup>. Additionally the Firmicutes / Bacteroidetes ratio was increased after 10 days of IF. Further analysis of bacterial composition at the level of order and class showed a slight elevation in Clostridia following an IF regimen, which was in line with findings by Li et al. in mice that had undergone 30 days of IF<sup>264</sup>. Clostridia have previously been correlated with maintenance of gut homeostasis<sup>429</sup> and are the class of bacteria that contain the species *Clostridium sporogenes*, which is the main producer of IPA<sup>403</sup>. These results coincide with a previous publication by Liu et al, which was able to show increased plasma levels of IPA following IF and upregulation of the genus of Clostridiales by 16S sequencing<sup>213</sup>. IPA is primarily produced by *Clostridium sporogenes* via tryptophan fermentation by the enzyme (R)-phenyllactyl-CoA dehydratase<sup>254</sup> and reconstitution of IPA in the blood of germfree mice was shown to be completely dependent on the presence of the bacterium *Clostridium sporogenes*<sup>430</sup>. In line with this, axonal regeneration was reduced in animals recolonised with the mutant *FldC C.sporogenes* strain compared to the WT (Figure 16). This further supports the idea that *C.sporogenes* producing IPA is required for axonal regeneration.

However, a more specific analysis using shot gun metagenomics or qPCR will be required to further investigate eventual specific changes in *C.sporogenes* upon IF.

Collectively, the data indicate that IPA synthesis in the gut is required for successful axonal regeneration and may act as the main mediator of IF induced axonal regeneration.

#### **4.3 Indole-3-propionic Acid mimics IF facilitated axonal regeneration through immunoregulatory mechanisms**

Having established the impact of IPA on axonal regeneration, further experiments aimed to determine the mechanism of action underlying IPA-dependent regenerative effects. It has been shown to protect neurons from oxidative damage in animal models of Alzheimer's disease and following ischemia in the hippocampus in mice<sup>431,432</sup>. Additionally, IPA binds to the xenobiotic nuclear receptor PXR, which has been implicated in a variety of immune responses, ranging from suppression<sup>255,256,433</sup> to activation<sup>434,435</sup> of inflammatory regulatory mechanisms. A study by Venkatesh et al. showed that the loss of PXR in gut epithelial cells enhances inflammatory markers, by augmenting gut permeability through activation of Toll like receptor 4 (TLR-4) and subsequent loss of tight junctions<sup>256</sup>. Additionally, Dodd et al., found that loss of IPA synthesis in the gut results in a systemic increase in CD8 T-cells, CD4 T-cells, neutrophils, monocytes and increased gut permeability<sup>254</sup>. Both papers have shown that oral delivery of IPA increases gut integrity, which was closely correlated with decreased inflammatory markers systemically. In line with this Alexeev et al., showed that oral administration of IPA increased IL-10 receptor 1 (IL-10R1) and decreased inflammatory marker, such as IFN $\gamma$ , TNF $\alpha$  and IL1 $\beta$  in the colon tissue, augmenting symptoms of experimentally induced colitis<sup>433</sup>.

Other studies revealed a potentially different function of IPA in the immune cells and endothelial cells, peripheral to the gut. Hudson et al., and Wang et al. demonstrated that PXR activation in macrophages and vascular endothelial cells, resulted in the expression of the NOD-, LRR- and pyrin domain-containing protein 3 (NLRP3) protein complex, triggering the activation of the inflammasome. Wang et al., found that PXR activation in vascular endothelial cells increased the expression of TLRs, including TLR4, leading to the upregulation of IL-1 $\beta$ <sup>435</sup>. These findings were mirrored in macrophages with increased expression of NLRP3 and IL1 $\beta$  upon PXR activation<sup>434</sup>. From this we concluded that IPA may have distinct effects based on tissue and cell type, promoting increased gut integrity resulting in reduced systemic inflammation, but activating innate immune signalling pathways in immune cells and vascular endothelial cells. Therefore I wanted to further establish whether IPA passage through the gut is required for axonal regeneration. Ten days of systemic treatment with IPA increased axonal regeneration, independent of the administration methodology (Figure 16). Intraperitoneal injection of IPA promoted a 1.5-fold increase in axonal fibres regenerating past the crush site (Figure 16), which closely mirrored what was found with IPA gavage treatment. This indicated that the mechanism through which IPA promotes regeneration in the sciatic nerve does not require passage through the gut epithelium. These results suggest that the alteration of gut permeability is not required for IPA-dependent regeneration. It is

likely that IPA would modulate neuronal extrinsic systemic signalling mechanisms to promote the regenerative ability.

In order to investigate IPA mediated signalling in the DRG before and after sciatic nerve injury, I conducted RNA sequencing from DRG from PBS and IPA treated mice uninjured and 3 days post SNC (Figure 17). I found that the majority of upregulated pathways before and after injury were immune regulatory pathways. Most interestingly, Gene Ontology analysis suggested an increase in Interferon gamma signalling following IPA treatment, which was further supported by upregulation of genes categorised as “MHC I subunit and assembly”. Following injury, IPA- dependent upregulated GO pathways described an increase in genes involved in “neutrophil chemotaxis”. Importantly we found that neutrophil ligand Cd177, endothelial neutrophil chemoattractant Cxcl1 and its receptor Cxcr2 were solely upregulated in the IPA-SNC dataset. CXCL1 binding to its receptor on neutrophils (CXCR2) facilitates neutrophil migration and tissue infiltration<sup>436,437</sup>, including into the brain<sup>438</sup>. However, in the dorsal root ganglion upregulation of both, Cxcl1 and Cxcr2, have been associated with mechanical allodynia and neuropathic pain<sup>439</sup>. In order to address this, we included a standard test for mechanical allodynia, the Von Frey test, following SNC and 4 weeks of IPA treatment (Figure 21). We found no difference between the IPA and PBS treated groups, indicating that increased expression of Cxcl1 was not sufficient to increase neuropathic pain.

Based on these results I performed immunohistochemistry analysis and found neutrophils accumulated around the DRG tissue upon IPA treatment before and after a sciatic nerve crush injury (Figure 18). This supported the notion of the RNA sequencing analysis that IPA treatment promotes neutrophil infiltration to the DRG tissue.

Interestingly, mRNA coding for the Pregnane X Receptor (PXR, Nr1i2) was increased 3-fold in the DRG tissue from IPA treated mice 3 days following SNC injury, suggesting IPA signalling to cells of the DRG, including immune cells, DRG neurons or endothelial cells. The PXR receptor is a member of the nuclear receptor (NR) super family and acts as a ligand-activated transcription factor. It is a xenobiotic sensor that is highly expressed in the liver and regions of the small and large intestine<sup>440</sup>. However, it has also been found expressed in immune cells<sup>434,441-443</sup> and vascular endothelial cells<sup>435</sup>. The previously mentioned study by Hudson et al. demonstrated that PXR ligand binding in macrophages activated an innate inflammatory response triggering the nucleotide-binding oligomerization domain, leucine rich repeat, and pyrin domain-containing 3 (NLRP) inflammasome leading to Caspase 1 cleavage and IL1 $\beta$  secretion<sup>434</sup>. Similar results were found in vascular endothelial cells upon PXR agonist treatment resulting in upregulation of toll like receptor (TLR) expression and NLRP3 activation<sup>435</sup>. In line with this, a number of genes summarised as “innate immune signalling” were IPA dependently upregulated in our dataset (Figure 17, network),

including genes involved in inflammasome and IL1 $\beta$  signalling, such as Nlrp3, Caspase 4 (Casp4), Chemokine (C-C motif) ligand 19 (Ccl19) and Gasdermin D (Gsdmd). Interestingly, a study by Biondo et al found that IL1 $\beta$  released by inflammasome activation is required for CXCL1/2 chemokine production and subsequent neutrophil recruitment to several tissues, including the brain, following systemic streptococcus infection<sup>444</sup>. It was established that mice deficient for IL1 $\beta$  had reduced CXCL1 protein levels in brain and kidney and were defective for systemic and local neutrophil mobilisation upon infection. It is intriguing to hypothesise a potential role of inflammasome activation in the endothelial cells encompassing the DRG tissue, further resulting in neutrophil recruitment and infiltration into the DRG.

In line with the RNA sequencing results fluorescence activated cell sorting (FACS) analysis of the spleen showed an increase in neutrophils and, additionally, natural killer (NK) cells 3 days after SNC injury and 13 days of IPA treatment (Figure 19). Analysis of the mesenteric lymph nodes (the draining lymph nodes of the gastrointestinal system), showed a strong effect after IPA plus SNC injury, containing increased levels of neutrophils, NK cells, NKT cells and B-cells (Figure 19). This is likely because neutrophils migrate into the lymphatic system upon a range of stimuli<sup>445</sup>. Following an initial inflammatory insult neutrophils traffic to lymph nodes (LNs) within few hours<sup>446</sup>, which has been hypothesized to facilitate the transport of antigens into LNs. Research has shown neutrophils directly interact with T- and B-cells in draining lymph nodes, displaying activation as well as inhibition of adaptive immune cells via neutrophil infiltration<sup>446</sup>. Additionally, neutrophil activation releases the cytokine Interleukin 18 (IL18), which is key for NK-cell activation<sup>447</sup>. Note that IL18 synthesis and release from neutrophils and other cells, primarily macrophages, epithelia and endothelia, is induced by NLRP3 inflammasome activation<sup>448-450</sup>. In line with this, the IL18 receptor complex was upregulated by 1.5-fold in the RNA sequencing dataset from DRG following IPA treatment and sciatic nerve crush. One can hypothesise that activation and infiltration of neutrophils stimulates and recruits NK and NKT cells in the LNs and consequently in the DRG.

Surprisingly, I found that IPA treatment increased neutrophil numbers around the DRG tissue even prior to an injury, but it did not change the number of immune cells in the MLN or spleen. It can be hypothesised that IPA alone activates the PXR receptor, potentially in the vascular endothelial cells or neurons of the DRG, initiating the recruitment and chemotaxis of neutrophils, perhaps by mechanisms of inflammasome activation and via subsequent release of CXCL1.

Larger neutrophil changes in primary and secondary lymphoid tissues, such as the LNs and the spleen, are unlikely to happen before an injury considering that neutrophils are primarily recruited to lymphoid tissues upon an inflammatory activation due to pathogens<sup>445,446,451,452</sup>. IPA treatment alone may activate neutrophil chemotaxis systemically, which then may be recruited into lymphoid

tissue upon injury. Secondly, it could be that small changes in neutrophil infiltration that are quantifiable by IHC in DRG tissue are not detectable by FACS from large lymphoid tissues such as the spleen. However, either hypothesis remains to be tested. In summary these results indicate that IPA in combination with SNC injury induces a systemic immune response which may be further reinforced by IPA signalling.

The finding that monoclonal antibody depletion of neutrophils diminished the effect of IPA on axonal regeneration, further supported the idea of a significant role for neutrophils in IPA facilitated axonal regeneration (Figure 20). The investigation of immune regulation following nerve and spinal cord injury and its impact on axonal regeneration has gained traction over the past few years. Interestingly, several publications have shown a crucial role for neutrophils in recovery following CNS and PNS injury<sup>143,324,353,354</sup>. Neutrophils are the first immune cells to arrive at the injury site in the spinal cord<sup>350</sup>, and sciatic nerve<sup>318</sup>, and infiltrate the DRG following sciatic nerve injury<sup>453</sup>. Little is known about the interaction between neutrophils and neurons and currently the role of neutrophils in peripheral nerve axonal regeneration is limited to the injury site. Neutrophils function as the primary mediators of destruction of microorganisms and dying cells, releasing chemokines that can either be beneficial or detrimental to neighbouring cells<sup>321,454,455</sup>. During an infection, the body relies on neutrophil-mediated tissue injury as one of the main sources of inflammation and immunity<sup>321</sup>. Conversely, neutrophils are also important for wound healing, including phagocytosis of tissue debris and release of anti-inflammatory cytokines<sup>321</sup>. Neutrophils are crucially involved in myelin clearance following nerve crush<sup>324</sup> and as the first responders, are likely involved in the recruitment to and activation of other leukocytes following tissue injury<sup>321</sup>, suggesting a role beyond phagocytosis. In the spinal cord neutrophils are responsible for an early activation of astrocytes and recruitment of macrophages<sup>143</sup>. A study by Stirling et al. found mice depleted of neutrophils showed reduced early astrogliosis, resulting in a decrease in functional recovery and increased lesion size<sup>353</sup>. In the optic nerve, another model for central nervous system injury, neutrophils were found to be essential for inflammation-mediated regeneration by releasing oncomodulin, a protein strongly associated with retinal ganglion cell survival and regeneration<sup>456</sup>. These data suggest that neutrophils contribute to inflammation-mediated regeneration.

RNA sequencing analysis found IPA dependent upregulation of IFN $\gamma$  signalling and increased expression of downstream MHCI assembly proteins. Additionally, the T-cell, NKT-, and NK-cell transcription factor TBX-21, which is key to induce IFN $\gamma$  transcription, was upregulated in the RNA sequencing dataset following IPA and SNC injury (Figure 17, shown in network). Therefore, IFN $\gamma$  may be crucial for neutrophil mediated axonal regeneration through direct signalling to DRG neurons. IFN $\gamma$  is a signature Th1 cytokine and has been shown to have a pro-inflammatory role in a number of autoimmune and inflammatory diseases<sup>457</sup>. However, there is mounting evidence that

IFN $\gamma$  has inflammation mitigating properties, by inducing the expression of anti-inflammatory cytokines or cytokine antagonists<sup>458,459</sup>, and has been shown to be protective in a number of disease models<sup>459-461</sup>. Interestingly, IFN $\gamma$  has also been found, by us and others, to promote neurite outgrowth<sup>462</sup> (Figure 20) and significantly contribute to spinal cord injury recovery<sup>460,463-465</sup>. For instance, Ishii et al., found IFN $\gamma$ -dependent secretion of IL-10 by T-cells enhanced functional recovery after spinal cord injury<sup>463</sup>. Similar results were shown in a model of colitis, exhibiting increased IL10 and IL10R and decreased gut permeability upon IFN $\gamma$  treatment<sup>459</sup>. In line with this, our RNA sequencing dataset revealed a significant increase of Il10 in the DRG tissue upon IPA treatment alone, which was further elevated following injury (Figure 17, shown in network). Both, IFN $\gamma$ , as well as IL10, activate the JAK-STAT signalling pathway and DRG neurons express receptors for both<sup>466,467</sup>. It is possible that cytokine activated regenerative signalling pathways, such as JAK1/2-STAT3 mediated signalling, are triggered in DRG neurons upon IPA treatment. This provides a promising new research direction, potentially unravelling a novel immune regulatory mechanism in neutrophil-mediated axonal regeneration.

#### **4.4 Indole-3-propionic acid promotes functional recovery following Sciatic nerve and spinal cord injury.**

Following robust responses in the PNS with treatments before injury, I explored whether IPA facilitates functional recovery following sciatic nerve and spinal cord injury. Firstly, treatment with IPA following sciatic nerve crush resulted in functional improvements starting at 7 days and reaching significant difference at day 16 post injury in the Hargreaves test (Figure 21). Sensitivity to thermal heat pain was strongly reduced at 3 days post injury and gradually improved in the following 2 weeks. No difference was observed in Von Frey mechanic allodynia test. However, distinct neuronal fibers innervating the skin are responsible for mechanical and temperature related pain perception, indicating a different response to IPA treatment between mechanical A $\delta$ -fibers and thermal sensitive A $\delta$  neurons. Interestingly, neutrophils and macrophages have previously been linked to thermal and mechanical allodynia<sup>468,469</sup>, which occurs shortly after nerve injury at 3-5 days (thermal~) and 7-8 days (mechanical~) post injury<sup>469</sup>. However, no allodynia was observed following IPA treatment and sciatic nerve crush in our experiment. It is intriguing to hypothesise immune cell dependent, but allodynia preventing, signalling to pain fibres. IHC staining for neuronal skin reinnervation will further clarify the specific neurons responding to IPA treatment and a potential role in thermal nociception.

Additionally and in line with findings in the peripheral nervous system, treatment with IPA following a spinal cord injury resulted in a functional improvement starting at 7 days post injury in behavioural tests for sensory-motor recovery (grid walk) and sensory recovery (Sticky tape

removal) (Figure 22). Rapid recovery within a short time frame formed the basis for the hypothesis that IPA may promote remodelling of supraspinal axonal circuits, facilitating a faster recovery. To investigate this, IHC staining of vGLUT and vGAT in the spinal cord showed an increase in synaptic contacts to the motoneurons in the ventral horn, caudal to the injury (Figure 23). Both results suggest that IPA promotes synaptic plasticity in the spinal cord following spinal cord injury. CTB tracing of sensory fibre regeneration into and across the lesion site did not show robust tracing (Data not shown). However, it has been well established that functional recovery does not rely on regeneration or less die back of long ascending fibres, but rather on synaptic plasticity below the injury site<sup>470-473</sup>. Remodelling of structural synapses results in circuit reorganisation after spinal cord injury<sup>474</sup>, which can restore sensory and motor function<sup>471,475,476</sup>. This can be achieved by molecular and cellular interventions, but also by training and electrophysiological stimulation<sup>157,470,477</sup>. Here we can conclude that IPA treatment following SCI may increase synaptic plasticity leading to supraspinal axonal circuit reorganisation and finally resulting in improved functional recovery. Additionally, GFAP IHC staining of the lesion site revealed that IPA treated mice, compared to PBS treatment, had a 50% decrease in GFAP intensity within the lesion core. This indicates a decreased accumulation of astrocytes following injury resulting in a less dense and potentially more growth permissive glial scar.

Together with the previous data, these results then raise the question as to whether IPA has an immune component following spinal cord injury. Neutrophil and astrocyte quantification at earlier time points will be able to further clarify if IPA induced neutrophil infiltration may be linked to improved sensory-motor recovery and altered activation of astrocytes. Future work will be required to address the possible interconnection between immune response and synaptic plasticity.



#### **4.5 Limitations and future perspectives**

The complexity and systematic nature of intermittent fasting has attracted growing interest over the past few years as it affects many organs and cells throughout the body. In this study we unravelled the impact of 10 days of IF on the gut microbiome and identified a gut microbiome derived metabolite that promotes axonal regeneration. However, some limitations are to be taken into consideration. IF has been shown to affect nutrient sensing pathways, adapting intracellular metabolic signalling and affecting circadian clock gene expression<sup>191</sup>. Additionally, IF has been implicated in the activation of Transcription factors such as CREB<sup>423,478</sup> and has been shown to induce profound transcriptomic changes following brain injury<sup>479</sup>. Therefore, it is likely that IF might increase axonal regeneration through a combination of multiple signalling pathways in addition to the mechanisms described here. Further studies are required to understand the full extent in which IF might impact axonal regeneration.

In order to identify changes in the composition of the gut microbiome, we ran 16S-sequencing analysis at 10 days following IF (Figure 15). Even though 16S-sequencing is able to analyse some bacterial strains to the level of species, it was not sufficient to identify *Clostridium sporogenes*. For a more systematic analysis shot-gut metagenomics sequencing would provide more detailed information of all bacterial families at the species level.

Furthermore, RNA sequencing was conducted from DRG bulk tissue, containing not only neurons, but also satellite cells, endothelial cells and Immune cells (Figure 17). The significant upregulation of immune related genes led us to the hypothesis of an increased infiltration of immune cells following IPA treatment prior to and with injury. Specific FACS analysis from DRG tissue will aim to answer that question. However, single cell analysis of the DRG tissue would be required to uncover to what extent differentially expressed genes are the source of immune cells, neurons or endothelial cells. It is noteworthy to mention that single cell RNAseq would further enable to define if IPA impacts specific neuronal populations over others, through mechanism that might be overshadowed by the vast increase in immune regulatory genes after injury.

Also, more mechanistic investigations are required to understand the signalling induced by IPA in neutrophils and neurons. Firstly, it will be interesting to investigate the sequence of events in more detail. Immunohistochemistry (IHC) staining of the spinal cord lesion site at 24h, 72h and 7 days after injury will uncover if IPA induces the infiltration of higher numbers of neutrophils following SCI and if that is linked to astrocyte activation. Further IHC staining of the SC injury site for NK and T-cells will identify if these are, additional to the findings in DRG, activated and recruited to the spinal cord following injury. Secondly, I hypothesise direct signalling of IPA to the PXR receptor expressed by vascular endothelial cells of the DRG potentially resulting in the recruitment of neutrophils and increased levels of IFN $\gamma$  in DRG tissue, possibly through signalling to NK, NKT

or T-cells. IHC and western blot analysis for markers of neutrophil chemotaxis, such as CXCL1 and CXCR2, from DRG tissue will verify the RNAseq results. Neutrophil recruitment by chemotaxis will be tested via monoclonal antibody injections of anti-CXCR2 in combination with IPA treatment including all the controls, to assess if loss of CXCL1 binding to CXCR2 will deplete the effect of IPA. CXCL1 is expressed and released by vascular endothelial cells upon inflammatory stimulation in the brain<sup>438</sup> and disruption of its signalling to neutrophils will consequently shed light on the dependency of neutrophil recruitment upon IPA treatment.

Secondly, PXR dependency of neutrophil chemotaxis on IPA signalling can be tested in vitro using a microfluidic co-culture platform. Taking advantage of WT and PXR<sup>-/-</sup> mice, this setup will enable the spatial separation of endothelial cells and neutrophils with and without PXR expression and therefore specifically investigate IPA mediated neutrophil chemotaxis reliance on the nuclear receptor in both cell types. Additionally, IPA treatment of a PXR<sup>-/-</sup> mouse should deplete its effect on axonal regeneration and neutrophil infiltration to the DRG. IFN $\gamma$  signalling through its receptor, expressed in DRG neurons, activates the JAK/STAT signalling cascade which has been correlated to axonal regeneration through the expression of regeneration associated genes<sup>96</sup>. A final translational experiment could explore IFNGR enhancing DRG JAK/STAT signalling as a treatment after SCI.

In the present study I identified a novel mechanism interlinking intermittent fasting. More systematic in-depth studies will be needed to fully unravel the sequence of events encompassing immune cell infiltration, signalling and evasion following a sciatic nerve and spinal cord injury. For instance, mass cytometry combined with IHC at different time points post injury together with single cell sequencing from DRG tissue and the spinal cord injury site would be required to fully understand key mechanisms that drive immune modulated axonal regeneration.

#### **4.6 Conclusion**

In Conclusion, this thesis has characterized a novel mechanism interlinking diet induced changes of a gut microbiome derived metabolite with immune-mediated axonal regeneration of the sciatic nerve. Results showed 10 days of IF increased axonal regeneration in the sciatic nerve. It was demonstrated that IF dependent changes of the gut microbiome composition mediate axonal regeneration, specifically via increased synthesis of the gut microbiome derived metabolite IPA. IPA treatment was found to promote axonal regeneration and functional recovery of the sciatic nerve, as well as improved functional recovery and increased synaptic plasticity following spinal cord injury. Further investigation suggested IPA dependent mechanisms involve neutrophils and IFN $\gamma$  signalling.

Pro-inflammatory signalling within a specific time-frame supports axonal regeneration following injury in the peripheral and central nervous system. This study has identified a metabolite that promotes axonal regeneration to the level of functional recovery through mechanisms of inflammation. Therefore, a therapy involving regular IPA administration, orally or intravenously, could further support the physiological efforts of the body to heal and promote axonal regeneration following injury.

Despite the growing interest in gut microbiome impact on health and disease and gut microbiome derived metabolites, currently very little is known within the field. An increasing number of studies supports the application of probiotics for treatment and a recent review even discussed Clostridium transplantation therapy suitability<sup>480</sup>, however more precise understanding of all the signalling targets will be required for therapeutic application.

IPA's mode of action requires further investigation, though recent results and supporting literature indicate IPA constitutes a promising small molecule for regenerative therapy of the injured PNS and CNS.

## Bibliography

- 1 Kandel, E. R. J. H. S., J.H.; Jessell, T.M.; Siegelbaum, S.A.; Hudspeth, A.J.; Mack, S. *Principles of Neural Science*. Vol. 5 (The McGraw-Hill Companies, Inc, 2013).
- 2 Afsoun Seddighi, A. N., Amir Saied Seddighi, Ali Reza Zali, Seyed Mahmood Tabatabaei, Ali Reza Sheykhi, Fatemeh Yourdkhani, Shoayb Naeimian. Peripheral Nerve Injury: A Review Article. *International Clinical Neuroscience Journal* **3**, 6 (2016).
- 3 Asplund, M., Nilsson, M., Jacobsson, A. & von Holst, H. Incidence of traumatic peripheral nerve injuries and amputations in Sweden between 1998 and 2006. *Neuroepidemiology* **32**, 217-228, doi:10.1159/000197900 (2009).
- 4 Evans, G. R. Peripheral nerve injury: a review and approach to tissue engineered constructs. *Anat Rec* **263**, 396-404, doi:10.1002/ar.1120 (2001).
- 5 Taylor, C. A., Braza, D., Rice, J. B. & Dillingham, T. The Incidence of Peripheral Nerve Injury in Extremity Trauma. *American Journal of Physical Medicine & Rehabilitation* **87**, 381-385, doi:10.1097/PHM.0b013e31815e6370 (2008).
- 6 Contractor, S. & Hardman, J. G. Injury during anaesthesia. *Continuing Education in Anaesthesia Critical Care & Pain* **6**, 67-70, doi:10.1093/bjaceaccp/mkl004 (2006).
- 7 Li, R. *et al.* Peripheral nerve injuries treatment: a systematic review. *Cell Biochem Biophys* **68**, 449-454, doi:10.1007/s12013-013-9742-1 (2014).
- 8 Venkatesh, I., Mehra, V., Wang, Z., Califf, B. & Blackmore, M. G. Developmental Chromatin Restriction of Pro-Growth Gene Networks Acts as an Epigenetic Barrier to Axon Regeneration in Cortical Neurons. *Dev Neurobiol* **78**, 960-977, doi:10.1002/dneu.22605 (2018).
- 9 Huebner, E. A. & Strittmatter, S. M. Axon regeneration in the peripheral and central nervous systems. *Results Probl Cell Differ* **48**, 339-351, doi:10.1007/400\_2009\_19 (2009).
- 10 Strand, N. S. *et al.* Wnt/beta-catenin signaling promotes regeneration after adult zebrafish spinal cord injury. *Biochem Biophys Res Commun* **477**, 952-956, doi:10.1016/j.bbrc.2016.07.006 (2016).
- 11 Lindsay, R. M. Nerve growth factors (NGF, BDNF) enhance axonal regeneration but are not required for survival of adult sensory neurons. *J Neurosci* **8**, 2394-2405 (1988).
- 12 Ghosh, S. & Hui, S. P. Axonal regeneration in zebrafish spinal cord. *Regeneration (Oxf)* **5**, 43-60, doi:10.1002/reg2.99 (2018).
- 13 Shimizu, Y., Ueda, Y. & Ohshima, T. Wnt signaling regulates proliferation and differentiation of radial glia in regenerative processes after stab injury in the optic tectum of adult zebrafish. *Glia* **66**, 1382-1394, doi:10.1002/glia.23311 (2018).
- 14 Hoffman, P. N. A conditioning lesion induces changes in gene expression and axonal transport that enhance regeneration by increasing the intrinsic growth state of axons. *Exp Neurol* **223**, 11-18, doi:10.1016/j.expneurol.2009.09.006 (2010).
- 15 Case, J. F. The median nerves and cockroach spiracular function. *Journal of Insect Physiology* **1**, 85-94, doi:[https://doi.org/10.1016/0022-1910\(57\)90025-2](https://doi.org/10.1016/0022-1910(57)90025-2) (1957).
- 16 Hoy, R. R., Bittner, G. D. & Kennedy, D. Regeneration in Crustacean Motoneurons: Evidence for Axonal Fusion. *Science* **156**, 251, doi:10.1126/science.156.3772.251 (1967).
- 17 Muller, K. J. & Carbonetto, S. The morphological and physiological properties of a regenerating synapse in the C.N.S. of the leech. *J Comp Neurol* **185**, 485-516, doi:10.1002/cne.901850305 (1979).
- 18 Allison, P. B., P.R. Anatomical studies of central regeneration of an identified molluscan interneuron. *The Royal Society* **226**, doi:<https://doi.org/10.1098/rspb.1985.0088> (1985).
- 19 Benjamin, P. R. A., P. Regeneration of excitatory, inhibitory and biphasic synaptic connections made by a snail giant interneuron. *Proceedings of the Royal Society of London. Series B. Biological Sciences* **226**, 159-176, doi:10.1098/rspb.1985.0089 (1985).

- 20 Zhang, X.-P. & Ambron, R. T. Positive injury signals induce growth and prolong survival in Aplysia neurons. *Journal of Neurobiology* **45**, 84-94, doi:10.1002/1097-4695(20001105)45:2<84::aid-neu3>3.0.co;2-4 (2000).
- 21 Sung, Y. J., Povelones, M. & Ambron, R. T. RISK-1: A novel MAPK homologue in axoplasm that is activated and retrogradely transported after nerve injury. *Journal of Neurobiology* **47**, 67-79, doi:10.1002/neu.1016 (2001).
- 22 Sung, Y. J., Walters, E. T. & Ambron, R. T. A neuronal isoform of protein kinase G couples mitogen-activated protein kinase nuclear import to axotomy-induced long-term hyperexcitability in Aplysia sensory neurons. *J Neurosci* **24**, 7583-7595, doi:10.1523/JNEUROSCI.1445-04.2004 (2004).
- 23 Schmied, R. & Ambron, R. T. A nuclear localization signal targets proteins to the retrograde transport system, thereby evading uptake into organelles in aplysia axons. *Journal of Neurobiology* **33**, 151-160, doi:10.1002/(sici)1097-4695(199708)33:2<151::aid-neu4>3.0.co;2-1 (1997).
- 24 Lindwall, C. & Kanje, M. Retrograde axonal transport of JNK signaling molecules influence injury induced nuclear changes in p-c-Jun and ATF3 in adult rat sensory neurons. *Mol Cell Neurosci* **29**, 269-282, doi:10.1016/j.mcn.2005.03.002 (2005).
- 25 Perlson, E. *et al.* Vimentin-dependent spatial translocation of an activated MAP kinase in injured nerve. *Neuron* **45**, 715-726, doi:10.1016/j.neuron.2005.01.023 (2005).
- 26 Ben-Yaakov, K. *et al.* Axonal transcription factors signal retrogradely in lesioned peripheral nerve. *EMBO J* **31**, 1350-1363, doi:10.1038/emboj.2011.494 (2012).
- 27 Soares, L., Parisi, M. & Bonini, N. M. Axon injury and regeneration in the adult Drosophila. *Sci Rep* **4**, 6199, doi:10.1038/srep06199 (2014).
- 28 Byrne, A. B. & Hammarlund, M. Axon regeneration in *C. elegans*: Worming our way to mechanisms of axon regeneration. *Exp Neurol* **287**, 300-309, doi:10.1016/j.expneurol.2016.08.015 (2017).
- 29 Lai, C. H., Chou, C. Y., Ch'ang, L. Y., Liu, C. S. & Lin, W. Identification of novel human genes evolutionarily conserved in *Caenorhabditis elegans* by comparative proteomics. *Genome research* **10**, 703-713, doi:10.1101/gr.10.5.703 (2000).
- 30 Hammarlund, M., Nix, P., Hauth, L., Jorgensen, E. M. & Bastiani, M. Axon regeneration requires a conserved MAP kinase pathway. *Science* **323**, 802-806, doi:10.1126/science.1165527 (2009).
- 31 Yan, D. & Jin, Y. Regulation of DLK-1 kinase activity by calcium-mediated dissociation from an inhibitory isoform. *Neuron* **76**, 534-548, doi:10.1016/j.neuron.2012.08.043 (2012).
- 32 Yan, D., Wu, Z., Chisholm, A. D. & Jin, Y. The DLK-1 kinase promotes mRNA stability and local translation in *C. elegans* synapses and axon regeneration. *Cell* **138**, 1005-1018, doi:10.1016/j.cell.2009.06.023 (2009).
- 33 Byrne, A. B. *et al.* Insulin/IGF1 signaling inhibits age-dependent axon regeneration. *Neuron* **81**, 561-573, doi:10.1016/j.neuron.2013.11.019 (2014).
- 34 El Bejjani, R. & Hammarlund, M. Notch signaling inhibits axon regeneration. *Neuron* **73**, 268-278, doi:10.1016/j.neuron.2011.11.017 (2012).
- 35 Tessier-Lavigne, M. & Placzek, M. Target attraction: Are developing axons guided by chemotropism? *Trends in Neurosciences* **14**, 303-310, doi:10.1016/0166-2236(91)90142-H (1991).
- 36 Xu, P. *et al.* Nerve injury induces glial cell line-derived neurotrophic factor (GDNF) expression in Schwann cells through purinergic signaling and the PKC-PKD pathway. *Glia* **61**, 1029-1040, doi:10.1002/glia.22491 (2013).
- 37 Borschel, G. H. *et al.* Glial-derived neurotrophic factor (GDNF) delivered from microspheres enhances peripheral nerve regeneration after delayed nerve repair. *Journal of the American College of Surgeons* **215**, S90, doi:10.1016/j.jamcollsurg.2012.06.241 (2012).

- 38 Eggers, R. *et al.* Lentiviral vector-mediated gradients of GDNF in the injured peripheral nerve: effects on nerve coil formation, Schwann cell maturation and myelination. *PLoS One* **8**, e71076, doi:10.1371/journal.pone.0071076 (2013).
- 39 Namgung, U. The role of Schwann cell-axon interaction in peripheral nerve regeneration. *Cells Tissues Organs* **200**, 6-12, doi:10.1159/000370324 (2014).
- 40 Neumann, S. & Woolf, C. J. Regeneration of Dorsal Column Fibers into and beyond the Lesion Site following Adult Spinal Cord Injury. *Neuron* **23**, 83-91, doi:[https://doi.org/10.1016/S0896-6273\(00\)80755-2](https://doi.org/10.1016/S0896-6273(00)80755-2) (1999).
- 41 Waller, A. Experiments on the Section of the Glossopharyngeal and Hypoglossal Nerves of the Frog, and Observations of the Alterations Produced Thereby in the Structure of Their Primitive Fibres. *Philosophical Transactions of the Royal Society of London* **140**, 423-429 (1850).
- 42 Rotshenker, S. Wallerian degeneration: the innate-immune response to traumatic nerve injury. *J Neuroinflammation* **8**, 109, doi:10.1186/1742-2094-8-109 (2011).
- 43 Sievers, C., Platt, N., Perry, V. H., Coleman, M. P. & Conforti, L. Neurites undergoing Wallerian degeneration show an apoptotic-like process with annexin V positive staining and loss of mitochondrial membrane potential. *Neuroscience Research* **46**, 161-169, doi:10.1016/s0168-0102(03)00039-7 (2003).
- 44 Spira, M. E., Oren, R., Dormann, A. & Gitler, D. Critical calpain-dependent ultrastructural alterations underlie the transformation of an axonal segment into a growth cone after axotomy of cultured Aplysia neurons. *J Comp Neurol* **457**, 293-312, doi:10.1002/cne.10569 (2003).
- 45 Spira, M. E., Oren, R., Dormann, A., Ilouz, N. & Lev, S. Calcium, protease activation, and cytoskeleton remodeling underlie growth cone formation and neuronal regeneration. *Cell Mol Neurobiol* **21**, 591-604, doi:10.1023/a:1015135617557 (2001).
- 46 Howard, M. J., David, G. & Barrett, J. N. Resealing of transected myelinated mammalian axons in vivo: evidence for involvement of calpain. *Neuroscience* **93**, 807-815, doi:[https://doi.org/10.1016/S0306-4522\(99\)00195-5](https://doi.org/10.1016/S0306-4522(99)00195-5) (1999).
- 47 Gray, M., Palispis, W., Popovich, P. G., van Rooijen, N. & Gupta, R. Macrophage depletion alters the blood-nerve barrier without affecting Schwann cell function after neural injury. *J Neurosci Res* **85**, 766-777, doi:10.1002/jnr.21166 (2007).
- 48 Weerasuriya, A. & Hockman, C. H. Perineurial permeability to sodium during Wallerian degeneration in rat sciatic nerve. *Brain Research* **581**, 327-333, doi:[https://doi.org/10.1016/0006-8993\(92\)90727-Q](https://doi.org/10.1016/0006-8993(92)90727-Q) (1992).
- 49 Mizisin, A. P. & Weerasuriya, A. Homeostatic regulation of the endoneurial microenvironment during development, aging and in response to trauma, disease and toxic insult. *Acta Neuropathol* **121**, 291-312, doi:10.1007/s00401-010-0783-x (2011).
- 50 Guertin, A. D., Zhang, D. P., Mak, K. S., Alberta, J. A. & Kim, H. A. Microanatomy of axon/glial signaling during Wallerian degeneration. *J Neurosci* **25**, 3478-3487, doi:10.1523/JNEUROSCI.3766-04.2005 (2005).
- 51 Murinson, B. B., Archer, D. R., Li, Y. & Griffin, J. W. Degeneration of myelinated efferent fibers prompts mitosis in Remak Schwann cells of uninjured C-fiber afferents. *J Neurosci* **25**, 1179-1187, doi:10.1523/JNEUROSCI.1372-04.2005 (2005).
- 52 Fex Svennigsen, A. & Dahlin, L. B. Repair of the Peripheral Nerve-Remyelination that Works. *Brain Sci* **3**, 1182-1197, doi:10.3390/brainsci3031182 (2013).
- 53 Tofaris, G. K., Patterson, P. H., Jessen, K. R. & Mirsky, R. Denervated Schwann cells attract macrophages by secretion of leukemia inhibitory factor (LIF) and monocyte chemoattractant protein-1 in a process regulated by interleukin-6 and LIF. *J Neurosci* **22**, 6696-6703, doi:20026699 (2002).
- 54 Madduri, S. & Gander, B. Schwann cell delivery of neurotrophic factors for peripheral nerve regeneration. *Journal of the peripheral nervous system : JPNS* **15**, 93-103, doi:10.1111/j.1529-8027.2010.00257.x (2010).

- 55 Hervera, A. *et al.* Reactive oxygen species regulate axonal regeneration through the release of exosomal NADPH oxidase 2 complexes into injured axons. *Nat Cell Biol* **20**, 307-319, doi:10.1038/s41556-018-0039-x (2018).
- 56 Gaudet, A. D., Popovich, P. G. & Ramer, M. S. Wallerian degeneration: gaining perspective on inflammatory events after peripheral nerve injury. *J Neuroinflammation* **8**, 110, doi:10.1186/1742-2094-8-110 (2011).
- 57 Doyu, M. *et al.* Laminin A, B1, and B2 Chain Gene Expression in Transected and Regenerating Nerves: Regulation by Axonal Signals. *Journal of Neurochemistry* **60**, 543-551, doi:10.1111/j.1471-4159.1993.tb03183.x (1993).
- 58 Kuecherer-Ehret, A., Graeber, M. B., Edgar, D., Thoenen, H. & Kreutzberg, G. W. Immunoelectron microscopic localization of laminin in normal and regenerating mouse sciatic nerve. *Journal of Neurocytology* **19**, 101-109, doi:10.1007/BF01188442 (1990).
- 59 Wallquist, W. *et al.* Laminin chains in rat and human peripheral nerve: Distribution and regulation during development and after axonal injury. *Journal of Comparative Neurology* **454**, 284-293, doi:10.1002/cne.10434 (2002).
- 60 Agius, E. & Cochard, P. Comparison of Neurite Outgrowth Induced by Intact and Injured Sciatic Nerves: A Confocal and Functional Analysis. *The Journal of Neuroscience* **18**, 328, doi:10.1523/JNEUROSCI.18-01-00328.1998 (1998).
- 61 Chen, Z. L. & Strickland, S. Laminin gamma1 is critical for Schwann cell differentiation, axon myelination, and regeneration in the peripheral nerve. *J Cell Biol* **163**, 889-899, doi:10.1083/jcb.200307068 (2003).
- 62 Condic, M. L. Adult Neuronal Regeneration Induced by Transgenic Integrin Expression. *The Journal of Neuroscience* **21**, 4782, doi:10.1523/JNEUROSCI.21-13-04782.2001 (2001).
- 63 Nieuwenhuis, B., Haenzi, B., Andrews, M. R., Verhaagen, J. & Fawcett, J. W. Integrins promote axonal regeneration after injury of the nervous system. *Biol Rev Camb Philos Soc* **93**, 1339-1362, doi:10.1111/brv.12398 (2018).
- 64 Gary, D. S. & Mattson, M. P. Integrin signaling via the PI3-kinase–Akt pathway increases neuronal resistance to glutamate-induced apoptosis. *Journal of Neurochemistry* **76**, 1485-1496, doi:10.1046/j.1471-4159.2001.00173.x (2001).
- 65 Schäfer, M., Fruttiger, M., Montag, D., Schachner, M. & Martini, R. Disruption of the Gene for the Myelin-Associated Glycoprotein Improves Axonal Regrowth along Myelin in C57BL/Wlds Mice. *Neuron* **16**, 1107-1113, doi:[https://doi.org/10.1016/S0896-6273\(00\)80137-3](https://doi.org/10.1016/S0896-6273(00)80137-3) (1996).
- 66 Neumann, S., Bradke, F., Tessier-Lavigne, M. & Basbaum, A. I. Regeneration of Sensory Axons within the Injured Spinal Cord Induced by Intraganglionic cAMP Elevation. *Neuron* **34**, 885-893, doi:[https://doi.org/10.1016/S0896-6273\(02\)00702-X](https://doi.org/10.1016/S0896-6273(02)00702-X) (2002).
- 67 Qiu, J. *et al.* Spinal Axon Regeneration Induced by Elevation of Cyclic AMP. *Neuron* **34**, 895-903, doi:[https://doi.org/10.1016/S0896-6273\(02\)00730-4](https://doi.org/10.1016/S0896-6273(02)00730-4) (2002).
- 68 Griffin, J. W. & Thompson, W. J. Biology and pathology of nonmyelinating Schwann cells. *Glia* **56**, 1518-1531, doi:10.1002/glia.20778 (2008).
- 69 Stoll, G., Griffin, J. W., Li, C. Y. & Trapp, B. D. Wallerian degeneration in the peripheral nervous system: participation of both Schwann cells and macrophages in myelin degradation. *Journal of Neurocytology* **18**, 671-683, doi:10.1007/BF01187086 (1989).
- 70 Chen, Z. L., Yu, W. M. & Strickland, S. Peripheral regeneration. *Annu Rev Neurosci* **30**, 209-233, doi:10.1146/annurev.neuro.30.051606.094337 (2007).
- 71 Huang, E. J. & Reichardt, L. F. Neurotrophins: roles in neuronal development and function. *Annu Rev Neurosci* **24**, 677-736, doi:10.1146/annurev.neuro.24.1.677 (2001).
- 72 Makwana, M. & Raivich, G. Molecular mechanisms in successful peripheral regeneration. *FEBS J* **272**, 2628-2638, doi:10.1111/j.1742-4658.2005.04699.x (2005).



- 73 Markus, A., Patel, T. D. & Snider, W. D. Neurotrophic factors and axonal growth. *Current Opinion in Neurobiology* **12**, 523-531, doi:[https://doi.org/10.1016/S0959-4388\(02\)00372-0](https://doi.org/10.1016/S0959-4388(02)00372-0) (2002).
- 74 Snider, W. D., Zhou, F.-Q., Zhong, J. & Markus, A. Signaling the Pathway to Regeneration. *Neuron* **35**, 13-16, doi:[https://doi.org/10.1016/S0896-6273\(02\)00762-6](https://doi.org/10.1016/S0896-6273(02)00762-6) (2002).
- 75 Yoshimura, T. *et al.* GSK-3beta regulates phosphorylation of CRMP-2 and neuronal polarity. *Cell* **120**, 137-149, doi:10.1016/j.cell.2004.11.012 (2005).
- 76 Zhou, F. Q. *et al.* Neurotrophins support regenerative axon assembly over CSPGs by an ECM-integrin-independent mechanism. *J Cell Sci* **119**, 2787-2796, doi:10.1242/jcs.03016 (2006).
- 77 Zhou, F. Q., Zhou, J., Dedhar, S., Wu, Y. H. & Snider, W. D. NGF-induced axon growth is mediated by localized inactivation of GSK-3beta and functions of the microtubule plus end binding protein APC. *Neuron* **42**, 897-912, doi:10.1016/j.neuron.2004.05.011 (2004).
- 78 Boyd, J. Glial cell line-derived neurotrophic factor and brain-derived neurotrophic factor sustain the axonal regeneration of chronically axotomized motoneurons in vivo. *Experimental Neurology* **183**, 610-619, doi:10.1016/s0014-4886(03)00183-3 (2003).
- 79 Boyd, J. G. & Gordon, T. A dose-dependent facilitation and inhibition of peripheral nerve regeneration by brain-derived neurotrophic factor. *European Journal of Neuroscience* **15**, 613-626, doi:10.1046/j.1460-9568.2002.01891.x (2002).
- 80 Chan, J. R., Cosgaya, J. M., Wu, Y. J. & Shooter, E. M. Neurotrophins are key mediators of the myelination program in the peripheral nervous system. *Proceedings of the National Academy of Sciences* **98**, 14661, doi:10.1073/pnas.251543398 (2001).
- 81 Höke, A. *et al.* Glial Cell Line-Derived Neurotrophic Factor Alters Axon Schwann Cell Units and Promotes Myelination in Unmyelinated Nerve Fibers. *The Journal of Neuroscience* **23**, 561, doi:10.1523/JNEUROSCI.23-02-00561.2003 (2003).
- 82 Iwase, T., Jung, C. G., Bae, H., Zhang, M. & Soliven, B. Glial cell line-derived neurotrophic factor-induced signaling in Schwann cells. *J Neurochem* **94**, 1488-1499, doi:10.1111/j.1471-4159.2005.03290.x (2005).
- 83 Carroll, S. L., Miller, M. L., Frohnert, P. W., Kim, S. S. & Corbett, J. A. Expression of Neuregulins and their Putative Receptors, ErbB2 and ErbB3, Is Induced during Wallerian Degeneration. *The Journal of Neuroscience* **17**, 1642, doi:10.1523/JNEUROSCI.17-05-01642.1997 (1997).
- 84 Yawo, H. & Kuno, M. Calcium dependence of membrane sealing at the cut end of the cockroach giant axon. *The Journal of neuroscience : the official journal of the Society for Neuroscience* **5**, 1626-1632, doi:10.1523/JNEUROSCI.05-06-01626.1985 (1985).
- 85 Rishal, I. & Fainzilber, M. Axon-soma communication in neuronal injury. *Nat Rev Neurosci* **15**, 32-42, doi:10.1038/nrn3609 (2014).
- 86 Saito, A. & Cavalli, V. Signaling Over Distances. *Mol Cell Proteomics* **15**, 382-393, doi:10.1074/mcp.R115.052753 (2016).
- 87 Abe, N. & Cavalli, V. Nerve injury signaling. *Curr Opin Neurobiol* **18**, 276-283, doi:10.1016/j.conb.2008.06.005 (2008).
- 88 Ghosh-Roy, A., Wu, Z., Goncharov, A., Jin, Y. & Chisholm, A. D. Calcium and cyclic AMP promote axonal regeneration in *Caenorhabditis elegans* and require DLK-1 kinase. *J Neurosci* **30**, 3175-3183, doi:10.1523/JNEUROSCI.5464-09.2010 (2010).
- 89 Shin, J. E. *et al.* Dual leucine zipper kinase is required for retrograde injury signaling and axonal regeneration. *Neuron* **74**, 1015-1022, doi:10.1016/j.neuron.2012.04.028 (2012).
- 90 Puttagunta, R. *et al.* PCAF-dependent epigenetic changes promote axonal regeneration in the central nervous system. *Nat Commun* **5**, 3527, doi:10.1038/ncomms4527 (2014).
- 91 Cho, Y. & Cavalli, V. HDAC5 is a novel injury-regulated tubulin deacetylase controlling axon regeneration. *EMBO J* **31**, 3063-3078, doi:10.1038/emboj.2012.160 (2012).



- 92 Cho, Y., Sloutsky, R., Naegle, K. M. & Cavalli, V. Injury-induced HDAC5 nuclear export is essential for axon regeneration. *Cell* **155**, 894-908, doi:10.1016/j.cell.2013.10.004 (2013).
- 93 Mahar, M. & Cavalli, V. Intrinsic mechanisms of neuronal axon regeneration. *Nat Rev Neurosci* **19**, 323-337, doi:10.1038/s41583-018-0001-8 (2018).
- 94 Palmisano, I. *et al.* Epigenomic signatures underpin the axonal regenerative ability of dorsal root ganglia sensory neurons. *Nat Neurosci* **22**, 1913-1924, doi:10.1038/s41593-019-0490-4 (2019).
- 95 Weng, Y. L. *et al.* An Intrinsic Epigenetic Barrier for Functional Axon Regeneration. *Neuron* **94**, 337-346 e336, doi:10.1016/j.neuron.2017.03.034 (2017).
- 96 Qiu, J., Cafferty, W. B., McMahon, S. B. & Thompson, S. W. Conditioning injury-induced spinal axon regeneration requires signal transducer and activator of transcription 3 activation. *J Neurosci* **25**, 1645-1653, doi:10.1523/JNEUROSCI.3269-04.2005 (2005).
- 97 Seiffers, R., Mills, C. D. & Woolf, C. J. ATF3 increases the intrinsic growth state of DRG neurons to enhance peripheral nerve regeneration. *J Neurosci* **27**, 7911-7920, doi:10.1523/JNEUROSCI.5313-06.2007 (2007).
- 98 Lonze, B. E., Riccio, A., Cohen, S. & Ginty, D. D. Apoptosis, Axonal Growth Defects, and Degeneration of Peripheral Neurons in Mice Lacking CREB. *Neuron* **34**, 371-385, doi:[https://doi.org/10.1016/S0896-6273\(02\)00686-4](https://doi.org/10.1016/S0896-6273(02)00686-4) (2002).
- 99 Liu, R. Y. & Snider, W. D. Different signaling pathways mediate regenerative versus developmental sensory axon growth. *The Journal of neuroscience : the official journal of the Society for Neuroscience* **21**, RC164-RC164, doi:10.1523/JNEUROSCI.21-17-j0003.2001 (2001).
- 100 Zhou, F. Q., Walzer, M. A. & Snider, W. D. Turning on the machine: genetic control of axon regeneration by c-Jun. *Neuron* **43**, 1-2, doi:10.1016/j.neuron.2004.06.020 (2004).
- 101 Jing, X., Wang, T., Huang, S., Glorioso, J. C. & Albers, K. M. The transcription factor Sox11 promotes nerve regeneration through activation of the regeneration-associated gene *Sprr1a*. *Exp Neurol* **233**, 221-232, doi:10.1016/j.expneurol.2011.10.005 (2012).
- 102 Gaub, P. *et al.* The histone acetyltransferase p300 promotes intrinsic axonal regeneration. *Brain* **134**, 2134-2148, doi:10.1093/brain/awr142 (2011).
- 103 Wang, Z., Reynolds, A., Kirry, A., Nienhaus, C. & Blackmore, M. G. Overexpression of Sox11 Promotes Corticospinal Tract Regeneration after Spinal Injury While Interfering with Functional Recovery. *The Journal of Neuroscience* **35**, 3139, doi:10.1523/JNEUROSCI.2832-14.2015 (2015).
- 104 Huang, X. *et al.* Overexpression of the transcription factors OCT4 and KLF4 improves motor function after spinal cord injury. *CNS Neurosci Ther*, doi:10.1111/cns.13390 (2020).
- 105 Fagoe, N. D., Attwell, C. L., Kouwenhoven, D., Verhaagen, J. & Mason, M. R. Overexpression of ATF3 or the combination of ATF3, c-Jun, STAT3 and Smad1 promotes regeneration of the central axon branch of sensory neurons but without synergistic effects. *Hum Mol Genet* **24**, 6788-6800, doi:10.1093/hmg/ddv383 (2015).
- 106 Mehta, S. T., Luo, X., Park, K. K., Bixby, J. L. & Lemmon, V. P. Hyperactivated Stat3 boosts axon regeneration in the CNS. *Exp Neurol* **280**, 115-120, doi:10.1016/j.expneurol.2016.03.004 (2016).
- 107 Bareyre, F. M. *et al.* In vivo imaging reveals a phase-specific role of STAT3 during central and peripheral nervous system axon regeneration. *Proc Natl Acad Sci U S A* **108**, 6282-6287, doi:10.1073/pnas.1015239108 (2011).
- 108 Tedeschi, A. *et al.* The Calcium Channel Subunit Alpha2delta2 Suppresses Axon Regeneration in the Adult CNS. *Neuron* **92**, 419-434, doi:10.1016/j.neuron.2016.09.026 (2016).

- 109 Quadrato, G. & Di Giovanni, S. Waking up the sleepers: shared transcriptional pathways in axonal regeneration and neurogenesis. *Cell Mol Life Sci* **70**, 993-1007, doi:10.1007/s00018-012-1099-x (2013).
- 110 Christie, K. J., Webber, C. A., Martinez, J. A., Singh, B. & Zochodne, D. W. PTEN inhibition to facilitate intrinsic regenerative outgrowth of adult peripheral axons. *J Neurosci* **30**, 9306-9315, doi:10.1523/JNEUROSCI.6271-09.2010 (2010).
- 111 Fox, I. K. & Mackinnon, S. E. Adult peripheral nerve disorders: nerve entrapment, repair, transfer, and brachial plexus disorders. *Plast Reconstr Surg* **127**, 105e-118e, doi:10.1097/PRS.0b013e31820cf556 (2011).
- 112 Hagen, E. M. Acute complications of spinal cord injuries. *World J Orthop* **6**, 17-23, doi:10.5312/wjo.v6.i1.17 (2015).
- 113 Sekhon, L. H. S. & Fehlings, M. G. Epidemiology, Demographics, and Pathophysiology of Acute Spinal Cord Injury. *Spine* **26** (2001).
- 114 Young, W. & Koreh, I. Potassium and calcium changes in injured spinal cords. *Brain Research* **365**, 42-53, doi:[https://doi.org/10.1016/0006-8993\(86\)90720-1](https://doi.org/10.1016/0006-8993(86)90720-1) (1986).
- 115 Carulli, D., Laabs, T., Geller, H. M. & Fawcett, J. W. Chondroitin sulfate proteoglycans in neural development and regeneration. *Curr Opin Neurobiol* **15**, 116-120, doi:10.1016/j.conb.2005.01.014 (2005).
- 116 Bradbury, E. J. *et al.* Chondroitinase ABC promotes functional recovery after spinal cord injury. *Nature* **416**, 636-640, doi:10.1038/416636a (2002).
- 117 Karimi-Abdolrezaee, S., Eftekharpour, E., Wang, J., Schut, D. & Fehlings, M. G. Synergistic effects of transplanted adult neural stem/progenitor cells, chondroitinase, and growth factors promote functional repair and plasticity of the chronically injured spinal cord. *J Neurosci* **30**, 1657-1676, doi:10.1523/JNEUROSCI.3111-09.2010 (2010).
- 118 Sandvig, A., Berry, M., Barrett, L. B., Butt, A. & Logan, A. Myelin-, reactive glia-, and scar-derived CNS axon growth inhibitors: expression, receptor signaling, and correlation with axon regeneration. *Glia* **46**, 225-251, doi:10.1002/glia.10315 (2004).
- 119 Yiu, G. & He, Z. Glial inhibition of CNS axon regeneration. *Nat Rev Neurosci* **7**, 617-627, doi:10.1038/nrn1956 (2006).
- 120 Fawcett, J. W., Schwab, M. E., Montani, L., Brazda, N. & Müller, H. W. in *Handbook of Clinical Neurology* Vol. 109 (eds Joost Verhaagen & John W. McDonald) 503-522 (Elsevier, 2012).
- 121 Filbin, M. T. Myelin-associated inhibitors of axonal regeneration in the adult mammalian CNS. *Nature Reviews Neuroscience* **4**, 703-713, doi:10.1038/nrn1195 (2003).
- 122 Sartori, A. M., Hofer, A.-S. & Schwab, M. E. Recovery after spinal cord injury is enhanced by anti-Nogo-A antibody therapy — from animal models to clinical trials. *Current Opinion in Physiology* **14**, 1-6, doi:10.1016/j.cophys.2019.11.001 (2020).
- 123 Sivasankaran, R. *et al.* PKC mediates inhibitory effects of myelin and chondroitin sulfate proteoglycans on axonal regeneration. *Nature Neuroscience* **7**, 261-268, doi:10.1038/nn1193 (2004).
- 124 Wang, X., Hu, J., She, Y., Smith, G. M. & Xu, X. M. Cortical PKC inhibition promotes axonal regeneration of the corticospinal tract and forelimb functional recovery after cervical dorsal spinal hemisection in adult rats. *Cereb Cortex* **24**, 3069-3079, doi:10.1093/cercor/bht162 (2014).
- 125 Peruzzotti-Jametti, L. *et al.* The role of the immune system in central nervous system plasticity after acute injury. *Neuroscience* **283**, 210-221, doi:10.1016/j.neuroscience.2014.04.036 (2014).
- 126 Sofroniew, M. V. Astrogliosis. *Cold Spring Harb Perspect Biol* **7**, a020420, doi:10.1101/cshperspect.a020420 (2014).
- 127 Zamanian, J. L. *et al.* Genomic analysis of reactive astrogliosis. *J Neurosci* **32**, 6391-6410, doi:10.1523/JNEUROSCI.6221-11.2012 (2012).

- 128 Chen, M. *et al.* Leucine Zipper-Bearing Kinase Is a Critical Regulator of Astrocyte Reactivity in the Adult Mammalian CNS. *Cell Rep* **22**, 3587-3597, doi:10.1016/j.celrep.2018.02.102 (2018).
- 129 Rhodes, K. E. & Fawcett, J. W. Chondroitin sulphate proteoglycans: preventing plasticity or protecting the CNS? *J Anat* **204**, 33-48, doi:10.1111/j.1469-7580.2004.00261.x (2004).
- 130 Avram, S., Shaposhnikov, S., Buiu, C. & Mernea, M. Chondroitin Sulfate Proteoglycans: Structure-Function Relationship with Implication in Neural Development and Brain Disorders. *BioMed Research International* **2014**, 642798, doi:10.1155/2014/642798 (2014).
- 131 Siebert, J. R., Conta Steencken, A. & Osterhout, D. J. Chondroitin Sulfate Proteoglycans in the Nervous System: Inhibitors to Repair. *BioMed Research International* **2014**, 845323, doi:10.1155/2014/845323 (2014).
- 132 Irvine, S. F. & Kwok, J. C. F. Perineuronal Nets in Spinal Motoneurons: Chondroitin Sulphate Proteoglycan around Alpha Motoneurons. *International journal of molecular sciences* **19**, 1172, doi:10.3390/ijms19041172 (2018).
- 133 Wen, T. H., Binder, D. K., Ethell, I. M. & Razak, K. A. The Perineuronal 'Safety' Net? Perineuronal Net Abnormalities in Neurological Disorders. *Front Mol Neurosci* **11**, 270, doi:10.3389/fnmol.2018.00270 (2018).
- 134 McKeon, R. J., Höke, A. & Silver, J. Injury-Induced Proteoglycans Inhibit the Potential for Laminin-Mediated Axon Growth on Astrocytic Scars. *Experimental Neurology* **136**, 32-43, doi:<https://doi.org/10.1006/exnr.1995.1081> (1995).
- 135 Jones, L. L., Yamaguchi, Y., Stallcup, W. B. & Tuszynski, M. H. NG2 is a major chondroitin sulfate proteoglycan produced after spinal cord injury and is expressed by macrophages and oligodendrocyte progenitors. *The Journal of neuroscience : the official journal of the Society for Neuroscience* **22**, 2792-2803, doi:10.1523/JNEUROSCI.22-07-02792.2002 (2002).
- 136 Tan, C. L. *et al.* Integrin activation promotes axon growth on inhibitory chondroitin sulfate proteoglycans by enhancing integrin signaling. *J Neurosci* **31**, 6289-6295, doi:10.1523/JNEUROSCI.0008-11.2011 (2011).
- 137 Shen, Y. *et al.* PTP $\sigma$  Is a Receptor for Chondroitin Sulfate Proteoglycan, an Inhibitor of Neural Regeneration. *Science* **326**, 592, doi:10.1126/science.1178310 (2009).
- 138 Fisher, D. *et al.* Leukocyte common antigen-related phosphatase is a functional receptor for chondroitin sulfate proteoglycan axon growth inhibitors. *The Journal of neuroscience : the official journal of the Society for Neuroscience* **31**, 14051-14066, doi:10.1523/JNEUROSCI.1737-11.2011 (2011).
- 139 Lang, B. T. *et al.* Modulation of the proteoglycan receptor PTP $\sigma$  promotes recovery after spinal cord injury. *Nature* **518**, 404-408, doi:10.1038/nature13974 (2015).
- 140 Dickendesher, T. L. *et al.* NgR1 and NgR3 are receptors for chondroitin sulfate proteoglycans. *Nature neuroscience* **15**, 703-712, doi:10.1038/nn.3070 (2012).
- 141 Xu, B. *et al.* Role of CSPG receptor LAR phosphatase in restricting axon regeneration after CNS injury. *Neurobiology of disease* **73**, 36-48, doi:10.1016/j.nbd.2014.08.030 (2015).
- 142 Ohtake, Y., Wong, D., Abdul-Muneer, P. M., Selzer, M. E. & Li, S. Two PTP receptors mediate CSPG inhibition by convergent and divergent signaling pathways in neurons. *Sci Rep* **6**, 37152, doi:10.1038/srep37152 (2016).
- 143 Silver, J. & Miller, J. H. Regeneration beyond the glial scar. *Nat Rev Neurosci* **5**, 146-156, doi:10.1038/nrn1326 (2004).
- 144 Anderson, M. A. *et al.* Astrocyte scar formation aids central nervous system axon regeneration. *Nature* **532**, 195-200, doi:10.1038/nature17623 (2016).
- 145 Blackmore, M. G. *et al.* Kruppel-like Factor 7 engineered for transcriptional activation promotes axon regeneration in the adult corticospinal tract. *Proc Natl Acad Sci U S A* **109**, 7517-7522, doi:10.1073/pnas.1120684109 (2012).

- 146 Wang, Z. *et al.* KLF6 and STAT3 co-occupy regulatory DNA and functionally synergize  
to promote axon growth in CNS neurons. *Sci Rep* **8**, 12565, doi:10.1038/s41598-018-  
31101-5 (2018).
- 147 Norsworthy, M. W. *et al.* Sox11 Expression Promotes Regeneration of Some Retinal  
Ganglion Cell Types but Kills Others. *Neuron* **94**, 1112-1120 e1114,  
doi:10.1016/j.neuron.2017.05.035 (2017).
- 148 Baker, B. J., Akhtar, L. N. & Benveniste, E. N. SOCS1 and SOCS3 in the control of CNS  
immunity. *Trends Immunol* **30**, 392-400, doi:10.1016/j.it.2009.07.001 (2009).
- 149 Smith, P. D. *et al.* SOCS3 deletion promotes optic nerve regeneration in vivo. *Neuron* **64**,  
617-623, doi:10.1016/j.neuron.2009.11.021 (2009).
- 150 Lee, D.-H. *et al.* Mammalian target of rapamycin's distinct roles and effectiveness in  
promoting compensatory axonal sprouting in the injured CNS. *The Journal of  
neuroscience : the official journal of the Society for Neuroscience* **34**, 15347-15355,  
doi:10.1523/jneurosci.1935-14.2014 (2014).
- 151 Park, K. K. *et al.* Promoting axon regeneration in the adult CNS by modulation of the  
PTEN/mTOR pathway. *Science* **322**, 963-966, doi:10.1126/science.1161566 (2008).
- 152 Park, K. K., Liu, K., Hu, Y., Kanter, J. L. & He, Z. PTEN/mTOR and axon regeneration.  
*Experimental neurology* **223**, 45-50, doi:10.1016/j.expneurol.2009.12.032 (2010).
- 153 Liu, K. *et al.* PTEN deletion enhances the regenerative ability of adult corticospinal  
neurons. *Nat Neurosci* **13**, 1075-1081, doi:10.1038/nn.2603 (2010).
- 154 Danilov, C. A. & Steward, O. Conditional genetic deletion of PTEN after a spinal cord  
injury enhances regenerative growth of CST axons and motor function recovery in mice.  
*Exp Neurol* **266**, 147-160, doi:10.1016/j.expneurol.2015.02.012 (2015).
- 155 Abe, N., Borson, S. H., Gambello, M. J., Wang, F. & Cavalli, V. Mammalian target of  
rapamycin (mTOR) activation increases axonal growth capacity of injured peripheral  
nerves. *J Biol Chem* **285**, 28034-28043, doi:10.1074/jbc.M110.125336 (2010).
- 156 Mattson, M. P., Moehl, K., Ghena, N., Schmaedick, M. & Cheng, A. Intermittent  
metabolic switching, neuroplasticity and brain health. *Nat Rev Neurosci* **19**, 63-80,  
doi:10.1038/nrn.2017.156 (2018).
- 157 Hutson, T. H. *et al.* Cbp-dependent histone acetylation mediates axon regeneration  
induced by environmental enrichment in rodent spinal cord injury models. *Science  
Translational Medicine* **11**, eaaw2064, doi:10.1126/scitranslmed.aaw2064 (2019).
- 158 Molina-Serrano, D., Kyriakou, D. & Kirmizis, A. Histone Modifications as an  
Intersection Between Diet and Longevity. *Front Genet* **10**, 192,  
doi:10.3389/fgene.2019.00192 (2019).
- 159 Gensous, N. *et al.* The Impact of Caloric Restriction on the Epigenetic Signatures of  
Aging. *Int J Mol Sci* **20**, doi:10.3390/ijms20082022 (2019).
- 160 Han, S. M., Baig, H. S. & Hammarlund, M. Mitochondria Localize to Injured Axons to  
Support Regeneration. *Neuron* **92**, 1308-1323, doi:10.1016/j.neuron.2016.11.025 (2016).
- 161 Zhou, B. *et al.* Facilitation of axon regeneration by enhancing mitochondrial transport and  
rescuing energy deficits. *J Cell Biol* **214**, 103-119, doi:10.1083/jcb.201605101 (2016).
- 162 Agostinone, J. *et al.* Insulin signalling promotes dendrite and synapse regeneration and  
restores circuit function after axonal injury. *Brain* **141**, 1963-1980,  
doi:10.1093/brain/awy142 (2018).
- 163 Liu, Y. *et al.* A Sensitized IGF1 Treatment Restores Corticospinal Axon-Dependent  
Functions. *Neuron* **95**, 817-833 e814, doi:10.1016/j.neuron.2017.07.037 (2017).
- 164 Hwang, D. H., Park, H. H., Shin, H. Y., Cui, Y. & Kim, B. G. Insulin-like Growth Factor-  
1 Receptor Dictates Beneficial Effects of Treadmill Training by Regulating Survival and  
Migration of Neural Stem Cell Grafts in the Injured Spinal Cord. *Exp Neurobiol* **27**, 489-  
507, doi:10.5607/en.2018.27.6.489 (2018).

- 165 Karlsson, M. *et al.* Changes in energy metabolism due to acute rotenone-induced mitochondrial complex I dysfunction - An in vivo large animal model. *Mitochondrion* **31**, 56-62, doi:10.1016/j.mito.2016.10.003 (2016).
- 166 Duckworth, W. C. *et al.* Glucose Intolerance Due to Insulin Resistance in Patients with Spinal Cord Injuries. *Diabetes* **29**, 906, doi:10.2337/diab.29.11.906 (1980).
- 167 Mattson, M. P., Longo, V. D. & Harvie, M. Impact of intermittent fasting on health and disease processes. *Ageing Res Rev*, doi:10.1016/j.arr.2016.10.005 (2016).
- 168 Anson, R. M. *et al.* Intermittent fasting dissociates beneficial effects of dietary restriction on glucose metabolism and neuronal resistance to injury from calorie intake. *P Natl Acad Sci USA* **100**, 6216-6220, doi:DOI 10.1073/pnas.1035720100 (2003).
- 169 Mandal, A. & Drerup, C. M. Axonal Transport and Mitochondrial Function in Neurons. *Front Cell Neurosci* **13**, 373, doi:10.3389/fncel.2019.00373 (2019).
- 170 Misgeld, T., Kerschensteiner, M., Bareyre, F. M., Burgess, R. W. & Lichtman, J. W. Imaging axonal transport of mitochondria in vivo. *Nat Methods* **4**, 559-561, doi:10.1038/nmeth1055 (2007).
- 171 Mar, F. M. *et al.* CNS axons globally increase axonal transport after peripheral conditioning. *J Neurosci* **34**, 5965-5970, doi:10.1523/JNEUROSCI.4680-13.2014 (2014).
- 172 Parry, H. A. *et al.* Ketogenic diet increases mitochondria volume in the liver and skeletal muscle without altering oxidative stress markers in rats. *Heliyon* **4**, e00975, doi:10.1016/j.heliyon.2018.e00975 (2018).
- 173 Zhang, Q. *et al.* Exercise induces mitochondrial biogenesis after brain ischemia in rats. *Neuroscience* **205**, 10-17, doi:10.1016/j.neuroscience.2011.12.053 (2012).
- 174 Lettieri Barbato, D., Baldelli, S., Pagliei, B., Aquilano, K. & Ciriolo, M. R. Caloric Restriction and the Nutrient-Sensing PGC-1alpha in Mitochondrial Homeostasis: New Perspectives in Neurodegeneration. *Int J Cell Biol* **2012**, 759583, doi:10.1155/2012/759583 (2012).
- 175 Chausse, B., Vieira-Lara, M. A., Sanchez, A. B., Medeiros, M. H. & Kowaltowski, A. J. Intermittent fasting results in tissue-specific changes in bioenergetics and redox state. *PLoS One* **10**, e0120413, doi:10.1371/journal.pone.0120413 (2015).
- 176 Longo, V. D. & Mattson, M. P. Fasting: molecular mechanisms and clinical applications. *Cell Metab* **19**, 181-192, doi:10.1016/j.cmet.2013.12.008 (2014).
- 177 Kerr, J. S. *et al.* Mitophagy and Alzheimer's Disease: Cellular and Molecular Mechanisms. *Trends Neurosci* **40**, 151-166, doi:10.1016/j.tins.2017.01.002 (2017).
- 178 Saxton, R. A. & Sabatini, D. M. mTOR Signaling in Growth, Metabolism, and Disease. *Cell* **168**, 960-976, doi:10.1016/j.cell.2017.02.004 (2017).
- 179 He, M. *et al.* Autophagy induction stabilizes microtubules and promotes axon regeneration after spinal cord injury. *Proc Natl Acad Sci U S A* **113**, 11324-11329, doi:10.1073/pnas.1611282113 (2016).
- 180 Vachon, P. *et al.* Alleviation of chronic neuropathic pain by environmental enrichment in mice well after the establishment of chronic pain. *Behav Brain Funct* **9**, 22, doi:10.1186/1744-9081-9-22 (2013).
- 181 Madorsky, I. *et al.* Intermittent fasting alleviates the neuropathic phenotype in a mouse model of Charcot-Marie-Tooth disease. *Neurobiology of Disease* **34**, 146-154, doi:10.1016/j.nbd.2009.01.002 (2009).
- 182 Lu, C. & Thompson, C. B. Metabolic regulation of epigenetics. *Cell Metab* **16**, 9-17, doi:10.1016/j.cmet.2012.06.001 (2012).
- 183 Berger, S. L. & Sassone-Corsi, P. Metabolic Signaling to Chromatin. *Cold Spring Harb Perspect Biol* **8**, doi:10.1101/cshperspect.a019463 (2016).
- 184 Boukouris, A. E., Zervopoulos, S. D. & Michelakis, E. D. Metabolic Enzymes Moonlighting in the Nucleus: Metabolic Regulation of Gene Transcription. *Trends Biochem Sci* **41**, 712-730, doi:10.1016/j.tibs.2016.05.013 (2016).

- 185 Shin, J. E. & Cho, Y. Epigenetic Regulation of Axon Regeneration after Neural Injury. *Mol Cells* **40**, 10-16, doi:10.14348/molcells.2017.2311 (2017).
- 186 Streijger, F. *et al.* Ketogenic diet improves forelimb motor function after spinal cord injury in rodents. *PLoS One* **8**, e78765, doi:10.1371/journal.pone.0078765 (2013).
- 187 Wang, X. *et al.* Ketogenic Metabolism Inhibits Histone Deacetylase (HDAC) and Reduces Oxidative Stress After Spinal Cord Injury in Rats. *Neuroscience* **366**, 36-43, doi:10.1016/j.neuroscience.2017.09.056 (2017).
- 188 Zhao, M. *et al.* Ketogenic diet improves the spatial memory impairment caused by exposure to hypobaric hypoxia through increased acetylation of histones in rats. *PLoS One* **12**, e0174477, doi:10.1371/journal.pone.0174477 (2017).
- 189 Shimazu, T. *et al.* Suppression of oxidative stress by beta-hydroxybutyrate, an endogenous histone deacetylase inhibitor. *Science* **339**, 211-214, doi:10.1126/science.1227166 (2013).
- 190 Achanta, L. B. & Rae, C. D. beta-Hydroxybutyrate in the Brain: One Molecule, Multiple Mechanisms. *Neurochem Res* **42**, 35-49, doi:10.1007/s11064-016-2099-2 (2017).
- 191 Longo, V. D. & Panda, S. Fasting, Circadian Rhythms, and Time-Restricted Feeding in Healthy Lifespan. *Cell Metab* **23**, 1048-1059, doi:10.1016/j.cmet.2016.06.001 (2016).
- 192 Mattson, M. P. & Arumugam, T. V. Hallmarks of Brain Aging: Adaptive and Pathological Modification by Metabolic States. *Cell Metab* **27**, 1176-1199, doi:10.1016/j.cmet.2018.05.011 (2018).
- 193 Goodrick, C. L., Ingram, D. K., Reynolds, M. A., Freeman, J. R. & Cider, N. L. Differential Effects of Intermittent Feeding and Voluntary Exercise on Body Weight and Lifespan in Adult Rats1. *Journal of Gerontology* **38**, 36-45, doi:10.1093/geronj/38.1.36 (1983).
- 194 Patterson, R. E. & Sears, D. D. Metabolic Effects of Intermittent Fasting. *Annu Rev Nutr*, doi:10.1146/annurev-nutr-071816-064634 (2017).
- 195 Li, L., Wang, Z. & Zuo, Z. Chronic intermittent fasting improves cognitive functions and brain structures in mice. *PLoS One* **8**, e66069, doi:10.1371/journal.pone.0066069 (2013).
- 196 Gomez-Pinilla, F. & Tyagi, E. Diet and cognition: interplay between cell metabolism and neuronal plasticity. *Curr Opin Clin Nutr* **16**, 726-733, doi:10.1097/MCO.0b013e328365aae3 (2013).
- 197 de Cabo, R. & Mattson, M. P. Effects of Intermittent Fasting on Health, Aging, and Disease. *N Engl J Med* **381**, 2541-2551, doi:10.1056/NEJMra1905136 (2019).
- 198 Fusco, S. *et al.* A role for neuronal cAMP responsive-element binding (CREB)-1 in brain responses to calorie restriction. *Proc Natl Acad Sci U S A* **109**, 621-626, doi:10.1073/pnas.1109237109 (2012).
- 199 De Souza, A. M. A. *et al.* Severe food restriction activates the central renin angiotensin system. *Physiol Rep* **8**, e14338, doi:10.14814/phy2.14338 (2020).
- 200 Johnson, J. B. *et al.* Alternate day calorie restriction improves clinical findings and reduces markers of oxidative stress and inflammation in overweight adults with moderate asthma. *Free radical biology & medicine* **42**, 665-674, doi:10.1016/j.freeradbiomed.2006.12.005 (2007).
- 201 Varady, K. A., Allister, C. A., Roohk, D. J. & Hellerstein, M. K. Improvements in body fat distribution and circulating adiponectin by alternate-day fasting versus calorie restriction. *J Nutr Biochem* **21**, 188-195, doi:10.1016/j.jnutbio.2008.11.001 (2010).
- 202 Barnosky, A. R., Hoddy, K. K., Unterman, T. G. & Varady, K. A. Intermittent fasting vs daily calorie restriction for type 2 diabetes prevention: a review of human findings. *Transl Res* **164**, 302-311, doi:10.1016/j.trsl.2014.05.013 (2014).
- 203 Froy, O. & Miskin, R. Effect of feeding regimens on circadian rhythms: implications for aging and longevity. *Aging (Albany NY)* **2**, 7-27, doi:10.18632/aging.100116 (2010).
- 204 Gonidakis, S., Finkel, S. E. & Longo, V. D. Genome-wide screen identifies *Escherichia coli* TCA-cycle-related mutants with extended chronological lifespan dependent on



- acetate metabolism and the hypoxia-inducible transcription factor ArcA. *Aging Cell* **9**, 868-881, doi:10.1111/j.1474-9726.2010.00618.x (2010).
- 205 Longo, V. D., Shadel, G. S., Kaerberlein, M. & Kennedy, B. Replicative and  
chronological aging in *Saccharomyces cerevisiae*. *Cell Metab* **16**, 18-31,  
doi:10.1016/j.cmet.2012.06.002 (2012).
- 206 Kaerberlein, T. L. *et al.* Lifespan extension in *Caenorhabditis elegans* by complete  
removal of food. *Aging Cell* **5**, 487-494, doi:10.1111/j.1474-9726.2006.00238.x (2006).
- 207 Lee, G. D. *et al.* Dietary deprivation extends lifespan in *Caenorhabditis elegans*. *Aging  
Cell* **5**, 515-524, doi:10.1111/j.1474-9726.2006.00241.x (2006).
- 208 Goodrick, C. L., Ingram, D. K., Reynolds, M. A., Freeman, J. R. & Cider, N. L. Effects of  
Intermittent Feeding Upon Growth and Life Span in Rats. *Gerontology* **28**, 233-241,  
doi:10.1159/000212538 (1982).
- 209 Davis, K., Chamseddine, D. & Harper, J. M. Nutritional limitation in early postnatal life  
and its effect on aging and longevity in rodents. *Experimental Gerontology* **86**, 84-89,  
doi:10.1016/j.exger.2016.05.001 (2016).
- 210 Xie, K. *et al.* Every-other-day feeding extends lifespan but fails to delay many symptoms  
of aging in mice. *Nat Commun* **8**, 155, doi:10.1038/s41467-017-00178-3 (2017).
- 211 Pifferi, F. & Aujard, F. Caloric restriction, longevity and aging: Recent contributions  
from human and non-human primate studies. *Prog Neuropsychopharmacol Biol  
Psychiatry* **95**, 109702, doi:10.1016/j.pnpbp.2019.109702 (2019).
- 212 Wan, R., Camandola, S. & Mattson, M. P. Intermittent food deprivation improves  
cardiovascular and neuroendocrine responses to stress in rats. *J Nutr* **133**, 1921-1929,  
doi:10.1093/jn/133.6.1921 (2003).
- 213 Liu, Z. *et al.* Gut microbiota mediates intermittent-fasting alleviation of diabetes-induced  
cognitive impairment. *Nat Commun* **11**, 855, doi:10.1038/s41467-020-14676-4 (2020).
- 214 Alzoughaibi, M. A., Pandi-Perumal, S. R., Sharif, M. M. & BaHammam, A. S. Diurnal  
Intermittent Fasting during Ramadan: The Effects on Leptin and Ghrelin Levels. *Plos  
One* **9**, doi:ARTN e92214  
10.1371/journal.pone.0092214 (2014).
- 215 Santos, H. O. & Macedo, R. C. O. Impact of intermittent fasting on the lipid profile:  
Assessment associated with diet and weight loss. *Clin Nutr ESPEN* **24**, 14-21,  
doi:10.1016/j.clnesp.2018.01.002 (2018).
- 216 Wan, R. *et al.* Cardioprotective effect of intermittent fasting is associated with an  
elevation of adiponectin levels in rats. *J Nutr Biochem* **21**, 413-417,  
doi:10.1016/j.jnutbio.2009.01.020 (2010).
- 217 Newman, J. C. & Verdin, E. beta-Hydroxybutyrate: A Signaling Metabolite. *Annu Rev  
Nutr* **37**, 51-76, doi:10.1146/annurev-nutr-071816-064916 (2017).
- 218 Speakman, J. R. & Mitchell, S. E. Caloric restriction. *Mol Aspects Med* **32**, 159-221,  
doi:10.1016/j.mam.2011.07.001 (2011).
- 219 Arumugam, T. V. *et al.* Age and energy intake interact to modify cell stress pathways and  
stroke outcome. *Ann Neurol* **67**, 41-52, doi:10.1002/ana.21798 (2010).
- 220 Fann, D. Y. *et al.* Intermittent fasting attenuates inflammasome activity in ischemic  
stroke. *Exp Neurol* **257**, 114-119, doi:10.1016/j.expneurol.2014.04.017 (2014).
- 221 Qiu, G. *et al.* Neuroprotection provided by dietary restriction in rats is further enhanced  
by reducing glucocorticoids. *Neurobiol Aging* **33**, 2398-2410,  
doi:10.1016/j.neurobiolaging.2011.11.025 (2012).
- 222 Vasconcelos, A. R. *et al.* Intermittent fasting attenuates lipopolysaccharide-induced  
neuroinflammation and memory impairment. *J Neuroinflammation* **11**, 85,  
doi:10.1186/1742-2094-11-85 (2014).
- 223 Johnson, J. B. *et al.* Alternate day calorie restriction improves clinical findings and  
reduces markers of oxidative stress and inflammation in overweight adults with moderate

- asthma. *Free Radic Biol Med* **42**, 665-674, doi:10.1016/j.freeradbiomed.2006.12.005 (2007).
- 224 Fann, D. Y., Ng, G. Y., Poh, L. & Arumugam, T. V. Positive effects of intermittent fasting in ischemic stroke. *Exp Gerontol* **89**, 93-102, doi:10.1016/j.exger.2017.01.014 (2017).
- 225 Mayans, L. Metabolic Syndrome: Insulin Resistance and Prediabetes. *FP Essent* **435**, 11-16 (2015).
- 226 Sequea, D., Sharma, N., Arias, E. & Cartee, G. Calorie Restriction Enhances Insulin-Stimulated Glucose Uptake and Akt Phosphorylation in Both Fast-Twitch and Slow-Twitch Skeletal Muscle of 24-Month-Old Rats. *The journals of gerontology. Series A, Biological sciences and medical sciences* **67**, doi:10.1093/gerona/gls085 (2012).
- 227 Tinsley, G. M. & La Bounty, P. M. Effects of intermittent fasting on body composition and clinical health markers in humans. *Nutr Rev* **73**, 661-674, doi:10.1093/nutrit/nuv041 (2015).
- 228 Fontana, L., Meyer, T. E., Klein, S. & Holloszy, J. O. Long-term calorie restriction is highly effective in reducing the risk for atherosclerosis in humans. *P Natl Acad Sci USA* **101**, 6659-6663, doi:10.1073/pnas.0308291101 (2004).
- 229 Lefevre, M. *et al.* Caloric restriction alone and with exercise improves CVD risk in healthy non-obese individuals. *Atherosclerosis* **203**, 206-213, doi:10.1016/j.atherosclerosis.2008.05.036 (2009).
- 230 Klempel, M. C., Kroeger, C. M., Bhutani, S., Trepanowski, J. F. & Varady, K. A. Intermittent fasting combined with calorie restriction is effective for weight loss and cardio-protection in obese women. *Nutr J* **11**, 98-98, doi:10.1186/1475-2891-11-98 (2012).
- 231 Rochon, J. *et al.* Design and conduct of the CALERIE study: comprehensive assessment of the long-term effects of reducing intake of energy. *J Gerontol A Biol Sci Med Sci* **66**, 97-108, doi:10.1093/gerona/glq168 (2011).
- 232 Martin, C. K. *et al.* Effect of Calorie Restriction on Mood, Quality of Life, Sleep, and Sexual Function in Healthy Nonobese Adults: The CALERIE 2 Randomized Clinical Trial. *JAMA Intern Med* **176**, 743-752, doi:10.1001/jamainternmed.2016.1189 (2016).
- 233 Ravussin, E. *et al.* A 2-Year Randomized Controlled Trial of Human Caloric Restriction: Feasibility and Effects on Predictors of Health Span and Longevity. *J Gerontol A Biol Sci Med Sci* **70**, 1097-1104, doi:10.1093/gerona/glv057 (2015).
- 234 Menzies, F. M. *et al.* Autophagy and Neurodegeneration: Pathogenic Mechanisms and Therapeutic Opportunities. *Neuron* **93**, 1015-1034, doi:10.1016/j.neuron.2017.01.022 (2017).
- 235 Godar, R. J. *et al.* Repetitive stimulation of autophagy-lysosome machinery by intermittent fasting preconditions the myocardium to ischemia-reperfusion injury. *Autophagy* **11**, 1537-1560, doi:10.1080/15548627.2015.1063768 (2015).
- 236 Mattson, M. P. Energy intake and exercise as determinants of brain health and vulnerability to injury and disease. *Cell Metab* **16**, 706-722, doi:10.1016/j.cmet.2012.08.012 (2012).
- 237 Zhang, J. *et al.* Intermittent Fasting Protects against Alzheimer's Disease Possible through Restoring Aquaporin-4 Polarity. *Front Mol Neurosci* **10**, 395, doi:10.3389/fnmol.2017.00395 (2017).
- 238 Halagappa, V. K. M. *et al.* Intermittent fasting and caloric restriction ameliorate age-related behavioral deficits in the triple-transgenic mouse model of Alzheimer's disease. *Neurobiology of Disease* **26**, 212-220, doi:10.1016/j.nbd.2006.12.019 (2007).
- 239 Duan, W. *et al.* Dietary restriction normalizes glucose metabolism and BDNF levels, slows disease progression, and increases survival in huntingtin mutant mice. *P Natl Acad Sci USA* **100**, 2911-2916, doi:10.1073/pnas.0536856100 (2003).



- 240 Shin, B. K., Kang, S., Kim, D. S. & Park, S. Intermittent fasting protects against the deterioration of cognitive function, energy metabolism and dyslipidemia in Alzheimer's disease-induced estrogen deficient rats. *Exp Biol Med (Maywood)* **243**, 334-343, doi:10.1177/1535370217751610 (2018).
- 241 Liu, Y. *et al.* SIRT3 mediates hippocampal synaptic adaptations to intermittent fasting and ameliorates deficits in APP mutant mice. *Nat Commun* **10**, 1886, doi:10.1038/s41467-019-09897-1 (2019).
- 242 Fontan-Lozano, A. *et al.* Caloric restriction increases learning consolidation and facilitates synaptic plasticity through mechanisms dependent on NR2B subunits of the NMDA receptor. *J Neurosci* **27**, 10185-10195, doi:10.1523/JNEUROSCI.2757-07.2007 (2007).
- 243 Dasgupta, A., Kim, J., Manakkadan, A., Arumugam, T. V. & Sajikumar, S. Intermittent fasting promotes prolonged associative interactions during synaptic tagging/capture by altering the metaplastic properties of the CA1 hippocampal neurons. *Neurobiol Learn Mem*, doi:10.1016/j.nlm.2017.12.004 (2017).
- 244 Wahl, D. *et al.* Cognitive and behavioral evaluation of nutritional interventions in rodent models of brain aging and dementia. *Clin Interv Aging* **12**, 1419-1428, doi:10.2147/CIA.S145247 (2017).
- 245 Lee, J., Seroogy, K. B. & Mattson, M. P. Dietary restriction enhances neurotrophin expression and neurogenesis in the hippocampus of adult mice. *J Neurochem* **80**, 539-547 (2002).
- 246 Numakawa, T., Odaka, H. & Adachi, N. Actions of Brain-Derived Neurotrophin Factor in the Neurogenesis and Neuronal Function, and Its Involvement in the Pathophysiology of Brain Diseases. *Int J Mol Sci* **19**, doi:10.3390/ijms19113650 (2018).
- 247 von Bohlen und Halbach, O. & von Bohlen und Halbach, V. BDNF effects on dendritic spine morphology and hippocampal function. *Cell and Tissue Research* **373**, 729-741, doi:10.1007/s00441-017-2782-x (2018).
- 248 Jeong, M. A. *et al.* Intermittent fasting improves functional recovery after rat thoracic contusion spinal cord injury. *J Neurotrauma* **28**, 479-492, doi:10.1089/neu.2010.1609 (2011).
- 249 Plunet, W. T. *et al.* Dietary restriction started after spinal cord injury improves functional recovery. *Exp Neurol* **213**, 28-35, doi:10.1016/j.expneurol.2008.04.011 (2008).
- 250 Bäckhed, F., Ley, R. E., Sonnenburg, J. L., Peterson, D. A. & Gordon, J. I. Host-Bacterial Mutualism in the Human Intestine. *Science* **307**, 1915, doi:10.1126/science.1104816 (2005).
- 251 Sender, R., Fuchs, S. & Milo, R. Revised Estimates for the Number of Human and Bacteria Cells in the Body. *PLOS Biology* **14**, e1002533, doi:10.1371/journal.pbio.1002533 (2016).
- 252 Neish, A. S. Microbes in gastrointestinal health and disease. *Gastroenterology* **136**, 65-80, doi:10.1053/j.gastro.2008.10.080 (2009).
- 253 Natividad, J. M. & Verdu, E. F. Modulation of intestinal barrier by intestinal microbiota: pathological and therapeutic implications. *Pharmacol Res* **69**, 42-51, doi:10.1016/j.phrs.2012.10.007 (2013).
- 254 Dodd, D. *et al.* A gut bacterial pathway metabolizes aromatic amino acids into nine circulating metabolites. *Nature* **551**, 648-652, doi:10.1038/nature24661 (2017).
- 255 Qiu, Z. *et al.* Pregnane X Receptor Regulates Pathogen-Induced Inflammation and Host Defense against an Intracellular Bacterial Infection through Toll-like Receptor 4. *Sci Rep* **6**, 31936, doi:10.1038/srep31936 (2016).
- 256 Venkatesh, M. *et al.* Symbiotic bacterial metabolites regulate gastrointestinal barrier function via the xenobiotic sensor PXR and Toll-like receptor 4. *Immunity* **41**, 296-310, doi:10.1016/j.immuni.2014.06.014 (2014).

- 257 den Besten, G. *et al.* The role of short-chain fatty acids in the interplay between diet, gut  
microbiota, and host energy metabolism. *J Lipid Res* **54**, 2325-2340,  
doi:10.1194/jlr.R036012 (2013).
- 258 Baumler, A. J. & Sperandio, V. Interactions between the microbiota and pathogenic  
bacteria in the gut. *Nature* **535**, 85-93, doi:10.1038/nature18849 (2016).
- 259 Gao, J. *et al.* Impact of the Gut Microbiota on Intestinal Immunity Mediated by  
Tryptophan Metabolism. *Front Cell Infect Microbiol* **8**, 13,  
doi:10.3389/fcimb.2018.00013 (2018).
- 260 Gensollen, T., Iyer, S. S., Kasper, D. L. & Blumberg, R. S. How colonization by  
microbiota in early life shapes the immune system. *Science* **352**, 539-544,  
doi:10.1126/science.aad9378 (2016).
- 261 Duca, F. A. & Lam, T. K. Gut microbiota, nutrient sensing and energy balance. *Diabetes  
Obes Metab* **16 Suppl 1**, 68-76, doi:10.1111/dom.12340 (2014).
- 262 Titgemeyer, E. C., Bourquin, L. D., Fahey, G. C., Jr & Garleb, K. A. Fermentability of  
various fiber sources by human fecal bacteria in vitro. *The American Journal of Clinical  
Nutrition* **53**, 1418-1424, doi:10.1093/ajcn/53.6.1418 (1991).
- 263 Guillon, F. & Champ, M. Structural and physical properties of dietary fibres, and  
consequences of processing on human physiology. *Food Research International* **33**, 233-  
245, doi:10.1016/S0963-9969(00)00038-7 (2000).
- 264 Li, G. *et al.* Intermittent Fasting Promotes White Adipose Browning and Decreases  
Obesity by Shaping the Gut Microbiota. *Cell Metab*, doi:10.1016/j.cmet.2017.08.019  
(2017).
- 265 Krautkramer, K. A. *et al.* Diet-Microbiota Interactions Mediate Global Epigenetic  
Programming in Multiple Host Tissues. *Mol Cell* **64**, 982-992,  
doi:10.1016/j.molcel.2016.10.025 (2016).
- 266 Bourassa, M. W., Alim, I., Bultman, S. J. & Ratan, R. R. Butyrate, neuroepigenetics and  
the gut microbiome: Can a high fiber diet improve brain health? *Neurosci Lett* **625**, 56-63,  
doi:10.1016/j.neulet.2016.02.009 (2016).
- 267 Frost, G. *et al.* The short-chain fatty acid acetate reduces appetite via a central  
homeostatic mechanism. *Nat Commun* **5**, 3611, doi:10.1038/ncomms4611 (2014).
- 268 Lin, H. V. *et al.* Butyrate and propionate protect against diet-induced obesity and regulate  
gut hormones via free fatty acid receptor 3-independent mechanisms. *PLoS One* **7**,  
e35240, doi:10.1371/journal.pone.0035240 (2012).
- 269 Lu, Y. *et al.* Short Chain Fatty Acids Prevent High-fat-diet-induced Obesity in Mice by  
Regulating G Protein-coupled Receptors and Gut Microbiota. *Sci Rep* **6**, 37589,  
doi:10.1038/srep37589 (2016).
- 270 Kimura, I. *et al.* Short-chain fatty acids and ketones directly regulate sympathetic nervous  
system via G protein-coupled receptor 41 (GPR41). *Proc Natl Acad Sci U S A* **108**, 8030-  
8035, doi:10.1073/pnas.1016088108 (2011).
- 271 Inoue, D. *et al.* Short-chain fatty acid receptor GPR41-mediated activation of sympathetic  
neurons involves synapsin 2b phosphorylation. *FEBS Lett* **586**, 1547-1554,  
doi:10.1016/j.febslet.2012.04.021 (2012).
- 272 Ge, X. *et al.* Antibiotics-induced depletion of mice microbiota induces changes in host  
serotonin biosynthesis and intestinal motility. *J Transl Med* **15**, 13, doi:10.1186/s12967-  
016-1105-4 (2017).
- 273 Tang, C. *et al.* Loss of FFA2 and FFA3 increases insulin secretion and improves glucose  
tolerance in type 2 diabetes. *Nat Med* **21**, 173-177, doi:10.1038/nm.3779 (2015).
- 274 Nguyen, N. H. *et al.* Propionate increases neuronal histone acetylation, but is metabolized  
oxidatively by glia. Relevance for propionic acidemia. *J Neurochem* **101**, 806-814,  
doi:10.1111/j.1471-4159.2006.04397.x (2007).
- 275 Hashimoto, T. *et al.* ACE2 links amino acid malnutrition to microbial ecology and  
intestinal inflammation. *Nature* **487**, 477-481, doi:10.1038/nature11228 (2012).

- 276 Kim, C. J. *et al.* L-Tryptophan exhibits therapeutic function in a porcine model of dextran sodium sulfate (DSS)-induced colitis. *J Nutr Biochem* **21**, 468-475, doi:10.1016/j.jnutbio.2009.01.019 (2010).
- 277 Krishnan, S. *et al.* Gut Microbiota-Derived Tryptophan Metabolites Modulate Inflammatory Response in Hepatocytes and Macrophages. *Cell Rep* **23**, 1099-1111, doi:10.1016/j.celrep.2018.03.109 (2018).
- 278 Zelante, T. *et al.* Tryptophan Catabolites from Microbiota Engage Aryl Hydrocarbon Receptor and Balance Mucosal Reactivity via Interleukin-22. *Immunity* **39**, 372-385, doi:10.1016/j.immuni.2013.08.003 (2013).
- 279 Burokas, A., Moloney, R. D., Dinan, T. G. & Cryan, J. F. in *Advances in Applied Microbiology* Vol. 91 (eds Sima Sariaslani & Geoffrey Michael Gadd) 1-62 (Academic Press, 2015).
- 280 O'Mahony, S. M., Clarke, G., Borre, Y. E., Dinan, T. G. & Cryan, J. F. Serotonin, tryptophan metabolism and the brain-gut-microbiome axis. *Behav Brain Res* **277**, 32-48, doi:10.1016/j.bbr.2014.07.027 (2015).
- 281 Diaz Heijtz, R. *et al.* Normal gut microbiota modulates brain development and behavior. *Proc Natl Acad Sci U S A* **108**, 3047-3052, doi:10.1073/pnas.1010529108 (2011).
- 282 Kelly, J. R. *et al.* Transferring the blues: Depression-associated gut microbiota induces neurobehavioural changes in the rat. *J Psychiatr Res* **82**, 109-118, doi:10.1016/j.jpsychires.2016.07.019 (2016).
- 283 Zheng, P. *et al.* Gut microbiome remodeling induces depressive-like behaviors through a pathway mediated by the host's metabolism. *Mol Psychiatry* **21**, 786-796, doi:10.1038/mp.2016.44 (2016).
- 284 De Palma, G. *et al.* Transplantation of fecal microbiota from patients with irritable bowel syndrome alters gut function and behavior in recipient mice. *Science Translational Medicine* **9**, eaaf6397, doi:10.1126/scitranslmed.aaf6397 (2017).
- 285 Sudo, N. *et al.* Postnatal microbial colonization programs the hypothalamic-pituitary-adrenal system for stress response in mice. *J Physiol* **558**, 263-275, doi:10.1113/jphysiol.2004.063388 (2004).
- 286 Bedarf, J. R., Hildebrand, F., Goeser, F., Bork, P. & Wullner, U. [The gut microbiome in Parkinson's disease]. *Nervenarzt* **90**, 160-166, doi:10.1007/s00115-018-0601-6 (2019).
- 287 Emery, D. C. *et al.* 16S rRNA Next Generation Sequencing Analysis Shows Bacteria in Alzheimer's Post-Mortem Brain. *Front Aging Neurosci* **9**, 195, doi:10.3389/fnagi.2017.00195 (2017).
- 288 Gazerani, P. Probiotics for Parkinson's Disease. *Int J Mol Sci* **20**, doi:10.3390/ijms20174121 (2019).
- 289 Sampson, T. R. *et al.* Gut Microbiota Regulate Motor Deficits and Neuroinflammation in a Model of Parkinson's Disease. *Cell* **167**, 1469-1480 e1412, doi:10.1016/j.cell.2016.11.018 (2016).
- 290 Fujii, Y. *et al.* Fecal metabolite of a gnotobiotic mouse transplanted with gut microbiota from a patient with Alzheimer's disease. *Bioscience, Biotechnology, and Biochemistry* **83**, 2144-2152, doi:10.1080/09168451.2019.1644149 (2019).
- 291 Nimgampalle, M. & Kuna, Y. Anti-Alzheimer Properties of Probiotic, Lactobacillus plantarum MTCC 1325 in Alzheimer's Disease induced Albino Rats. *J Clin Diagn Res* **11**, KC01-KC05, doi:10.7860/JCDR/2017/26106.10428 (2017).
- 292 Gungor, B., Adiguzel, E., Gursel, I., Yilmaz, B. & Gursel, M. Intestinal Microbiota in Patients with Spinal Cord Injury. *PLoS One* **11**, e0145878, doi:10.1371/journal.pone.0145878 (2016).
- 293 O'Connor, G. *et al.* Investigation of Microbiota Alterations and Intestinal Inflammation Post-Spinal Cord Injury in Rat Model. *J Neurotrauma* **35**, 2159-2166, doi:10.1089/neu.2017.5349 (2018).

- 294 Kigerl, K. A. *et al.* Gut dysbiosis impairs recovery after spinal cord injury. *J Exp Med* **213**, 2603-2620, doi:10.1084/jem.20151345 (2016).
- 295 Sherwin, E., Dinan, T. G. & Cryan, J. F. Recent developments in understanding the role of the gut microbiota in brain health and disease. *Ann N Y Acad Sci*, doi:10.1111/nyas.13416 (2017).
- 296 Qin, J. *et al.* A human gut microbial gene catalogue established by metagenomic sequencing. *Nature* **464**, 59-65, doi:10.1038/nature08821 (2010).
- 297 De Filippo, C. *et al.* Impact of diet in shaping gut microbiota revealed by a comparative study in children from Europe and rural Africa. *Proc Natl Acad Sci U S A* **107**, 14691-14696, doi:10.1073/pnas.1005963107 (2010).
- 298 Muegge, B. D. *et al.* Diet drives convergence in gut microbiome functions across mammalian phylogeny and within humans. *Science* **332**, 970-974, doi:10.1126/science.1198719 (2011).
- 299 Wu, G. D. *et al.* Linking long-term dietary patterns with gut microbial enterotypes. *Science* **334**, 105-108, doi:10.1126/science.1208344 (2011).
- 300 David, L. A. *et al.* Diet rapidly and reproducibly alters the human gut microbiome. *Nature* **505**, 559-563, doi:10.1038/nature12820 (2014).
- 301 Kohl, K. D., Amaya, J., Passemant, C. A., Dearing, M. D. & McCue, M. D. Unique and shared responses of the gut microbiota to prolonged fasting: a comparative study across five classes of vertebrate hosts. *FEMS Microbiol Ecol* **90**, 883-894, doi:10.1111/1574-6941.12442 (2014).
- 302 Cignarella, F. *et al.* Intermittent Fasting Confers Protection in CNS Autoimmunity by Altering the Gut Microbiota. *Cell Metab* **27**, 1222-1235 e1226, doi:10.1016/j.cmet.2018.05.006 (2018).
- 303 Wang, S. *et al.* Gut microbiota mediates the anti-obesity effect of calorie restriction in mice. *Sci Rep* **8**, 13037, doi:10.1038/s41598-018-31353-1 (2018).
- 304 Cotillard, A. *et al.* Dietary intervention impact on gut microbial gene richness. *Nature* **500**, 585-588, doi:10.1038/nature12480 (2013).
- 305 Le Chatelier, E. *et al.* Richness of human gut microbiome correlates with metabolic markers. *Nature* **500**, 541-546, doi:10.1038/nature12506 (2013).
- 306 Castaner, O. *et al.* The Gut Microbiome Profile in Obesity: A Systematic Review. *Int J Endocrinol* **2018**, 4095789, doi:10.1155/2018/4095789 (2018).
- 307 Beli, E. *et al.* Restructuring of the Gut Microbiome by Intermittent Fasting Prevents Retinopathy and Prolongs Survival in db/db Mice. *Diabetes* **67**, 1867-1879, doi:10.2337/db18-0158 (2018).
- 308 Brück, W. & Friede, R. L. The role of complement in myelin phagocytosis during PNS wallerian degeneration. *Journal of the Neurological Sciences* **103**, 182-187, doi:[https://doi.org/10.1016/0022-510X\(91\)90162-Z](https://doi.org/10.1016/0022-510X(91)90162-Z) (1991).
- 309 Dailey, A. T., Avellino, A. M., Benthem, L., Silver, J. & Kliot, M. Complement depletion reduces macrophage infiltration and activation during Wallerian degeneration and axonal regeneration. *The Journal of neuroscience : the official journal of the Society for Neuroscience* **18**, 6713-6722, doi:10.1523/JNEUROSCI.18-17-06713.1998 (1998).
- 310 Liu, L. *et al.* Hereditary absence of complement C5 in adult mice influences Wallerian degeneration, but not retrograde responses, following injury to peripheral nerve. *Journal of the peripheral nervous system : JPNS* **4**, 123-133 (1999).
- 311 Galli, S. J., Nakae, S. & Tsai, M. Mast cells in the development of adaptive immune responses. *Nat Immunol* **6**, 135-142, doi:10.1038/ni1158 (2005).
- 312 Metcalfe, D. D., Baram, D. & Mekori, Y. A. Mast cells. *Physiological Reviews* **77**, 1033-1079, doi:10.1152/physrev.1997.77.4.1033 (1997).
- 313 Kleij, H. P. v. d. & Bienenstock, J. Significance of Conversation between Mast Cells and Nerves. *Allergy Asthma Clin Immunol* **1**, 65-80, doi:10.1186/1710-1492-1-2-65 (2005).

- 314 Gottwald, T., Coerper, S., Schäffer, M., Köveker, G. & Stead, R. H. The mast cell-nerve axis in wound healing: a hypothesis. *Wound Repair and Regeneration* **6**, 8-20, doi:10.1046/j.1524-475X.1998.60104.x (1998).
- 315 Wezel, A. *et al.* Mast cells mediate neutrophil recruitment during atherosclerotic plaque progression. *Atherosclerosis* **241**, 289-296, doi:<https://doi.org/10.1016/j.atherosclerosis.2015.05.028> (2015).
- 316 Sahu, S. K. *et al.* Mast Cells Initiate the Recruitment of Neutrophils Following Ocular Surface Injury. *Investigative Ophthalmology & Visual Science* **59**, 1732-1740, doi:10.1167/iovs.17-23398 (2018).
- 317 Hughes, E. L., Becker, F., Flower, R. J., Buckingham, J. C. & Gavins, F. N. E. Mast cells mediate early neutrophil recruitment and exhibit anti-inflammatory properties via the formyl peptide receptor 2/lipoxin A4 receptor. *British Journal of Pharmacology* **174**, 2393-2408, doi:10.1111/bph.13847 (2017).
- 318 Kim, C. F. & Moalem-Taylor, G. Detailed characterization of neuro-immune responses following neuropathic injury in mice. *Brain Res* **1405**, 95-108, doi:10.1016/j.brainres.2011.06.022 (2011).
- 319 Johnston, B. *et al.* Chronic inflammation upregulates chemokine receptors and induces neutrophil migration to monocyte chemoattractant protein-1. *The Journal of clinical investigation* **103**, 1269-1276, doi:10.1172/JCI5208 (1999).
- 320 Scholz, J. & Woolf, C. J. The neuropathic pain triad: neurons, immune cells and glia. *Nat Neurosci* **10**, 1361-1368, doi:10.1038/nn1992 (2007).
- 321 Nathan, C. Neutrophils and immunity: challenges and opportunities. *Nat Rev Immunol* **6**, 173-182, doi:10.1038/nri1785 (2006).
- 322 Perkins, N. M. & Tracey, D. J. Hyperalgesia due to nerve injury: role of neutrophils. *Neuroscience* **101**, 745-757, doi:[https://doi.org/10.1016/S0306-4522\(00\)00396-1](https://doi.org/10.1016/S0306-4522(00)00396-1) (2000).
- 323 Fleming, J. C. *et al.* Timing and duration of anti-alpha4beta1 integrin treatment after spinal cord injury: effect on therapeutic efficacy. *J Neurosurg Spine* **11**, 575-587, doi:10.3171/2009.6.spine08915 (2009).
- 324 Lindborg, J. A., Mack, M. & Zigmond, R. E. Neutrophils Are Critical for Myelin Removal in a Peripheral Nerve Injury Model of Wallerian Degeneration. *J Neurosci* **37**, 10258-10277, doi:10.1523/JNEUROSCI.2085-17.2017 (2017).
- 325 Scapini, P. *et al.* The neutrophil as a cellular source of chemokines. *Immunological Reviews* **177**, 195-203, doi:10.1034/j.1600-065X.2000.17706.x (2000).
- 326 Welling, M. M. *et al.* Antibacterial activity of human neutrophil defensins in experimental infections in mice is accompanied by increased leukocyte accumulation. *The Journal of clinical investigation* **102**, 1583-1590, doi:10.1172/JCI3664 (1998).
- 327 Witko-Sarsat, V., Rieu, P., Descamps-Latscha, B., Lesavre, P. & Halbwachs-Mecarelli, L. Neutrophils: Molecules, Functions and Pathophysiological Aspects. *Laboratory Investigation* **80**, 617-653, doi:10.1038/labinvest.3780067 (2000).
- 328 Shamash, S., Reichert, F. & Rotshenker, S. The cytokine network of Wallerian degeneration: tumor necrosis factor-alpha, interleukin-1alpha, and interleukin-1beta. *The Journal of neuroscience : the official journal of the Society for Neuroscience* **22**, 3052-3060, doi:10.1523/JNEUROSCI.22-08-03052.2002 (2002).
- 329 Kurek, J. B., Austin, L., Cheema, S. S., Bartlett, P. F. & Murphy, M. Up-regulation of leukaemia inhibitory factor and interleukin-6 in transected sciatic nerve and muscle following denervation. *Neuromuscular Disorders* **6**, 105-114, doi:[https://doi.org/10.1016/0960-8966\(95\)00029-1](https://doi.org/10.1016/0960-8966(95)00029-1) (1996).
- 330 Cafferty, W. B. *et al.* Conditioning injury-induced spinal axon regeneration fails in interleukin-6 knock-out mice. *J Neurosci* **24**, 4432-4443, doi:10.1523/JNEUROSCI.2245-02.2004 (2004).

- 331 Cao, Z. *et al.* The cytokine interleukin-6 is sufficient but not necessary to mimic the peripheral conditioning lesion effect on axonal growth. *J Neurosci* **26**, 5565-5573, doi:10.1523/JNEUROSCI.0815-06.2006 (2006).
- 332 Perrin, F. E., Lacroix, S., Aviles-Trigueros, M. & David, S. Involvement of monocyte chemoattractant protein-1, macrophage inflammatory protein-1alpha and interleukin-1beta in Wallerian degeneration. *Brain* **128**, 854-866, doi:10.1093/brain/awh407 (2005).
- 333 Siebert, H., Sachse, A., Kuziel, W., Maeda, N. & Brück, W. The chemokine receptor CCR2 is involved in macrophage recruitment of the injured nervous system. *Journal of neuroimmunology* **110**, 177-185, doi:10.1016/S0165-5728(00)00343-X (2000).
- 334 Cafferty, W. B. *et al.* Leukemia inhibitory factor determines the growth status of injured adult sensory neurons. *The Journal of neuroscience : the official journal of the Society for Neuroscience* **21**, 7161-7170, doi:10.1523/JNEUROSCI.21-18-07161.2001 (2001).
- 335 Zhong, J., Dietzel, I. D., Wahle, P., Kopf, M. & Heumann, R. Sensory impairments and delayed regeneration of sensory axons in interleukin-6-deficient mice. *The Journal of neuroscience : the official journal of the Society for Neuroscience* **19**, 4305-4313, doi:10.1523/JNEUROSCI.19-11-04305.1999 (1999).
- 336 Heinrich, P. C., Behrmann, I., Müller-Newen, G., Schaper, F. & Graeve, L. Interleukin-6-type cytokine signalling through the gp130/Jak/STAT pathway. *The Biochemical journal* **334 ( Pt 2)**, 297-314, doi:10.1042/bj3340297 (1998).
- 337 Zigmond, R. E. Cytokines that promote nerve regeneration. *Exp Neurol* **238**, 101-106, doi:10.1016/j.expneurol.2012.08.017 (2012).
- 338 Li, M., Peake, P. W., Charlesworth, J. A., Tracey, D. J. & Moalem-Taylor, G. Complement activation contributes to leukocyte recruitment and neuropathic pain following peripheral nerve injury in rats. *Eur J Neurosci* **26**, 3486-3500, doi:10.1111/j.1460-9568.2007.05971.x (2007).
- 339 Mosley, K. & Cuzner, M. L. Receptor-mediated phagocytosis of myelin by macrophages and microglia: effect of opsonization and receptor blocking agents. *Neurochemical research* **21**, 481-487, doi:10.1007/bf02527713 (1996).
- 340 Barrette, B. *et al.* Requirement of myeloid cells for axon regeneration. *J Neurosci* **28**, 9363-9376, doi:10.1523/JNEUROSCI.1447-08.2008 (2008).
- 341 Stratton, J. A. *et al.* Macrophages Regulate Schwann Cell Maturation after Nerve Injury. *Cell Rep* **24**, 2561-2572 e2566, doi:10.1016/j.celrep.2018.08.004 (2018).
- 342 Siqueira Mietto, B. *et al.* Role of IL-10 in Resolution of Inflammation and Functional Recovery after Peripheral Nerve Injury. *J Neurosci* **35**, 16431-16442, doi:10.1523/JNEUROSCI.2119-15.2015 (2015).
- 343 Kwon, M. J. *et al.* Contribution of macrophages to enhanced regenerative capacity of dorsal root ganglia sensory neurons by conditioning injury. *J Neurosci* **33**, 15095-15108, doi:10.1523/JNEUROSCI.0278-13.2013 (2013).
- 344 Aguilar Salegio, E. A., Pollard, A. N., Smith, M. & Zhou, X.-F. Macrophage presence is essential for the regeneration of ascending afferent fibres following a conditioning sciatic nerve lesion in adult rats. *BMC Neuroscience* **12**, 11, doi:10.1186/1471-2202-12-11 (2011).
- 345 Niemi, J. P. *et al.* A critical role for macrophages near axotomized neuronal cell bodies in stimulating nerve regeneration. *J Neurosci* **33**, 16236-16248, doi:10.1523/JNEUROSCI.3319-12.2013 (2013).
- 346 McLachlan, E., Hu, P. & Geczy, C. Neutrophils rarely invade dorsal root ganglia after peripheral nerve lesions. *J Neuroimmunol* **187**, 212-213; author reply 214-215, doi:10.1016/j.jneuroim.2007.05.001 (2007).
- 347 Moalem, G., Xu, K. & Yu, L. T lymphocytes play a role in neuropathic pain following peripheral nerve injury in rats. *Neuroscience* **129**, 767-777, doi:10.1016/j.neuroscience.2004.08.035 (2004).

- 348 Greenhalgh, A. D. & David, S. Differences in the phagocytic response of microglia and peripheral macrophages after spinal cord injury and its effects on cell death. *J Neurosci* **34**, 6316-6322, doi:10.1523/JNEUROSCI.4912-13.2014 (2014).
- 349 Bellver-Landete, V. *et al.* Microglia are an essential component of the neuroprotective scar that forms after spinal cord injury. *Nat Commun* **10**, 518, doi:10.1038/s41467-019-08446-0 (2019).
- 350 Nguyen, H. X., Beck, K. D. & Anderson, A. J. Quantitative assessment of immune cells in the injured spinal cord tissue by flow cytometry: a novel use for a cell purification method. *J Vis Exp*, doi:10.3791/2698 (2011).
- 351 Campbell, S. J., Wilcockson, D. C., Butchart, A. G., Perry, V. H. & Anthony, D. C. Altered chemokine expression in the spinal cord and brain contributes to differential interleukin-1 $\beta$ -induced neutrophil recruitment. *Journal of Neurochemistry* **83**, 432-441, doi:10.1046/j.1471-4159.2002.01166.x (2002).
- 352 Neirinckx, V. *et al.* Neutrophil contribution to spinal cord injury and repair. *Journal of Neuroinflammation* **11**, 150, doi:10.1186/s12974-014-0150-2 (2014).
- 353 Stirling, D. P., Liu, S., Kubes, P. & Yong, V. W. Depletion of Ly6G/Gr-1 leukocytes after spinal cord injury in mice alters wound healing and worsens neurological outcome. *J Neurosci* **29**, 753-764, doi:10.1523/JNEUROSCI.4918-08.2009 (2009).
- 354 de Castro, R., Jr. *et al.* Evidence that infiltrating neutrophils do not release reactive oxygen species in the site of spinal cord injury. *Exp Neurol* **190**, 414-424, doi:10.1016/j.expneurol.2004.05.046 (2004).
- 355 Martinez, F. O., Helming, L. & Gordon, S. Alternative activation of macrophages: an immunologic functional perspective. *Annu Rev Immunol* **27**, 451-483, doi:10.1146/annurev.immunol.021908.132532 (2009).
- 356 Kigerl, K. A., McGaughy, V. M. & Popovich, P. G. Comparative analysis of lesion development and intraspinal inflammation in four strains of mice following spinal contusion injury. *J Comp Neurol* **494**, 578-594, doi:10.1002/cne.20827 (2006).
- 357 Wang, X. *et al.* Macrophages in spinal cord injury: phenotypic and functional change from exposure to myelin debris. *Glia* **63**, 635-651, doi:10.1002/glia.22774 (2015).
- 358 Totoiu, M. O. & Keirstead, H. S. Spinal cord injury is accompanied by chronic progressive demyelination. *J Comp Neurol* **486**, 373-383, doi:10.1002/cne.20517 (2005).
- 359 Alvarez, J. I., Katayama, T. & Prat, A. Glial influence on the blood brain barrier. *Glia* **61**, 1939-1958, doi:10.1002/glia.22575 (2013).
- 360 Bush, T. G. *et al.* Leukocyte Infiltration, Neuronal Degeneration, and Neurite Outgrowth after Ablation of Scar-Forming, Reactive Astrocytes in Adult Transgenic Mice. *Neuron* **23**, 297-308, doi:10.1016/S0896-6273(00)80781-3 (1999).
- 361 Shechter, R., Raposo, C., London, A., Sagi, I. & Schwartz, M. The glial scar-monocyte interplay: a pivotal resolution phase in spinal cord repair. *PLoS One* **6**, e27969, doi:10.1371/journal.pone.0027969 (2011).
- 362 Miron, V. E. *et al.* M2 microglia and macrophages drive oligodendrocyte differentiation during CNS remyelination. *Nat Neurosci* **16**, 1211-1218, doi:10.1038/nn.3469 (2013).
- 363 Kigerl, K. A. *et al.* Identification of two distinct macrophage subsets with divergent effects causing either neurotoxicity or regeneration in the injured mouse spinal cord. *J Neurosci* **29**, 13435-13444, doi:10.1523/JNEUROSCI.3257-09.2009 (2009).
- 364 Zhu, Y. *et al.* Hematogenous macrophage depletion reduces the fibrotic scar and increases axonal growth after spinal cord injury. *Neurobiol Dis* **74**, 114-125, doi:10.1016/j.nbd.2014.10.024 (2015).
- 365 Shechter, R. *et al.* Infiltrating blood-derived macrophages are vital cells playing an anti-inflammatory role in recovery from spinal cord injury in mice. *PLoS Med* **6**, e1000113, doi:10.1371/journal.pmed.1000113 (2009).



- 366 Jones, T. B., Hart, R. P. & Popovich, P. G. Molecular control of physiological and pathological T-cell recruitment after mouse spinal cord injury. *J Neurosci* **25**, 6576-6583, doi:10.1523/JNEUROSCI.0305-05.2005 (2005).
- 367 Gonzalez, R., Glaser, J., Liu, M. T., Lane, T. E. & Keirstead, H. S. Reducing inflammation decreases secondary degeneration and functional deficit after spinal cord injury. *Experimental Neurology* **184**, 456-463, doi:10.1016/s0014-4886(03)00257-7 (2003).
- 368 Schwartz, M. & Kipnis, J. Protective autoimmunity: regulation and prospects for vaccination after brain and spinal cord injuries. *Trends in Molecular Medicine* **7**, 252-258, doi:[https://doi.org/10.1016/S1471-4914\(01\)01993-1](https://doi.org/10.1016/S1471-4914(01)01993-1) (2001).
- 369 Kipnis, J. *et al.* Neuroprotective autoimmunity: naturally occurring CD4+CD25+ regulatory T cells suppress the ability to withstand injury to the central nervous system. *P Natl Acad Sci USA* **99**, 15620-15625, doi:10.1073/pnas.232565399 (2002).
- 370 Walsh, J. T. *et al.* Regulatory T cells in central nervous system injury: a double-edged sword. *J Immunol* **193**, 5013-5022, doi:10.4049/jimmunol.1302401 (2014).
- 371 Vignali, D. A. A., Collison, L. W. & Workman, C. J. How regulatory T cells work. *Nature reviews. Immunology* **8**, 523-532, doi:10.1038/nri2343 (2008).
- 372 Kipnis, J. *et al.* Low-dose  $\gamma$ -irradiation promotes survival of injured neurons in the central nervous system via homeostasis-driven proliferation of T cells. *European Journal of Neuroscience* **19**, 1191-1198, doi:10.1111/j.1460-9568.2004.03207.x (2004).
- 373 Kipnis, J., Avidan, H., Caspi, R. R. & Schwartz, M. Dual effect of CD4+CD25+ regulatory T cells in neurodegeneration: a dialogue with microglia. *P Natl Acad Sci USA* **101 Suppl 2**, 14663-14669, doi:10.1073/pnas.0404842101 (2004).
- 374 Popovich, P. G. *et al.* Depletion of Hematogenous Macrophages Promotes Partial Hindlimb Recovery and Neuroanatomical Repair after Experimental Spinal Cord Injury. *Experimental Neurology* **158**, 351-365, doi:<https://doi.org/10.1006/exnr.1999.7118> (1999).
- 375 Mietto, B. S., Mostacada, K. & Martinez, A. M. Neurotrauma and inflammation: CNS and PNS responses. *Mediators Inflamm* **2015**, 251204, doi:10.1155/2015/251204 (2015).
- 376 Zhang, N., Fang, M., Chen, H., Gou, F. & Ding, M. Evaluation of spinal cord injury animal models. *Neural regeneration research* **9**, 2008-2012, doi:10.4103/1673-5374.143436 (2014).
- 377 Angius, D. *et al.* A systematic review of animal models used to study nerve regeneration in tissue-engineered scaffolds. *Biomaterials* **33**, 8034-8039, doi:10.1016/j.biomaterials.2012.07.056 (2012).
- 378 Lee, J. H. T. *et al.* A Novel Porcine Model of Traumatic Thoracic Spinal Cord Injury. *Journal of Neurotrauma* **30**, 142-159, doi:10.1089/neu.2012.2386 (2013).
- 379 Kuluz, J. *et al.* Pediatric spinal cord injury in infant piglets: description of a new large animal model and review of the literature. *J Spinal Cord Med* **33**, 43-57, doi:10.1080/10790268.2010.11689673 (2010).
- 380 Rosenzweig, E. S. *et al.* Extensive spontaneous plasticity of corticospinal projections after primate spinal cord injury. *Nature neuroscience* **13**, 1505-1510, doi:10.1038/nn.2691 (2010).
- 381 Ethier, C., Oby, E. R., Bauman, M. J. & Miller, L. E. Restoration of grasp following paralysis through brain-controlled stimulation of muscles. *Nature* **485**, 368-371, doi:10.1038/nature10987 (2012).
- 382 Courtine, G. *et al.* Can experiments in nonhuman primates expedite the translation of treatments for spinal cord injury in humans? *Nature medicine* **13**, 561-566, doi:10.1038/nm1595 (2007).
- 383 Byrnes, K. R., Fricke, S. T. & Faden, A. I. Neuropathological differences between rats and mice after spinal cord injury. *J Magn Reson Imaging* **32**, 836-846, doi:10.1002/jmri.22323 (2010).



- 384 Ellenbroek, B. & Youn, J. Rodent models in neuroscience research: is it a rat race? *Dis Model Mech* **9**, 1079-1087, doi:10.1242/dmm.026120 (2016).
- 385 Lee, D.-H. & Lee, J. K. Animal models of axon regeneration after spinal cord injury. *Neurosci Bull* **29**, 436-444, doi:10.1007/s12264-013-1365-4 (2013).
- 386 Varejao, A. S., Melo-Pinto, P., Meek, M. F., Filipe, V. M. & Bulas-Cruz, J. Methods for the experimental functional assessment of rat sciatic nerve regeneration. *Neurol Res* **26**, 186-194, doi:10.1179/016164104225013833 (2004).
- 387 Kaplan, H. M., Mishra, P. & Kohn, J. The overwhelming use of rat models in nerve regeneration research may compromise designs of nerve guidance conduits for humans. *J Mater Sci Mater Med* **26**, 226-226, doi:10.1007/s10856-015-5558-4 (2015).
- 388 Basso, D. M., Beattie, M. S. & Bresnahan, J. C. A Sensitive and Reliable Locomotor Rating Scale for Open Field Testing in Rats. *Journal of Neurotrauma* **12**, 1-21, doi:10.1089/neu.1995.12.1 (1995).
- 389 Trygg, J. & Wold, S. Orthogonal projections to latent structures (O-PLS). *Journal of Chemometrics* **16**, 119-128, doi:10.1002/cem.695 (2002).
- 390 Thévenot, E. A., Roux, A., Xu, Y., Ezan, E. & Junot, C. Analysis of the Human Adult Urinary Metabolome Variations with Age, Body Mass Index, and Gender by Implementing a Comprehensive Workflow for Univariate and OPLS Statistical Analyses. *Journal of Proteome Research* **14**, 3322-3335, doi:10.1021/acs.jproteome.5b00354 (2015).
- 391 Callahan, B. J. *et al.* DADA2: High-resolution sample inference from Illumina amplicon data. *Nat Methods* **13**, 581-583, doi:10.1038/nmeth.3869 (2016).
- 392 McMurdie, P. J. & Holmes, S. phyloseq: an R package for reproducible interactive analysis and graphics of microbiome census data. *PLoS One* **8**, e61217, doi:10.1371/journal.pone.0061217 (2013).
- 393 McMurdie, P. J. & Holmes, S. Waste not, want not: why rarefying microbiome data is inadmissible. *PLoS Comput Biol* **10**, e1003531, doi:10.1371/journal.pcbi.1003531 (2014).
- 394 Love, M. I., Huber, W. & Anders, S. Moderated estimation of fold change and dispersion for RNA-seq data with DESeq2. *Genome Biol* **15**, 550, doi:10.1186/s13059-014-0550-8 (2014).
- 395 Poplawski, G. *et al.* Schwann cells regulate sensory neuron gene expression before and after peripheral nerve injury. *Glia*, doi:10.1002/glia.23325 (2018).
- 396 Hollis, E. R., 2nd, Jamshidi, P., Löw, K., Blesch, A. & Tuszynski, M. H. Induction of corticospinal regeneration by lentiviral trkB-induced Erk activation. *P Natl Acad Sci USA* **106**, 7215-7220, doi:10.1073/pnas.0810624106 (2009).
- 397 Liu, Y. *et al.* NT-3 promotes proprioceptive axon regeneration when combined with activation of the mTor intrinsic growth pathway but not with reduction of myelin extrinsic inhibitors. *Exp Neurol* **283**, 73-84, doi:10.1016/j.expneurol.2016.05.021 (2016).
- 398 Boyd, J. G. & Gordon, T. Neurotrophic Factors and Their Receptors in Axonal Regeneration and Functional Recovery After Peripheral Nerve Injury. *Molecular neurobiology* **27**, 277-324, doi:10.1385/MN:27:3:277 (2003).
- 399 Hoke, A. *et al.* Schwann cells express motor and sensory phenotypes that regulate axon regeneration. *J Neurosci* **26**, 9646-9655, doi:10.1523/JNEUROSCI.1620-06.2006 (2006).
- 400 Choi, I. Y. *et al.* A Diet Mimicking Fasting Promotes Regeneration and Reduces Autoimmunity and Multiple Sclerosis Symptoms. *Cell Rep* **15**, 2136-2146, doi:10.1016/j.celrep.2016.05.009 (2016).
- 401 Isaac, S. *et al.* Short- and long-term effects of oral vancomycin on the human intestinal microbiota. *J Antimicrob Chemother* **72**, 128-136, doi:10.1093/jac/dkw383 (2017).
- 402 Aragozzini, F., Ferrari, A., Pacini, N. & Gualandris, R. Indole-3-lactic acid as a tryptophan metabolite produced by *Bifidobacterium* spp. *Applied and Environmental Microbiology* **38**, 544-546 (1979).

- 403 Zhang, L. S. & Davies, S. S. Microbial metabolism of dietary components to bioactive metabolites: opportunities for new therapeutic interventions. *Genome Med* **8**, 46, doi:10.1186/s13073-016-0296-x (2016).
- 404 Huntley, N. F. & Patience, J. F. Xylose: absorption, fermentation, and post-absorptive metabolism in the pig. *J Anim Sci Biotechnol* **9**, 4, doi:10.1186/s40104-017-0226-9 (2018).
- 405 Westfall, S. *et al.* Microbiome, probiotics and neurodegenerative diseases: deciphering the gut brain axis. *Cell Mol Life Sci*, doi:10.1007/s00018-017-2550-9 (2017).
- 406 Correa-Oliveira, R., Fachi, J. L., Vieira, A., Sato, F. T. & Vinolo, M. A. Regulation of immune cell function by short-chain fatty acids. *Clin Transl Immunology* **5**, e73, doi:10.1038/cti.2016.17 (2016).
- 407 Menni, C. *et al.* Gut microbiome diversity and high-fibre intake are related to lower long-term weight gain. *Int J Obes (Lond)* **41**, 1099-1105, doi:10.1038/ijo.2017.66 (2017).
- 408 Sundqvist, M. *et al.* Similarities and differences between the responses induced in human phagocytes through activation of the medium chain fatty acid receptor GPR84 and the short chain fatty acid receptor FFA2R. *Biochim Biophys Acta Mol Cell Res* **1865**, 695-708, doi:10.1016/j.bbamcr.2018.02.008 (2018).
- 409 Oyoshi, M. K. *et al.* Leukotriene B4-driven neutrophil recruitment to the skin is essential for allergic skin inflammation. *Immunity* **37**, 747-758, doi:10.1016/j.immuni.2012.06.018 (2012).
- 410 Eun, J. C. *et al.* Leukotriene b4 and its metabolites prime the neutrophil oxidase and induce proinflammatory activation of human pulmonary microvascular endothelial cells. *Shock* **35**, 240-244, doi:10.1097/SHK.0b013e3181faceb3 (2011).
- 411 Eash, K. J., Greenbaum, A. M., Gopalan, P. K. & Link, D. C. CXCR2 and CXCR4 antagonistically regulate neutrophil trafficking from murine bone marrow. *J Clin Invest* **120**, 2423-2431, doi:10.1172/JCI41649 (2010).
- 412 Sulaiman, W. & Gordon, T. Neurobiology of peripheral nerve injury, regeneration, and functional recovery: from bench top research to bedside application. *Ochsner J* **13**, 100-108 (2013).
- 413 Fitch, M. T. & Silver, J. CNS injury, glial scars, and inflammation: Inhibitory extracellular matrices and regeneration failure. *Exp Neurol* **209**, 294-301, doi:10.1016/j.expneurol.2007.05.014 (2008).
- 414 Brownstone, R. M. & Bui, T. V. Spinal interneurons providing input to the final common path during locomotion. *Prog Brain Res* **187**, 81-95, doi:10.1016/B978-0-444-53613-6.00006-X (2010).
- 415 Adams, M. M. & Hicks, A. L. Spasticity after spinal cord injury. *Spinal Cord* **43**, 577-586, doi:10.1038/sj.sc.3101757 (2005).
- 416 Kathe, C., Hutson, T. H., McMahon, S. B. & Moon, L. D. Intramuscular Neurotrophin-3 normalizes low threshold spinal reflexes, reduces spasms and improves mobility after bilateral corticospinal tract injury in rats. *Elife* **5**, doi:10.7554/eLife.18146 (2016).
- 417 Bergami, M. *et al.* A critical period for experience-dependent remodeling of adult-born neuron connectivity. *Neuron* **85**, 710-717, doi:10.1016/j.neuron.2015.01.001 (2015).
- 418 Farmer, J. *et al.* Effects of voluntary exercise on synaptic plasticity and gene expression in the dentate gyrus of adult male Sprague-Dawley rats in vivo. *Neuroscience* **124**, 71-79, doi:10.1016/j.neuroscience.2003.09.029 (2004).
- 419 Olson, A. K., Eadie, B. D., Ernst, C. & Christie, B. R. Environmental enrichment and voluntary exercise massively increase neurogenesis in the adult hippocampus via dissociable pathways. *Hippocampus* **16**, 250-260, doi:10.1002/hipo.20157 (2006).
- 420 Bayat, M., Sharifi, M. D., Haghani, M. & Shabani, M. Enriched environment improves synaptic plasticity and cognitive deficiency in chronic cerebral hypoperfused rats. *Brain Res Bull* **119**, 34-40, doi:10.1016/j.brainresbull.2015.10.001 (2015).

- 421 Marosi, K. & Mattson, M. P. BDNF mediates adaptive brain and body responses to energetic challenges. *Trends Endocrinol Metab* **25**, 89-98, doi:10.1016/j.tem.2013.10.006 (2014).
- 422 Marini, A. M. *et al.* Preconditioning and neurotrophins: a model for brain adaptation to seizures, ischemia and other stressful stimuli. *Amino Acids* **32**, 299-304, doi:10.1007/s00726-006-0414-y (2007).
- 423 Baik, S. H., Rajeev, V., Fann, D. Y., Jo, D. G. & Arumugam, T. V. Intermittent fasting increases adult hippocampal neurogenesis. *Brain Behav* **10**, e01444, doi:10.1002/brb3.1444 (2020).
- 424 Be'eri, H., Reichert, F., Saada, A. & Rotshenker, S. The cytokine network of Wallerian degeneration: IL-10 and GM-CSF. *European Journal of Neuroscience* **10**, 2707-2713, doi:10.1046/j.1460-9568.1998.00277.x (1998).
- 425 Ishida, A., Nakajima, W. & Takada, G. Short-term fasting alters neonatal rat striatal dopamine levels and serotonin metabolism: an in vivo microdialysis study. *Developmental Brain Research* **104**, 131-136, doi:[https://doi.org/10.1016/S0165-3806\(97\)00149-1](https://doi.org/10.1016/S0165-3806(97)00149-1) (1997).
- 426 Shawky, S., Anis, A., Orabi, S., Shoghy, K. & Hassan, W. Effect of Intermittent Fasting on Brain Neurotransmitters, Neutrophils Phagocytic Activity, and Histopathological Finding in Some Organs in Rats. *International Journal of Research Studies in Biosciences(IJRSB)* **3**, 38-45 (2015).
- 427 Wheeler, M. A., Rothhammer, V. & Quintana, F. J. Control of immune-mediated pathology via the aryl hydrocarbon receptor. *J Biol Chem* **292**, 12383-12389, doi:10.1074/jbc.R116.767723 (2017).
- 428 Rothhammer, V. *et al.* Type I interferons and microbial metabolites of tryptophan modulate astrocyte activity and central nervous system inflammation via the aryl hydrocarbon receptor. *Nat Med* **22**, 586-597, doi:10.1038/nm.4106 (2016).
- 429 Lopetuso, L. R., Scaldaferrri, F., Petito, V. & Gasbarrini, A. Commensal Clostridia: leading players in the maintenance of gut homeostasis. *Gut Pathogens* **5**, 23, doi:10.1186/1757-4749-5-23 (2013).
- 430 Wikoff, W. R. *et al.* Metabolomics analysis reveals large effects of gut microflora on mammalian blood metabolites. *Proceedings of the National Academy of Sciences* **106**, 3698, doi:10.1073/pnas.0812874106 (2009).
- 431 Hwang, I. K. *et al.* Indole-3-propionic acid attenuates neuronal damage and oxidative stress in the ischemic hippocampus. *J Neurosci Res* **87**, 2126-2137, doi:10.1002/jnr.22030 (2009).
- 432 Chyan, Y. J. *et al.* Potent neuroprotective properties against the Alzheimer beta-amyloid by an endogenous melatonin-related indole structure, indole-3-propionic acid. *J Biol Chem* **274**, 21937-21942 (1999).
- 433 Alexeev, E. E. *et al.* Microbiota-Derived Indole Metabolites Promote Human and Murine Intestinal Homeostasis through Regulation of Interleukin-10 Receptor. *Am J Pathol* **188**, 1183-1194, doi:10.1016/j.ajpath.2018.01.011 (2018).
- 434 Hudson, G. *et al.* Pregnane X Receptor Activation Triggers Rapid ATP Release in Primed Macrophages That Mediates NLRP3 Inflammasome Activation. *J Pharmacol Exp Ther* **370**, 44-53, doi:10.1124/jpet.118.255679 (2019).
- 435 Wang, S. *et al.* Xenobiotic pregnane X receptor (PXR) regulates innate immunity via activation of NLRP3 inflammasome in vascular endothelial cells. *J Biol Chem* **289**, 30075-30081, doi:10.1074/jbc.M114.578781 (2014).
- 436 Metzemaekers, M., Gouwy, M. & Proost, P. Neutrophil chemoattractant receptors in health and disease: double-edged swords. *Cell Mol Immunol*, doi:10.1038/s41423-020-0412-0 (2020).
- 437 Sawant, K. V. *et al.* Chemokine CXCL1-Mediated Neutrophil Trafficking in the Lung: Role of CXCR2 Activation. *J Innate Immun* **7**, 647-658, doi:10.1159/000430914 (2015).

- 438 Wu, F. *et al.* CXCR2 is essential for cerebral endothelial activation and leukocyte recruitment during neuroinflammation. *J Neuroinflammation* **12**, 98, doi:10.1186/s12974-015-0316-6 (2015).
- 439 Cao, D.-L., Qian, B., Zhang, Z.-J., Gao, Y.-J. & Wu, X.-B. Chemokine receptor CXCR2 in dorsal root ganglion contributes to the maintenance of inflammatory pain. *Brain Research Bulletin* **127**, 219-225, doi:<https://doi.org/10.1016/j.brainresbull.2016.09.016> (2016).
- 440 Ioannis, K., Stamatios, T., Efstratios, P. & Constantinos, G. Pregnane X Receptor (PXR) at the Crossroads of Human Metabolism and Disease. *Current Drug Metabolism* **14**, 341-350, doi:<http://dx.doi.org/10.2174/1389200211314030009> (2013).
- 441 Dubrac, S., Elentner, A., Ebner, S., Horejs-Hoeck, J. & Schmuth, M. Modulation of T lymphocyte function by the pregnane X receptor. *J Immunol* **184**, 2949-2957, doi:10.4049/jimmunol.0902151 (2010).
- 442 Schote, A. B., Turner, J. D., Schiltz, J. & Muller, C. P. Nuclear receptors in human immune cells: expression and correlations. *Mol Immunol* **44**, 1436-1445, doi:10.1016/j.molimm.2006.04.021 (2007).
- 443 Casey, S. C. & Blumberg, B. The steroid and xenobiotic receptor negatively regulates B-1 cell development in the fetal liver. *Mol Endocrinol* **26**, 916-925, doi:10.1210/me.2011-1303 (2012).
- 444 Biondo, C. *et al.* The interleukin-1beta/CXCL1/2/neutrophil axis mediates host protection against group B streptococcal infection. *Infect Immun* **82**, 4508-4517, doi:10.1128/IAI.02104-14 (2014).
- 445 Voisin, M. B. & Nourshargh, S. Neutrophil trafficking to lymphoid tissues: physiological and pathological implications. *J Pathol* **247**, 662-671, doi:10.1002/path.5227 (2019).
- 446 Hampton, H. R., Bailey, J., Tomura, M., Brink, R. & Chtanova, T. Microbe-dependent lymphatic migration of neutrophils modulates lymphocyte proliferation in lymph nodes. *Nat Commun* **6**, 7139, doi:10.1038/ncomms8139 (2015).
- 447 Sporri, R., Joller, N., Hilbi, H. & Oxenius, A. A novel role for neutrophils as critical activators of NK cells. *J Immunol* **181**, 7121-7130, doi:10.4049/jimmunol.181.10.7121 (2008).
- 448 Bakele, M. *et al.* Localization and functionality of the inflammasome in neutrophils. *J Biol Chem* **289**, 5320-5329, doi:10.1074/jbc.M113.505636 (2014).
- 449 Ketelut-Carneiro, N. *et al.* IL-18 triggered by the Nlrp3 inflammasome induces host innate resistance in a pulmonary model of fungal infection. *J Immunol* **194**, 4507-4517, doi:10.4049/jimmunol.1402321 (2015).
- 450 Sahoo, M., Ceballos-Olvera, I., del Barrio, L. & Re, F. Role of the inflammasome, IL-1beta, and IL-18 in bacterial infections. *ScientificWorldJournal* **11**, 2037-2050, doi:10.1100/2011/212680 (2011).
- 451 Hyun, Y. M. & Hong, C. W. Deep insight into neutrophil trafficking in various organs. *J Leukoc Biol* **102**, 617-629, doi:10.1189/jlb.1RU1216-521R (2017).
- 452 Norris, B. A. *et al.* Chronic but not acute virus infection induces sustained expansion of myeloid suppressor cell numbers that inhibit viral-specific T cell immunity. *Immunity* **38**, 309-321, doi:10.1016/j.immuni.2012.10.022 (2013).
- 453 Morin, N. *et al.* Neutrophils invade lumbar dorsal root ganglia after chronic constriction injury of the sciatic nerve. *J Neuroimmunol* **184**, 164-171, doi:10.1016/j.jneuroim.2006.12.009 (2007).
- 454 Popovich, P. G. & Longbrake, E. E. Can the immune system be harnessed to repair the CNS? *Nature Reviews Neuroscience* **9**, 481-493, doi:10.1038/nrn2398 (2008).
- 455 Brinkmann, V. & Zychlinsky, A. Neutrophil extracellular traps: Is immunity the second function of chromatin? *The Journal of Cell Biology* **198**, 773-783, doi:10.1083/jcb.201203170 (2012).

- 456 Kurimoto, T. *et al.* Neutrophils express oncomodulin and promote optic nerve  
regeneration. *J Neurosci* **33**, 14816-14824, doi:10.1523/JNEUROSCI.5511-12.2013  
(2013).
- 457 Ivashkiv, L. B. IFN $\gamma$ : signalling, epigenetics and roles in immunity, metabolism,  
disease and cancer immunotherapy. *Nat Rev Immunol* **18**, 545-558, doi:10.1038/s41577-  
018-0029-z (2018).
- 458 Mühl, H. & Pfeilschifter, J. Anti-inflammatory properties of pro-inflammatory interferon- $\gamma$ .  
*International Immunopharmacology* **3**, 1247-1255, doi:10.1016/s1567-5769(03)00131-  
0 (2003).
- 459 Kominsky, D. J. *et al.* IFN-gamma-mediated induction of an apical IL-10 receptor on  
polarized intestinal epithelia. *J Immunol* **192**, 1267-1276, doi:10.4049/jimmunol.1301757  
(2014).
- 460 Kunis, G. *et al.* IFN-gamma-dependent activation of the brain's choroid plexus for CNS  
immune surveillance and repair. *Brain* **136**, 3427-3440, doi:10.1093/brain/awt259 (2013).
- 461 Kelchtermans, H., Billiau, A. & Matthys, P. How interferon-gamma keeps autoimmune  
diseases in check. *Trends Immunol* **29**, 479-486, doi:10.1016/j.it.2008.07.002 (2008).
- 462 Song, J. H. *et al.* Interferon gamma induces neurite outgrowth by up-regulation of p35  
neuron-specific cyclin-dependent kinase 5 activator via activation of ERK1/2 pathway. *J  
Biol Chem* **280**, 12896-12901, doi:10.1074/jbc.M412139200 (2005).
- 463 Ishii, H. *et al.* ifn-gamma-dependent secretion of IL-10 from Th1 cells and  
microglia/macrophages contributes to functional recovery after spinal cord injury. *Cell  
Death Dis* **4**, e710, doi:10.1038/cddis.2013.234 (2013).
- 464 Fujiyoshi, T. *et al.* Interferon- $\gamma$  Decreases Chondroitin Sulfate Proteoglycan Expression  
and Enhances Hindlimb Function after Spinal Cord Injury in Mice. *Journal of  
Neurotrauma* **27**, 2283-2294, doi:10.1089/neu.2009.1144 (2010).
- 465 Victório, S. C. S., Havton, L. A. & Oliveira, A. L. R. Absence of IFN $\gamma$  expression induces  
neuronal degeneration in the spinal cord of adult mice. *Journal of Neuroinflammation* **7**,  
77, doi:10.1186/1742-2094-7-77 (2010).
- 466 Neumann, H., Schmidt, H., Wilharm, E., Behrens, L. & Wekerle, H. Interferon gamma  
gene expression in sensory neurons: evidence for autocrine gene regulation. *The Journal  
of experimental medicine* **186**, 2023-2031, doi:10.1084/jem.186.12.2023 (1997).
- 467 Shen, K.-F. *et al.* Interleukin-10 down-regulates voltage gated sodium channels in rat  
dorsal root ganglion neurons. *Experimental Neurology* **247**, 466-475,  
doi:<https://doi.org/10.1016/j.expneurol.2013.01.018> (2013).
- 468 Cunha, T. M. *et al.* Treatment with DF 2162, a non-competitive allosteric inhibitor of  
CXCR1/2, diminishes neutrophil influx and inflammatory hypernociception in mice. *Br J  
Pharmacol* **154**, 460-470, doi:10.1038/bjp.2008.94 (2008).
- 469 Cobos, E. J. *et al.* Mechanistic Differences in Neuropathic Pain Modalities Revealed by  
Correlating Behavior with Global Expression Profiling. *Cell Rep* **22**, 1301-1312,  
doi:10.1016/j.celrep.2018.01.006 (2018).
- 470 Courtine, G. *et al.* Transformation of nonfunctional spinal circuits into functional states  
after the loss of brain input. *Nat Neurosci* **12**, 1333-1342, doi:10.1038/nn.2401 (2009).
- 471 Courtine, G. *et al.* Recovery of supraspinal control of stepping via indirect propriospinal  
relay connections after spinal cord injury. *Nat Med* **14**, 69-74, doi:10.1038/nm1682  
(2008).
- 472 Blesch, A. & Tuszynski, M. H. Spinal cord injury: plasticity, regeneration and the  
challenge of translational drug development. *Trends Neurosci* **32**, 41-47,  
doi:10.1016/j.tins.2008.09.008 (2009).
- 473 Taccola, G., Sayenko, D., Gad, P., Gerasimenko, Y. & Edgerton, V. R. And yet it moves:  
Recovery of volitional control after spinal cord injury. *Prog Neurobiol* **160**, 64-81,  
doi:10.1016/j.pneurobio.2017.10.004 (2018).

- 474 Sofroniew, M. V. Dissecting spinal cord regeneration. *Nature* **557**, 343-350, doi:10.1038/s41586-018-0068-4 (2018).
- 475 Takeoka, A., Vollenweider, I., Courtine, G. & Arber, S. Muscle spindle feedback directs locomotor recovery and circuit reorganization after spinal cord injury. *Cell* **159**, 1626-1639, doi:10.1016/j.cell.2014.11.019 (2014).
- 476 Bareyre, F. M. *et al.* The injured spinal cord spontaneously forms a new intraspinal circuit in adult rats. *Nat Neurosci* **7**, 269-277, doi:10.1038/nn1195 (2004).
- 477 Harkema, S. *et al.* Effect of epidural stimulation of the lumbosacral spinal cord on voluntary movement, standing, and assisted stepping after motor complete paraplegia: a case study. *The Lancet* **377**, 1938-1947, doi:10.1016/s0140-6736(11)60547-3 (2011).
- 478 Everett, L. J. *et al.* Integrative genomic analysis of CREB defines a critical role for transcription factor networks in mediating the fed/fasted switch in liver. *BMC Genomics* **14**, 337, doi:10.1186/1471-2164-14-337 (2013).
- 479 Kim, J. *et al.* Transcriptome analysis reveals intermittent fasting-induced genetic changes in ischemic stroke. *Hum Mol Genet* **27**, 1497-1513, doi:10.1093/hmg/ddy057 (2018).
- 480 Guo, P., Zhang, K., Ma, X. & He, P. Clostridium species as probiotics: potentials and challenges. *Journal of animal science and biotechnology* **11**, 24-24, doi:10.1186/s40104-019-0402-1 (2020).